Clonogenicity and Stem Cells

Charlotte Mary Beaver

Submitted for the degree of Doctor of Philosophy

to University College London

Division of Surgery and Interventional Science, UCL

March 2013

I, Charlotte Beaver, confirm that the work presented in this thesis is my own. Where information has been derived from other sources, I confirm that this has been indicated in the thesis.

Abstract

Primary keratinocytes form 3 types of colony with different morphologies termed holoclones, meroclones and paraclones, thought to be derived from stem, early and late stage precursor cells respectively (Barrandon and Green, 1987b, Rochat et al., 1994). Cancer cell lines produce colonies with morphologies analogous to those of holoclones, meroclones and paraclones, and consequently holoclone morphology is used as a surrogate marker for stem cell colonies. The aim of this study was to elucidate the relationship between clonogenicity, colony morphology and stem cells.

Colonies formed by primary prostate epithelial cells and prostate cancer cell lines (DU145, PC3, LNCaP) were characterised. The proportions of colonies were not altered significantly by modification of culture conditions. In contrast to cancer cells, primary prostate epithelial cells form only two types of colony, termed types 1 and 2, which are analogous to holoclones and paraclones. Only type 1 colonies were highly proliferative, able to self-renew and express putative stem cell markers.

Paradoxically, cells from DU145 meroclones formed holoclones and had self-renewal capacity (by serial cloning and xenografting). It is concluded that the major difference between holoclone and meroclone colonies from the cancer cell line DU145 is the proportion of stem cells within each colony, not the presence or absence of stem cells. Phage display was used to look for targets on the surface of cells in Type 1 colonies. Various experimental protocols were tested, but no targets were identified.

Acknowledgements

To my supervisors Professor John Masters and Dr Aamir Ahmed for their guidance and support.

To Dr Stephen Hart for his help and knowledge of phage display.

To Ben Challacombe at Guy's hospital for providing tissue, even when he was on holiday on the other side of the world.

To those at the Prostate Cancer Research Centre and the Cecil Pilkington Charitable Trust who generously funded this work (2009-2013).

To all my friends PCRC. Thanks for all the help, support and friendship. It's been a great few years.

To my family and especially my parents who have supported by ambitions. I wouldn't be here without you.

To Mark who has supported me all these years and made me lots of cups of tea.

Table of Contents

List of Figures

List of Tables

Abbreviations

°C	Degree Celsius
µg	Microgram
µl	Microliter
ABCG2	ABC family member G2 (alias BCRP1)
ABTS	2,2'-azino-bis(3-ethylbenzthiazoline-6-sulphonic acid)
Akt	Protein Kinase B
ALDH	Aldehyde dehydrogenase 1
ALL	Acute lymphoblastic leukaemia
AML	Acute Myeloid Leukaemia
AR	Androgen receptor
bcl-2	B-cell lymphoma 2
BM	Bone marrow
BPH	Benign prostatic hyperplasia
BPH-1	Benign prostatic hyperplasia epithelial cell line
BrdU	Bromodeoxyuridine
BSA	Bovine serum albumin
CFE	Colony forming efficiency
c-kit	Tyrosine-protein kinase Kit (CD117)
CSC	Cancer stem cells
CV	Crystal Violet
CWR22	Prostate xenograft model
DAPI	4',6-diamidino-2-phenylindole
DC	Differentiated cell
dH_2O	Distilled water
DHT	Dihydrotestosterone

Dkk1	Dickkopf1
DMSO	Dimethyl sulfoxide
DNA	Deoxyribonucleic acid
DRE	Digital rectal examination
DU145	Human prostate adenocarcinoma cell line
E.coli	Escherichia coli
EGFR	Epidermal growth factor receptor
ELISA	Enzyme-linked immunosorbent assay
EMT	Epithelial-mesenchymal transition
EPC	Endothelial progenitor cells
E-TA	Early transit amplifying
Fab	Fragment antigen-binding
FACS	Flow-cytometery based sorting
FBS	Foetal bovine serum
FITC	Fluorescein isothiocyanate
Fz	Frizzled
g	Gram
g	Gravity
GCT27	Human germ cell tumour line
h18	Ribosomal idiosyncratic pseudoknot structure
HCl	Hydrogen chloride
HeLa	Human cervical carcinoma cells
Hh	Hedgehog
HoLEP	Holmium Laser Enucleation of the Prostate
HSC	Haematopoetic stem cells
hTERT	Telomerase reverse transcriptase

HTSCA	Human tumour stem cell assay
HUVEC	Human umbilical vein endothelial cells
Il2rg2/2	Interleukin-2 receptor gamma chain null
IMS	Industrial methylated spirit
IPTG	Isopropyl-β-D-thiogalactoside
K14	Cytokeratin 14
K18	Cytokeratin 18
K5	Cytokeratin 5
K8	Cytokeratin 8
LB	Lysogeny Broth
LNCaP	Human prostate adenocarcinoma cell line
LRP6	Lipoprotein receptor-related protein-6
LSC	Leukemic stem cells
L-TA	Late transit amplifying
M	Molar
mAb	Monoclonal antibody
MANOVA	Multivariate analysis of variance
mg	Milligram
ml	Millilitre
MRI	Magnetic Resonance Imaging
MSC	Mesenchymal stem cells
NaCl	Sodium chloride
NBS	New born calf serum
NGS	Normal goat serum
NOD/SCID	Non-obese diabetic severe combined immunodeficiency

Oct4	Octamer-binding transcription factor 4 (POU5F1)
p63	Tumor protein p63
PAP	Prostatic acid phosphatase
PBS	Phosphate buffered saline
PC-3	Human prostate adenocarcinoma cell line
Pca	Prostate cancer
PcG	Polycomb group protein
PEG	Polyethylene glycol
PFA	Paraformaldehyde
PIN	Prostatic intraepithelial neoplasia
PrEBM	Prostate Epithelial Basal Medium
PrEGM	Prostate epithelial growth medium
PSA	Prostate-specific antigen
PSMA	Prostate-specific membrane antigen
PTCH1	Patched 1
RF	Replicative form
RNA	Ribonucleic acid
RNAi	RNA interference
rpm	Revolutions per minute
RT-PCR	Reverse transcription polymerase chain reaction
rUGM	Rat urogenital mesenchyme
S.E.M	Standard error of the mean
SC	Stem cell
Sca-1	Stem cell antigen-1
scFv	Single-chain variable fragment
SD	Shine–Dalgarno

SFE	Sphere forming efficiency
SMO	Signalling molecule
Sox2	SRY (sex determining region Y)-box 2
SP	Side population
ssDNA	Single stranded viral DNA
TA	Transit amplifying
TBS	Tris buffered saline
TGF-β	Transforming growth factor beta
TRITC	Tetramethylrhodamine-isothiocyanate
TUNA	Transurethral needle ablation
TUP	Target-unrelated peptides
TURP	Transurethral resection of the prostate
VC	Vehicle control
VEGF	Vascular endothelial growth factor
Xgal	5-Bromo-4-chloro-3-indolyl-β-D-galactoside

1 Introduction

1.1 The Prostate and it's Diseases

1.1.1 Prostate Anatomy

The prostate is an exocrine gland of the male reproductive system located inferior to the bladder, which surrounds the initial part of the urethra and some of the ejaculatory duct. The function of the prostate is to secrete an alkaline fluid into the semen to help neutralise the acidity of the female vaginal tract, and prostate-specific antigen (PSA) which liquefies the semen (Kirby, 2003).

The prostate gland is a pyramid-shaped organ with its *apex* adjacent to the urethra and directed downward and its *bases* adjacent to the bladder and directed upward. It lies below the urinary bladder and is located in front of the rectum and the seminal vesicles are located at its base. The prostate weighs about 20 g by early adulthood and is made up of several glandular and non-glandular components with no obvious capsular morphology (McNeal, 1988). The prostate can be divided into 5 lobes: an anterior, two lateral, a median and a posterior lobe (Kirby, 2003). However, this idea is disputed and alternatively 3 distinct zones of the prostate can be identified: the central zone (CZ), peripheral zone (PZ), and transition zone (TZ) (McNeal, 1981, McNeal, 1988) (Figure 1). These zones differ both physiologically and biologically and a zonal description of prostate morphology is central to present understanding of prostatic diseases, particularly prostate cancer.

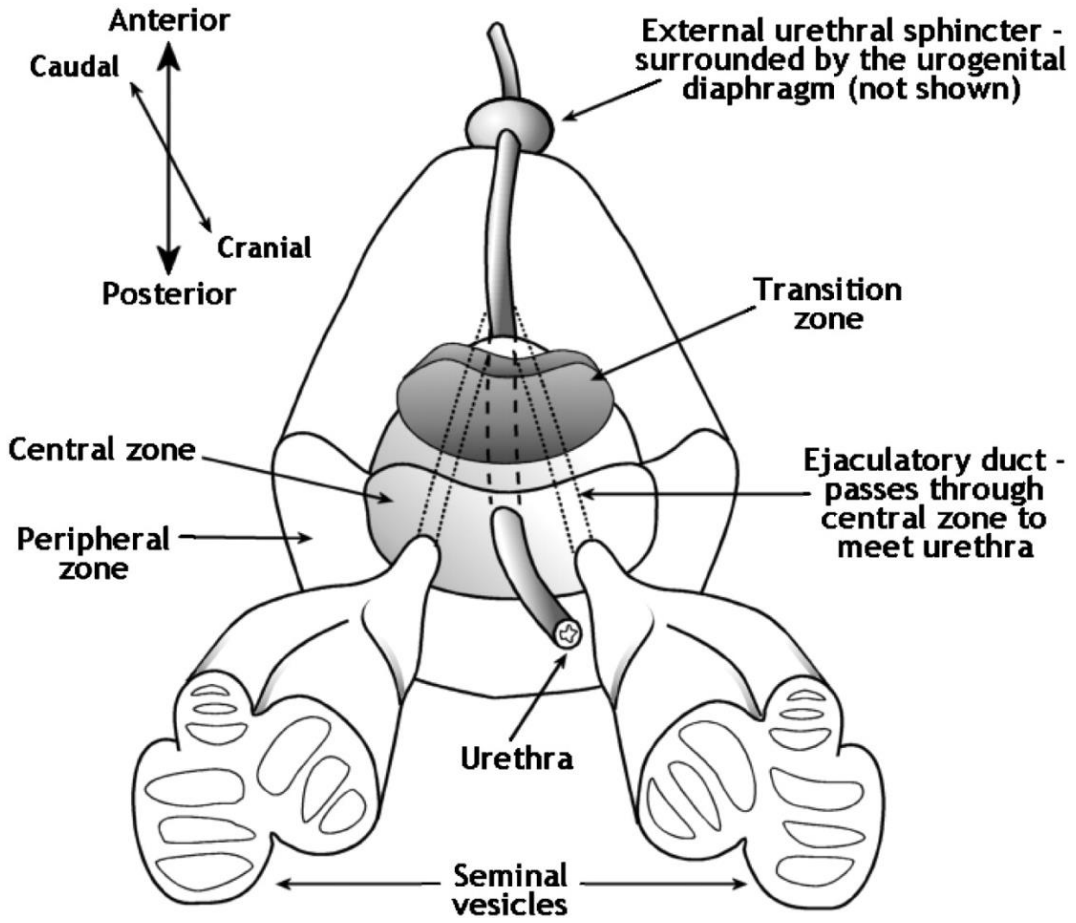

Figure 1. Anatomy the normal prostate gland.
Cartoon showing peripheral, central and transitional zones (Potter et al., 2005).

The peripheral zone comprises about 70% of the glandular prostate in young men and is predominantly mesodermal in origin (Argani et al., 1998). Its ducts exit from the posteriolateral recess of the urethral wall and extend mainly laterally in the coronal plane, branching both anteriorly and posteriorly (McNeal, 1988). The central zone is a cone shaped region that surrounds the ejaculatory ducts and makes up approximately 25% of the glandular prostate mass in young adults. The transition zone accounts for only 5% of the glandular prostate tissue and surrounds the proximal urethra. The non-glandular prostate tissue comprises of the preprostatic sphincter, striated

sphincter, anterior fibromuscular stroma and the prostatic capsule (McNeal, 1988).

There are three diseases of the prostate: prostatitis (inflammation), benign prostatic hyperplasia (BPH) and prostate cancer (PCa), which affect the different zones of the prostate. BPH develops predominantly in the transition zone and PCa in the peripheral zone.

1.1.1 Prostate Histology

The human prostate gland comprises of two distinct epithelial cell types: basal and secretory luminal cells which along with rarer neuroendocrine cells to form a complex branching ductal structure embedded in a muscular stroma containing smooth muscle cells and fibroblasts (Kirby, 2003). Basal cells form a layer along the basement membrane and luminal cells sit above the basal cells and secrete prostatic proteins into the lumen (Figure 2). The primary role of luminal epithelial cells is to secrete PSA, a single-chain glycoprotein consisting of 237 acids.

The two layers of epithelial cells are distinguished by their protein marker expression and secretions, as shown in Figure 2. Luminal cells express prostate specific antigen (PSA), prostatic acid phosphatase (PAP), androgen receptor (AR), CD57, 15-lipoxygenase (15-LOX2) and low molecular weight cytokeratins K8 and K18. Basal cells express high molecular weight cytokeratins K5 and K14, CD44, p63, telomerase and bcl-2 (Hudson, 2004, Bagley R.G. , 2009).

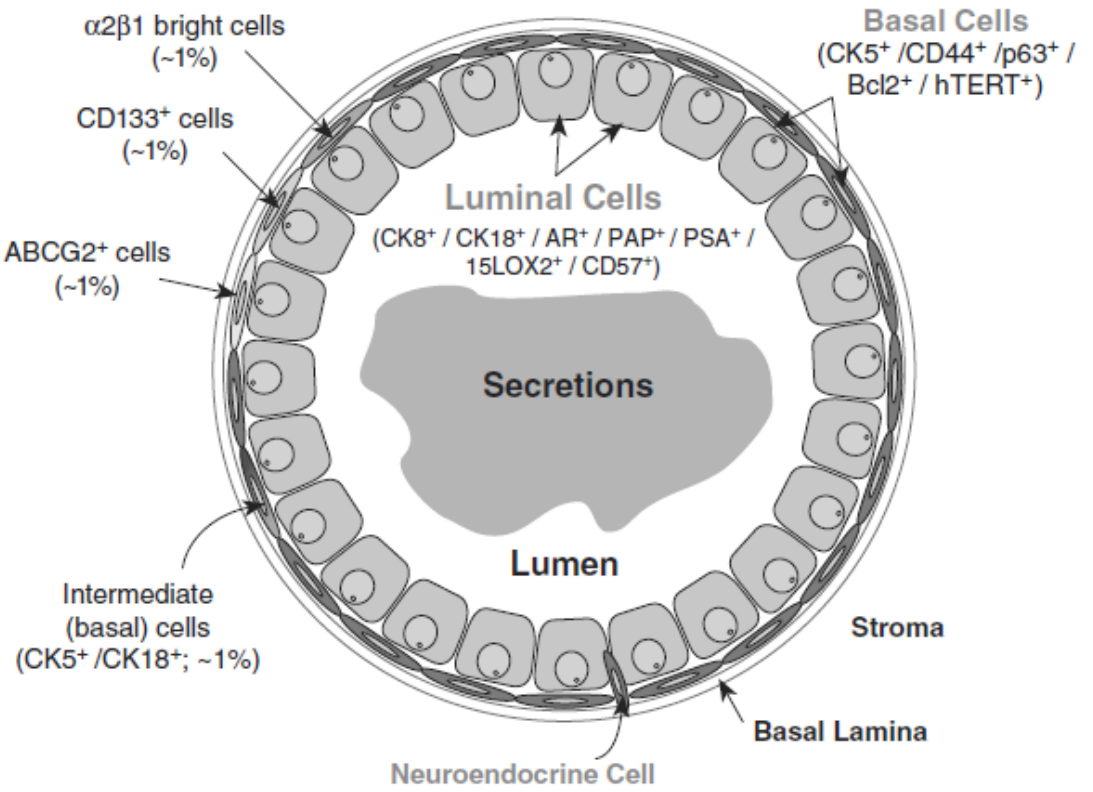

Figure 2. Structure of the human prostatic gland.
Cartoon of the structure and marker expression of the prostatic ducts, which comprise a basal and a luminal epithelial layer with distinct protein expression (Honorio 2009).

1.1.2 Benign Prostatic Hyperplasia

BPH occurs mainly in the transition zone, and is caused by hyperplasia of the prostatic stromal and epithelial cells (McNeal, 2006). Large fibromuscular nodules form in the periurethral region of the prostate, which can compress the urethral canal and cause obstruction of the urethra and interfere with the flow of urine. Symptoms include urinary hesitancy, dysuria (painful urination), nocturia, increased risk of urinary tract infections, and urinary retention. Although age is the major risk factor for BPH, androgens influence the

disease etiology as men castrated before puberty do not develop the disease (Wilson and Roehrborn, 1999).

Diagnosis is usually by digital rectal examination (DRE) and biopsy to rule out PCa. Treatments include 5α-reductase inhibitors that reduce conversion of testosterone to DHT and alpha-adrenergic blockers to relax smooth muscle in the prostate and the bladder neck, thereby increasing urine flow (Timms and Hofkamp, 2011). Both 5α-reductase and alpha-adrenoceptor blockade are well tolerated and effective treatments (Tammela, 1997). A surgical alternative is transurethral resection of the prostate (TURP), thus removing the urethral blockage. However, TURP can result in considerable side effects (Tammela, 1997). Other alternatives are transurethral needle ablation (TUNA) and transurethral microwave thermotherapy and although these have lower associated risks, are not as effective as TURP (Schatzl et al., 2000).

1.1.3 Prostate Cancer

Prostate cancer is an adenocarcinoma most frequently found in the peripheral zone of the prostate. Initially, small clumps of cancer cells are confined to otherwise normal prostate glands, a condition known as prostatic intraepithelial neoplasia (PIN), which can develop into invasive cancers. Prostate cancer most commonly metastasizes to the bone via the lymph nodes, and also can invade rectum, bladder and lower ureters after local progression (Kirby, 2003).

PCa diagnosis is confirmed by a combination of PSA screening, DRE, Magnetic Resonance Imaging (MRI) and prostate biopsy. PSA is a protein produced by normal epithelial cells as well as PCa, and can be elevated in

prostatic disorders. Biopsy samples of PCa are classified according to their Gleason score based the morphology of the cancer (Epstein et al., 2005). Cytological features may include hyperchromatic, enlarged nuclei with prominent nucleoli and abundant cytoplasm (Kirby and Madhavan, 2010).

Clinically, localized disease is treated by surgery (prostatectomy) or radiation therapy (external beam or brachytherapy), which have high success rates. An alternative is active surveillance which involves monitoring PSA levels (Bannuru et al., 2011). The use of surgery to treat localized disease can be controversial and some studies have shown no survival advantages when compared to active surveillance in men with low grade disease (Wilt et al., 2012).

Treatment of advanced disease is less successful. First line treatment depends on the androgen sensitivity of PCa, using androgen ablation or blockade of androgen action through the androgen receptor (Miyamoto et al., 2004). Although this treatment initially leads to tumour regression in the majority of patients, the cancer recurs in a median period of 18-24 months, leading to castrate resistance (Miyamoto et al., 2004). Recently two new treatments, Abiraterone and Enzalutamide have been developed to target castrate resistant disease. Abiraterone is an inhibitor of CYP17 activity which significantly decreases testosterone levels (Barrie et al., 1994). In Phase III trials, it extended median survival to 14.8 months versus 10.9 months. Phase III trials of the androgen receptor antagonist Enzalutamide increased survival to 18.4 months compared to 13.6 months in the control group (Scher et al., 2012). Both drugs have now received FDA approval and offer promising new therapy regimes. Development of alternative treatments is required to treat

metastatic disease and further improve the long term prognosis of men with advanced disease (Wolff and Mason, 2012).

1.2 Adult Stem Cells

Organs are composed of differentiated cells that perform discrete functions (Miller et al., 2005) and comprise the bulk the cells (Ichim and Wells, 2006). The continuous replacement of differentiated, functional cells by more primitive cells is a normal homeostatic process driven by multi-potential stem cells (SCs). These cells are also known as somatic or adult stem cells and have been identified in most tissues. They replenish dying cells and maintain organ health and functionality. Adult stem cells have features in common, including a large nuclear-to-cytoplasmic ratio, few organelles and they are structurally unspecialised or undifferentiated (Miller et al., 2005).

1.2.1 The Adult Stem Cell Hierarchy

An adult stem cell has two properties which allow it to maintain organ function: *Potency* and *self-renewal*. The potential the cell has to differentiate to form all the functional cell types within a tissue is called *potency.* The SC is at the apex of the hierarchy and is the initiating cell in the cell division and differentiation process producing a large family of differentiated descendants known as clonal expansion. To replenish the stem cell compartment lost during differentiation, the SC can undergo symmetrical division to produce two identical stem cell daughters, a process termed *self-renewal* (Mackillop et al., 1983).

In addition to self-renewing stem cells, the hierarchy model predicts two other types of cell: proliferating, non-self-renewing cells (transit amplifying) (TA) and non-proliferating, differentiated end cells (DC). The hierarchy in Figure 3

illustrates how the potential for division and differentiation changes as a cell moves down the hierarchy. Following division, the stem cell can give rise to a transit amplifying cell that will undergo further proliferation. The cells progressively differentiate and irreversibly commit to one of the lineages specific to the tissue (Miller et al., 2005). As cells move down the hierarchy acquiring the differentiated features associated with tissue function, the proportion of differentiated cells increases.

Somatic SCs reside in confined tissue compartments, referred to as niches (Loeffler and Roeder, 2002), where the microenvironment suppresses SC proliferation, resulting in a quiescent SC population. The SCs may be triggered to proliferate and differentiate in response to injury to repair damaged tissue (Ghotra et al., 2009). In this way the stem cell has the ability to maintain the organ over its lifetime (Miller et al., 2005).

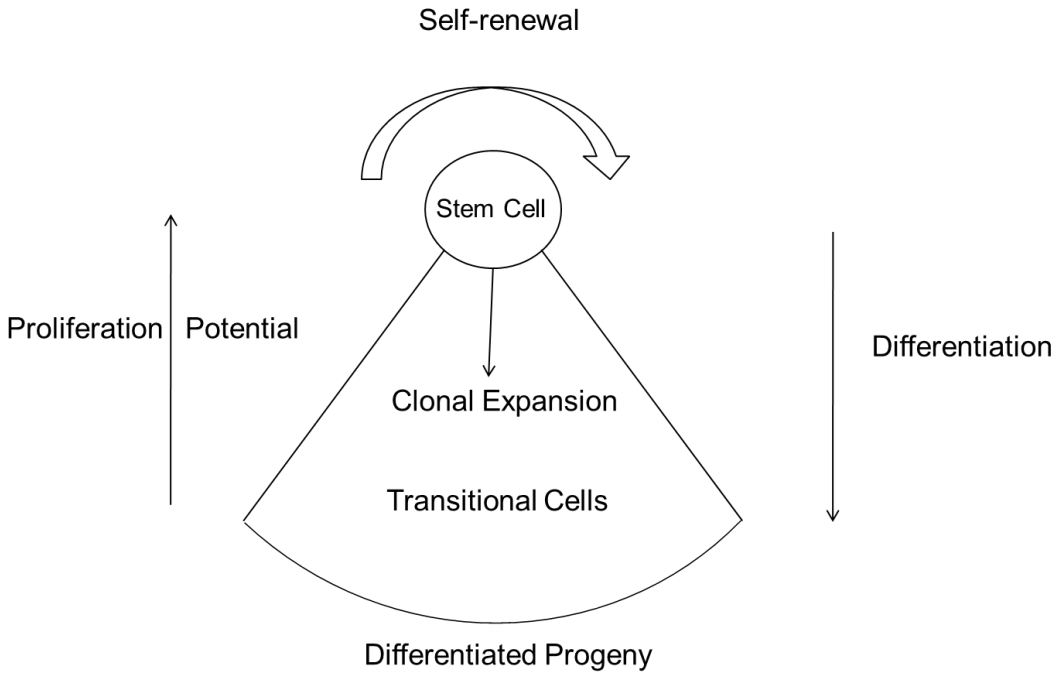

Figure 3. Adult Stem Cell Hierarchy.
The stem cell can self-renew or divide to produce proliferative transitional cells expand clonally. As cells differentiate they lose their proliferative potential and become more abundant.

1.2.2 Stem Cells in the Haematopoietic System

The first evidence for the existence of SCs in adult animals was generated by Till and McCulloch, who showed that mouse bone marrow (BM) cells injected into irradiated recipient mice developed visible spleen colonies derived from grafted cells. (Till and McCulloch, 1961, McCulloch and Till, 1962) The number of donor cells was directly proportional to the number of colonies that developed within the spleen. This result suggested that the transplanted BM cells were capable of self-renewal and it was hypothesised that these cells were stem cells. In addition, the radiation survival curve of cells that form colonies closely resembled the *in vitro* cell survival curves of clonogenic cells developed by Puck and Marcus (1956). The clonal origin of spleen colonies

was confirmed by transplantation of sub lethally irradiated bone marrow into heavily irradiated recipient mice. Some donor bone marrow cells containing genetic abnormalities caused by the irradiation cells, retained the ability to proliferate and produce clones containing the abnormality, demonstrating their clonal origin (Becker et al., 1963).

If the capacity to form colonies is to be considered as a criterion to identify stem cells, the cell must lose this capacity upon undergoing differentiation. The differentiation and subsequent loss of colony forming capacity was confirmed by applying hypoxia as a differentiating pressure which resulted in a reduction in colony formation in the spleens of hypoxic mice (Bruce and McCulloch, 1964). This result was thought to be due erythropoiesis which stimulates erythropoietin stimulated by hypoxia. The data suggested that an increased demand for differentiated cells reduced the number of stem cells, resulting in a reduction of colony forming ability. This confirmed the property of these stem cells as able to undergo both self-renewal and differentiation.

This data inspired further work studying stem cells, particularly within the haematopoietic system, leading to the discovery that BM contains at least 3 different stem cell populations: haematopoetic stem cells (HSCs), mesenchymal stem cells (MSCs) and endothelial progenitor cells (EPCs) (Alison and Islam, 2009). Single unselected BM cells can also form colonies in non-lympho-haematopoietic tissue, such as hepatocytes (Petersen et al., 1999), muscle fibre (Ferrari et al., 1998), microglia and astroglia (Eglitis and Mezey, 1997) and neuronal tissue (Brazelton et al., 2000, Mezey et al., 2000). The morphology and marker expression of these colonies are similar to the native cells.

1.2.3 Adult Stem Cell Identification

Morphology, proliferative/ cycling rates, location and marker expression are all used to identify and characterise stem cells in adult tissues. Advances in the identification and characterisation of adult stem cells have been aided by the development of techniques to label cells based on surface marker expression. Stem cells are identified by staining cell surface markers with monoclonal antibodies (mAb), exclusion of fluorescent dyes such as Hoechst 33342 or long term labelling with tritiated thymidine (Mittal et al., 2009). mAb technology and flow-cytometery based sorting (FACS) and analysis have been the main driving force in recent SC developments to enrich SC populations.

The identification of SCs is confirmed by the ability of the selected cells to recapitulate the organ of origin. The haematopoietic system and tissues with high cell turnover rates, such as the cells of the digestive tracts and skin, have been extensively studied, although SC in almost all organs have been identified and enriched for based on cell surface marker expression (Alison and Islam 2009). Table 1 lists markers for the identification and selection of adult stem cells in both blood and solid tissues. Of note is CD133 (Prominin 1), a marker which is a potential stem cell marker in several tissues, although its function in this context remains unclear.

The putative SC markers are also compared by clonogenicity, growth in non-adherent culture, the ability to reconstitute the organ when transplanted orthotopically *in vivo* and lineage tracing studies. Potential molecular markers for stem cells have also been identified in embryonic stem cells. These markers include the transcription factors Oct4, Sox2 and Nanog which are

known to control self-renewal and differentiation. These markers can identified *in situ* by immunocytochemistry and are used in combination to identify the location of the stem cell niche. Reverse transcription polymerase chain reaction (RT-PCR) analysis of cells retrieved from the mouse stomach stem cell niche by laser capture micro-dissection revealed a gene expression profile closely matching that of HSCs (Mills et al., 2002).

Table 1. Prospective Adult Stem Cell Markers.

Tissue/ stem cells	Markers Used to Enrich for SCs
Brain	CD133 (Lee et al., 2005) CD184+ CD271− CD44− CD24+ (Yuan et al., 2011)
Bone marrow (HSC)	CD34+ CD133+ CD45+ and c-kit+ (Bhatia, 2001)
Bone marrow/ (MSC)	$CD105^{+}/CD73^{+}/CD90^{+}/CD34^{-}/$ $CD45^{-}$, (Dominici et al., 2006)
Breast	*α*6integrin + $CK19^{+}$ ESA^{+} $MUC1^{-}$ $CALLA^{-}$ (Clarke et al., 2005)
Cardiac	Lin− c-kit+ (Beltrami et al., 2003)
Intestinal	Lgr5+ (Barker et al., 2007)
Kidney	CD133+ CD73+ CD29+ and CD44+ (Bussolati et al., 2005)
Liver	CD29+ CD73+ CD44+ and CD90+ (Herrera et al., 2006)
Skin	CK19+ (Michel et al., 1996) CD34+ and CK15+ (Blanpain et al., 2004) Lgr6+ (Snippert et al., 2010)

Potential cell surface markers for the identification of adult stem cells in the respective tissues.

1.3 Prostate Stem Cells

The earliest evidence for the existence of stem cells in the adult prostate came from androgen-ablation studies, where it was observed that adult rodent prostate can undergo multiple rounds of castration-induced regression and testosterone-induced regeneration (Isaacs and Coffey, 1989). Following castration there is a rapid reduction in prostate volume due to apoptosis. The remaining epithelial cell population can survive long periods and regenerate the prostate following androgen replacement (English et al., 1987, Evans and Chandler, 1987). This suggests that a small population of SCs possess the ability to self-renew and differentiate to regenerate the prostate, whilst the bulk of the prostate cells which are androgen dependent lack this function.

The castration studies suggest that SCs reside within the basal epithelial compartment of the prostate, as the majority of cells that survive castration have a basal rather than a luminal phenotype. (Kirby, 2003). Expression of proliferation and survival markers such as telomerase, p63 and Bcl-2 are localised in the basal compartment, which further supports this theory (Kasper, 2008). During regeneration SCs differentiate to produce androgen-independent TA cells that give rise to androgen-dependent fully differentiated secretory luminal cells providing evidence for a cellular hierarchy within the adult human prostate (English et al., 1987).

1.3.1 Prostate Stem Cell Identification

Several candidate prostate SC populations have been isolated based on marker expression observed only in the basal layer of the epithelium. Potential markers include K5/K18 double positive cells (Hudson et al., 2000) and CD44+ α2β1hi CD133+ cells (Richardson et al., 2004). α2β1 integrin

selects for cells which have a higher colony forming efficiency, are positive for the basal markers K5 and K14 and form prostate-like glands *in vivo* (Collins et al., 2001). Other potential markers for enrichment of prostate SCs include CD44, CD49f (Yamamoto et al., 2012), CD117 (c-kit) and CD133 (Collins et al., 2001), alone and in combination . Cells expressing these markers demonstrate increased colony forming efficiency (CFE) and can generate glandular structures when implanted under the renal capsule when recombined with rat urogenital mesenchyme (rUGM) (Leong et al., 2008). SCs from the prostate also appear to be enriched in side population (SP) cells. SP cells express the ATP-binding cassette membrane transporter ABCG2 transporter, which actively effluxes Hoechst 33342 from the cell which allows enrichment by FACS (Brown et al., 2007).

1.4 Cancer Stem Cells

1.4.1 Models of Tumour Heterogeneity

Like normal tissue, cancers are composed of a heterogeneous mixture of cells with range of capacity to differentiate, proliferate and form tumours (Pierce and Speers, 1988). Studies *in vivo* have demonstrated that, within a cancer population, only a small percentage of cells are able to initiate tumour development (Bonnet and Dick, 1997, Al-Hajj et al., 2003, Singh et al., 2004). Two models have been proposed to explain phenotypic and functional tumour heterogeneity: the stochastic and hierarchical, which are described in Figure 4.

1.4.1.1 *Stochastic Model of Stem Cells*

The stochastic model predicts that all tumour cells have similar proliferative capacity, but their behaviour is influenced by extrinsic factors (e.g. host factors, immune response, and microenvironment) or intrinsic (e.g. signalling pathways, levels of transcription factors). The randomness and unpredictability of these variables results in heterogeneity in marker expression, proliferation and tumour initiation capacity (Dick, 2008).

For the stochastic model to be correct, tumour cells cannot be permanently affected by these factors and all cells must have equal capacity to act as stem cells (Wang and Dick, 2005). The stochastic models predicts a growth fraction of less than 100% due to cell loss and the result of the constraints of the micro-environment (Miller et al., 2005). In this model tumour initiating activity cannot be enriched or selected for, because no markers are available.

1.4.1.2 *CSC Hierarchy Model of Stem Cells*

The second model is the cancer stem cells (CSC) hierarchy model which predicts that the tumour is a 'caricature of normal tissue development (Pierce and Speers, 1988). Like normal tissue, tumours are hierarchically organised, with the CSCs at the apex, driving tumour growth and regeneration. Like normal SCs, CSCs maintain the hierarchy by self-renewal or they generate transit amplifying cells which divide to produce differentiated offspring which form the bulk of the tumour and lack stem cell properties. The CSCs are thought to be a relatively small population of cells essential for tumour initiation (Frank et al., Reya et al., 2001). As in normal tissue only a small percentage of the tumour population maintain the capacity for long term proliferation, while most cells proceed down the differentiation pathway resulting in terminal differentiation (Miller et al., 2005). Due to differences in their characteristics, including proliferative capacity and marker expression, CSCs can be selected for.

Current cancer treatments may eradicate the tumour bulk but spare the populations of stem cells which are able to regenerate the cancer (Wang et al., 2012). This process may explain why tumour regression does not translate to improved patient survival in many clinical trials. It is still not clear whether CSCs are originally somatic SCs which have undergone oncogenic changes, or TA or DCs which have gained genetic changes which result in SC behaviour. The evidence for the hierarchical model which underlies the CSC theory comes from clonogenic and tumourigenic assays, which will be discussed further.

1.4.1.3 *Clonal Evolution*

A parallel and popular idea is the clonal evolution model of cancer in which cancer is a stepwise evolutionary process of Darwinian natural selection (Greaves and Maley, 2012). Intrinsic differences can be caused by stochastic genetic (Nowell, 1986) or epigenetic changes (Baylin and Jones, 2011). This model complements both the CSC and the stochastic model (Shackleton et al., 2009). It proposes that most neoplasms arise from a single cell of origin, and tumour progression results from acquired stepwise genetic changes. The newly acquired genetic changes within the original clone allow the sequential selection of more aggressive sub-lines (Nowell, 1976).

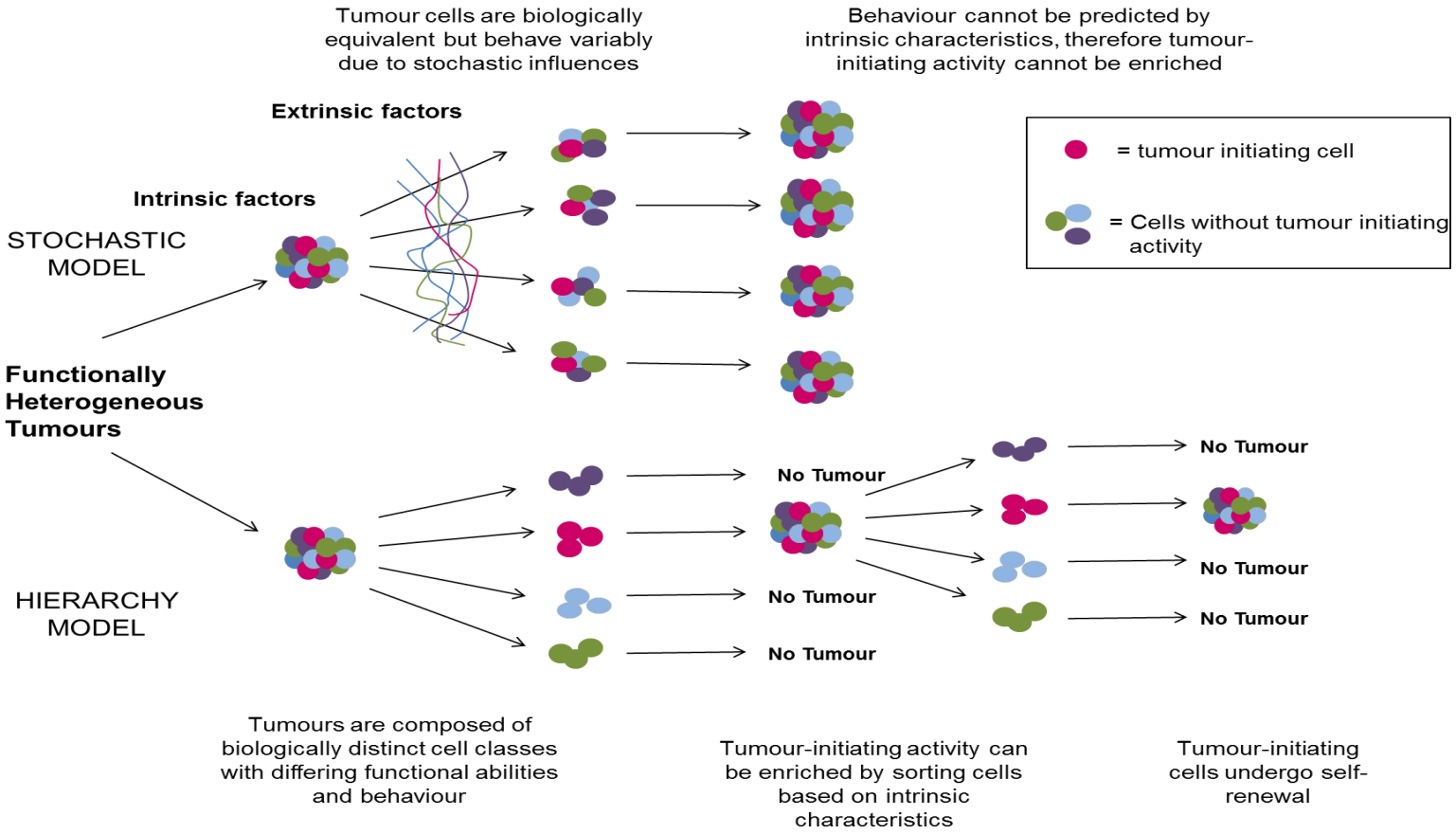

Figure 4 Stochastic and Hierarchical Models of Cancer Stem Cells.

The hierarchical model predicts that tumours are composed of functionally distinct cells, including cancer stem cells, which have different functional properties. The stochastic model predicts that all cells are functionally equal and that cell heterogeneity is due to intrinsic and extrinsic influences which affect cell behaviour. Adapted from Dick, 2008.

1.4.2 Cancer Stem Cell Definition

The CSC is defined as “A cell within a tumour that possesses the capacity to self-renew and to cause the heterogeneous lineages of cancer cells that comprise the tumour. CSCs can thus only be defined experimentally by their ability to recapitulate the generation of a continuously growing tumour” (Clarke et al., 2006). Therefore CSCs express the stem cell properties of self-renewal and potency. Self-renewal is the ability to undergo cell division while maintaining stem cell capacity. Potency is the ability of cells to differentiate into the cells that comprise the tumour of origin (Mittal et al., 2009). Experimentally, the ‘gold standard’ for CSC identification is the ability to serially xenograft (Clarke et al., 2006).

1.4.3 Identification of Cancer Stem Cells

The first evidence for the existence of CSCs came from cell proliferation studies. Radiolabelling of cells and the use of autoradiography enabled measurements of proliferation, hierarchical relationships and lifespan in normal and neoplastic tissues (Belanger and Leblond, 1946, Dick, 2008). From these studies came the proposal that tumours are caricatures of normal development and contain stem cells (Pierce and Speers, 1988).

1.4.3.1 *Haematopoietic CSCs*

Like somatic stem cells, much of the early work on CSCs relied on cancers of the haematopoietic system. In the 1970s, cytokinetic studies of cell lines, murine models of acute leukaemias and *in vivo* examination of leukaemia blast proliferation kinetics in human AML (Acute Myeloid Leukaemia) and ALL (Acute Lymphoblastic Leukaemia) patients demonstrated functional heterogeneity (Clarkson et al., 1970, Dick, 2008). The majority of leukaemic

blasts were post mitotic the population was replenished from a relatively small fraction of proliferative cells. Only a small number of leukemic blast cells were cycling *in vivo* and two proliferative fractions were observed: a larger, fast cycling subset with a 24 hour cell cycle time and a smaller, slow cycling subset with a dormancy of weeks to months. It was proposed that the slow cycling fraction generates the fast cycling fraction. These kinetic properties were similar to normal haematopoietic stem cells (Cheshier et al., 1999) and this observation indicates that cancers also exhibit functional heterogeneity in terms of proliferative potential.

The inability of conventional therapies to kill slow cycling leukemic stem cells (LSCs) is predicted to be the cause of relapse and failure of chemotherapy (Cronkite, 1970). LSCs respond to the depletion of the leukemic cell mass following chemotherapy by entering the cell cycle to regenerate the cancer (Clarkson et al., 1975). It has been suggested that the way to eliminate dormant LSCs was to find the time frame in which they are cycling, but the eradication of dormant LSCs by chemotherapeutic agents has, so far, not been fully achieved (Dick, 2008). The inability to identify and assay potential LSCs was a major stumbling block to these studies, and characterising LSCs was impossible due to an inability to identify markers. Therefore attention was focused on the clonogenic assay which was adapted by several groups to study AML. By using the clonogenic assay, these groups managed to identify the phenotype of AML cultures *in vitro* with differing proliferative potential, providing further proof for hierarchy in AML (McCulloch et al., 1981, McCulloch, 1983, Griffin and Lowenberg, 1986).

1.4.4 Identification of CSCs: In Vivo Tumourigenicity

Advances in the types of immunocompromised animal models makes *in vivo* serial xeno-transplantation assay the gold standard of CSC identification (Clarke et al., 2006). A CSC enriched cell fraction must display significantly increased tumourigenic capacity to validate the cell surface markers upon which it was selected.

The serial xeno-transplantation model is shown diagrammatically in Figure 5**.** Cells from the original tumour are dissociated, usually by enzymatic or mechanical means. The CSCs population is enriched for based on molecular marker expression with mAbs. The cells are then injected either subcutaneously or orthotopically into immunocompromised mice and form a xenograft. The xenografted tumour is in turn harvested, digested and transplanted into the same site into further mice. *In vivo* limiting dilution assays must be performed with both the target and depleted cell fractions to confirm enhanced tumourigenicity in the positive fraction.

The CSC containing fraction must re-establish the phenotypic characteristics of the original tumour. The non CSC fraction is also injected as a control which, if selection is successful, fails to form a tumour (Visvader and Lindeman, 2008). Clonogenicity *in vitro* can also be used to estimate CSC frequency and results often correlate with tumourigenicity (O'Brien et al., 2010).

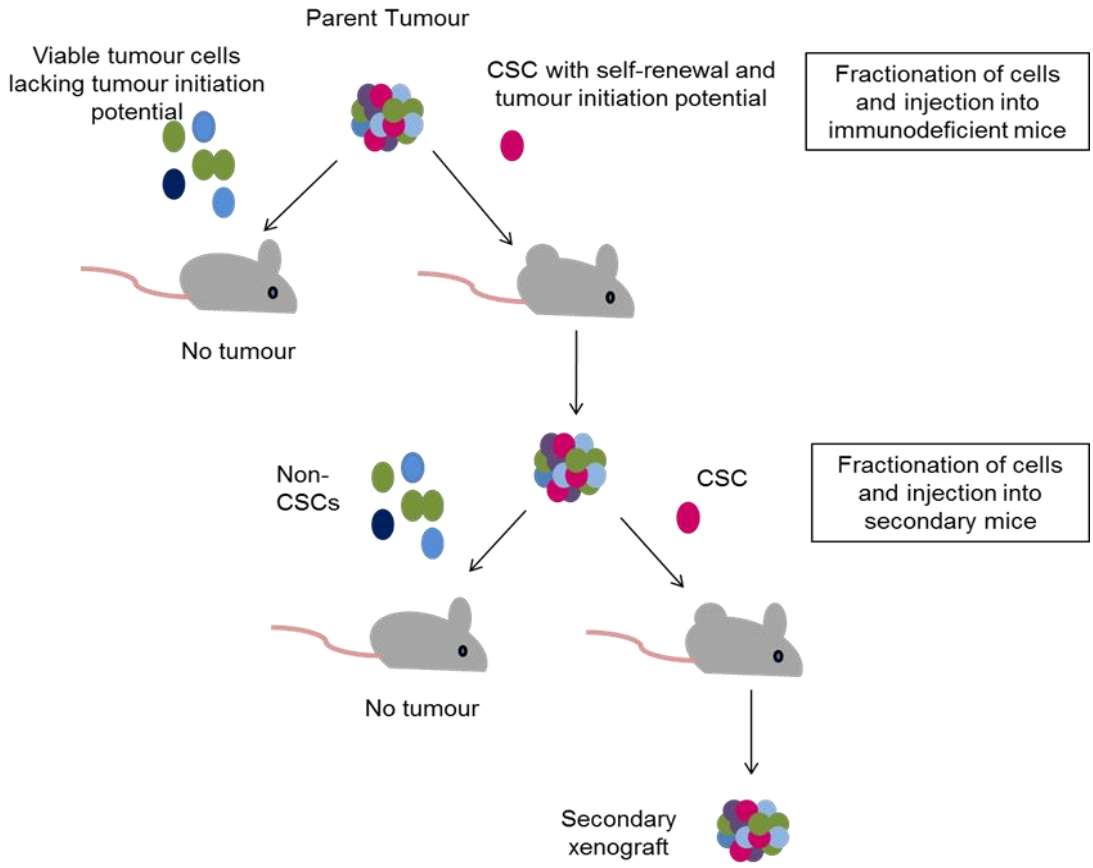

Figure 5. *In Vivo* Serial Xeno-transplantation Assay.
Human CSCs from human tumours are enriched for by marker selection and injected subcutaneously or orthotopically into immunodeficient mice. The resulting tumour is removed, digested and either reselected or transferred directly into secondary mice. Adapted from (O'Brien et al., 2010).

The xenotransplantation assay was first used to show that human leukaemias contain a small population (≤1%) of cells, with a CD34+, CD38- phenotype, which give rise to differentiated leukaemia cells and recapitulate the heterogeneous phenotype of the bulk tumour cancer in NOD/SCID mice (Bonnet and Dick, 1997). This finding was a crucial first step in demonstrating that subsets of cancer cells with enhanced tumourigenicity can be isolated based on molecular markers. The phenotypically more mature cells failed to engraft in mice, suggesting the presence of an identifiable tumour cell

hierarchy. This experiment also demonstrated the hierarchical organisation of human AML.

1.4.4.1 *CSCs in Solid Tissues*

Fractions of serially tumourigenic cells have been identified in solid tumours, such as breast (CD44+ CD24-/low) and brain (CD133+) (Singh et al., 2004). In these experiments small numbers of selected cells produced tumours in recipient mice. CD44 and CD133, which are markers frequently used to isolate somatic SC populations, are often used to isolate CSCs. A list of potential CSC markers shown to enrich for tumourigenicity in mice are shown in Table 2. Other CSC markers have been suggested, but although they increased CFE, they have so far failed to enhance tumourigenicity of primary human tumour samples in mice. Most of the currently used markers recognise molecules on the cell surface and not functional stem cell activity. Interestingly, there is a noticeable similarity between markers used to enrich normal adult SCs and CSCs, suggesting that they share some phenotypic traits. However, in some cases it has proven difficult to confirm markers that originally appeared to distinguish tumorigenic from non-tumourigenic cells. Following the initial discovery of some markers, conflicting results have been published and the suitability of several markers refuted (Magee et al., 2012).

Table 2. Putative Cancer Stem Cell Markers.

Cancer	Marker Used to Enrich for CSCs
Haematopoietic (AML)	$CD34^{+}$, $CD38^{-}$ (Lapidot et al., 1994, Bonnet and Dick, 1997)
Brain	$CD133^{+}$ (Singh et al., 2004)
Breast	$CD44^{+}$ $CD24^{-/low}$ (Al-Hajj et al., 2003)
Colon	$CD133^{+}$ (O'Brien et al., 2007, Ricci-Vitiani et al., 2007)
Pancreas	$CD133^{+}$ (Hermann et al., 2007) $ESA^{+}CD44^{+}$ $CD24^{+}$ (Li et al., 2007)
Melanoma	$ABC5^{+}$ (Schatton et al., 2008) CD20+ CD166+ Nestin+ (Klein et al., 2007)

Phenotypic populations which enrich for tumour initiating cells when serially transplanted immunocompromised mice.

Studying CSCs in solid tumours has proved more challenging than those in the haematopoietic system and the frequency of CSCs in solid tumours identified by current methods is highly variable (Visvader and Lindeman 2008). Evidence for the existence of cancer stem cells in solid tumours has been more difficult to obtain than in the haematopoietic system for several reasons:

1) The cells within the tumour are less accessible and tissue has to undergo mechanical or enzymatic digestion to obtain a single cell suspension which can be analysed;

2) There is a lack of functional assays suitable for detecting and quantifying non-cancerous stem cells from many organs;

3) Only a few cell surface stem cell markers have been identified and characterised. The identified markers are often used in combination as for

most tumour types and no single marker can select for a 100% pure stem cell population.

Improvements to the NOD/SCID murine model by engineering mice to be deficient in natural killer and macrophage activity has increased the reliability of these assays. These improvements have also raised questions about the frequency of CSCs observed in tumours. The number of CSCs estimated in cancer tissue may be affected by the xeno-transplantation model used and the extent to which the host immune system is suppressed may account for some of the variation between studies (Brehm et al., 2010). A study into the frequency of cancer stem cells in melanoma has suggested that the number of stem cells within a tumour can be much higher than previously thought. Using NOD/SCID interleukin-2 receptor gamma chain null (Il2rg2/2) mice, 25% of unsorted primary and metastatic melanoma cells were tumourigenic. Enrichment using markers had no effect on the tumourigenicity of the cells (Quintana et al., 2008).

1.5 Prostate Cancer Stem Cells

Like other cancers, there is evidence for CSCs in the progression of prostate cancer, much of which comes from clonogenic assays. Small percentages of cells can establish serially passagable clones or spheres, which are enriched in putative stem cell markers (Tang et al., 2007, Li et al., 2008). However, the majority of these studies involve cancer cell lines rather than primary tumour samples. A combination of markers from primary human cancers which can reconstitute the tumour in immune-compromised mice has not yet been identified.

1.5.1 Cellular Origin of Prostate Cancer

The cell of origin of prostate cancer is still unknown, although recent studies suggest that it may originate in the basal epithelial compartment (Goldstein et al., 2010). The majority of cells in prostate cancer have a luminal phenotype, expressing K8, K18, AR and PSA, which has to suggestions that prostate cancer may arise by the malignant transformation of a luminal cell (Okada et al., 1992). Emerging evidence suggests, however, that this theory may be incorrect and that the 'cell of origin' lies within the basal epithelial cell layer of the prostate which is more susceptible to malignant transformation (Goldstein et al., 2010). This theory is supported by the fact that most prostate cancers contain a minor fraction of basal-like cells which express markers such as CD44, p63, ABGG2 and CD133. Surprisingly, one study has shown that the CD133 negative population (the non-stem cell population) of BPH-1(SV-40 transformed normal prostate epithelial) is more susceptible to malignant transformation than CD133 positive cells (Taylor et al., 2012).

1.5.2 Prostate Cancer Stem Cell Identification

Like other cancers, putative populations of prostate CSCs have been sorted and enriched for based on their cell surface marker expression. In both primary human prostate cancers and cell lines, $CD44^{+}/\alpha2\beta1^{hi}/CD133^{+}$ populations isolated by FACS demonstrate increased CFE and SFE (Collins et al., 2005, Gu et al., 2007, Patrawala et al., 2007). Increased serial tumourigenicity is also observed in CD44+ PC-3 cells and CD44+CD24- LNCaP prostate cells, where as few as 100 cells form tumours in mice (Patrawala et al., 2006). These CD44+ CSCs express embryonic stem cell genes such as Oct4, Bmi-1, β-catenin and Smo which are more invasive suggesting a role in metastases (Klarmann et al., 2009). TRA-1-60, CD151 and CD166 triple positive cells from the prostate xenograft model CWR22 have enhanced tumourigenicity and also demonstrate enhanced nuclear factor-κB activity (Rajasekhar et al., 2011).

1.6 Clonogenicity

1.6.1 The Clonogenic Assay

In 1956 Puck and Marcus published a paper describing a cell culture technique for assessment of colony forming ability of single mammalian cells (Puck, Marcus et al. 1956). Plated in culture dishes with a suitable medium, human cervical carcinoma cells (HeLa) were supplemented with a large number of irradiated feeder cells and the number of colonies formed was counted. This technique is a simple rapid method for growing single mammalian cells into macroscopic colonies with a colony forming efficiency of 80-100%. The assay was developed further to enable quantification of the effects of x-rays on cell populations *in vitro*, to produce the first *in vitro* radiation cell survival curves (Puck and Marcus 1955; Cieciura, Marcus et al. 1956; Puck, Marcus et al. 1956).

The colony forming assay demonstrates heterogeneity *in vitro*. A clone is defined as a group of cells derived from a single ancestor cell and clonogenicity is the ability of a given cell population, when plated as single cells, to produce one or more clones. The clonogenic potential of a cell population can be measured by clonogenic assay, which quantifies the proportion of colony forming cells, as a percentage of the plated cell number, referred to as colony forming efficiency (CFE). It is believed that colony-forming cells are able to both self-renew and differentiate (Bruce and McCulloch, 1964). Therefore, the ability to measure the capacity of cells to form clones is a useful tool and much of the evidence for the hierarchy model of tumour heterogeneity derives from clonogenic assays.

Several adaptations to the original method have been made. Immobilising cells in a top layer of 0.3% agar avoids formation of tumour cell aggregates by random movement, which can be confused with colony growth (Bizzari and Mackillop 1985). Agar can be replaced by agarose, which is easier to handle or methylcellulose which allows better recovery of the colony for replating (Bizzari and Mackillop 1985). Other groups have simplified the culture medium and omitted feeder cells, although this is dependent on cell type (Franken et al., 2006).

The clonogenic assay has been used for a wide variety of studies, with many cell types, using a range of culture conditions, and for the testing of many potential chemotherapeutic agents. It has played a crucial role in the identification and characterisation of CSCs. Secondary cloning has allowed study of self-renewal and longer term proliferation of CSCs and has the advantage of being able to identify cells that undergo a large number of cell divisions, a fundamental property of SCs (Bizzari and Mackillop 1985). This technique involves selecting specific colonies to determine their proliferative potential over a number of passages.

The role of CSCs in multiple myeloma has been studied using an anchorage independent growth clonogenic assay (Hamburger and Salmon, 1977), Anchorage independence growth is thought to be a characteristic of stem cells (Mori et al., 2009). Bone marrow samples from patients with multiple myeloma and normal volunteers cultured in the presence of an agar feeder layer prepared by either human type O+ washed erythrocytes or adherent spleen cells of BALB/c mice, have a linear relationship between colony formation and the number of nucleated bone marrow cells. Multiple myeloma

patient samples have a higher CFE compared to normal volunteers and, crucially, the number of colonies is proportional to the number of cells seeded, suggesting a single cell origin (Hamburger and Salmon, 1977).

The study of stem cell capacity using clonogenic assays demonstrated the presence of a cellular hierarchy in many human cancers, lending support to the stem cell model of tumour growth (Mackillop et al., 1983). A few cells in each tumour are able to give rise to colonies in culture. Some colonies contain transit amplifying cells capable of undergoing a limited number of further divisions (Dick, 2008). Studies of serial CFE and colony size of human tumours has demonstrated the proliferative heterogeneity of a wide range of tumour types including neoplastic human urothelium (Mackillop et al., 1985), melanoma (Asano and Riglar, 1981, Meyskens et al., 1985) and squamous carcinoma (Grenman et al., 1989).

1.6.2 The Human Tumour Stem Cell Assay (HTSCA)

The success of Hamburger and Salmon in showing a relationship between multiple myeloma and colony forming efficiency led to the human tumour stem cell assay (HTSCA) as an *in vitro* method to test sensitivity of individual tumours to anticancer drugs (Friedman and Glaubiger, 1982, Panasci et al., 1985). Semi-solid agar enriched with medium supports colony growth from cell suspensions from a variety of malignant human tumours (Hamburger and Salmon, 1977). The aim of the HTSCA was to tailor chemotherapeutic regimes to the individual patient and test the effectiveness of new cytotoxic agents (Kirkels et al., 1983) including sensitivity of both leukaemias (Santini et al., 1989) and solid tumours (Von Hoff et al., 1983, Kuczek and Axelrod, 1987).

Although the development of the HTSCA looked promising the results were controversial and it was invalidated (Daniels et al., 1997). Part of the failure is attributed to the relatively small proportion of patient tumour samples that produce sufficient colonies for in vitro testing. Also, only a small proportion of tumours exhibited detectable *in vitro* sensitivity (Selby et al., 1983).

The response of clonogenic cells to drugs *in vitro* should correlate with the response of the tumour to the same drug in the patient (Dick, 2008). The stem cell model of human cancer suggests that cure or duration of remission after clinical treatment should correlate with killing of CSCs. Assessment of treatment effects on an unselected cell population (e.g. on the basis of morphological criteria) could be misleading since the effects on a small population of stem cells will be masked by those on the large population of stem cells (Selby et al., 1983).

Some studies directly compared the response in vitro with the subsequent clinical response and showed poor correlation. There have been a wide range of predictive value positives reported for the human clonogenic tumour cell assay when applied to a patient population with an expected clinical response rate of 15-49% (Hug et al., 1984). This value could be misleading and in practice may only be workable for cytotoxicity testing for only one third of specimens tested.

Other problems with the use and interpretation of human tumour clonogenic assays include technical issue such as difficulty in preparing single cell suspensions, production of only small quantities of data, and problems defining drug sensitivity and response criteria (Selby et al., 1983, Hug et al.,

1984). These problems lead to the failure of the HTSCA to become a routine tool for analysis and treatment of cancers.

1.6.3 Non-adherent Colonies

Culture of single cells in non-adherent conditions is a clonogenic assay which is used to measure the number of self-renewing cells, by the formation of spheres. Prior to the early 1990s, it was believed that the brain was incapable of regeneration due to an absence of SCs. However, the propagation of neurospheres in a non-adherent system has demonstrated the brain does contain SCs capable of self-renewal and differentiation (Reynolds and Weiss, 1992). In a non-adherent culture system containing growth factors which select for primitive cells, more committed progenitors and mature cells die, positively selecting for proliferating neural stem cells (Galli et al., 2003).

In the sphere forming assay, either freshly digested or previously adherent cells are dissociated and cultured as single cells in non-adherent conditions, either on low attachment tissue culture plates or in a basement membrane matrix suspension (Pastrana et al., 2011). The resultant spheres are dissociated and re-plated under identical growth conditions. Differentiated cells within the original sphere die rapidly, while the neural SCs continue to proliferate exponentially to give rise to secondary spheres. This technique has led to the generation of stable neural SC lines (Galli et al., 2003). The selection of self-renewing cells in non-adherent culture is also possible in mammary cells, which have been shown to form floating structures known as mammospheres, (Dontu et al., 2003a, Dontu et al., 2003b, Dontu and Wicha, 2005) and prostate (prostapheres) (Garraway et al., 2010) which are

similarly enriched in stem cells. Putative SC markers have been observed and identified in these systems, although formation of spheres alone is not enough to define a SC (Pastrana et al., 2011).

1.6.4 Barrandon and Green: Holoclones, Meroclones and Paraclones

In a seminal paper, Barrandon and Green (1987b) showed that freshly isolated clonogenic human epidermal cells form colonies with distinct morphologies, which are linked to their proliferative potential. Inoculation of single keratinocyte cells into dishes and transfer of the subsequent colonies into indicator dishes for further growth demonstrated that the founding cells were heterogeneous in their capacity for sustained growth. This provided the first evidence of a relationship between stem cells and colony morphology.

The founding single cells were classified as holoclones, meroclones and paraclones, based on the frequency of terminal colonies produced when the clone was transferred to indicator dishes, shown in Table 3. When 100% of colonies were terminal the cell was classified as paraclone; when more than 5% but less than 100% of the colonies were terminal, the clone was classified as meroclone; when 0-5% of colonies were terminal the clone was classified as a holoclone. A link between proliferative capacity and colony morphology was also observed with holoclones tending to form large colonies with a smooth outline and consisting of small cells (Figure 6). Meroclones tended to form smaller colonies with a wrinkled outline and heterogeneity of cell size and morphology within the colony. Paraclones tended to form small colonies with irregular edges and terminally differentiated cells, which were generally incapable of further division.

Table 3. Barrandon and Green Colonies.

Typically formed by	Colony Morphology	Colony Area	Cell Size	Proliferative Capacity
Holoclone	Large nearly circular with smooth perimeter.	10-30mm^2	Small	<5% cells terminal
Meroclone	Wrinkled colony that is in between holoclone and paraclones in size.	5-10mm^2	Mixture	5-95% cells terminal
Paraclone	Small, highly irregular perimeter	<5mm^2	Large and flattened	>95% terminal

Colony morphology and proliferative heterogeneity of keratinocyte clones *in vitro.* (Barrandon and Green, 1987b)

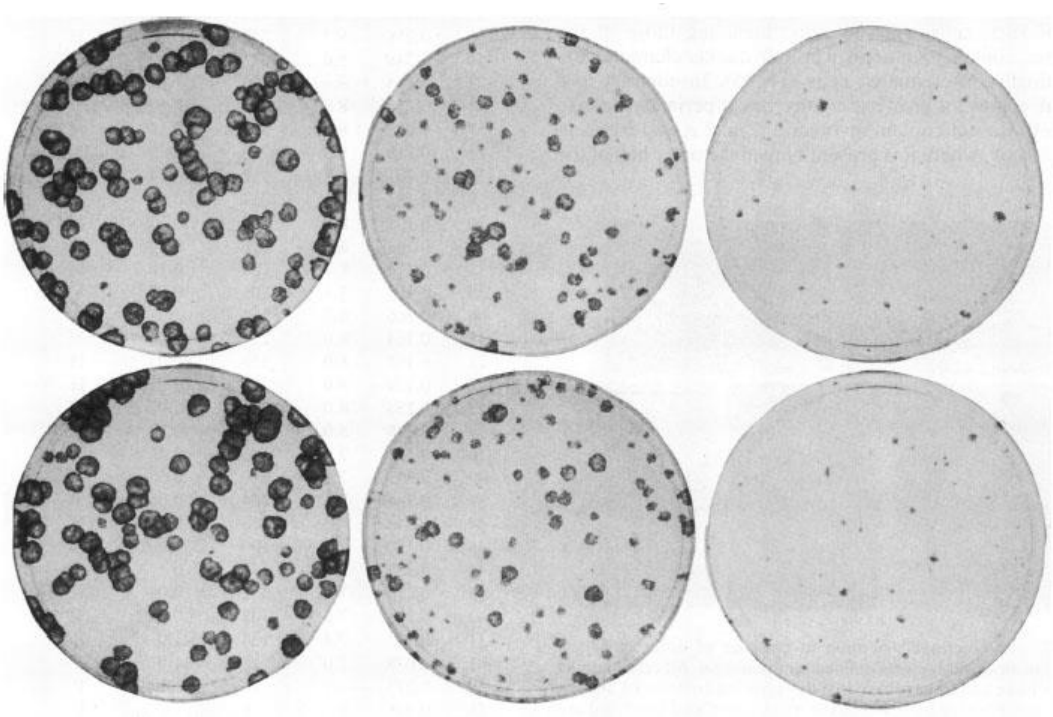

Figure 6. Barrandon and Green Colonies.

Morphologies of colonies derived from holoclone (left), meroclone (middle) and paraclone (right) keratinocyte cells (Barrandon and Green, 1987b).

The terms holoclone, meroclone and paraclone are now synonymous with stem cells, early and late transit amplifying cells respectively (Barrandon and Green, 1987b, Barrandon and Green, 1987a, Rochat et al., 1994). Further analysis in murine keratinocytes has shown that only holoclones can form secondary holoclones and be serially passaged long term (Tudor et al., 2004, Tudor et al., 2007). This has led to the holoclone forming assay being adopted as a surrogate assay to identify adult SCs, particularly in the skin (Mavilio et al., 2006, Murayama et al., 2007, Szabo et al., 2013) , follicular (Rochat et al., 1994) and limbal (Pellegrini et al., 2001, Shortt et al., 2007) tissues. Holoclones also demonstrate expression of survival genes such as p63 (Pellegrini et al., 2001), activation of β-catenin and Akt pathways (Murayama et al., 2007) and increased expression of self-renewal genes such as Bmi1 (Claudinot et al., 2005).

1.6.5 Cancer Colony Morphology

Cell lines derived from cancer are a useful tool for studying CSCs. The three colony types including holoclone have been observed in cancer cell lines including head and neck, breast (Locke et al., 2005), prostate (Locke et al., 2005, Wei et al., 2007, Li et al., 2008, Pfeiffer and Schalken, 2010) and pancreas (Li et al., 2007, Wang et al., 2013). These cell lines are heterogeneous in terms of CFE, secondary plating efficiency, tumourigenicity and marker expression. There is further evidence to indicate the presence of stem cells, including dye-exclusion (Hirschmann-Jax et al., 2004, Setoguchi et al., 2004, Locke et al., 2005, Patrawala et al., 2006), and sphere formation in non-adherent culture conditions (Reynolds, 1992). A fraction of cells within

the cell lines also demonstrate increased serial tumourigenicity and chemo-resistance (Reynolds and Putnam, 1992).

Prostate cancer cell lines form colonies with three different morphologies when cultured at clonal density (Locke et al., 2005, Wei et al., 2007, Li et al., 2008, Pfeiffer and Schalken, 2010, Zhang and Waxman, 2010, Beaver, 2012). Their morphologies are similar to the Barrandon and Green definitions of holoclone, meroclone and paraclone. This suggests the presence of a cellular hierarchy similar to normal epithelial cell populations containing stem cells, transit amplifying cells and differentiating cells (Locke et al., 2005).

Previous studies have shown that holoclones can be passaged long term, (Pfeiffer and Schalken, 2010) are serially transplantable in immune-compromised mice, and show increased expression of stem cell markers such as CD44, α2β1 integrin and β-catenin in PC-3 (Li et al., 2008) and DU145 clones (Locke et al., 2005) and aldehyde dehydrogenase 1 (ALDH1) activity (Doherty et al., 2011). In contrast meroclones and paraclones can only be passaged for a limited period and are non-tumourigenic. Cells sorted based on $CD44^{+}$, integrin $\alpha2\beta1^{+}$, $CD133^{+}$ expression have a higher CFE and form more holoclones than $CD44^{+}$ integrin $\alpha2\beta1^{low}$ $CD133^{low}$ sorted DU145 cells. (Wei et al., 2007). However, the meroclone fraction has been studied in depth only in PC-3 cells, whilst other studies on other cell lines have concentrated on the differences between holoclones and paraclones and ignored meroclones.

The holoclone forming assay has been extensively utilised in cancer stem cell research, particularly within prostate cancer, as a surrogate stem cell assay. As well as confirming SC enrichment by cell surface expression

(Patrawala et al., 2006, Gao et al., 2009, Marian et al., 2010), dye exclusion (Marian et al., 2010) and reduced PSA expression (Qin et al., 2012) the holoclone assay has given insight into how CSCs are controlled and how this may affect metastasis and disease progression. In conjunction with tumourigenicity, an increase in the number of holoclones formed by overexpression of Nanog has demonstrated a functional role for the stem cell gene Nanog in prostate cancer, which supports stem cell model (Jeter et al., 2009, Jeter et al., 2011). The holoclones assay has also demonstrates role for miR-34a in the control of prostate cancer stem cells and metastases (Liu et al., 2011). Despite their frequent use, only the PC-3 cell line colonies have been rigorously characterised.

1.7 Drug Discovery by Phage Display

Phage display is a technology that can identify a wide range of biological targets, varying from small molecules to organ specific ligands. Developed by George Smith in 1985, phage display is essentially an affinity selection of random peptides displayed on the surface of a bacteriophage that binds strongly to the target (Smith, 1985).

Bacteriophages are viruses that infect bacterial cells, and a key property is that they can incorporate DNA and translate the sequence to be expressed as peptides on their surface (Smith and Petrenko, 1997). This ability is utilised in the phage display technique, where phage are manipulated to display a potentially infinite range of random peptides. The technique then relies on the ability to rapidly identify ligands with the desired target property from a large population of phage clones (called a library library) displaying diverse surface peptides (Vodnik et al., 2011). Phage display systems that display antibody fragments have also been developed (Clackson et al., 1991) which display either scFv or Fab fragments (Carmen and Jermutus, 2002). Both peptide and antibody phage display libraries have been used in *in vivo* selection and panning experiments, primarily in mice (Rajotte et al., 1998, Li et al., 2006, Newton et al., 2006, Du et al., 2010). The phage library is injected and the phage homes to and binds to organs. Following sacrifice harvested tissues can then analysed to recover clones binding to them.

1.7.1 Bacteriophages

Bacteriophages have a simple structure which consists of a protein capsid enclosing genetic material. A wide range of bacteriophages with differing protein coats and modes of infectivity exist, although most published phage

display work uses filamentous phage strains M13, fd, or f1 as the vector. Filamentous phage are shaped like flexible rods approximately 1 µm long and 6 nm in diameter composed mainly of a tube of helically arranged molecules of the 50-residue major coat protein pVIII, shown in

Figure 7. Inside the tube is single stranded viral DNA (ssDNA) consisting of 6407 bases coding for 11 genes, five of which are coat proteins. At one tip of the protein tube are five copies of each of the minor coat proteins pIII and pVI and at the other tip are minor coat proteins pVII and pIX. 2700 copies of the major coat protein pVIII encapsulate the phage encoded by gene 8 (Griffiths et al., 1994).

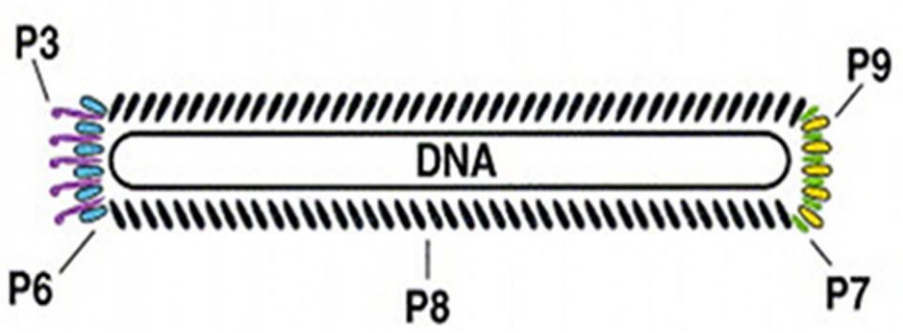

Figure 7. Filamentous Bacteriophage.
Structure of a filamentous bacteriophage showing the protein coats and their locations. pVIII coats the entire phage with pIX and pVII at one end and pIII and pVI at the other. pIII (or P3) coat protein is present in 5 copies and is frequently the site used to display the peptide library (Sidhu, 2001).

1.7.2 Bacteriophage Infection of an E.coli Host

Bacteriophages used in phage display can only infect an E.coli cell that displays the thread like appendage F pilus. They are non-lytic, meaning that they leave the host cell intact. The pIII protein has two N-terminal domains

(N1 and N2) and a C-terminal domain connected by glycine-rich linkers G1 and G2 (Figure 8). Infection is initiated when the N-terminal domain of pIII attaches to the tip of the host pilus and the particle enters the cell by dissolving coat proteins on the surface of the cell envelope and the uncoated ssDNA enters the cytoplasm. A complementary DNA strand is synthesised by the host, resulting in the double stranded replicative form (RF). The RF replicates to make progeny RFs and acts as the template for transcription of phage genes and synthesis of progeny ssDNAs. The new progeny ssDNAs are extruded through the cell envelope, acquiring new coat proteins from the membrane, emerging as complete virons which are excreted continuously from the host cell without killing it (Smith and Petrenko, 1997).

Figure 8. Phage coat protein pIII.
The modular structure of phage coat protein pIII which is essential for phage activity has two N-terminal domains (N1 and N2) and a C-terminal domain connected with glycine rich linkers (G1 and G2). It can be modified to display a peptide library between N2 and CT or at the N terminus (Carmen and Jermutus, 2002).

1.7.3 Peptide phage display

For phage display, foreign peptides have been fused to the coat proteins pIII, pVIII and pVI, although the most commonly used is pIII. The foreign random

DNA sequence is inserted between the amino-terminal half and the carboxyl-terminal half of pIII, which minimally disrupts its function, particularly its infectivity (Smith, 1985). A phage display library contains phage clones carrying a wide range of different, random gene inserts and when the phage replicates its foreign peptides are also replicated, producing identical progeny when infecting a new bacterial host (Smith and Petrenko, 1997).

A peptide display library contains a large number of clones, typically 10^9-10^{10} , although there can be up to 10^{12}, and each clone expresses multiple copies of the unique peptide sequence on its surface (Lunder et al., 2005). The library is used for affinity selection assays, where the peptide library vectors are incubated with an immobilised target, a process called panning. Phages that do not bind to the target are washed away, whilst bound phage are eluted and then amplified in the E.coli host.

Amplified phage are again incubated with the immobilised target and panning is repeated 3-4 times. Too many rounds of panning can result in phage with replicative advantage being selected for. The final round eluate should contain phage which are enriched for peptides which bind to the target.

Various targets can be panned for *in vitro*, from simple proteins to whole live cells, either in solution or adherent. Clones displaying peptides with high affinity for the target bind strongly whilst others are washed away. Selected clones are isolated and DNA coding the displayed peptide can be sequenced. Usually, peptide-encoding DNA libraries are based on partially randomised oligonucleotides (Lindner et al., 2012). Commercially available phage display libraries include Filamentous phage M13 Ph.D-7, Ph.D-12 and

Ph.D-C7C (New England Biolabs) and Spherical T7 phage called T7 Select (Merck).

1.7.4 Targeting Tumours by Phage Display

Phage display has been used for a wide range of targets. Although initially phage display was used for relatively simple targets, the system is also utilised for both in vitro whole cell phage display and in vivo panning. Peptide phage display has generally yielded peptide sequences which bind to previously known cellular targets. Studies have screened peptide phage libraries against proteins of interest in cancers such as PSA (Ferrieu-Weisbuch et al., 2006, Shanmugam et al., 2011) , prostate-specific membrane antigen (PSMA) (Lupold and Rodriguez, 2004), ErbB-2 (Karasseva et al., 2002) and isolated putative cancer stem cell protein markers such as CD44 (Park et al., 2011). Of particular interest commercially have been peptides targeting growth factor activity, such as the motif CVRAC which binds to epidermal growth factor receptor (EGFR) (Cardo-Vila et al., 2010) and peptides which inhibit Vascular endothelial growth factor (VEGF) mediated angiogenesis *in vitro* (Yayon et al., 1993).

Peptides have been screened against whole tumour cells, cancer cell lines and putative stem cell populations. In this way peptides influencing cell attachment and invasion (Romanov et al., 2001, Fukuchi et al., 2010) and targeting specific receptors such as urokinase receptor have been identified (Goodson et al., 1994, Fong et al., 2002).

Using cancer cells *in vitro* for selection has yielded some interesting potential targets for cancer such as peptide VHLGYAT (Zhang et al., 2007), and HEWSYLAPYPWF (Rasmussen et al., 2002) for colon and breast carcinoma

and CPLDIDFYC, believed to be a α4β1 integrin receptor for AML (Jager et al., 2007). Potential ligands have been identified panning against prostate cells using either several cancer cell lines and normal prostate epithelial cells as a negative selection step. Panning against PC-3 cells has yielded DTDSHVNL, DTPYDLTG and DVVYALSDD as potential ligands, and these have proved to be useful for in vivo imaging applications (Jayanna et al., 2010). Screening of the National Cancer Institute panel of human cancer cell lines (NCI-60) identified tri-peptide motifs which were recurrently selected across the panel, although much heterogeneity was observed (Kolonin et al., 2006). This study identified motifs that were similar to domains of human tumour ligands. Antibody phage display has identified antibody fragments which bind to prostate cancer cells but not normal prostate epithelium (Popkov et al., 2004) and single chain antibodies (scFv) which target a putative breast cancer stem cell population (Jakobsen et al., 2007, Gur et al., 2009) but not normal breast tissue.

Phage display has been used to target normal cells such as keratinocytes (Jensen et al., 2003), rat pancreatic islet-cells (Ueberberg and Schneider, 2010) and the luminal surface of polarised endothelium of human umbilical veins (Maruta et al., 2003). Some of these phage ligands have been shown to resemble binding proteins of bacterial and viral pathogens (Writer et al., 2004).

1.8 Experimental Aims

Clonogenic assays are widely used as a surrogate assay to identify highly proliferative cells in normal and neoplastic tissue. Prostate cancer cells are known to form three types of colony similar to the Barrandon and Green holoclones, meroclone and paraclones. The use of holoclones formation as a surrogate stem cell assay has become popular in the study of prostate cancer stem cells. However, the heterogeneity and characteristics of these colonies has not been fully studied and previously meroclones have been ignored.

The aim of this study was to elucidate relationship between clonogenicity, colony morphology and stem cells in normal and cancer cell populations. To do this the stem cell traits (proliferative capacity, self-renewal and differentiation) of each type of colony were compared. Full characterisation of the clonogenic cells will validate of this assay for the identification stem cells. Once validated, the clonogenic assay was used to identify potential therapeutic targets against cell surface molecules.

1.8.1 Hypothesis

The clonogenic assay can be used as a surrogate assay for stem cell identification. The number of stem cells in the cell population is directly proportional to the number of holoclones formed in both normal and cancerous cells. The formation of proliferative colonies can be used to identify peptides which target highly proliferative stem cells, by peptide phage display.

1.8.2 Objectives

The following objectives test the hypothesis:

- Identify the types of colonies formed by single cells from prostate cancer derived cell lines and primary prostate epithelial cells from patients undergoing TURP for BPH.
- Test the stability of the number of stem cell colonies under different conditions. Is the number of stem cell colonies inherent to the cell line or can it be significantly altered?
- Characterise colonies in terms of proliferative capacity, tumourigenicity and marker expression. Are all colonies equal? Is there a difference between colonies formed by cell lines and primary cells?
- Identify potential therapeutic targets by peptide phage display.

2 Materials and Methods

2.1 Prostate Cancer Cell Lines

The cell lines used in this study were derived from metastatic prostate cancers from men with castrate-resistant disease. DU145 was derived from a brain metastasis (Stone et al., 1978). PC-3 cells were derived from advanced androgen independent bone metastasis of prostate cancer (Kaighn et al., 1979). LNCaP cells were derived from a supraclavicular lymph node metastasis (Horoszewicz et al., 1983). All cell lines were obtained from their originators (Stone et al., 1978, Kaighn et al., 1979, Horoszewicz et al., 1983) and their identification confirmed by STR profiling.

The cells were maintained in 25cm^2 tissue culture flasks (Nunc) in RMPI-1640 (Invitrogen, UK) supplemented with 10% foetal bovine serum (FBS) (PAA, UK #A10409-1608) and 2 mM L-Glutamine (Invitrogen). A medium change was performed every 3-4 days or with sub-culturing when confluent. Cells were passaged by removing medium by aspiration. The remaining FBS, which inhibits trypsinisation, was removed by washing with Phosphate Buffered Saline (PBS) (Invitrogen). 1ml of 0.25% trypsin (Invitrogen) was added to each culture flask, the cells coated and incubated for approximately 5 minutes at 37°C in 5% CO_2 until cells rounded up and detached from the bottom of the flask. Standard culture medium containing serum was added to stop the trypsinisation process and cells diluted 1:10 and introduced into fresh culture flasks. Cells were used for a maximum of 10 passages before retrieving further cells from the liquid nitrogen cell bank.

2.2 Primary Human Prostate Epithelial Cells

2.2.1 Tissue Collection

Tissue was obtained from Guy's Hospital with ethical approval and in accordance with the Human Tissue Act 2006 regulations. Samples were collected from patients between the ages of 59-81 years undergoing treatment for benign prostatic hyperplasia. All patients underwent TURP or Holmium Laser Enucleation of the Prostate (HoLEP) which removed between 10 – 100 g tissue. A maximum of 10% of the tissue was placed in in 25ml of transport medium made up of Lebovitz L15 medium supplemented with 5% FBS, 1 % Penicillin/Streptomycin and 1% Ampicillin (all Invitrogen) and transported from theatre on ice to the laboratory within 1 h. Lebovitz medium is buffered with air, so a stable pH is maintained during transportation.

2.2.2 Tissue Digestion

Protocols for tissue digestion and clonogenic assays followed previously published protocols (Hudson et al., 2000, Hudson, 2004). The tissue was transferred to a sterile 10cm Petri dish and washed with fresh transport medium. Clumps of blood and charred tissue were removed with a sterile scalpel and forceps and the tissue minced finely using sterile, curved scissors. Tissue pieces were transferred to a 50ml centrifuge tube (BD Biosciences) and washed by the addition of 20ml PBS. Tissue pieces were allowed to sink to the bottom of the tube and the PBS was carefully removed by aspiration. The wash step was repeated until the sample was clear of blood. It was then digested in transport medium containing 200U/ml Collagenase IV (Worthington, New Jersey, USA) for 18-20 h at 37°C with gentle shaking. After digestion any remaining pieces were broken up by

gently pipetting up and down with a 5ml pipette. The cell suspension was centrifuged at 170 x g for 5 min to pellet the cells and the supernatant removed. 20 ml of PBS was added and centrifugation step was repeated.

2.2.3 Single Cell Suspension

To produce a single cell suspension, the cell pellet was resuspended in 2 ml of 0.25% trypsin and incubated for 2 minutes at 37°C with gentle shaking. Trypsinisation was stopped by the addition of 2 ml of 1mg/ml soybean trypsin inhibitor (Sigma-Aldrich) in PBS. To remove large cell aggregates and produce a single cell suspension, the cell suspension was made up to 10ml with PBS and passed through a 100 µm cell sieve (BD-Biosciences, UK). The cells were washed twice with PBS, centrifuged, as previously described, and re-suspended in 2 ml Prostate Epithelial Basal Medium (PrEBM) (Lonza, UK) supplemented with prostate epithelial growth medium (PrEGM) bullet kit (Lonza) and 1% Penicillin/Streptomycin and 1% Ampicillin.

2.3 Clonogenic Assays

2.3.1 Cell Lines

The cell line clonogenic assay was adapted from previously published methods (Franken et al., 2006). Growth medium was aspirated from a cell monolayer at approximately 70% confluence and the cells were washed with PBS. 1 ml of 0.25% trypsin was added to the flask and incubated at 37°C for 5 minutes until the cells became rounded and detached from the culture flask. Nine ml of growth medium was added to stop the trypsinisation process. The cell suspension was gently pipetted up and down several times to break up clumps and produce a single cell suspension. 50µl of cell suspension was diluted 1:1 (v/v) with trypan blue (Sigma-Aldrich, UK) and

about 10µl was added to each side of a Neubauer haemocytometer chamber.

The number of viable cells was counted in 8 separate squares of the haemocytometer. Viable cells are phase bright and dark cells which took up trypan blue as a result of a permeable cell membrane were deemed to be non-viable. On the basis that each of the large squares is equivalent is 0.1µl, the number of cells per ml can calculated from the number of cells per grid x 10^4 ml. The average number of live cells per grid was determined and was multiplied by the dilution factor by 10^4 to give the viable cell count per ml. Cell suspensions which contained fewer than 95% single, viable cells were rejected.

Cells were seeded into 60mm petri-dishes at a density of 200 (DU145 and PC-3) or 500 (LNCaP) cells per dish in 5ml growth medium in triplicate. The dishes were gently shaken side to side and front to back to evenly distribute the cells and incubated for either two weeks (DU145 and PC-3) or three weeks (LNCaP) at 37°C in 5% CO_2. The medium was changed every 7 days.

2.3.2 Primary Prostate Epithelial Cells

Cells isolated from TURP or HoLEP tissue (described in section 2.2.3) were counted using trypan blue exclusion and the number of single cells determined. Only samples containing >90% single cells were used for clonogenic assays. 1000 or 10,000 single cells were seeded into collagen coated petri dishes supported by a feeder layer of Swiss 3T3 fibroblasts with 5ml PrEGM in triplicate. Cells were incubated at 37°C at 5% CO_2 for 12 days. Following 4 days incubation, the cells were removed from the incubator and washed gently by removing PrEGM and adding 5ml PBS. The liquid was

aspirated and fresh PrEGM added gently, so as not to disturb adherent colonies.

2.3.2.1 *Preparation of Collagen Coated Dishes*

Sixty mm diameter petri dishes were coated with 2µg / cm^2 of Type I Collagen from rat tail (Sigma-Aldrich) by diluting 15 µl of the 4 mg / ml stock in 1ml dH_2O and swirling to coat the bottom of the dish. The dishes were incubated at 37 °C for 2 hours and then washed with dH_2O, allowed to dry, sealed with laboratory film and stored at 4°C for up to 1 month.

2.3.2.2 *Preparation of Feeder Layer*

Murine Swiss 3T3 cells (ATCC) were maintained in RPMI-1640 supplemented with 2 mM L-Glutamine and 10 % new born calf serum (NBS) (Sigma-Aldrich). When the cells were approximately 70 % confluent they were treated with 4 µg/ml Mitomycin C in culture medium (Sigma-Aldrich) for 2 hours at 37 °C. The cells were washed with 5ml PBS and harvested by incubation with 3 ml of 0.25 % trypsin for 5 minutes, counted by trypan Blue exclusion and frozen at – 80 °C in 10 % dimethylsulfoxide (DMSO) in complete culture medium. To check mitotic inhibition, 2 x 10^5 treated cells were cultured in a 75 cm^2 flask for 7 days. Only treated cells which did not proliferate within the 7 days were used to provide a supportive feeder layer for primary prostate epithelial growth. 24 hours prior to clonogenic assay, 3T3 cells were defrosted rapidly at 37 °C and seeded into 60 mm petri dishes at a density of 1 x 10^5 cells and incubated overnight at 37 ° C, 5 % CO_2.

2.3.3 Analysis

Following incubation, cells were fixed by the addition of 3 ml of 70% industrial methylated spirit (IMS) in dH_2O for 30 minutes. The IMS was removed and

the cells stained by with 0.1 % Crystal Violet (CV) (Sigma-Aldrich) dissolved in 20 % IMS in dH_20 for 30 min. The CV was removed and the dishes were washed gently with tap water so as not to disturb the colonies, and allowed to air dry for 24 hours.

The colonies which contain >32 cells were scored and counted under a dissection microscope. Colonies were colour coded by pen for easy identification and measurement. The total number of colonies and the number of each colony type were determined and the CFE calculated as a percentage of the number of input cells.

Mean colony size, cell size and number of cells per colony were determined by measuring the colony size and counting the number of cells across the diameter. Twenty colonies of each type were measured using a graticule and calibrated eye piece across the x and y axis.

From these measurements the area (a) of each colony was calculated based on the following equation:

$$a = \pi * x * y$$

The number (n) of cells across the y axis of each colony was counted and the average cell diameter (d) was calculated by diving it by the length of the y axis: $d = \frac{n}{y}$

The colony diameter was then used to estimate the area (A) taken up by each of each cell: $A = \pi * (0.5 * d) * (0.5 * d)$

The number of cells per colony (N) was estimated by calculating the number of cells based on the equation: $N = \frac{a}{A}$

In later experiments, the mean number of cells per mm^2 from twenty colonies of each morphological type was used to estimate the number of cells in colonies, based on colony diameter, by multiplying the estimated colony area by the mean number of cells per mm^2 (c):

$$N = A * c$$

2.4 Effect of Culture Conditions on Clonogenicity

Conditions that affect CFE were assessed by clonogenic assay. Firstly the optimum seeding densities for DU145, PC-3 and LNCaP cell lines were determined. Optimal cell numbers were then cultured with different concentrations of FBS, on different substrates and with different media. The same incubation times and parameters were applied for each condition, changing only the test condition each time. Finally, optimum conditions for each cell line were tested in combination.

2.4.1 Seeding Density

The following numbers of single cells were seeded in triplicate in 60mm petri-dishes containing 5ml growth medium: 1000, 500, 200, 100, 50 and 20. Dishes were gently shaken side to side and front to back to evenly distribute the cells and incubated for either two weeks (DU145 and PC-3) or three weeks (LNCaP) at 37°C 5% CO_2. The medium was changed every 7 days.

2.4.2 FBS Concentration

A clonogenic assay was used to analyse the effect of FBS concentration on the prostate cancer colonies. To acclimatise cells to new conditions, one $25cm^2$ flask of 70% confluent cells was spilt into 5 fresh flasks and cultured

with 50, 20, 10, 5 or 1% FBS in RPMI-1640. Following 7 days incubation, each flask was trypisinsed to produce a single cell suspension and cells counted by trypan Blue exclusion. 200 cells (DU145 and PC-3) or 500 cells (LNCaP) were seeded in triplicate in 60mm petri-dishes containing 5ml of the corresponding FBS containing medium.

2.4.2.1 *Substrate*

The effect of the substrates collagen, fibronectin, laminin, vitronectin and a feeder layer of mitomycin C treated Swiss 3t3 cells was tested by clonogenic assay. All substrates were prepared in 60mm petri-dishes according to manufacturer's instructions and the final concentrations are shown in Table 4. Petri dishes were coated with 2µg / cm^2 Type I Collagen from rat tail (Sigma-Aldrich) by diluting 15 µl of the 4 mg / ml stock in 1ml dH_2O and coating the bottom of the dish with 1ml. The dishes were incubated at 37 °C for 2 hours and then washed with dH_2O, allowed to dry, sealed and stored at 4°C for up to 1 month. A 0.5 µg / ml fibronectin solution was made by diluting stock fibronectin (Invitrogen) in growth medium and 3ml was added per dish and incubated for 1 hour at 37 °C in 5 % CO_2 prior to seeding cells. At seeding a further 2 ml of growth medium was also added. A working solution of 0.5 µg/ml of Laminin (Sigma-Aldrich) was prepared by diluting 50 µg in PBS. 3 ml of the working solution was added to each dish and incubated at 37 °C for 2 hours and washed with PBS, sealed and stored at 4 °C for up to 1 month. A working solution of vitronectin (Sigma-Aldrich) was prepared at a concentration of 0.5 µg / ml in dH_2O and 3 ml added to each 60 mm petri dish, incubated at 37 °C for 2 hours and washed with PBS. Vitronectin dishes were prepared fresh for each assay. A feeder layer of $1x10^4$ mitomycin C treated 3t3 cells per cm was prepared as in 2.3.2.2. Into each of the prepared

dishes, 200 (DU145 and PC-3) or 500 single cells (LNCaP) were seeded as described above. Again, the cells were incubated for 14 or 21 days and the medium changed every 7 days.

Table 4. Substrates Tested By Clonogenic Assay

Substrate	Concentration	Supplier
Tissue Culture Plastic	N/A	Nunc (UK)
Type I rat tail Collagen	2µg/cm^2	Sigma-Aldrich (C3867-1VL)
Fibronectin	50ng/cm^2	Invitrogen (#33010-018)
Laminin	50ng/cm^2	Sigma-Aldrich (L4544)
Vitronectin	50ng/cm^2	Sigma-Aldrich (V8379)
3T3 feeder cells	1x10^4 /cm	N/A

2.4.2.2 *Culture Medium*

The commonly used cell culture media shown in Table 5 were tested for their ability to support colony forming cells. Each medium was supplemented with 10% FBS. As with the FBS assay, 7 days prior to the assay, cells were introduced to the test culture medium to allow acclimatisation to new conditions. Again, following 7 days incubation, each flask was trypsinised to produce a single cell suspension and cells counted by trypan blue exclusion. 200 cells (DU145 and PC-3) or 500 cells (LNCaP) were seeded in triplicate in 60mm petri-dishes containing 5ml of each medium.

Table 5. Cell Culture Medium Tested by Clonogenic Assay.

Medium	Manufacturer
RPMI-1640	Gibco #31870
DMEM High Glucose	Gibco #41966
DMEM Low Glucose	Gibco #31885
Ham's F12	Gibco #21765
Hams' F12/ DMEM High Glucose	1:1 mixture of Gibco #21765 and #41966
Advanced MEM	Gibco #12492

2.4.2.3 *Analysis*

After the incubation period, the colonies were fixed and stained with crystal violet as previously described. All colonies were counted and scored based on previously determined parameters. Twenty colonies of each colony type for each condition for each experiment were measured using a graticule and eye piece. Colony size and cell number were determined based on mean cell number of measured colonies (see section 2.3.3). An estimation of the number of cells in LNCaP colonies was not possible due to the three-dimensional nature of the colonies.

2.4.2.4 *Statistical Analysis*

The total number of colonies, the number of each colony type and colony size were analysed by MANOVA followed by Tukey's honestly significant difference (HSD) post hoc pairwise comparison using the statistics package PAWS Statistics 18 (formerly SPSS). This post hoc test was chosen to compare all possible means based on Studentised Range Distribution. Tukey's HSD allows comparison of each pair of conditions to see of their difference is significant. The Tukey test looks at the random variation that exists between the pair of means (the standard error of the differences

between pairs of means). The variation between the pairs of means is then compared to the standard error of the sample. To transform the colony size data to ensure that the data has a normal distribution essential for Tukey's HSD, the log of each measurement was taken. Results with a $p < 0.05$ were deemed significant.

2.5 Secondary Cloning

Under a phase contrast light microscope well isolated colonies were selected, circled with a pen and numbered for identification. Colony diameter was measured using a calibrated eye piece and graticule to estimate cell number based on previous calculations (see section 2.3.3).

Culture medium was removed from the petri-dish by aspiration and cells washed with 5ml of PBS. A sterile glass cloning ring coated with vacuum grease around the bottom edge was placed around each selected colony with sterile forceps and gently twisted to produce a seal. The colony was inspected under a light microscope to ensure the correct placement of the ring and to ensure vacuum grease did not touch the colony. 100µl of 0.25% trypsin was added to each ring and the cells incubated at 37°C in 5% CO_2 for 10 minutes until the cells rounded and detached.

2.5.1 Cell Lines

The contents of each cloning ring were transferred to a sterile universal tube and the ring washed with growth medium to collect any remaining cells. The cell suspension was diluted with growth medium to a concentration of 1000 cells per ml, based on the estimation of the number of cells within each colony. 200 cells were seeded in triplicate into 60mm petri-dishes in 5ml

growth medium and cultured for a further 2 weeks. If the colony consisted of fewer than 200 cells, the entire colony was transferred directly to a fresh petri dish. Following 2 weeks incubation the colonies were analysed as in section 2.3.3 and CFE determined as the percentage of colonies per number of input cells.

2.5.2 Primary Prostate Epithelial Cells

The contents of each cloning ring were transferred to a sterile universal tube and the ring washed with growth medium to collect any remaining cells. Trypsin activity was inhibited by the addition of 100µl of 1mg/ml soybean trypsin inhibitor and the tube centrifuged at 170 xg. The cell suspension was diluted with complete PrEGM to a concentration of 1000 cells per ml, based on the estimation of the number of cells within each colony. 1000 cells were seeded in triplicate into collagen coated 60mm petri-dishes supported by a feeder cells with 5ml PrEGM and cultured for a further 2 weeks. If the colony consisted of fewer than 1000 cells, the entire colony was transferred directly to a fresh petri dish.

2.6 Serial Cloning

DU145 colonies were serially cloned to compare the proliferative capacity of each of the colony types. Three colonies of each type generated by a standard clonogenic assay were ring cloned and seeded at clonal density to generate secondary colonies. Subsequent colonies of each lineage were then ring cloned and the process repeated until either no colonies were formed or until the end of the experiment (Figure 9). At each generation, remaining dishes not sued for further cloning were fixed with 70% IMS and stained with Crystal Violet to analyse CFE and colony morphology.

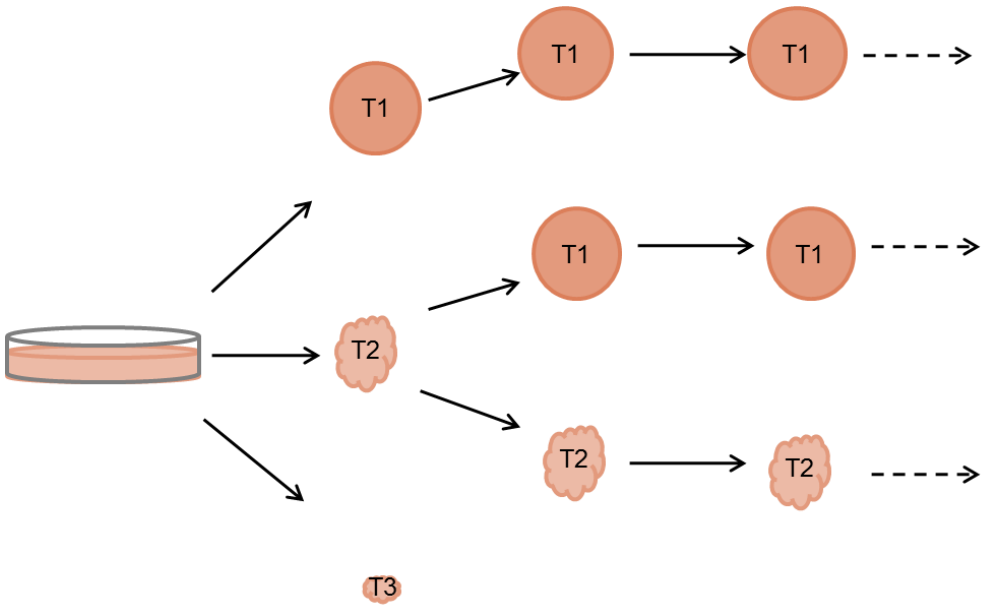

Figure 9. Long term serial cloning of prostate colonies.
Type 1, 2 and 3 colonies were serially cloned until terminal or until the 200 cell divisions were reached. Pure lineages were cloned e.g. secondary type 1 colonies from primary type 1 colonies, secondary type 2 colonies from primary type 2 colonies. As secondary type 1 colonies were observed from a primary type 2 colony this lineage was also serially cloned. Type 3 colonies were terminal upon secondary plating.

2.7 Serial Passage

2.7.1 Cell Lines

The long term growth potential of prostate cancer cells under normal cell line maintenance conditions were compared. Each colony was ring cloned and transferred to a T25cm^2 flasks for long term culture. In three separate experiments, 5 colonies of each type were ring cloned, as previously described, resuspended in 5ml culture medium and transferred to a T25cm^2 flask. The cells were incubated at 37°C in 5% CO_2 until 70-90% confluent. Flasks were monitored 2-3 times per week and once the cells reached confluence they were passaged using standard subculture techniques, as

previously described in (section 2.1), and seeded at a 1:10 dilution. The cells were serially passaged when confluent until they reached 20 passages, at which point they were deemed immortal. Flasks that failed to reach confluence were monitored until the other flasks containing actively dividing cells reached 20 passages, a period of approximately 14 weeks.

2.7.2 Prostate Epithelial Cells

The long term growth potential of primary prostate epithelial cells was compared by serial passage. Each colony was ring cloned and transferred to a T25cm^2 flasks for long term culture. Using 3 patient samples, 5 colonies of each type were ring cloned, as previously described, resuspended in 5ml culture medium and transferred to a collagen coated T25cm^2 flask. The cells were incubated at 37°C in 5% CO_2 until 70-90% confluent. Flasks were monitored daily and, once cells reached confluence, passaged using standard subculture techniques and seeded at a 1:6 dilution. Cells were serially passaged until no further growth was observed. Colonies that failed to reach confluence were monitored until flasks containing actively dividing cells ceased to proliferate.

2.8 Sphere Formation

The sphere forming assay under non-adherent conditions is a measure of self-renewal (Reynolds and Weiss, 1992). Colonies were selected by ring cloning, cultured under non-adherent conditions (Hudson et al., 2000, Rybak et al., 2011) and the resulting number and size of spheres determined.

2.8.1 Cell Lines

Colonies were prepared and ring cloned as previously described. The single cell suspension was diluted to a concentration of $1x10^4$ cells/ ml in sphere forming medium (serum-free DMEM/F12 medium, 20 ng/ml basic FGF, 20 ng/ml EGF 1x B27 (all Invitrogen) and 3 µg/ml insulin (Sigma)). 100µl of cell suspension (1000 cells) was placed into a 1.5 eppendorf tube and made up to 135µl with sphere forming medium. 135µl of Matrigel™ (BD Bioscience, Michigan, USA), which had been kept on ice to prevent setting, was added and pipetted up and down gently to mix. The 1:1 cell suspension:Matrigel mixture was transferred to one well of a 6 well plate and gently pipetted around the edges of the dish. Up to 3 wells were prepared for each colony, depending the number of cells it contained, and the dish was incubated at 37°C until Matrigel had set. When the cell suspension had solidified, 3ml of sphere medium was added to the centre of the well to avoid dislodging the cells. The spheres were incubated for 2 weeks at 37°C in 5% CO_2 with a medium change at 7 days.

2.8.1.1 *Prostate Epithelial Cells*

Primary prostate epithelial colonies from 5 patient samples were prepared and ring cloned as previously described. The single cell suspension was diluted to a concentration of $1x10^4$ cells/ ml in PrEGM. 100µl of cell suspension (1000 cells) was transferred to a 1.5 eppendorf tube and made up to 135µl with sphere forming medium. 135µl of Matrigel™ was added to each one well of a 6 well plate and gently pipetted around the edges of the dish. Up to 3 wells were prepared for each colony, depending the number of cells, and the dish was incubated at 37°C until the Matrigel had set. When the cell suspension had solidified, 3ml of sphere medium was added to the

centre of the well to avoid dislodging the cells. The spheres were incubated for 2 weeks at 37°C in 5% CO_2 with a medium change at 7 days.

2.8.2 Analysis

Following two weeks incubation the spheres were examined under phase contrast microscopy. The number of spheres in each well was counted and each sphere was measured using an eye piece and graticule to determine its diameter. The sphere forming efficiency (% SFE) was determined as the number of spheres formed as a percentage of the number of cells seeded.

2.9 Tumourigenicity

The ‘gold standard’ for confirming a cancer stem cell is the ability to form serially transplantable tumours in immuno-compromised mice (Clarke et al., 2006). In this study, colonies of each morphological type were harvested and pooled. 10,000 or 1,000 cells were injected subcutaneously into the flanks of nude mice and the resultant tumour rate determined. Some of the primary tumours were digested, expanded *in vitro* and re-injected to form secondary tumours. The protocol is shown diagrammatically in Figure 10.

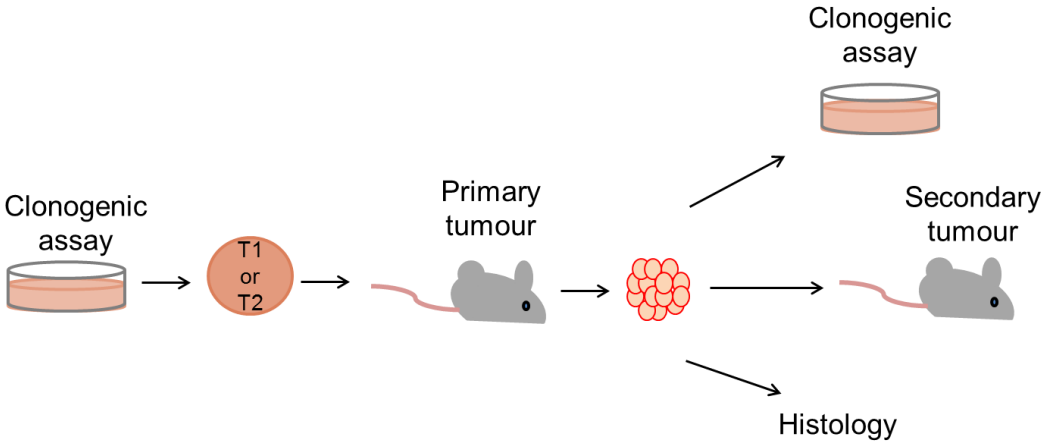

Figure 10. Assessment of Colony Tumourigencity *In Vivo*.

Type 1 and 2 DU145 colonies were ring cloned and injected subcutaneously with Matrigel™ into the flanks of nude mice. After 12 weeks the tumours were removed and analysed. Tumours were and digested and cultured at clonal density to assess Clonogenicity and confirm formation of colony types. Tumours were also fixed, paraffin embedded, sectioned and stained for histology. Some tumour samples were digested and the cells re-injected into secondary mice to assess their ability to form secondary tumours.

2.9.1 Primary Tumourigenicity

DU145 cells were cultured under standard clonogenic conditions for two weeks. Colonies were scored and measured to determine the number of cells per colony (as previously described). Colonies were ring cloned and smaller colonies were pooled to produce enough cells for each injection and resuspended in 10 ml of culture medium. Cells were washed by centrifuging at 120xg for 5 minutes, the supernatant removed and the cell pellet resuspended at a density of $1x10^4$ cells per ml. As a positive control DU145 cells cultured in a monolayer were harvested by trypisinisation, counted and resuspended at a density of $1x10^4$. Either 10,000 or 1,000 cells were transferred to individual 1.5ml microfuge tubes, made up to 1ml with culture medium and centrifuged again at 120xg. The supernatant was removed and the cells resuspended in a mixture of 100µl 1:1 Matrigel™: RPMI-1640 + 10% FBS which had been kept on ice to prevent solidification. The tubes were kept on ice until injection to prevent Matrigel™ solidifying.

Cell suspensions were injected into the flanks of 7 week old (19-20 g) male BALB/cOlaHsd-Foxn1nu Nu/nu (Nude) mice from Harlan, UK, with a 100-U insulin syringe with a 28 Gauge ½ inch Micro-Fine™ IV needle (BD Biosciences). Once injected Matrigel™ rapidly forms a gel at temperatures above 22°C, retaining the cell suspension at the injection site. As a control 100µl culture medium:Matrigel™ alone (vehicle control) was injected into mice. Three separate experiments were performed with 2-6 replicates for each condition, dependent on the number of colonies harvested.

Tumour development was monitored weekly and tumour growth measured using 150mm digital callipers (World Precision Instruments, Hitchin, UK).

Tumour volume was calculated using the formula $0.5(ab^2)$, where a is the longer and b the shorter of the two perpendicular diameters. Mice were killed by cervical dislocation after 12 weeks or earlier if the maximum tumour burden of 5% of body weight was reached. As the average body weight of the nude mouse is 20g this was calculated as 1g, which corresponds to a live volume of around $3500mm^3$.

The mice were dissected, photographed, and the tumour removed using a fine sterile scalpel. Each tumour was weighed and placed in transport buffer consisting of PBS + 1% penicillin/ streptomycin, for transport to the laboratory. Each tumour was cut in to two. One piece was washed in PBS and fixed in 4% paraformaldehyde (PFA) and stored at 4°C. The other piece was either snap frozen in liquid nitrogen and stored at -80°C or digested and cultured (section 2.9.2). Samples fixed in 4% PFA were sent to the cryosectioning facility at the University of Dundee, paraffin embedded, cut into 10µm sections, mounted on microscope slides and stained with Haematoxylin and Eosin (H&E). Tumour sections were photographed analysed.

2.9.2 Clonogenicity of Xenografts

Xenografts were transferred to a 10cm petri dish and washed with transport buffer. The buffer was aspirated and replaced with 2ml PBS and the tissue was finely minced using curved 14.5cm scissors (World Precision Instruments). Tissue was transferred to a 15ml centrifuge tube and 10ml transport buffer added. The cells were centrifuged for 5 minutes at 120xg, the supernatant removed and the cells resuspended in 600U/ml filter-sterilised type 1 collagenase (Sigma-Aldrich) in 10ml RPMI-1640 (5% FBS + 1%

penicillin / streptomycin) and digested for 2 hours at 37°C with continuous shaking on a Luckham R100 orbital shaker on medium setting. The digested cell suspension was centrifuged at 120 *xg* for 5 minutes, the supernatant removed and the cells re-suspended in 5ml of RPMI-1640 supplemented with 10% FBS. Viable cells were counted by trypan blue exclusion and either 200 or 1000 viable cells were seeded into 60mm petri-dishes containing 5ml RPMI-1640 and cultured for 2 weeks in a clonogenic assay. Following 2 weeks incubation the cells were fixed, stained and CFE and colony morphology was determined.

2.9.3 Secondary Tumourigenicity

Cells from digested tumour samples were used to assess the ability of clones to form secondary tumours. Digested cells were seeded into T25cm^2 flasks and expanded for 2 weeks until confluent. Cells were washed, trypsinised, resuspended and counted using trypan blue exclusion. The cell samples for injection in the flanks of nude mice were prepared as described above for the DU145 monolayer at a cell number of 10,000 per injection and monitored over 12 week as previously described for the primary experiment. Tumours were removed and analysed as previously described.

2.10 Immunocytochemistry

The markers expressed by DU145 and prostate epithelial colonies were analysed by immunocytochemistry. Each type of colony was stained with a primary antibody against proliferation marker (Ki67), stem cell (CD44, α2β1, Oct4 and Bmi1) and differentiation (Cytokeratin 5 and 18) markers.

2.10.1 Sample Preparation

2.10.1.1 *DU145 Cells*

DU145 cells grown in a T25cm^2 flask were washed, trypsinised and counted. Ten cells were seeded with 1ml of culture medium in to each well of a 24-well plates and incubated for 2 weeks with a medium change after 7 days. After 2 weeks, the medium was removed and the cells were washed with PBS. The PBS was aspirated and the cells were fixed with 200µl of 4% PFA (Sigma-Aldrich) in PBS for 20 minutes at room temperature. The PFA was removed and PBS added, and the plates were sealed and stored at 4°C for up to 1 month.

2.10.1.2 *Prostate Epithelial Cells*

Primary prostate epithelial cells derived from 3 patients were cultured in a clonogenic assay for 2 weeks supported by a feeder layer. After 2 weeks, the medium was removed and the cells were washed with PBS. The PBS was aspirated and the cells were fixed with 1ml of 4% PFA (Sigma-Aldrich) in PBS for 20 minutes at room temperature. The PFA was removed and PBS added, and the plates were sealed and stored at 4°C for up to 1 month.

2.10.1.3 *Positive Controls*

PC-3 (Ki67, K18, K5) and GCT27 (α2β1, CD44, Oct4 and Bmi1) cells were used as positive controls for immunohistochemistry. Cells grown in a T25cm^2 flask were washed, trypsinised and counted. 1 x 10^4 cells were seeded with 1ml of culture medium in to each well of a 24-well plates and incubated for 2 days. The medium was removed and the cells were washed with PBS. The PBS was aspirated and the cells were fixed with 200µl of 4% PFA (Sigma-Aldrich) in PBS for 20 minutes at room temperature. The PFA was removed and PBS added, and the plates were sealed and stored at 4°C for up to 1 month.

2.10.2 Staining

The PBS was removed and the colonies which were to be stained for intracellular markers (Ki67, K5, K18, Bmi1 and Oct4) were permeabilised by adding 200µl 0.2% Triton X-100 (Sigma-Aldrich) in PBS for 10 minutes at room temperature. The permeabilisation buffer was removed and cells blocked with 10% normal goat serum (NGS) (PAA) in PBS for 30 minutes at room temperature to prevent non-specific binding. Primary antibody dilutions (Table 6) were prepared in 1% NGS in PBS and the blocking buffer was removed and replaced with the primary antibody and incubated overnight at 4°C in a humidity box, to prevent drying. For negative control, antibody diluent containing no antibody was added to the target well. Following an overnight incubation, the primary antibody was removed and the wells were washed 4 times with PBS containing 1% NGS. Secondary antibody dilutions (Table 6) were prepared and added to the target wells for 1 hour at room temperature in the dark to prevent photo bleaching. The antibodies were removed and wells washed 4 times. The final wash buffer was aspirated and

the plates turned upside down on tissue paper to allow any excess liquid to drain. A drop of Vectashield® mounting medium with DAPI (Vector Laboratories Inc, Peterborough, U.K.) was added to each well and the cells were covered with a 13mm coverslip (VWR, Lutterworth, UK) using fine forceps. The plates were stored at 4°C in the dark.

2.10.3 Two Colour Staining

To determine cytokeratin expression of prostate cells, colonies were sequentially stained with antibodies against K5 and K18 antibodies. Colonies were first stained with antibodies against K5 as in section 2.10.2. Following incubation with the first secondary antibody, cells were blocked again with 1% NGS. Blocking buffer was removed and the diluted antibody against K18 was added and incubated overnight at 4°C. Overnight antibody was removed and the cells washed 4 times with 1% NGS in PBS. The second secondary antibody was added and incubated at room temperature for 1 hour. The samples were washed again and mounted as described above.

Table 6. Antibodies For Immunocytochemistry

Target	Primary Antibody	Secondary Antibody
Ki67 (Proliferation)	Rabbit polyclonal to Ki67 (Abcam #ab15580) 5µg/ml	Goat anti rabbit IgG FITC (Southern Biotech) 4µg/ml
K5 (Basal)	Mouse monoclonal (clone XM26) (Abcam #ab17130) 5µg/ml	Goat anti mouse IgG1 FITC (Southern Biotech) 4µg/ml
K5 (Basal)	Rabbit polyclonal (Abcam #ab24647) 4µg/ml	Goat anti rabbit IgG FITC (Southern Biotech) 4µg/ml
K18 (Luminal)	Mouse monoclonal (clone C-04) to cytokeratin 18 (Abcam #ab668) 5µg/ml	Goat anti mouse IgG1 FITC (Southern Biotech) 4µg/ml Goat anti mouse IgG H&L TRITC (Abcam #ab6786)
α2β1 Intergrin (stem cell)	Mouse monoclonal (clone 16B4) to (Abcam #30483) 1µg/ml	Goat anti mouse IgG1 FITC (Southern Biotech) 4µg/ml
CD44 (stem cell)	Mouse monoclonal (clone G44-26) (BD Biosciences) 5µg/ml	Goat anti mouse IgG1 FITC (Southern Biotech) 4µg/ml
Oct-4 (stem cell)	Rabbit Polyclonal 4µg/ml	Goat anti rabbit IgG FITC (Southern Biotech) 4µg/ml
Bmi1 (stem cell)	Rabbit Polyclonal (Abcam #ab38295) 4µg/ml	Goat anti rabbit IgG FITC (Southern Biotech) 4µg/ml

2.10.4 Image Analysis

Colonies were analysed using an Olympus Total Internal Reflection inverted confocal microscope and Fluoview 2000 software. All photographic images were taken using a 10 times (x10) or 20 times (x20) objective. Laser power and voltage was set using control samples. Z stack images were taken at an interval of 1 µm and composite images were produced for both DAPI and FITC channels and a merged image. Large type 1 colonies were too wide to

image in 1 frame so mosaic images were produced using the same Z-stack dimensions and stitched together using the software. To determine the proportion of positive cells in a colony, the samples were viewed at x20 magnification. If the colony was small (<200 cells) all cells were counted and the positive fraction (green) calculated as a percentage of the total number of cells (DAPI stained nuclei). The proportion of positive cells in larger colonies was estimated by counting at least 200 cells in 5 random frames.

2.11 Incucyte Analysis of Clonal Growth

The clonogenic assay is based on the growth of colonies from single cells. To check the proportion of colonies that arose from single cells, colony growth was monitored using the Incucyte Live Cell Imaging System. DU145 cells were trypsinised and seeded at clonal density into 6 well plates. Phase contrast photographs of each well were taken at intervals of 4 hours by the Incucyte System for the duration of the 2 week incubation period. Incucyte images were viewed and each colony was tracked from when cell first adhered to the plastic to the end of the growth period. The number of cells from which the colony developed and the merging of colonies observed and the number of colonies derived from single cells calculated. The results are from 4 separate experiments from 4 individual flasks of DU145 cells.

2.12 Peptide Phage Display

2.12.1 The Ph.D.™-7 Phage Library

The Ph.D.™-7 library was purchased from New England Biolabs, UK. The library is based on a combinatorial library of random heptapeptides fused to a minor coat protein (pIII) of M13KE phage. The displayed peptide (7-mer) is expressed at the N-terminus of pIII and is present in 5 copies. The peptide is followed by a short spacer (Gly-Gly-Gly-Ser) and then the wild-type pIII sequence. The library consists of approximately 10^9 sequences amplified once to yield approximately 100 copies of each sequence in 10 µl of the supplied phage. The manufacturer's guidlines for panning against live cells were followed.

2.12.2 Culture of Host E.coli

E.coli host strain ER2738 (genotype F´proA$^+$B$^+$ lacI^q Δ(lacZ)M15 zzf::Tn10(Tet^R)/ fhuA2 glnV Δ(lac-proAB) thi-1 Δ(hsdS-mcrB)5) was purchased from New England Biolabs, (Hitchin, UK). This strain is a *fhuA2* version of *E. coli* NM522 in which the F' can be selected for using tetracycline. The stock was streaked on Lysogeny Broth (LB) agar, Miller plates (Sigma-Aldrich) supplemented with 20µg/ml tetracycline hydrochloride (Sigma-Aldrich) (LB-tet plates) and incubated overnight at 37°C. One colony was selected using a plastic loop and transferred to 5ml of Lysogeny Broth (LB) (Sigma-Aldrich) and incubated overnight at 37°C with vigorous shaking at 300 rpm. The ER2738 suspension culture was diluted 1:1 with sterile glycerol (Sigma-Aldrich) and stored at -80°C to create a new host stock. Colonies streaked onto LB-tet plates were stored at 4°C for up to one month.

2.12.3 Phage Titrations

To titrate the Ph.D.™-7 library, one colony of ER2738 cultured on LB-tet plates was selected and cultured in 5ml of LB with shaking at 300rpm at 37°C until the culture reached mid-log phase (OD_{600} ~ 0.5) (approximately 6 hours). Meanwhile, LB agar plates containing 50µg/ml isopropyl-β-D-thiogalactoside (IPTG) (Sigma-Aldrich), 40µg/ml 5-Bromo-4-chloro-3-indolyl-β-D-galactoside (Xgal) (Invitrogen) were pre-warmed to 37°C in the incubator. Top agar (10g LB media (Sigma) 2.7g agarose (Invitrogen) per litre) was prepared by melting in the microwave and kept warm in a 45°C water-bath. Phage dilutions were prepared from 10^1 - 10^{12} in LB and 10µl of each dilution was used to infect 200µl of the mid-log ER2738 cells. The infected cultures were vortexed briefly and incubated at room temperature for 5 minutes. Each dilution was added to 3ml of top agar, mixed by swirling and immediately poured onto one of the pre-warmed LB/IPTG/Xgal plates. The plates were allowed to set at room temperature for 15 minutes then inverted and transferred to a 37°C incubator for 18 hours. The M13 cloning vector used to manufacture the Ph.D.™-7 library carries the lacZα gene which results in blue plaques when cultured on media containing IPTG and Xgal. Contamination of wild type phage that do not contain a LacZ insert produce white plaques which are larger and fuzzier than blue plaques. The number of blue clones (Figure 11) is used to calculate the concentration of phage in the sample.

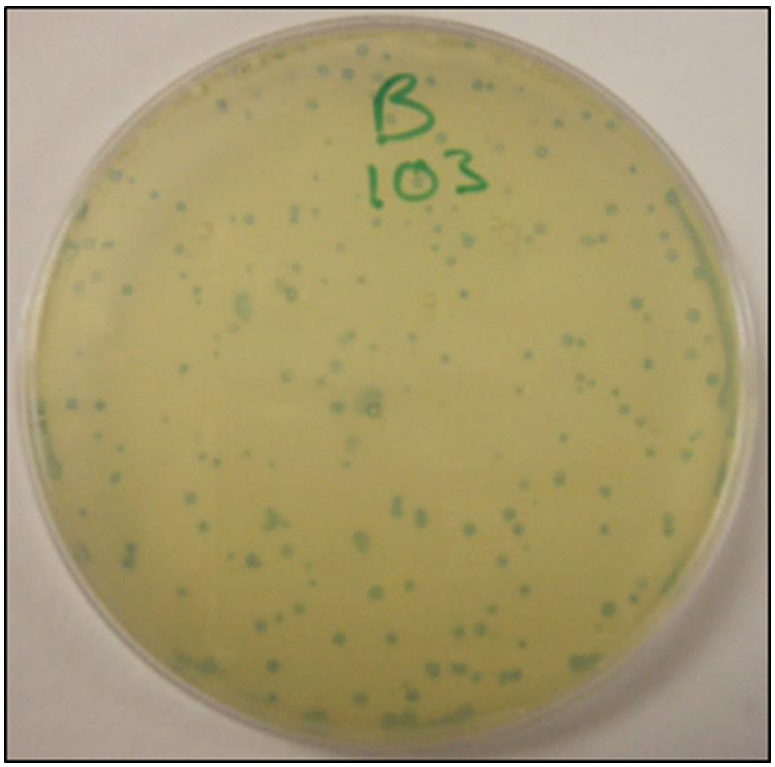

Figure 11. Titration of phage on IPTG/X-Gal LB plates.
Phage in the Ph.D.™-7 library carry the lacZα gene which results in blue plaques when they infect the ER2738 strain of E.Coli.

2.12.4 Sequencing of the Ph.D.™-7 Library

Fifty clones from the purchased Ph.D.™-7 were isolated and sequenced to confirm that no repeated sequences or motifs were present. Well-separated colonies were selected using a 1000µl pipette tip from titration plates following 18 hours of incubation. Each colony was transferred to a sterile 12ml culture tube containing 1.5ml of overnight ER2738 suspension culture (1 colony in 5ml LB shaken at 300rpm at 37°C overnight) diluted 1:100 in LB and incubated for 5 hours at 37°C with vigorous shaking. Single-stranded DNA was then isolated and sequenced.

2.12.4.1 *Single stranded DNA extraction*

The clones were transferred to 1.5ml Eppendorf tubes and centrifuged at 12,000 rpm for 5 minutes to remove E.coli. The supernatant was removed and transferred to a clean tube and single-stranded DNA was extracted using the M13 ssDNA extraction spin kit (Qiagen, UK). To 1ml of phage supernatant, 10µl of precipitation buffer was added and incubated for 5 minutes. The phage supernatant was added to the spin column and centrifuged in a microfuge at 8,000 rpm for 15 seconds. 700µl MLB lysis buffer (Qiagen kit) was added to each spin column and centrifuged tolyse phage and bind DNA to the column. The MLB step was repeated with a 1 minute incubation of MLB. The supernatant was removed and the column was washed by the addition of 700µl of PE buffer (Qiagen kit) was added to each tube and centrifuged. 50µl of DNase free dH_2O (Invitrogen) was added to the spin column and incubated at room temperature for 10 minutes to elute the DNA. The tubes were centrifuged again and ssDNA in solution collected in a fresh microfuge tube.

To ensure enough ssDNA had been isolated for sequencing each the ssDNA from each clone was visualised by agarose gel electrophoresis and compared to 25-100ng/µl of a known M13 ssDNA standard (New England Biolabs). A 1.2% agarose gel was cast containing 0.5µg/ml ethidium bromide (Sigma-Aldrich). DNA samples and the M13 ssDNA standard were diluted 1:1 with dH_2O and 1µl 10x Blue Juice loading dye (Sigma-Aldrich). 10µl of each sample was added to each well and the gel was run at 6 volts per cm for 45 minutes. The gel was viewed under UV and the samples compared to M13 ssDNA standard Figure 12.

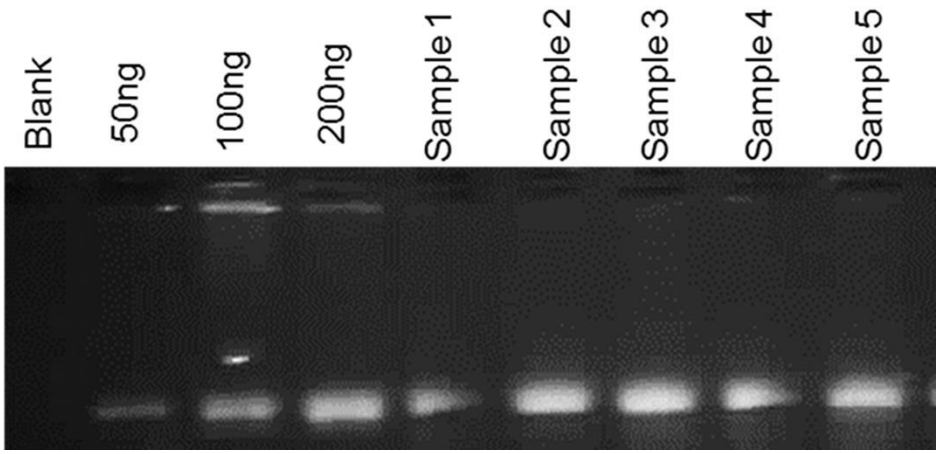

Figure 12. Agarose gel electrophoresis of ssDNA from phage clones.
An M13 ssDNA standard was diluted to 50-150ng/µl and run alongside ssDNA from phage clones to quantify the amount of ssDNA obtained from Qiagen M13 ssDNA extraction.

2.12.4.2 *DNA Sequencing and Analysis*

100ng of DNA from each sample was sequenced by Scientific Support Services at the Wolfson Institute for Biomedical Research, UCL, using ABI technology using the primer sequence 5´- $_{HO}$CCC TCA TAG TTA GCG TAA CG –3 (Invitrogen). Sequences were read using CLC Sequence Viewer 6 software and the variable region of each clone identified and translate to an amino acid sequence. Amino acid sequences were input into Pratt version 2.1 pattern recognition software (http://www.ebi.ac.uk/Tools/pratt/index.html). When given a set of unaligned protein sequences, the Pratt tool finds patterns matching a minimum number of these sequences. Pratt first searches the space of patterns and compiles a list of the most significant patterns (according to a non-statistical significance measure) found to be matching at least 4 sequences (Jonassen et al., 1995). Patterns and motifs repeated within and between sequences were identified.

2.12.5 Preparation of Target cells

Epithelial cells from samples of benign prostatic hyperplasia were used for positive selection of phage. HUVEC cells were used for the negative selection. Both cell types were seeded onto collagen coated 6 well plates and panning was performed when the cells reached 80% confluence (usually about 3 days).

Prostate epithelial cells were seeded in 60mm Petri-dishes containing mitomycin C treated fibroblasts at a density of 100 per dish and incubated for 12 days. Large type 1 colonies were ring cloned as previously described (chapter 3), pooled and seeded at a density of $5x10^4$ cells per well into 6 well plates with 3 ml PrEGM. Cells were incubated until 80% confluent for phage panning.

Human umbilical vein endothelial cells (HUVECs) were provided by Professor M O'Hare and maintained in Endothelial Growth Medium (EGM) supplemented with EGM Bullet Kit (Lonza, UK). The cells were passaged when 80% confluent and replated at a dilution of 1:6. $5x10^4$ HUVECs were seeded into each well of a 6 well plate and used for negative panning selection when 80% confluent.

2.12.6 Phage Panning

Four phage experiments were undertaken: A negative selection step was included after the first round using HUVEC cultures to remove phage that adhered to non-prostate cells and plastic or collagen binders.. The first two experiments used a different patient sample for each round of panning. The third and fourth experiments used only 1 patient sample to minimise phage loss due to sample variation. The post incubation washes were increased in stringency by raising the acidity of the wash buffer to reduce the number of non-specific and low affinity binders.

Table 7. Overview of Phage Display Panning Conditions

Experiment Number	Number of patient samples	Wash Stringency
1	4 (1 for each round)	Mild
2	4 (1 for each round)	Stringent
3	1 (1 for all rounds)	Mild
4	1 (1 for all rounds)	Stringent

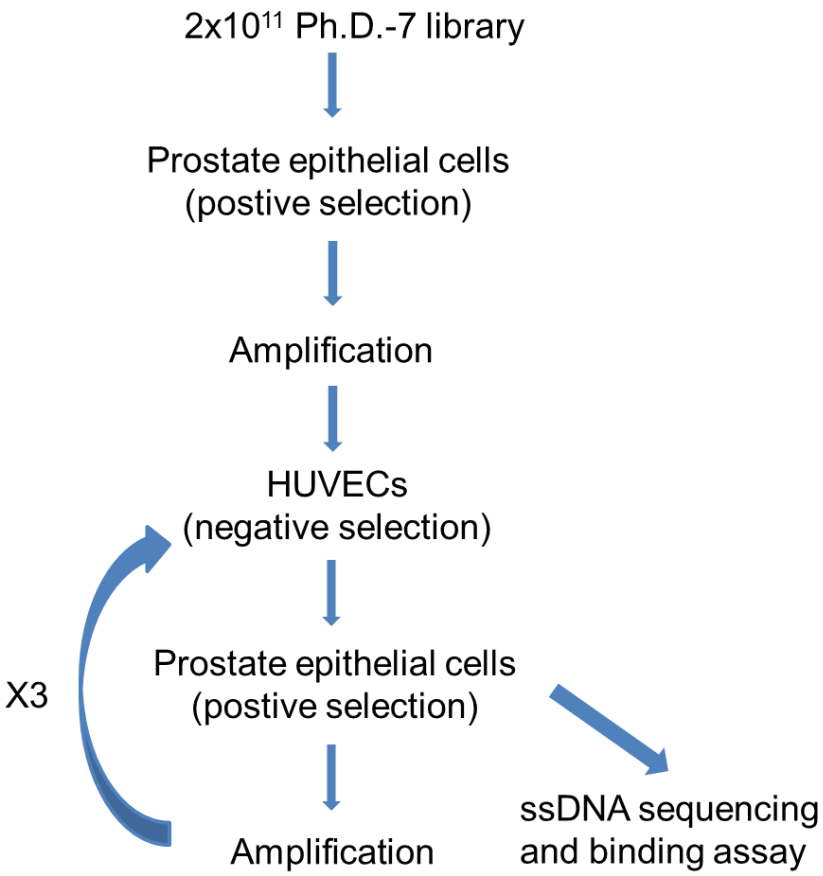

Figure 13. Phage Display Protocol.
Procedure used in this study to pan against prostate epithelial cells using HUVECs as a negative selection step.

2.12.6.1 *Round 1 (Day 1)*

The medium was removed from prostate epithelial cells and the cells were washed twice with 3ml of 50mM Tris-HCL pH 7.5, 150mM NaCl (TBS). The cells were blocked with 3ml of 2% Bovine serum albumin (BSA) (Sigma-Aldrich) in DMEM for 30 minutes at room temperature to reduce non-specific binding of phage. Blocking solution was removed and 10µl of Ph.D-7 library containing $2x10^{11}$ phage in 3ml of DMEM was added and incubated at room temperature for 1 hour with gentle shaking. Supernatant containing non-binding phage was removed and the cells were washed 5 times for 5 minutes

each with TBS-T (0.05% Tween 20 in TBS) Two ml of 0.2M Glycine-HCL (pH 2.2) containing 1 mg/ml BSA was added to elute the phage from the target cells. The cells were rocked for 20 minutes and 300 µl 1M Tris-HCL, pH 9.1 added to neutralise the elution buffer and the phage suspension was transferred to a microtube. A small volume of the phage was titrated (as section 2.12.3.) to determine the number of eluted phage. A colony of ER2738 was cultured in LB suspension over night at 37°C with shaking at 300rpm.

2.12.6.2 *Phage Amplification (Days 2 and 3)*

The first round eluate was transferred to a 50ml Erlenmeyer flask containing 20ml of overnight ER2738 culture diluted 1:100 in LB and incubated for 4 ½ hours at 37°C with shaking at 300 rpm. The culture was transferred to a centrifuge tube and centrifuged at 12,000g for 10 minutes at 4°C. The supernant was removed and a $1/6^{th}$ volume of 20% polyethylene glycol-8000 (Sigma-Aldrich), 2.5 M NaCl (Sigma-Aldrich) (PEG / NaCl) was added and allowed to precipitate overnight at 4°C. The mixture was centrifuged for 10 minutes at 12,000g to pellet the precipitate the phage and the supernatant was removed. The phage pellet was resuspended in 1ml TBS and the phage was reprecipitated for 1 hour on ice. The phage precipitation was microfuged at 14,000rpm for 10 minutes. The supernatant was removed and the phage particles resuspended in 200µl TBS. Phage were titered as in step 2.12.3.

2.12.6.3 *Round 2, 3 and 4 (Days 4 – 12)*

In rounds 2-4 a negative panning step was added to subtract non-prostate cell binders. Medium was removed from HuVECs and washed with 5ml TBS. $2x10^{11}$ phage from round 1 amplified eluate, diluted in 3ml DMEM, were

added to the HUVECS and incubated at 4 °C for 1 hour with gentle shaking at 60rpm. Meanwhile, the medium was removed from the prostate epithelial cells and the cells blocked with 3ml blocking solution for 30 minutes at room temperature. The blocking solution was removed and the cells. Non-binding phage were removed from the well containing HUVECs and transferred to the prostate epithelial cells. The HUVECs were washed twice with 1ml TBS-T and the supernatant added to the well containing prostate epithelial cells. Phage were incubated for 1 hour at 4°C with gentle shaking. Non-binding phage were removed and the cells were washed according to stringency (Table 8). Phage were eluted by the addition of 1ml 0.2 M Glycine-HCL (pH 2.2), 1 mg/ml BSA and gently shaken for 20 minutes. 300 µl of 1M Tris-HCL, pH 9.1, was added to neutralise the elution buffer and the phage suspension was transferred to a microtube. A small volume of the phage were titrated (as section 1.2.) to determine the number of eluted phage. After elution, phage were amplified, precipitated and titered as previously described. Following the fourth round of panning the phage eluate was not amplified and phage titration plates were set up to enable clone selection.

Table 8. Phage Panning Wash Protocols.

Stringency	Protocol
Mild	5 times 5 minutes with TBS-T (0.5% Tween-20)
Stringent	4 times for 5 minutes with 0.5% TBS-T, once for 1 minute with 76mM citrate buffer pH 3.5.

To optimise phage binding, different wash stringencies were used to select for high and low affinity binders during phage display panning.

2.12.6.4 *Clone Selection*

One hundred well separated plaques were selected and amplified in 2 ml of 1:100 dilution of overnight ER2738 suspension culture as described in 2.12.4. After 5 hours incubation at 37 °C with shaking, the culture was transferred in equal parts to two Eppendorf tubes. One of the Eppendorfs was diluted 1:1 with sterile glycerol and stored at -20°C and remaining the phage were used for ssDNA extraction and sequencing (see section 2.12.4.1). Clones which occurred at least twice were identified by Pratt analysis (2.12.4.2) and further amplified for phage binding assays.

2.12.7 Clone Binding Assays

Each phage clone was amplified and titered to determine adequate numbers of each clone for each binding assay. Two assays were used to determine the strength of binding of the clones and the pooled fourth round eluate in comparison to insert-less M13 control phage particles: a titration assay and a whole cell enzyme-linked immunosorbent assay (ELISA). 10 µl of each clone to be amplified, fourth round eluate and PhD7 library (New England Biolabs) were added to 20 ml 1:100 dilution of overnight ER2738 suspension culture in LB media in separate sterile Erlenmeyer flasks and cultured for 6 hours at 37 °C with vigorous shaking at 300rpm. The contents of each flask were decanted into sterile 50 ml tubes and centrifuged at 12,000 x *g* for 10 minutes at 4 °C. The supernatant was removed and placed in a clean tube and centrifuged again. The top 16ml of supernatant was placed in a clean tube and the phage were precipitated by adding 3.2 ml PEG/NaCl and allowing to precipitate at 4 °C overnight. The precipitated phage were centrifuged at 4 °C 12,000 x *g* for 15 minutes and the supernatant was removed. The phage pellet was re-spun for 1 minute and the remaining liquid carefully removed

with a 1ml pipette. The phage pellet was resuspended in 1ml TBS and transferred to a 1.5 ml Eppendorf tube and microfuged at 13,200 rpm for 10 minutes to remove any remaining host cells. The supernatant was transferred to a clean tube and the phage was re-precipitated for 60 minutes on ice by adding 200µl PEG/NaCl solution. The precipitate was centrifuged at 13,200 rpm for 10 minutes at 4°C and the supernatant removed. The phage pellet was resuspended in 200 µl of TBS and the concentration of phage determined by IPTG/Xgal titration (Section 2.12.3).

2.12.7.1 *Titration Binding Assay*

1 x 10^5 Prostate epithelial cells were seeded into 24 well plates with 1ml PrEGM and incubated overnight at 37°C in 5% CO_2. The medium was removed and the cells were washed twice with 1ml 0.05% TBS-T and the cells were blocked with 500µl of pre-warmed blocking buffer (2% BSA in DMEM) at 37°C for 30 minutes. An empty 24 well plate was also treated in the same way to test for background binding. Blocking buffer was removed and 1x10^{11} test phage clones, pooled round 4 clones and unselected PhD7 library clones were incubated in duplicate in the test well and blank wells in 150µl DMEM for 1 hour at 37°C. Then the wells were washed four times with 1ml TBS-T at room temperature, for 5 minutes per wash. Binding phage were eluted by adding 0.5ml of 0.2 M Glycine-HCL for 20 minutes with gentle rocking at room temperature and neutralised with 75 µl of Tris-HCL and transferred to a clean tube. The number of phage eluted was titered following the procedure in section 2.12.3 at dilutions of 10^1 – 10^6. The number of phage binding minus background binding was calculated by subtracting the number of phage recovered from wells containing target cells from those recovered from blank wells.

2.12.7.2 *Whole Cell ELISA*

$2x10^4$ Prostate epithelial cells were seeded into each well of a 96 well plate with 200µl PrEGM and incubated overnight at 37°C in 5% CO_2. The medium was removed and the cells were washed twice with 200µl 0.05% TBS-T and the cells were blocked with 200µl blocking buffer (2% BSA in DMEM) at 4°C for 30 minutes. Blocking buffer was removed and $1x10^{11}$ test phage (clones, pooled round 4 clones and insert-less phage) were incubated in duplicate in the test wells and blank wells in 100µl DMEM for 1 hour at 4°C. The wells were washed four times with 200µl PBS-T at 4°C for 5 minutes each. Cells were fixed with 100µl 4% PFA at 4°C for minutes and washed once with TBS. Each well was blocked with 200µl blocking buffer for 45 minutes at room temperature. Blocking buffer was removed and 100µl horseradish peroxidise-conjugated anti-M13 antibody (GE Healthcare) diluted 1/5000 in blocking buffer was added to each well and incubated for 1 hour at room temperature. The antibody solution was removed and the wells washed five times with TBS-T. 200µl of 2,2'-azino-bis(3-ethylbenzthiazoline-6-sulphonic acid) (ABTS) substrate dissolved in 0.05M phosphate-citrate buffer (both Sigma-Aldrich) was added to each well and allowed to develop in the dark for 60 minutes. Absorbance was measured at 405nm for 1 second per read on plate reader.

2.12.8 BLAST Search

A BLAST search of the SWISSPROT (http://www.ncbi.nlm.nih.gov/blast/) database with the phage peptide sequences was carried out to identify homology with proteins of interest in *Homo sapiens*. Only proteins with a minimum of 5 matching residues were compared.

3 Results: Colony Forming Ability and Culture Conditions

3.1 Chapter Introduction and Aims

Culture conditions can influence colony forming efficiency, but the effects on the morphology of the colonies produced and the proliferative capacity of individual colonies have not been studied. The aim of this study was to identify the colonies formed by prostate cancer cell lines DU145, LNCaP and PC-3 and determine the effect of culture conditions (seeding density, serum concentration, type of medium and substrate) on the proportion of each colony type and the cell number of individual colonies. This study will investigate whether colony forming ability is property of only a proportion of cells within a population or whether all cells within a cell line are clonogenic under optimum conditions.

3.2 Hypotheses

The work in this chapter will answer the following hypotheses:

1. All cells in a cell line are potentially stem cells.
2. Ability to form a stem cell colony is dependent on culture conditions.

3.3 Chapter Objectives

The following objectives were designed to test the hypotheses:

1. Classify the morphology of colonies derived from the prostate cancer cell lines DU145, PC-3 and LNCaP, under standard clonogenic assay conditions.
2. Characterise colonies on the basis of morphology and size.
3. Confirm the single cell origin of colonies.
4. Test the effects of culture conditions on the clonogenicity, morphology and size of the 3 prostate cancer cell line colonies, including:
    a. Cell seeding density
    b. FBS concentration
    c. Type of cell culture medium
    d. Cell substrate

3.4 Results

3.4.1 Prostate Cancer Cell Line Colony Forming Ability

200 DU145 and PC-3 and 500 LNCaP cells were seeded into 60mm petri-dishes as single cells and incubated for 2 weeks. Colonies were fixed and stained for counting and measurement. Under standard conditions in RPMI-1640 with 10 % FBS on tissue cultured treated plastic, the colony forming efficiency of DU145 was 27.4 ± 0.8 (mean ± standard error of the mean (S.E.M)), PC-3 was 22.8 ± 12.2 and LNCaP was 5.8 ± 3.5% based on 4 independent experiments (Figure 17 a).

3.4.1.1 *Prostate Cancer Colony Morphology*

Both DU145 (Figure 14) and LNCaP (Figure 16) cells formed three types of colony termed type 1, 2 and 3. Type 1 colonies were large and consisted mainly of small, tightly packed cells, with a generally smooth perimeter. Type 3 colonies contained enlarged, flattened cells. Type 2 colonies were of intermediate size and consisted of a mixture of cell types, with small tightly packed cells in the middle are larger flattened cells at the edges. LNCaP colonies were very densely packed and stained deeply with crystal violet. They also tended to form colonies with more jagged edges than type 1 colonies. PC-3 cells formed only two types of colony which were similar in morphology to type 2 and 3 colonies (Figure 15). Type 2 colonies were large, but only the cells in the middle were tightly packed, whereas type 3 colonies were sparse throughout the whole colony.

The relative proportions of the 3 colony types for each cell line are shown in Figure 17 b-d. Type 1 colonies were the most abundant type formed by DU145 and LNCaP cells, whereas Type 3 colonies were the least abundant.

PC-3 cells formed approximately equal number of Type 2 and 3 colonies, although the number of Type 3 colonies was more variable.

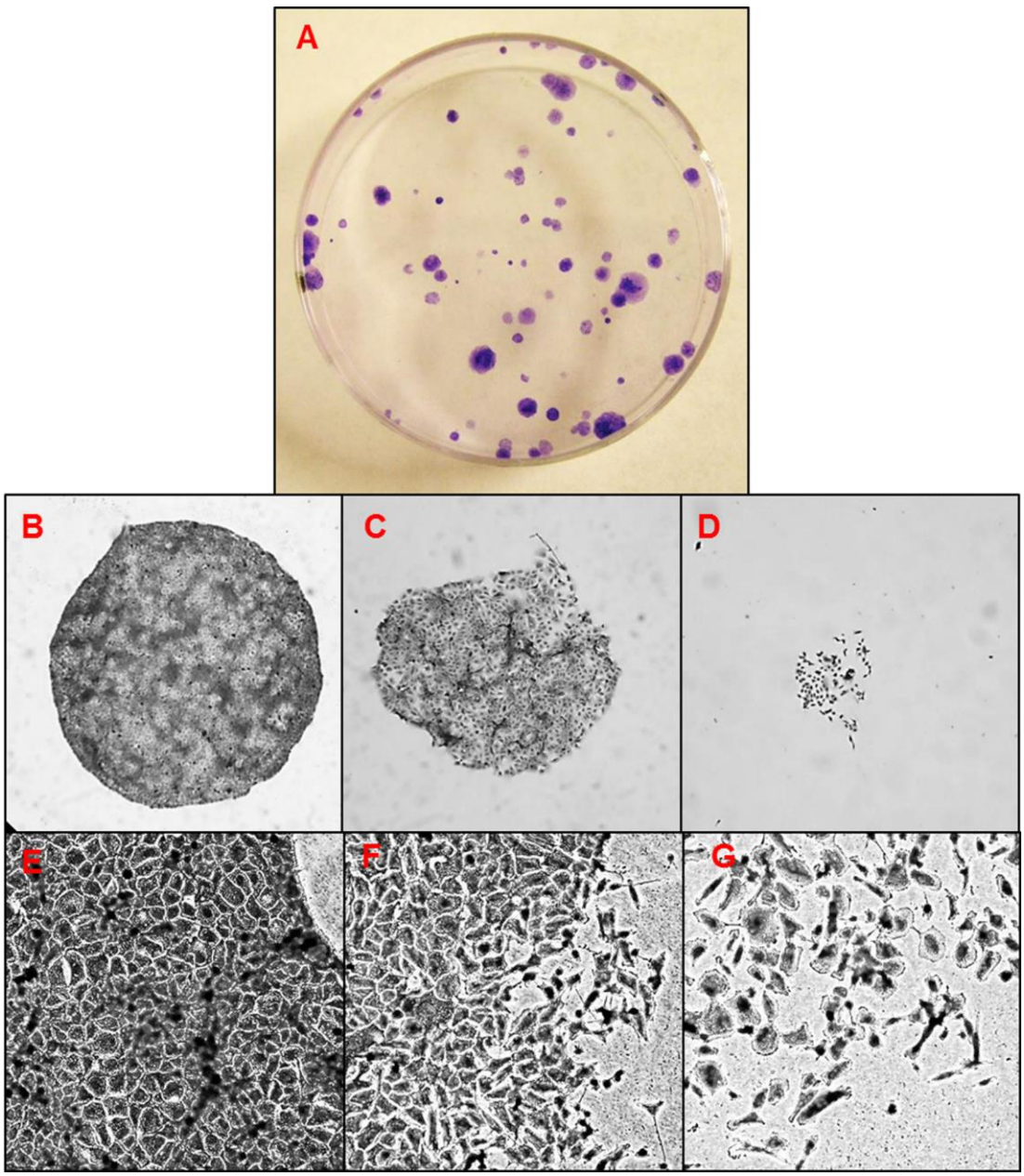

Figure 14. DU145 Colonies.

Single DU145 cells were seeded at low density into 60 mm petri-dishes (A). Single cells formed 3 morphological types of colony termed Type 1(B), 2 (C) and 3 (D). Type 1 colonies (E) contained small, densely packed cells with smooth edges. Type 2 colonies (F) contained a mixture of small tightly packed and larger more diffuse cells at the colony edge. Type 3 colonies (G) consisted of only enlarge flattened cells.

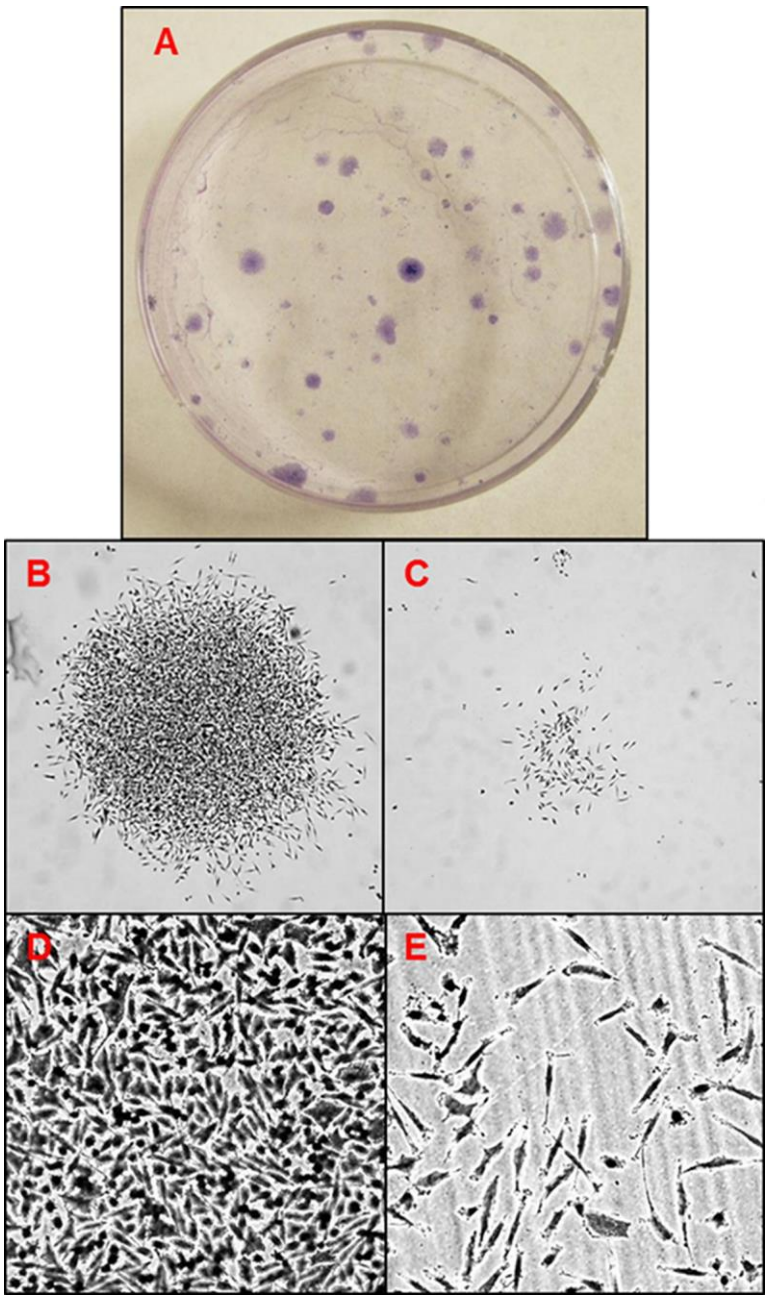

Figure 15. PC-3 Colonies.

Single PC-3 cells were seeded at low density into 60 mm petri-dishes (A). Single cells formed 2 morphological types of colony termed Type 2 (B) and 3 (C). No type 1 colonies were observed. Type 2 colonies (D) contained a mixture of small tightly packed and larger more diffuse cells at the colony edge. Type 3 colonies (E) consisted of only enlarge flattened cells.

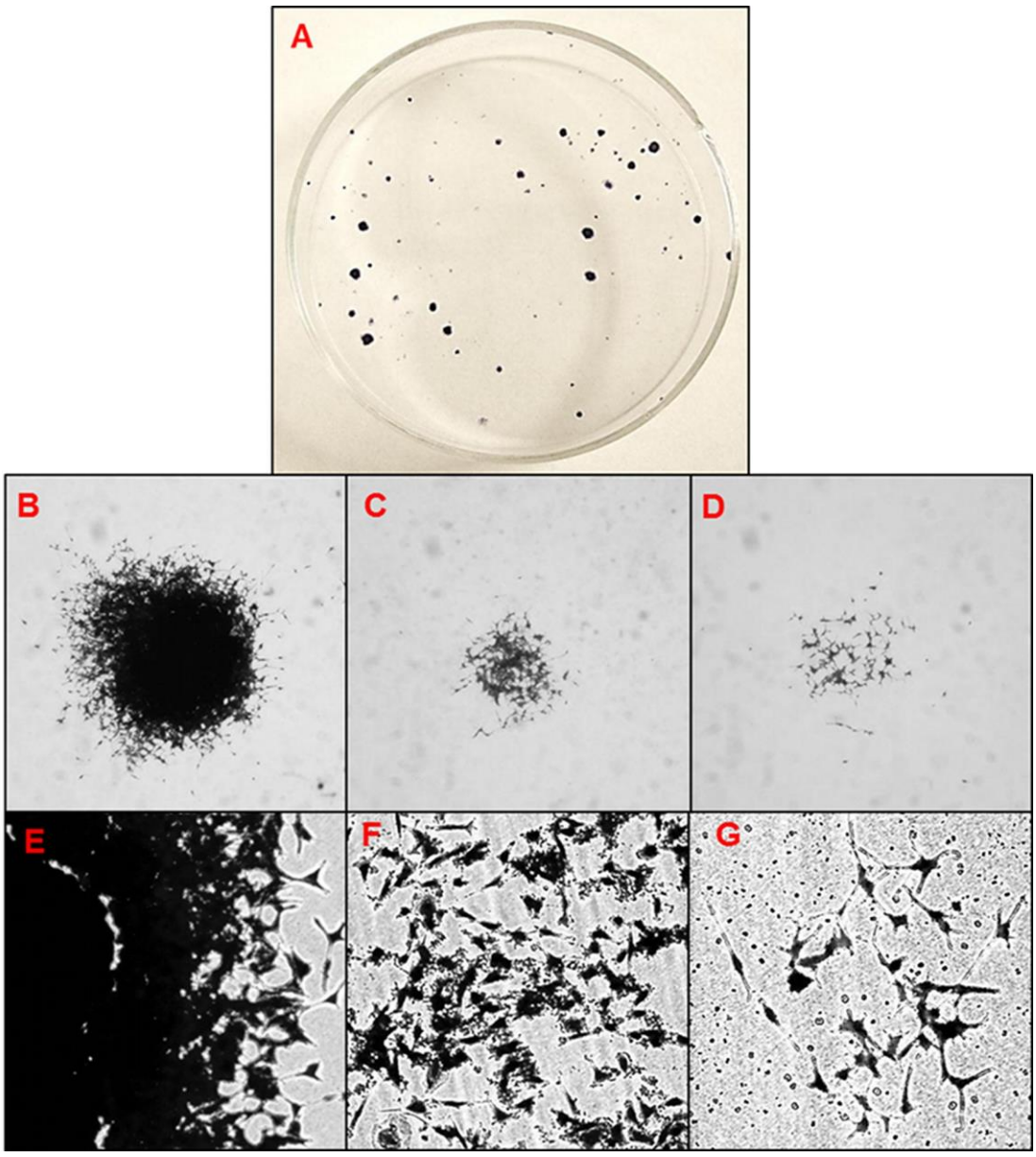

Figure 16. LNCaP Colonies.

Single LNCaP cells were seeded at low density into 60 mm petri-dishes (A). Single cells formed 3 morphological types of colony termed Type 1(B), 2 (C) and 3 (D). Type 1 colonies (E) contained small, densely packed cells, and it was not possible to identify single cells. Type 2 colonies (F) contained a mixture of small tightly packed and larger more diffuse cells. Type 3 colonies (G) consisted of only enlarge flattened cells.

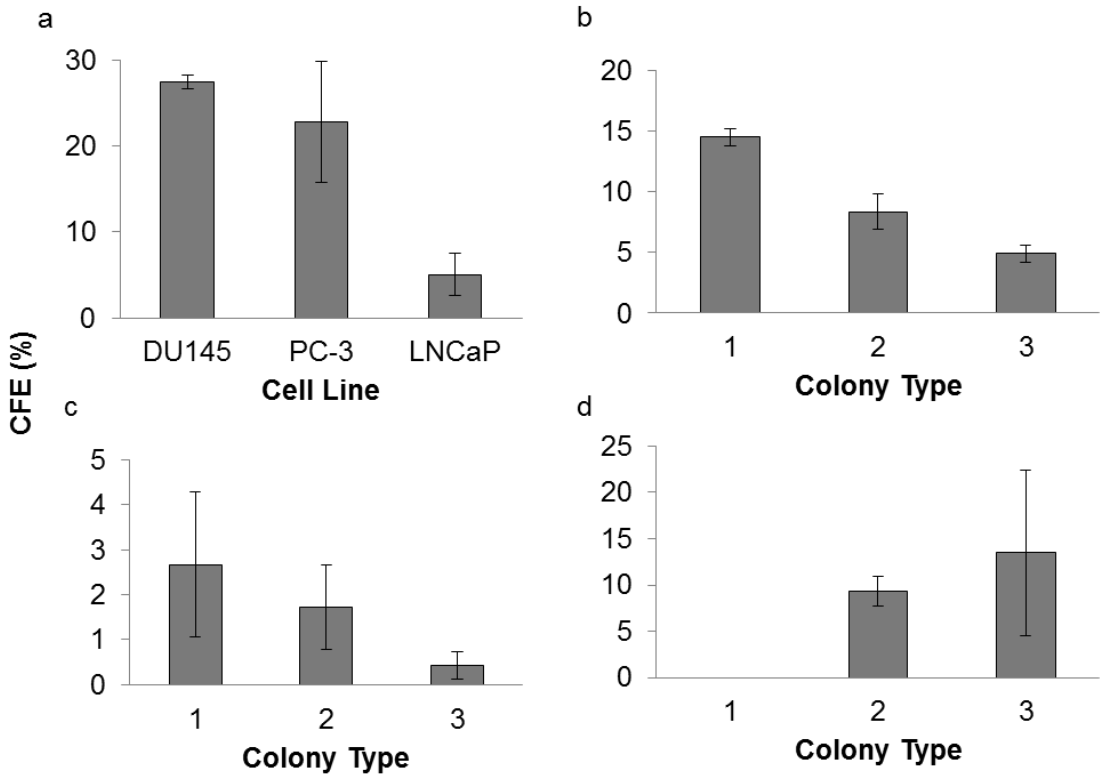

Figure 17. Colony forming efficiency of prostate cancer cells.

Total colony forming efficiency (a) and the colony forming efficiency of each type of (b) DU145, (c) LNCaP and (d) PC-3 cells. Bars represent Mean ± S.E.M of 4 experiments.

3.4.1.2 *Prostate Cancer Colony Size*

The properties of each colony type were determined from measurements of 20 colonies under standard conditions. Colony area, the number of cells per colony and number of cells per mm^2 are displayed in Table 9. LNCaP cells tended to form 3-dimensional colonies, which rendered estimation of the number of cells in LNCaP colonies impossible.

Type 1 DU145 colonies contained the most cells, and had the highest cell density of per mm^2 of 1470, nearly double the cell density of type 2 colonies of 753 cells per mm^2. The difference in cell densities between the colony types is due both to the differences in cell size and how tightly the cells are packed. Both type 2 and 3 colonies contain some cells which are not in direct contact with other cells.

From the number of cells per colony, the minimum number of cell divisions to achieve that number can be estimated (Figure 18). The largest Type 1 DU145 colonies underwent up to 13 cell divisions and Type 2 colonies up to 12, however type 3 colonies only divided 9 times within the 2 week incubation period. Type 2 PC-3 colonies underwent up to 11 cell divisions, whilst type 3 underwent up to 10 divisions.

Table 9. Prostate Cancer Colony Size.

Cell Line	Colony Type	Area (mm^2)	Total Number Cells	Cell Density (per mm^2)
DU145	1	2.16 (0.32)	3176 (569)	1470 (400)
	2	1.24 (0.21)	932 (201)	753 (218)
	3	0.92 (0.15)	240 (51)	261 (73)
PC-3	2	2.37 (0.38)	1420 (285)	568 (66)
	3	1.53 (0.23)	221 (62)	139 (23)
LNCaP	1	1.34 (0.28)	-	-
	2	0.82 (0.09)	-	-
	3	0.58 (0.07)	-	-

Mean colony area and number of cells per colony cultured under standard conditions. Estimation of the number of cells was not possible for the LNCaP cell line due to the structure of the colonies. Mean and S.E.M in parentheses of twenty colonies in 3 individual experiments.

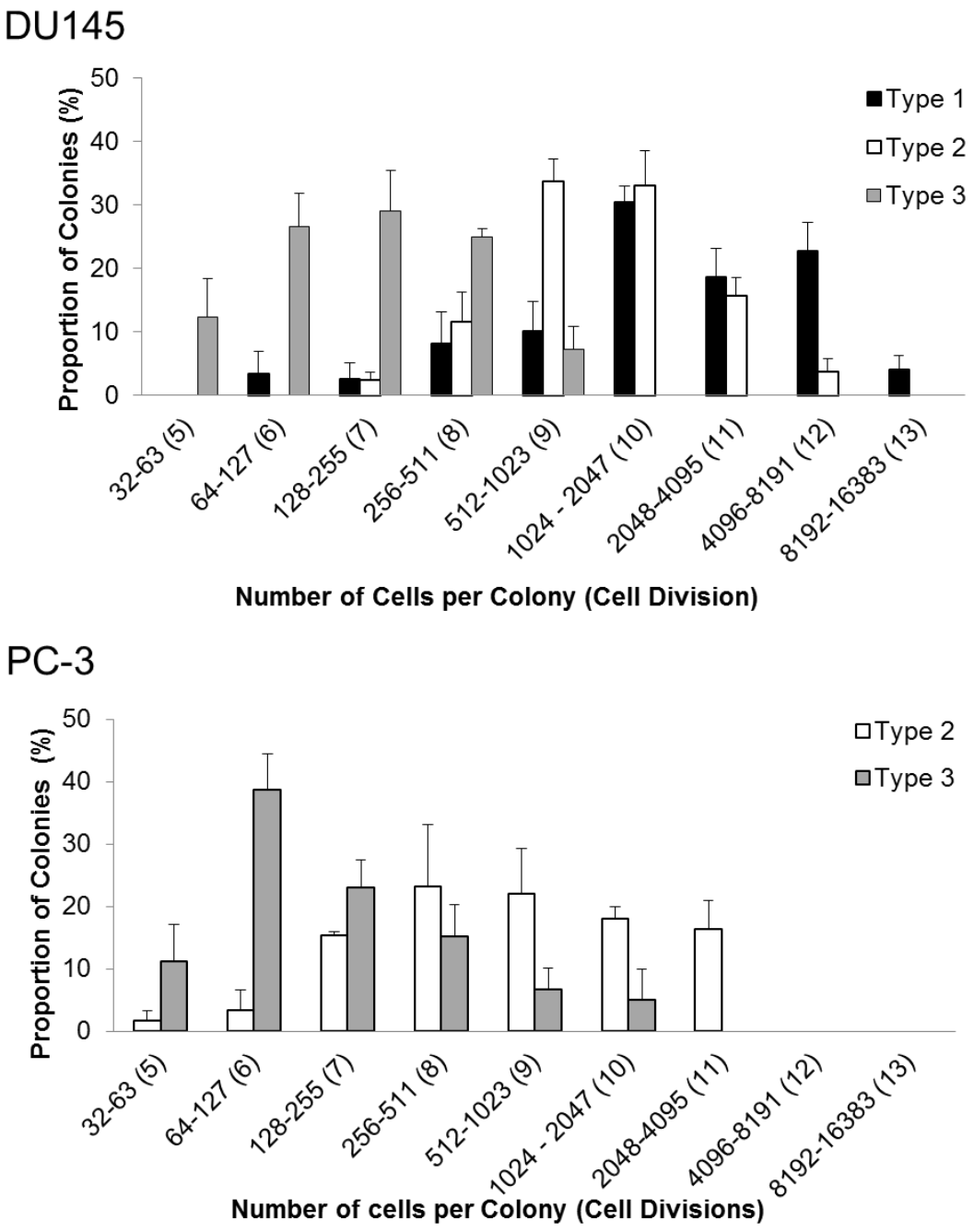

Figure 18. Distribution of Cancer Colony Sizes.

Comparison of the number of cells and number of cell divisions of the different colony types in DU145 and PC-3 cell lines. Distribution of the area and cell number of colonies formed by DU145 and PC-3 cells. (Mean ± SEM of 20 colonies in 3 individual experiments).

3.4.2 Seeding Density and Clonogenicity

A clonogenic assay was used to determine the effect of cell seeding density on the number of DU145, PC-3 and LNCaP colonies. Between 20 and 500 cells were seeded in a single cell suspension in triplicate and following 14 - 21 days incubation the CFE, the types of colonies and the sizes of colonies were determined. Figure 19, which shows the number of colonies at each seeding density, shows that there was no effect of on the number of colonies formed by any of the three cell lines ($p > 0.05$). At a seeding destiny of 500 cells per dish, which was optimum for LNCaP, both PC-3 and DU145 colonies were too confluent to count accurately.

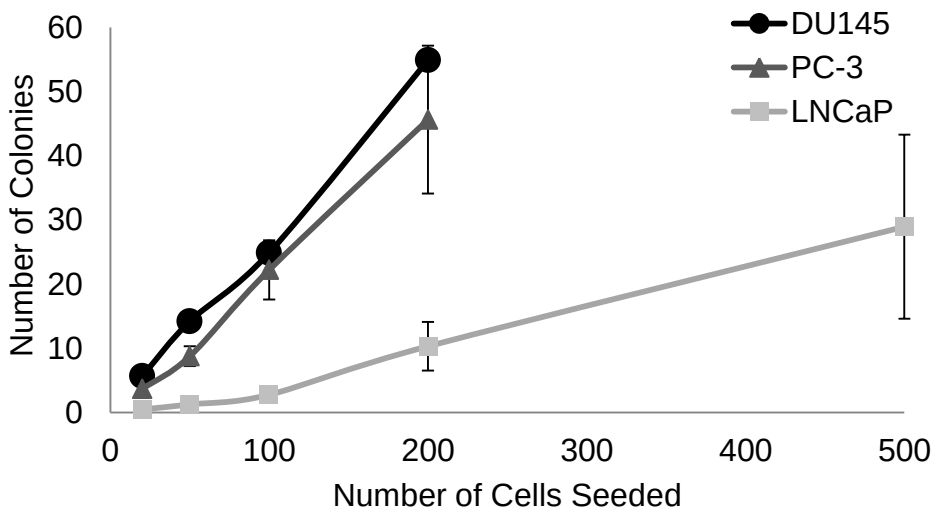

Figure 19. The effect of cell seeding density on colony forming efficiency.
The cell lines DU145, PC-3 and LNCaP. 20-500 cells were seeded in triplicate into 60 mm diameter petri-dishes and incubated for 14–21 days. Mean ± S.E.M of 3 experiments.

3.4.2.1 *Seeding Density and Colony Morphology*

Colonies were scored as Type 1, 2 or 3 based on colony size and morphology and the CFE of each colony type was determined as a percentage of the number of plated cells (Figure 20). Prostate cancer colony morphology is unaffected by seeding density ($p > 0.05$). Although a higher seeding density tended to increase the number of type 1 LNCaP colonies, the high variability meant that this observation was not statistically significant in this experiment ($p > 0.05$).

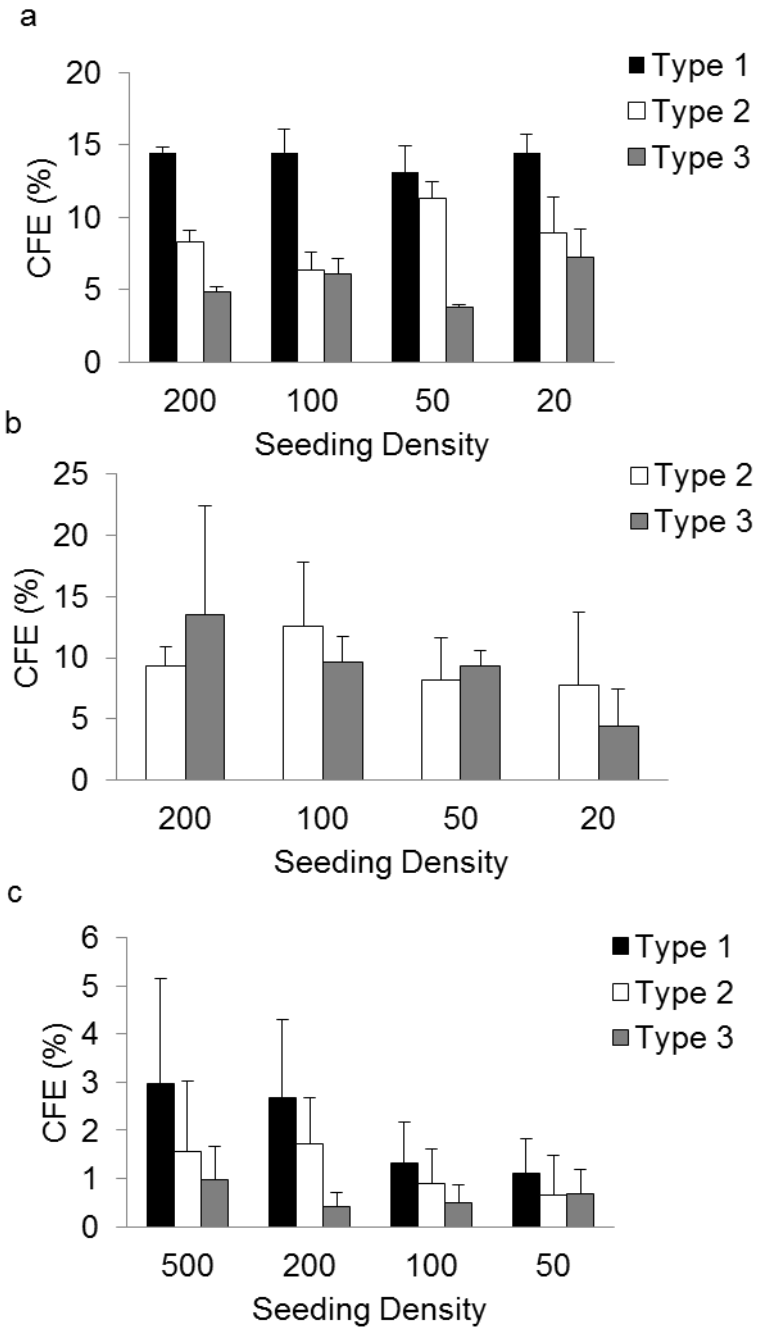

Figure 20. The effect of Seeding Density on Colony Morphology.

The colony forming efficiency of each of the different colony types as a percentage of the number of cells seeded. a) DU145, b) PC-3 and c) LNCaP. Mean ± S.E.M of 3 experiments.

3.4.2.2 *Seeding Density and Colony Size*

Mean colony area and cell number of twenty colonies of each type are displayed in Table 10. As previously mentioned, estimation of the number of cell per LNCaP colony was not possible due to the 3-dimensional nature of LNCaP cell colonies. Although higher seeding density appears to result in larger colonies, due to the larger variation in colony size this was not significant. Indeed, seeding density had no effect on colony size of any of the three cell lines ($p>0.05$) and also appears to not affect the potential for some colonies to consist of very large numbers of cells, as a few extremely larger colonies were observed at each seeding density.

Table 10. Seeding Density and Colony Size

Cell Line	Seeding Density	Type 1		Type 2		Type 3	
		Colony Area (mm2)	Cell Number Per Colony	Colony Area (mm2)	Cell Number Per Colony	Colony Area (mm2)	Cell Number Per Colony
DU145	200	1.85 (0.03)	2716 (46)	1.77 (0.07)	1338 (55)	0.88 (0.12)	229 (30)
	100	1.68 (0.32)	2468 (473)	1.67 (0.57)	1259 (433)	0.88 (0.19)	229 (49)
	50	1.85 (0.65)	2713 (957)	1.24 (0.12)	901(80)	0.63 (0.09)	164 (26)
	20	0.94 (0.19)	1381 (286)	1.03 (0.34)	773 (258)	0.65 (0.07)	169 (19)
PC-3	200	-	-	2.08 (0.44)	1183 (251)	1.05 (0.19)	146 (27)
	100	-	-	2.05 (0.41)	1163 (233)	1.03 (0.11)	143 (15)
	50	-	-	1.45 (0.46)	823 (259)	0.90 (0.06)	125 (8)
	20	-	-	1.13 (0.13)	643 (76)	0.85 (0.06)	118 (8)
LNCaP	500	1.34 (0.25)	-	0.53 (0.06)	-	0.48 (0.15)	-
	200	0.78 (0.21)	-	0.60 (0.11)	-	0.76 (0.20)	-
	100	1.00 (0.15)	-	0.66 (0.31)	-	0.39 (0.39)	-
	50	0.53 (0.20)	-	0.26 (0.00)	-	0.40 (0.11)	-

Colony size and number of cells per colony at each seeding density. Twenty colonies were measured at each seeding density. No Type 1 PC-3 colonies were observed. Estimation of the number of cells was not possible for the LNCaP cell line due to the structure of the colonies. Mean and S.E.M of 3 experiments in parentheses.

3.4.3 FBS concentration and Clonogenicity

A clonogenic assay was used to test the effect of FBS concentration on the CFE, colony morphology and colony size of DU145, PC-3 and LNCaP cell lines. As show in Figure 21, FBS concentration had a considerable effect on the CFE of all three cell lines.

The three cell lines responded differently to FBS modification. Both DU145 and PC-3 demonstrated an increase in CFE when cultured in a concentration of FBS up to 20%, although this was not significantly greater than standard conditions of 10% ($p > 0.05$). LNCaP cells on the other hand, demonstrated a preference for lower concentrations of FBS, with a peak CFE of 22.3% ± 6.9% when cultured at 5%, although again, this was not significantly higher than standard conditions ($p > 0.05$). Both extremely high (50%) and low (1%) resulted in reduced CFE in all three cell lines, with only very few colonies observed when culture with 1% ($p < 0.05$).

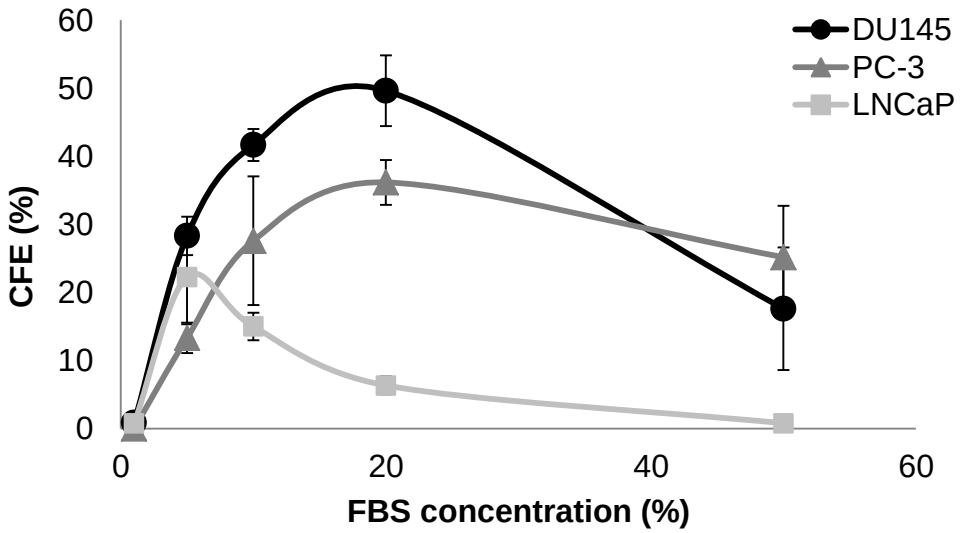

Figure 21. Colony forming efficiency of the prostate cancer cell lines.
DU145, PC-3 and LNCaP when cultured as single cells with 1 - 50% FB S in RPMI-1640. Results displayed as the mean of three independent experiments ± S.E.M.

3.4.3.1 *FBS Concentration and Colony Morphology*

The types of prostate cancer colonies formed when cultured in different FBS concentrations is displayed in Figure 22. As with observed with total CFE, the proportions of colony types can be modified by FBS concentration.

The Type 1 colonies were the most sensitive of the DU145 colonies to the suboptimal serum concentrations. At both 5 and 50 % serum concentrations, there was a marked reduction in Type 1 and 2 colonies, but no change in the number of Type 3 colonies, compared to the optimum concentrations of 10 and 20 %. A similar pattern was observed in PC-3 cells, where at suboptimal FBS concentrations, there was a significant reduction in the number of Type 2 colonies, but the number of Type 3 colonies remained stable, although this was less marked when cultured with 50 % FBS than in DU145 cells. All three types of LNCaP colonies were affected equally by the change in FBS conditions and the proportions of each type remained relatively stable.

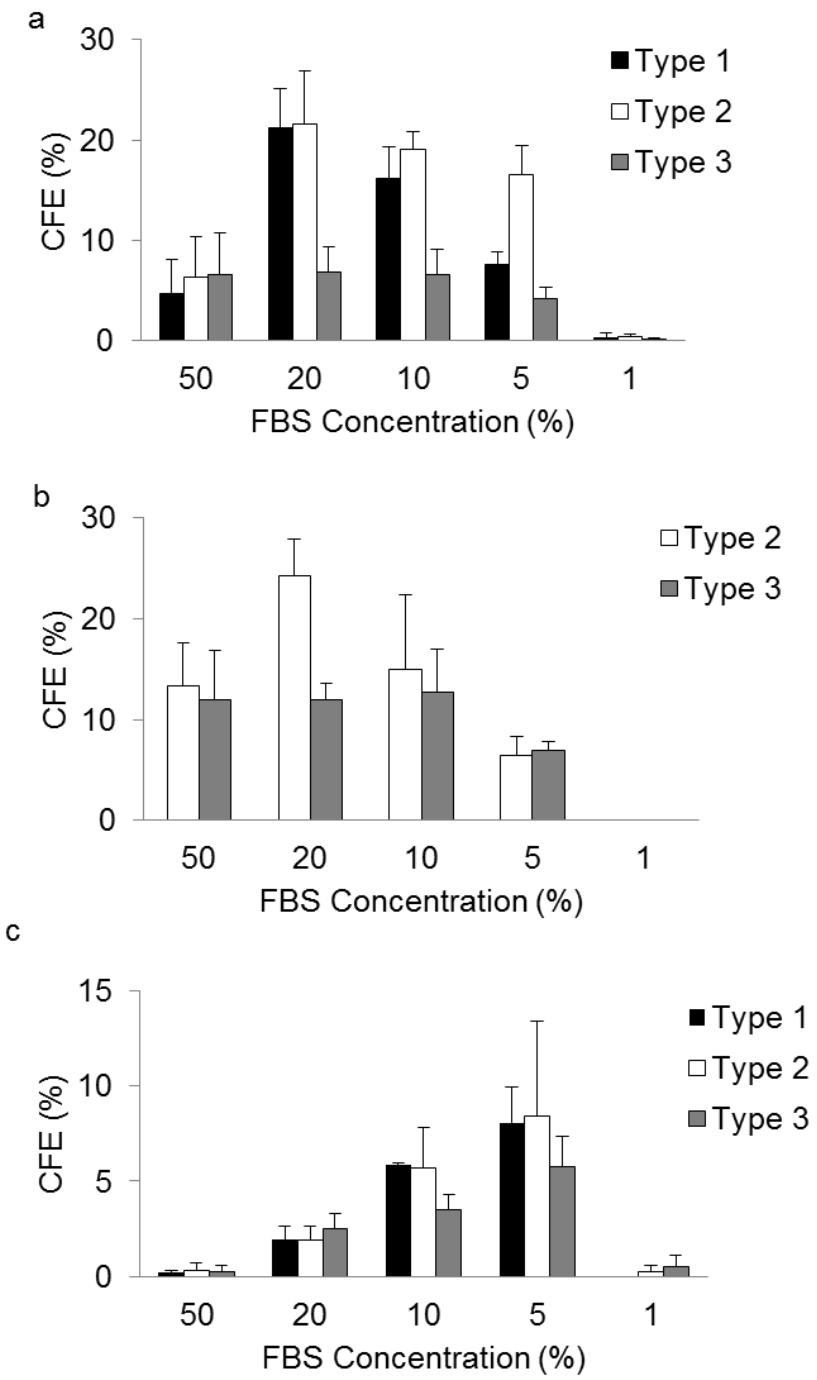

Figure 22. The Effect of FBS on Colony Morphology.

Colony forming efficiency of each colony type formed by the prostate cancer cell lines a) DU145, b) PC-3 and c) LNCaP when cultured as single cells with 1 - 50% FBS in RPMI-1640. Mean ± S.E.M of 3 independent experiments.

3.4.3.2 *FBS Concentration and Colony Size*

Serum concentration affected both colony area and the number of cells in each colony Table 11. The colony size of all three cell lines was reduced by culture in FBS concentrations sub-optimal for CFE. Type 1 colonies were most sensitive to sub-optimal serum concentrations. Type 1 DU145 colonies cultured with 5% FBS were significantly smaller than at all other concentrations ($p < 0.05$) with Type 1 colony size and cell number less than half those seen at higher serum concentrations. The optimum FBS concentration of 20 % FBS produced DU145 Type 1 and 2 colonies which were larger (2.61 and 2.16 mm^2 respectively) than at all other concentrations ($p < 0.05$). PC-3 colonies were also sensitive to low and higher FBS concentrations, and Type 2 colonies culture at 5 and 50 % were smaller than when cultured in standard conditions ($p < 0.05$). No concentration of FBS increased PC-3 colony size compared to the standard concentration of 10% ($p > 0.05$). All three type of LNCaP colony were sensitive to FBS concentration. Culture of LNCaP in the optimum FBS concentration of 5% FBS significantly increased the size of all three colony types compared to standard conditions ($p<0.05$).

Table 11. Serum Concentration and Colony Size

Cell Line	FBS (%)	Type 1		Type 2		Type 3	
		Colony Area (mm2)	Cell Number Per Colony	Colony Area (mm2)	Cell Number Per Colony	Colony Area (mm2)	Cell Number Per Colony
DU145	50	2.45 (0.43)	3604 (641)	1.66 (0.12)	1252 (92)	1.26 (0.35)	330 (91)
	20	2.61 (0.28)	3838 (414)	2.16 (0.33)	1630 (247)	1.04 (0.18)	272 (47)
	10	1.56 (0.29)	2291 (440)	1.40 (0.33)	1052 (247)	0.99 (0.18)	259 (47)
	5	0.86 (0.11)	1265 (161)	0.97 (0.15)	733 (112)	0.51 (0.05)	133 (13)
PC-3	50	-	-	1.84 (0.15)	1047 (80)	1.21 (0.08)	168 (11)
	20	-	-	2.26 (0.37)	1283 (210)	0.88 (0.21)	123 (29)
	10	-	-	2.58 (0.27)	1467 (154)	1.05 (0.16)	145 (22)
	5	-	-	1.54 (0.06)	875 (32)	0.78 (0.14)	108 (19)
LNCaP	50	0.53 (0.01)	-	0.24 (0.03)	-	0.43 (0.01)	-
	20	1.05 (0.44)	-	0.43 (0.12)	-	0.46 (0.10)	-
	10	1.00 (0.30)	-	0.43 (0.07)	-	0.48 (0.17)	-
	5	1.41 (0.10)	-	0.53 (0.08)	-	0.48 (0.06)	-

Colony size and number of cells per colony at each FBS concentration. Twenty colonies were measured at each seeding density. No type 1 PC-3 colonies were observed. Estimation of the number of cells was not possible for the LNCaP cell line due to the structure of the colonies. Mean and S.E.M in parentheses of 3 individual experiments.

3.4.4 Substrate and Clonogenicity

A clonogenic assay was used to test the effect of different substrates on the clonogenicity of the prostate cancer cell lines DU145, PC-3 and LNCaP, shown in Figure 23. Substrate modification did not increase the CFE of any of the three cell lines. Culture on 2µg/cm^2 type 1 rat tail collagen significantly decreased the CFE of PC-3 cells from 27.1 ± 2.4 to 7.8 ±1.9% ($p<0.01$). Although not significant, the optimum substrates for DU145 and PC-3 cells were 2µg/cm^2 type 1 rat tail collagen and 3T3 feeder layer respectively. No increase in LNCaP CFE was observed compared to tissue culture plastic.

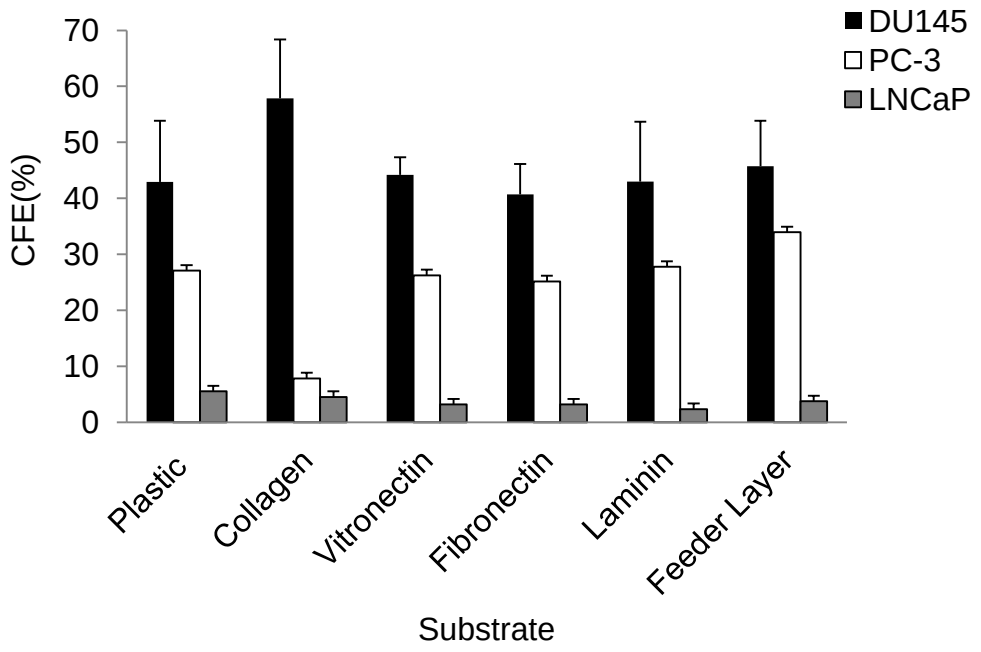

Figure 23. The effect of growth substrate on colony forming efficiency.
Substrates tested were: Tissue culture treated plastic (Nunc), 2µg/cm^2 Type 1 rat tail collagen, 50ng/ cm^2 Fibronectin, 50ng/ cm^2 Laminin, 50ng/ cm^2 Vitronectin and a feeder layer of Mitomycin C treated Swiss 3T3 cells at a density of 10^4 cells/ cm^2. Mean ± S.E.M of 3 individual experiments.

3.4.4.1 *Substrate and Colony Morphology*

The type of colonies formed when cultured on different growth substrates is displayed in Figure 24, as a proportion of the number of cells seeded. As observed with total CFE, modification of substrate had little effect on the morphology of DU145 or LNCaP colonies, although a moderate increase in the proportion of Type 2 and 3 DU145 colonies was observed when cultured with 2µg/cm^2 type 1 rat tail collagen ($p < 0.05$). The opposite effect was observed in PC-3 type 2 colonies, in which culture on collagen reduced type 2 CFE from 15.8 ± 1.2% to only 0.8% ± 0.3%, less than all other substrates ($p < 0.05$). The largest effect on colony morphology was observed in the PC-3 line when supported by a 3T3 feeder layer, although this was not statistically significant ($p<0.05$).

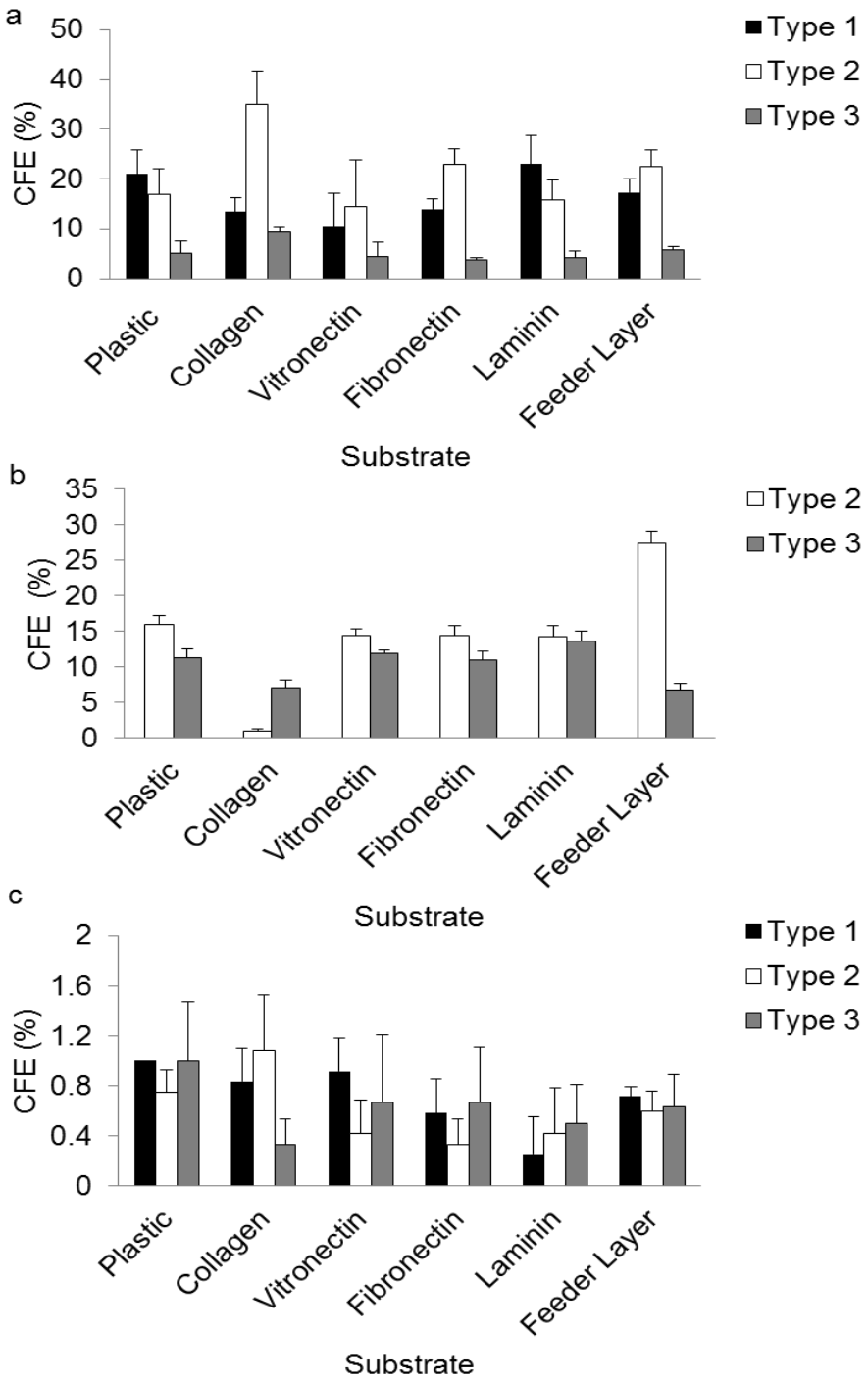

Figure 24. The Effect of Growth Substrate on Colony Morphology.

Colony forming efficiency of each colony type formed by the prostate cancer cell lines a) DU145, b) PC-3 and c) LNCaP when cultured with commonly used substrates in 10% FBS, RPMI-1640. Substrates tested were: Tissue culture treated plastic (Nunc), 2µg/cm^2 Type 1 rat tail collagen, 50ng/ cm^2 Fibronectin, 50ng/ cm^2 Laminin, 50ng/ cm^2 Vitronectin and a feeder layer of Mitomycin C treated Swiss 3T3 cells at a density of 10^4 cells/ cm^2. mean ± S.E.M of three independent experiments.

3.4.4.2 *Substrate and Colony Size*

The effect of substrate modification on DU145 and PC-3 colony size was more pronounced than CFE or colony morphology (Table 12). Type 1 and 2 colonies were more sensitive to the modification than Type 3 and some large increases in proliferation were observed. The size of LNCaP colonies were unaffected by substrates.

Both collagen and the feeder layer significantly increased the size of DU145 type 1 colonies to 6.56 ± 1.04mm^2 and 4.16 ± 0.18mm^2 respectively ($p < 0.05$). These are more than twice the size of colonies grown on tissue culture treated plastic. Collagen also increased the size of both Type 2 and 3 colonies ($p < 0.05$). Culture on collagen also increased the number of extremely large colonies with 88.4 % of Type 1 colonies containing 4096 (which equates to 12 or more divisions) or more cells, compared to 30% of those cultured on plastic. Collagen also increased the number of colonies that had undergone at least 14 cell divisions (>16,384) cells to 6.5 % of the Type 1 colonies. As with DU145 cells, culture on collagen increased the mean size of both Type 2 and 3 PC-3 colonies ($p < 0.05$), but not the number of colonies which had undergone at least 13 cell divisions.

Table 12. Substrate and Colony Size.

Cell Line	Substrate	Type 1		Type 2		Type 3	
		Colony Area (mm2)	Cell Number Per Colony	Colony Area (mm2)	Cell Number Per Colony	Colony Area (mm2)	Cell Number Per Colony
DU145	Plastic	2.59 (0.77)	3815 (1139)	1.58 (0.54)	1188 (405)	1.21 (0.00)	315 (10)
	Collagen	6.56 (0.74)	9641 (1087)	3.07 (0.12)	2314 (94)	1.72 (0.19)	450 (50)
	Fibronectin	2.88 (0.28)	4237 (408)	1.69 (0.02)	1275 (12)	0.89 (0.13)	232 (35)
	Laminin	1.76 (0.19)	2589 (281)	1.17 (0.04)	883 (27)	0.68 (0.09)	177 (23)
	Vitronectin	3.38 (0.78)	4973 (1141)	1.94 (0.21)	1465 (162)	0.86 (0.01)	224 (10)
	3T3	4.16 (0.13)	6115 (184)	2.51 (0.49)	1892 (368)	0.16 (0.00)	42 (4)
PC-3	Plastic	-	-	2.14 (0.14)	1217 (77)	1.09 (0.13)	152 (18)
	Collagen	-	-	2.84 (0.53)	1613 (303)	3.17 (0.67)	441 (93)
	Fibronectin	-	-	2.32 (0.09)	1316 (49)	0.99 (0.13)	138 (18)
	Laminin	-	-	1.81 (0.34)	1026 (190)	0.91 (0.16)	127 (23)
	Vitronectin	-	-	2.34 (0.28)	1331 (158)	1.27 (0.07)	177 (9)
	3T3	-	-	2.44 (0.29)	1388 (167)	0.94 (0.11)	131 (16)
LNCaP	Plastic	0.67 (0.14)	-	0.25 (0.08)	-	0.13 (0.05)	-
	Collagen	0.40 (0.08)	-	0.19 (0.06)	-	0.16 (0.03)	-
	Fibronectin	0.96 (0.16)	-	0.39 (0.05)	-	0.33 (0.05)	-
	Laminin	0.53 (0.01)	-	0.29 (0.19)	-	0.35 (0.07)	-
	Vitronectin	0.81 (0.21)	-	0.50 (0.10)	-	0.14 (0.03)	-
	3T3	0.79 (0.12)	-	0.35 (0.16)	-	0.22 (0.13)	-

Colony size and number of cells per colony when cultured on commercially available substrates. Substrates tested were: Tissue culture treated plastic (Nunc), 2µg/cm2 Type 1 rat tail collagen, 50ng/ cm2 Fibronectin, 50ng/ cm2 Laminin, 50ng/ cm2 Vitronectin and a feeder layer of Mitomycin C treated Swiss 3T3 cells at a density of 104 cells/ cm2. Estimation of the number of cells was not possible for the LNCaP cell line due to the structure of the colonies. Twenty colonies were measured at each seeding density. Mean and S.E.M of 3 independent experiments in parentheses.

3.4.5 Growth Medium and Clonogenicity

A clonogenic assay was used to test the proportion of DU145, PC-3 and LNCaP cells that are capable of forming colonies of greater than 32 cells when cultured in different commercially available media. The media tested were RPMI-1640, DMEM low glucose, DMEM high glucose, Hams F12, Hams F12/ DMEM and AMEM. The cells were adapted to the various media before the CFE was measured, and some profound effects on CFE were observed.

For all 3 cell lines, when compared to RPMI 1640, the use of Hams F12, Hams F12/ DMEM and AMEM resulted in small increases in the CFEs. ($p < 0.05$) (Figure 25). Culture with AMEM gave the highest CFE for both DU145 and PC-3 cells 64.2% ± 5.8% and 52.9 ± 5.7% respectively. Ham's F12 was optimal for LNCaP cells, with 15.2 ± 9.3 % of cells formed colonies. Interestingly, DMEM reduced the CFE of all three cell lines compared to all other culture media ($p < 0.05$).

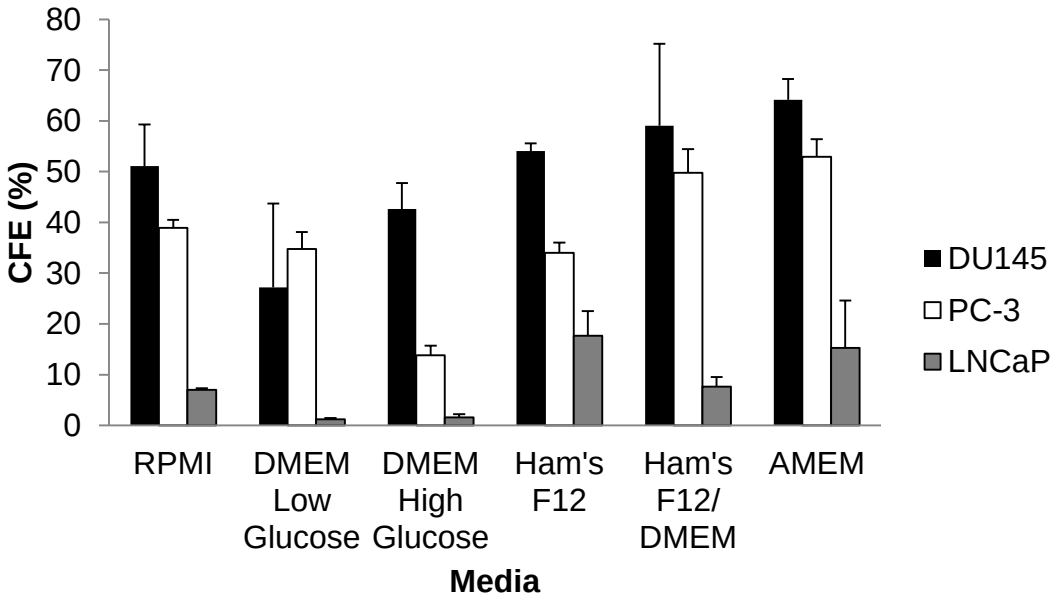

Figure 25. The effect of growth substrate on colony forming efficiency. The colony forming efficiency of prostate cancer cells. Mean ± S.E.M of three independent experiments.

3.4.5.1 *Culture Media and Colony Morphology*

The changes in total CFE observed in all three cell lines when cultured in different media were mainly due to changes in the proportion of Type 1 colonies, as shown in Figure 26. In sub-optimal conditions, significantly fewer ($p < 0.05$) Type 1 colonies developed in low glucose DMEM, compared to all other media except high glucose DMEM. AMEM increased the number of both type 1 and 2 colonies formed by DU145, LNCaP and PC-3 cells ($p < 0.05$).

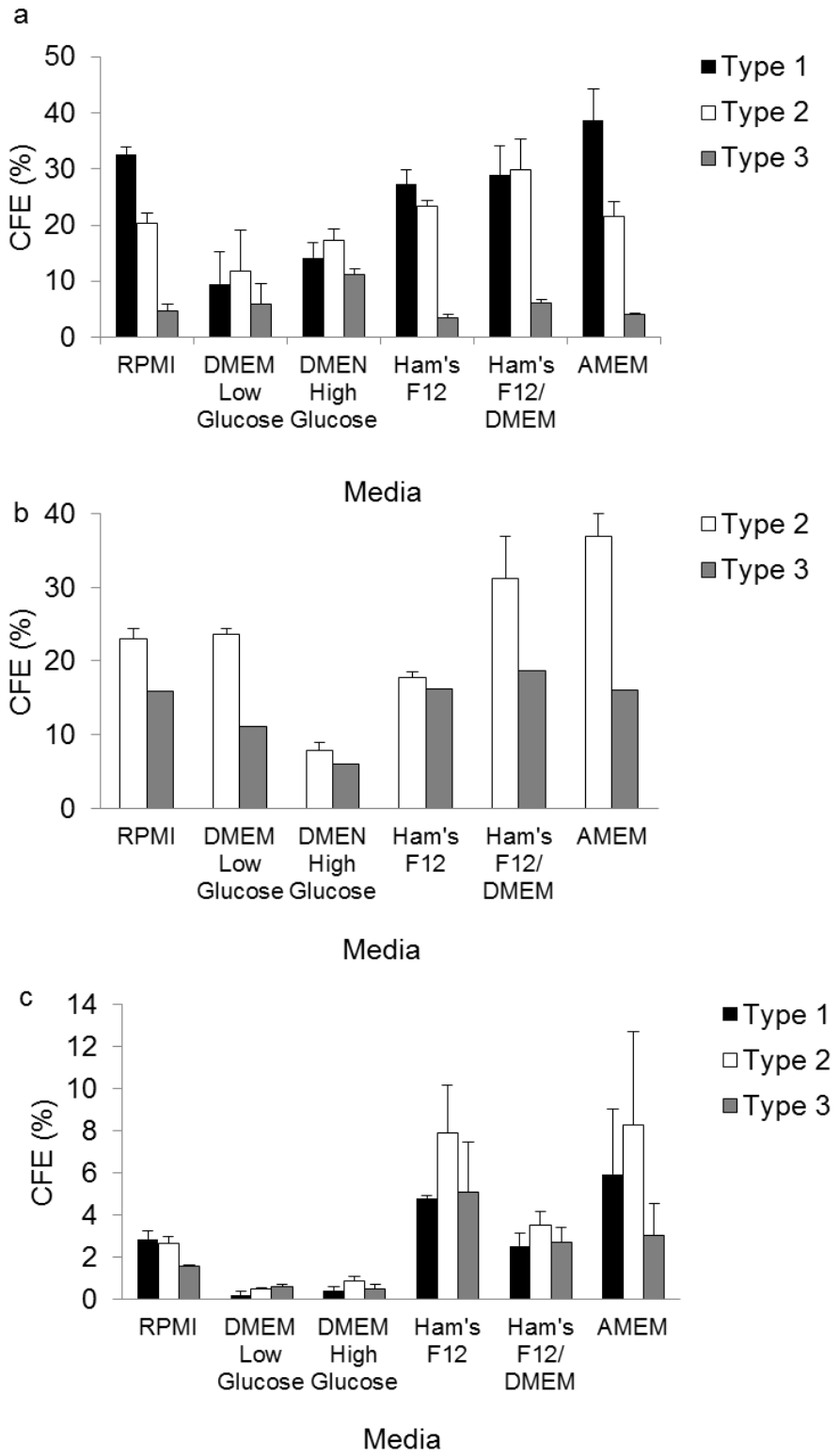

Figure 26. The effect of culture media on colony morphology.

Colony forming efficiency of each colony type formed by the prostate cancer cell lines a) DU145, b) PC-3 and c) LNCaP when cultured as single cells with commonly used substrates in 10% FBS, RPMI-1640. Mean ± S.E.M of three independent experiments .

3.4.5.2 *Media and Colony Size*

In contrast to the clear effects on CFE, there was little or no influence on the area or cell number of the DU145 or LNCaP colonies. However, culture with AMEM did significantly increase the size of PC-3 Type 2 colonies ($p < 0.05$), resulting in some very large colonies. As well as being detrimental to CFE, DMEM also inhibited colony proliferation resulting in significantly smaller PC-3 and LNCaP colonies.

Table 13. Media and Colony Size

Cell Line	Substrate	Type 1		Type 2		Type 3	
		Colony Area (mm2)	Cell Number Per Colony	Colony Area (mm2)	Cell Number Per Colony	Colony Area (mm2)	Cell Number Per Colony
DU145	RPMI -1640	1.66 (0.20)	2442 (288)	0.67 (0.07)	804 (50)	0.71 (0.18)	185 (50)
	DMEM Low Glucose	1.82 (0.15)	2671 (218)	0.97 (0.10)	729 (72)	0.54 (0.10)	142 (25)
	DMEM High Glucose	1.64 (0.26)	2406 (380)	0.65 (0.10)	487 (77)	0.84 (0.28)	221 (74)
	Ham's F12	1.00 (0.16)	1465 (242)	0.54 (0.09)	409 (65)	0.33 (0.19)	87 (50)
	Ham's F12/ DMEM	1.34 (0.22)	1965 (318)	0.64 (0.10)	480 (76)	0.90 (0.32)	235 (83)
	AMEM	1.77 (0.29)	2600 (421)	0.93 (0.15)	699 (111)	0.43 (0.16)	112 (42)
PC-3	RPMI -1640	-	-	2.60 (0.35)	1487 (200)	1.10 (0.1)	153 (13)
	DMEM Low Glucose	-	-	1.72 (0.10)	978 (56)	1.00 (0.2)	140 (27)
	DMEM High Glucose	-	-	1.05 (0.16)	599 (92)	0.70 (0.19)	97 (26)
	Ham's F12	-	-	3.6 (0.39)	2071 (255)	1.36 (0.30)	189 (42)
	Ham's F12/ DMEM	-	-	2.55 (0.31)	1456 (177)	1.27 (0.18)	176 (24)
	AMEM	-	-	4.70 (0.41)	2683 (232)	1.35 (0.08)	188 (10)
LNCaP	RPMI -1640	1.02 (0.14)	-	0.41 (0.19)	-	0.19 (0.01)	-
	DMEM Low Glucose	0.31 (0.04)	-	0.15 (0.04)	-	0.09 (0.02)	-
	DMEM High Glucose	0.63 (0.09)	-	0.14 (0.04)	-	0.23 (0.06)	-
	Ham's F12	0.94 (0.46)	-	0.46 (0.37)	-	0.48 (0.34)	-
	Ham's F12/ DMEM	0.80 (0.02)	-	0.60 (0.00)	-	0.34 (0.17)	-
	AMEM	1.00 (0.03)	-	0.46 (0.15)	-	0.36 (0.06)	-

Colony size and number of cells per colony when cultured with different growth media supplemented with 10% FBS. Twenty colonies of each type were measured for each experimental condition. Mean and S.E.M of three independent experiments in parentheses.

3.4.5.3 *Optimised Conditions*

As each cell line responded differently to the alterations in culture conditions a combination of optimum conditions was defined from the above results. The optimum conditions for each cell line are listed below in Table 14. CFE, number of each colony type and colony size under optimum conditions were compared to standard conditions of culture on tissue culture treated plastic in RPMI-1640 supplemented with 10 % FBS.

Table 14. Optimal Conditions for Clonogenicity of Prostate Cancer Cells.

Cell Line	Seeding Density (cells per dish)	FBS Concentration	Medium	Substrate
DU145	200	20%	AMEM	Collagen
PC-3	200	20%	AMEM	Feeder layer
LNCaP	500	5%	AMEM	Plastic

Only PC-3 cells demonstrated a moderate increase in the CFE when cultured under combined optimum conditions ($p<0.05$), mainly due to an increase in the number of type 2 colonies (Figure 27). DU145 and LNCaP cells showed no advantage of combined optimum conditions. Indeed, DU145 CFE was significantly reduced when cultured in AMEM, with 120% FBS on collagen ($p<0.05$) compared to standard conditions, mainly due to the significant decrease in type 2 colonies ($p<0.01$).

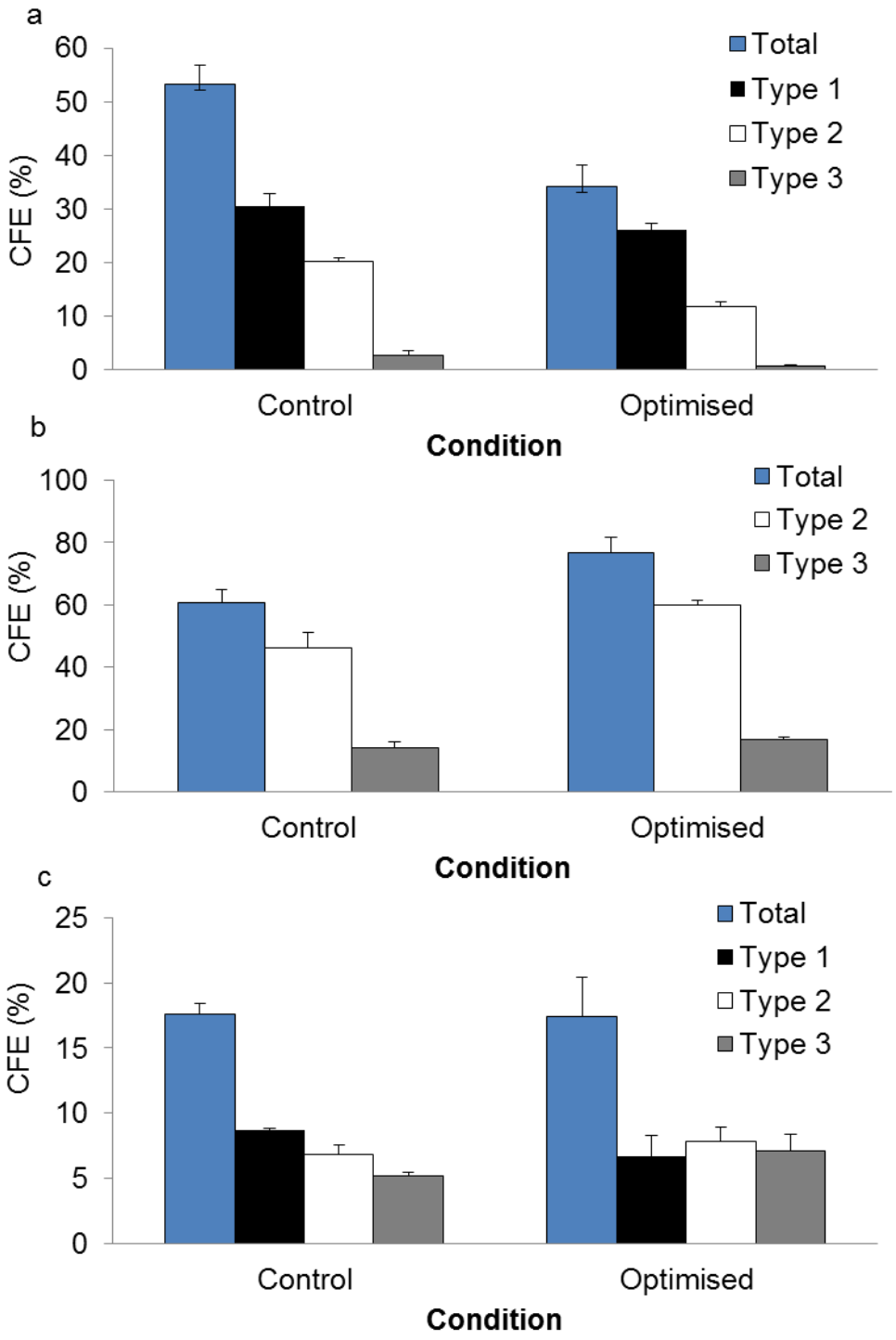

Figure 27. Optimised Colony Forming Efficiency.

The colony forming efficiency and the type of colonies formed when cultured in optimal conditions specific for each cell line, compared to control conditions of 200 cells per tissue culture treated plastic dish, cultured in RPMI-1640 supplemented with 10% FBS. a DU45, b PC-3, c LNCaP. Mean ± S.E.M of 3 independent experiments.

3.4.5.4 *Optimised Colony Size*

Culture in optimised conditions did not increase the size of either LNCaP or PC-3 colonies, however it did result in a significant increase in the size of type 1 and type 3 DU145 colonies from a mean of 2.17mm^2 ± 0.15 to 4.57 ± 0.42 mm^2 (type 1) and 0.23 ± 0.01 mm^2 to 0.59 ± 0.02 mm^2 (type 3), which is over double the number of cells ($p<0.01$).

Table 15. Size of Prostate Cancer Colonies Under Optimised Conditions.

Cell Line	Condition	Type 1		Type 2		Type 3	
		Colony Area (mm2)	Cell Number Per Colony	Colony Area (mm2)	Cell Number Per Colony	Colony Area (mm2)	Cell Number Per Colony
DU145	Control	2.17 (0.15)	3187 (226)	1.25 (0.18)	942 (139)	0.23 (0.01)	59 (4)
	Optimised	4.57 (0.42)	6721 (616)	1.89 (0.22)	1423 (134)	0.59 (0.02)	154 (6)
PC-3	Control	-	-	4.97 (0.24)	2823 (138)	1.12 (0.08)	156 (12)
	Optimised	-	-	5.98 (0.12)	3328 (123)	1.19 (0.11)	166 (16)
LNCaP	Control	1.01 (0.11)	-	0.46 (0.04)	-	0.19 (0.03)	-
	Optimised	0.85 (0.07)	-	0.46 (0.02)	-	0.22 (0.05)	-

Colony size and number of cells per colony when cultured under optimal conditions specific for each cell line compared to control conditions of 200 cells per tissue culture treated plastic dish, cultured in RPMI-1640 supplemented with 10% FBS. Twenty colonies of each type were measured for each experimental condition. Mean and S.E.M of three independent experiments in parentheses.

3.4.6 Incucyte Analysis of Single Cell Cloning

The quality of single cell suspensions for the purpose of cloning has not been checked systematically. Single DU145 cells were seeded into 6 well plates at clonal density and their growth tracked for 14 days by the Incucyte Live Cell Imaging System (Figure 28). In each of five separate experiments, the origins of 30-50 colonies were determined by back-tracking to monitor initial adhesion and subsequent growth. The number of cells at initial cell attachment and whether the cell merged with other colonies was determined.

Although the majority of colonies were derived from single cells, it was observed that some colonies originated from more than one cell or from colonies which merged and by the time of fixation appeared to be one colony (Figure 29). Of the type 1 colonies, 72.9% ± 9.8% were derived from single cells, compared to 89.5 ± 5.2% and 89.2% ± 5.5% of type 2 and 3. Type 1 colonies were more likely to be the product of more than one cell or colonies which had merged. Merged colonies which were indistinct from single cell colonies, merged within 9 days of culture. After 9 days the merged colonies were clearly the product of 2 or more colonies.

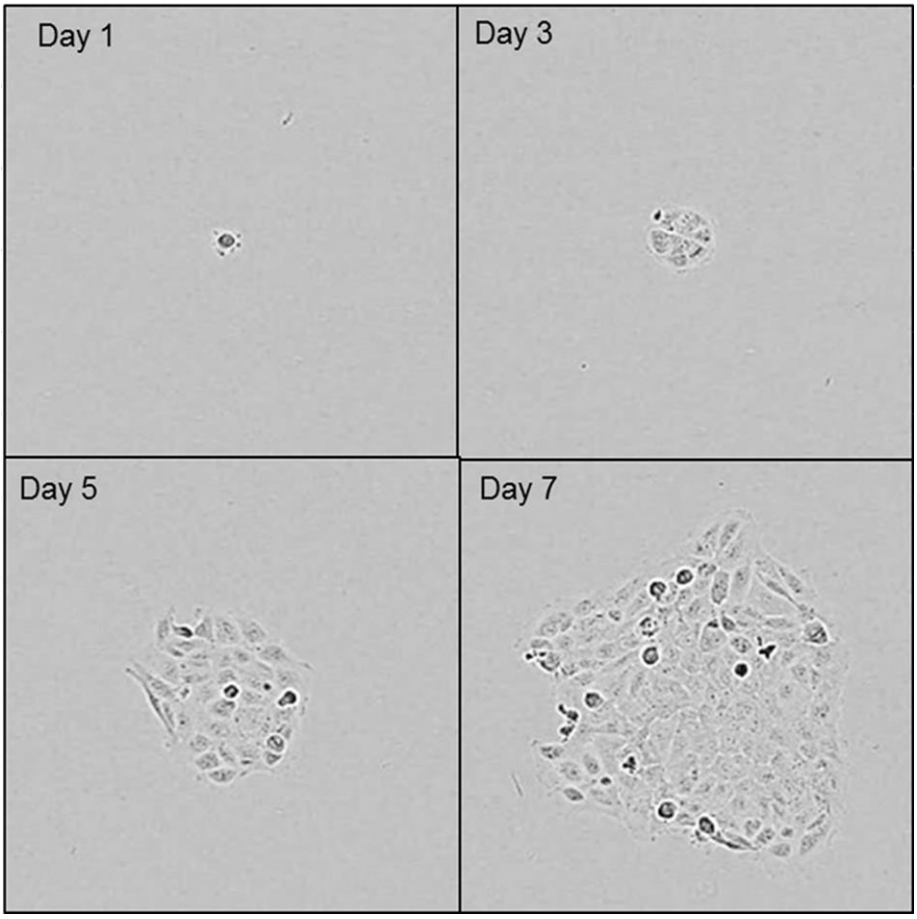

Figure 28. Clonal Tracking of DU145 Colonies.

The origin of colonies were tracked on the Incucyte system to observe the origin of each colony. At day 1 single cells which have adherent to the surface of the plate can be clearly observed.

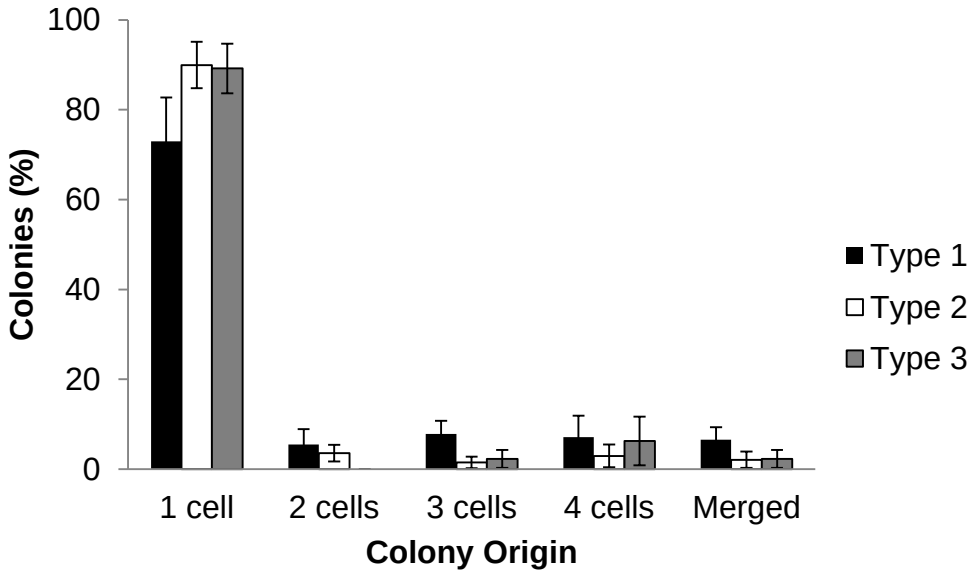

Figure 29. Origin of DU145 Colonies.

DU145 colony growth was tracked by time lapse photography (Incucyte). The number of colonies originating from 1 or more cells was determined. Colonies which were derived from a single cell upon initial adherence, but merged with other colonies were also determined. Results are displayed as mean ± S.E. from 5 independent experiments tracking 40 cells per experiment.

3.5 Discussion

The aim of this study was to identify the types of colonies formed by prostate cancer cell lines and to determine the extent to which the proportion of each colony type and number of cells in individual colonies are altered by culture conditions. The type 1 colonies, were most sensitive to unfavourable culture conditions, but increases in the proportion of type 1 colonies were modest. The results indicate that culture conditions can reduce the proportions of colonies, but can only increase the colony proportion by a small amount compared to our standard conditions. In some cases, cell number, but not CFE, was increased, suggesting that proliferation and colony forming ability are controlled in part by distinct factors.

3.5.1 Clonogenicity and Colony Morphology

The total number of colonies formed (CFE) varied depending on cell line, with approximately 50% of DU145 cells forming colonies compared to less than 5% of LNCaP cells, under standard conditions. Other cell lines also have varying degrees of clonogenicity (Locke et al., 2005, Li et al., 2008, Yu et al., 2008, Pfeiffer and Schalken, 2010). It is likely that the cells that fail to form colonies are killed during passaging or fail to attach upon plating or are terminally differentiated at the time of passage. This difference in colony forming ability clearly suggests that cell line population is highly heterogeneous in terms of their colony forming ability and proliferative capacity. The large range of colony sizes also demonstrates a high degree of heterogeneity within the cell line in terms of population doubling and cell cycle duration. Intrinsic differences in colony forming ability of cell lines suggests that have differing stem cell fractions driving clonogenic growth.

Both DU145 and LNCaP cells form three types of colony. The colonies were similar to the keratinocyte colonies described by Barrandon and Green. Colony definitions were set based on a combination of observations from previous studies and measurements of the colonies seen in this study. It is important to note that the classification of colony morphology is subjective which is why strict criteria were set. In previous studies, the colonies are referred to the Barrandon and Green description of colonies holoclone, meroclone and paraclone which correspond to Type 1, 2 and 3 respectively (Barrandon and Green, 1987b) therefore are predicted to be derived from SC and early and late TACs respectively. Similar colonies have been observed in other cancer cell lines and by Pfeiffer and Schalken (2009) who studied the same cell lines.

Unlike DU145 and LNCaP cells, PC-3 cells did not form colonies with a type 1 morphology, and only formed type 2 and 3 colonies, both of which contained loosely packed cells around the edges. These observations may be due to impaired cell–cell adhesion through E-cadherin due to a lack of alpha-catenin expression in PC-3 cells (Morton et al., 1993). In contrast the study by Li et al (Li et al., 2008) reported the existence of holoclones within the PC-3 cell population. These differences may arise due to the subjective nature of scoring colonies, and there can be overlap between colony types. It is also possible that these differences are due to varying culture conditions between laboratories.

3.5.2 The Effect of Culture Conditions on Clonogenicity

Seeding density had little effect on overall colony forming efficiency or the colony sizes of any of the cell lines tested. Previous studies have suggested that seeding at lower densities may results in an increased number holoclones, but this was not observed in this study (Pfeiffer and Schalken, 2010). However, FBS concentration, substrate and the type of culture medium all had effects on colony formation. The greatest effect was observed when altering FBS concentration. Type 1 and Type 2 colonies tend to be the most sensitive to modifications, whereas type 3 remained relatively stable.

3.5.2.1 *FBS Concentration*

FBS concentration influenced the CFE and colony size of all three cell lines. DU145 and PC-3 cells displayed maximum CFE when cultured with 20% FBS, whilst high serum conditions appeared to be detrimental to the growth of LNCaP. It is worth noting that conditions that were optimal for CFE were also optimal for the growth of Type 1 colonies for both DU145 and LNCaP cells and resulted in the largest colonies, suggesting that Type 1 colonies are most sensitive to changes in FBS concentration.

Only a modest increase in the proportion of Type 1 colonies was observed.. LNCaP have a higher CFE at relatively low FBS concentrations and type 1 colonies were particularly sensitive to toxic effects of high serum concentrations.

FBS concentration routinely varies from 5 and 20% FBS which may account for some differences in observation of CFE, colony morphology and colony size between studies. The content of bovine serum albumin (BSA) and other

proteins and growth factors can vary widely between batches of serum and impede or support cellular growth (Talbot et al., 2004). These results suggest that the concentration of serum used maybe an important factor when designing a clonogenicity experiment as cell lines are affected in different ways, increasing the possibility of getting misleading results and imparing reproducibility. The species of origin of the serum may also significantly alter CFE, particularly when culturing primary cells (Baker et al., 1988). The effect of FBS concentration on colony size has also been studied for the capillary human tumour clonogenic assay (Ali-Osman and Beltz, 1988). Like this study it was observed that the requirements of different primary cultures and cell lines differ with varying culture conditions and each cell type has different requirements. Cells, such as LNCaP, which are androgen receptor positive may be particularly sensitive to hormones contained within FBS (Horoszewicz et al., 1983).

3.5.2.2 *Media*

Type 1 colonies were most sensitive to changes in the type of media. AMEM increased the CFE of all three cell lines and increased the cellular proliferation of Type 1 colonies and Type 2 PC-3 colonies. The effect of media composition on the viability and morphology of cells is well known, (Cox and Gesner, 1968). Despite this, as with FBS, cell lines are routinely cultured in different growth media in different laboratories, which can significantly affect the results of clonogenic assays, due to the wide range of commercially available media which vary in concentration and composition of components such as glucose, amino acids supplements and vitamins. These cell lines, however, may have adapted to their differing culture conditions over time and only one week pre-incubation within this study may not

represent the results of fully conditioned cell lines. An example of this is DMEM which contains 44 mM bicarbonate and is designed for culture at 10% CO_2 atmosphere, however is often incubated in 5% CO_2 (as in this study) which raises the pH of the media and may account for the sensitivity of the cell lines and the lower CFEs observed in this study, as cells are known to be more sensitive to changes in pH at low clonal density, particularly within the first 24 hours of culture (Mackenzie et al., 1961). This also suggests that pH may be a further condition of interest.

3.5.2.3 *Substrate*

Unlike modification of FBS and media, changes in substrate had little effect on the CFE or the types of colony formed, but had a substantial effect on the size of colonies. All three DU145 and LNCaP colony types and type 3PC-3 colony sizes were affected by the substrate used and some particularly large Type 1 colonies were observed when cultured on collagen. These results are in contrast to previous work on keratinocytes in which the type of substrate used had no effect on CFE or colony size (Daniels et al., 1997). Some substrates are known to reduce cell attachment times by interaction with cell surface integrins which increases the number of cell divisions (Engler et al., 2006).

3.5.3 Single Cell Origin

Using the Incucyte to track cell growth it was found that the majority of DU145 colonies are derived from single cells. A proportion of colonies were derived by the fusion of two colonies or from small clumps of cells. It is well known that some cell lines, such as LNCaP, are more prone to clumping and therefore produce fewer single cell derived colonies (Horoszewicz et al.,

1983). Single cell suspension of primary cells can difficult to obtain and require rigorous mechanic and enzymatic digestions, which may damage the cells and result in reduced colony forming efficiency. The type of colonies produced will also be skewed towards larger holoclones.

3.5.4 Chapter 3 Conclusions

This chapter investigated the effect of culture conditions on clonogenicity and colony morphology of prostate cancer cell lines. The aim was test if the proportion of stem cells can be altered by culture conditions. The prostate cancer cell lines DU145 and LNCaP form three types of colony, whilst PC-3 form two. There is some degree of plasticity that enables small modifications in the numbers of type 1, 2 and 3 colony forming cells within a population when culture conditions allow, but there also appears to be factors regulating the proportion of CFE and growth rate. This indicates that heterogeneity and the number of stem cells within prostate cancer cell lines is relatively stable and not a product of the cellular microenvironment, which supports the CSC model. CFE and the proportion of each of the colony type may be controlled by unknown intrinsic mechanisms which control self-renewal and differentiation. Further characterisation of these colonies is required to confirm their identity and once characterised may be a useful model for biomarker discovery which target CSCs and improve understanding of their role in cancer.

4 Chapter 4: Characterisation of Prostate Cancer Colonies

4.1 Chapter Introduction and Aims

Barrandon and Greens work suggests that colonies with holoclone morphology are derived from stem cells with a high proliferative capacity whilst meroclones are derived from transit amplifying cells and paraclones from differentiated cells (Barrandon and Green, 1987b). Only holoclones are capable of extensive proliferation and self-renewal, whilst meroclones have a limited proliferative capacity and cannot self-renew and paraclones are incapable of further proliferation. The terms holoclone, meroclone and paraclone have since become synonymous with colonies derived respectively from stem, early and late stage transit amplifying (Barrandon and Green, 1987b, Pellegrini et al., 1999).

Consequently colony morphology has been used extensively as a surrogate assay to identify and characterise stem cells derived from normal primary tissue including skin (Tudor et al., 2004, Tudor et al., 2007), (Mavilio et al., 2006, Murayama et al., 2007), follicular (Rochat et al., 1994) and limbal (Pellegrini et al., 2001, Shortt et al., 2007) tissues. Holoclones, meroclones and paraclones have also been observed in cancer cell lines, including pancreatic (Jeter et al., 2011), head and neck (Harper et al., 2007), breast (Liu et al., 2012) and prostate cancer (Locke et al., 2005, Wei et al., 2007, Li et al., 2008, Pfeiffer and Schalken, 2010, Zhang and Waxman, 2010, Beaver, 2012) cell lines . In these studies an increased number of holoclones is regarded as enrichment for cancer stem cells (CSC) and used to study CSC marker expression as a surrogate CSC assay.

In the previous chapter, it was observed that the prostate cancer cell lines DU145 and LNCaP form 3 different types of colonies (Beaver, 2012). These colonies are robust and are affected little by varying culture conditions, suggesting an inherent hierarchy within the cell lines in terms of short term proliferative potential. Because we wanted to select stem cells and their progeny for use as targets in phage display experiments, we checked the validity of colony morphology by re-cloning the different colony types. Surprisingly we found that both type 1 and 2 colonies are able to form secondary type 1 colonies (Figure 31). This observation calls into question the widely held and applied assumption that colonies with the three characteristic morphologies are derived from stem, early and late transit-amplifying cells respectively. We therefore set out to re-investigate the relationship between clonogenicity and stem cell capacity by studying the colony forming ability, transplantation capacity and marker expression of each morphological type of colony derived from the prostate cancer cell line DU145. We tested the hypothesis that the colonies differ in the proportion, rather than the presence or absence, of stem cells.

4.2 Hypothesis

On the basis of Barrandon and Greens studies colony morphology reflects the nature of the founding cell. Stem cells form type 1 colonies (holoclones), whilst transit amplifying cells form type 2 colonies (meroclones) and late transit amplifying cells form type 3 colonies (paraclones). Colonies that contain stem cells have an infinite proliferative potential, can self-renew and are tumourigenic.

4.3 Objectives

To test this hypothesis that the three types of colony derived from DU145 cells were compared for their ability to self-renew, differentiate and form tumours *in vivo*. These features were investigated using the following experiments:

1. Serial cloning to test long term proliferative capacity
2. Serial passage in bulk culture to test long term proliferative capacity of the entire colony.
3. Sphere formation in non-adherent conditions to determine self-renewal capacity.
4. Serial xenotransplantation in Nude mice.
5. Immunocytochemistry to examine expression of differentiation and stem cell markers.

4.4 Material and Methods

To characterise DU145 colonies each colony type, identified in chapter 2, was compared for serial clonogenicity, long term serial passage ability, capacity for form spheres in non-adherent conditions, tumourigenicity and stem cell marker expression. This experimental plan is shown in Figure 30.

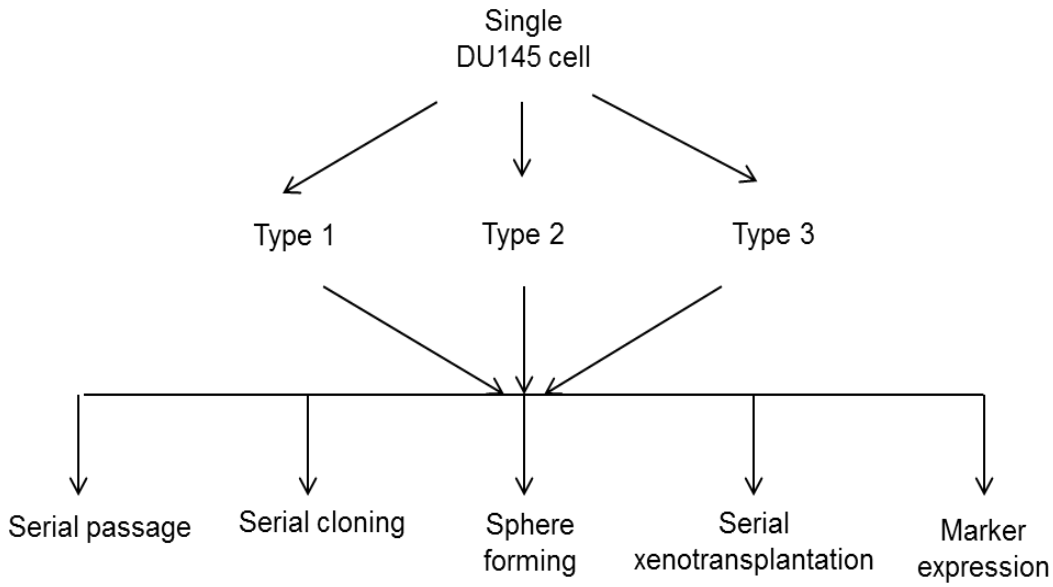

Figure 30. Characterisation of DU145 Colonies Experimental Plan.
Single DU145 cells form colonies of three types, with distinct morphologies, termed type 1, 2 and 3. The stem cell traits of self-renewal, proliferative capacity, tumourigenicity and differentiation of each colony were compared by serial passage, serial cloning, sphere formation, serial xenotransplantation and marker expression.

4.5 Results

4.5.1 Secondary Cloning

In order to measure secondary CFE, 30 colonies of each type of colony were cloned and plated at 200 cells/6cm dish in triplicate and the numbers of each type of colony produced were measured (Figure 31). Type 1 and 2 colonies produced similar numbers of secondary colonies overall with CFEs of 32.8 ± 3.2 % and 32.5 ± 3.3% respectively, whereas type 3 colonies produced few or no secondary colonies. The main difference between type 1 and 2 colonies was the number of secondary type 1 colonies each produced. Type 1 colonies produced mainly type 1 colonies (19.5 ±2.2%), whereas type 2 colonies produced slightly more type 2 colonies (16.3 ± 1.9%) than type 1 ($p>0.05$, 2-tailed independent t-test).

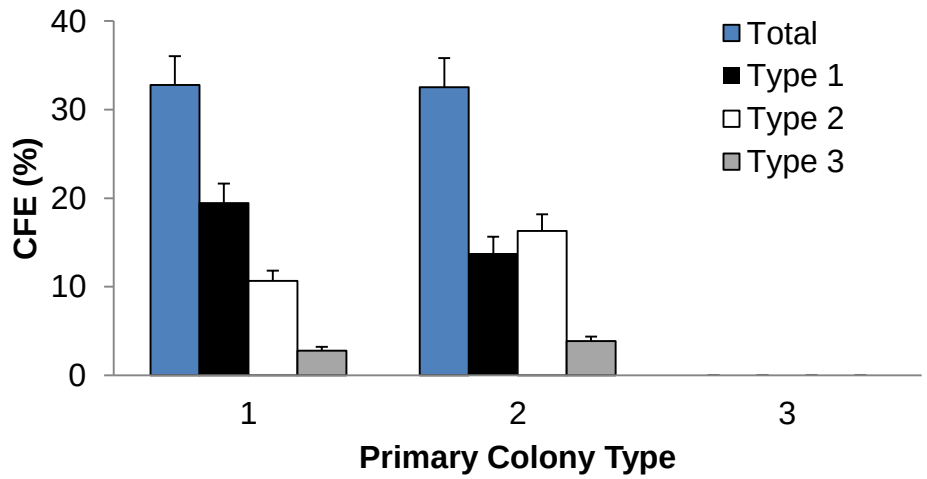

Figure 31. Types of Secondary Colonies.
DU145 colonies of each morphology were ring cloned and cultured at clonal density and the number and type of secondary colonies was observed. Mean ± S.E.M. of three individual experiments.

The relationship between colony size and ability to form a clone was also analysed. There is no clear relationship between type 1 or 2 colony size and colony forming efficiency, as shown in Figure 32. Small original colonies were just as likely to have high secondary CFEs as large ones. However colonies with a CFE of less than 10% were all derived from type 2 colonies containing fewer than 1200 cells.

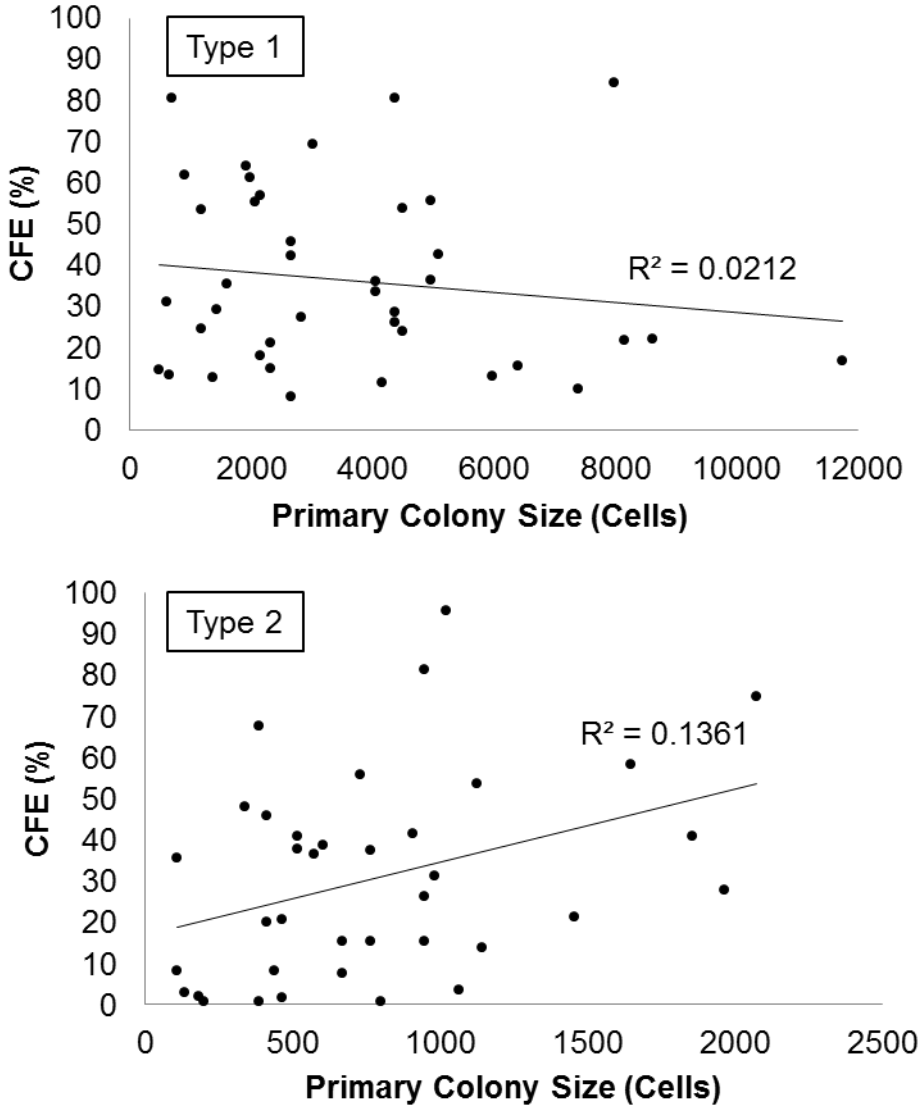

Figure 32. The Relationship Between Colony Size and Secondary CFE.
DU145 colonies were measured to determine the number of cells per colony. Colonies were cloned and cultured at 200 cells per dish to determine secondary CFE.

4.5.2 Serial Cloning

In order to measure the serial colony forming capacity of each colony type, 3 type 1 and 3 type 2 colonies were picked, and re-cloned at 200 cells/6cm dish in triplicate. Each colony was serially cloned a further 16 times or until terminal. Type 1 colonies derived from type 2 colonies were also serially cloned. Based on the estimate of the number of cells in each colony, it was possible to calculate the number of cell divisions needed to produce each colony, although this calculation assumed no cell loss and identical reproductive capacity throughout the colony.

Type 1 colonies are able to reproduce colonies of all three types over the 17 generations of this study (Figure 33), which is equates to more than 200 populations doublings (Table 16). Type 2 colonies were terminal after 6-8 generations following about 66 population doublings. Type 1 colonies derived from an initial type 2 colony underwent at least 117 population doublings before termination after 9-11 generation. These colonies were smaller than the type 1 colonies derived from a type 1 colony (Table 16).

CFE and colony morphology were more stable and consistently higher within the type 1 lineage cultures than type 2. From the second generation onwards, the ability of type 2 colonies to form further colonies gradually declines, until terminal. Type 1 colonies from an initial type 2 colony demonstrate an initial CFE similar to type 1, which is stable until about 4-5 generations, but gradually declined until terminal.

The proportion of the types of colonies was also altered over the generations of cloning. Initially both type 1 and 2 colonies produce all three colony types, but in subsequent generations the colonies formed by type 2 colonies shift

towards the more differentiated colony type. Although initially type 2 colonies can form all three colony types, second generation and onwards clones are mainly type 2 and 3 colonies and only very rare type 1 colonies were observed after 4 generations. Type 1 colonies demonstrated a stable CFE and proportion of each colony type throughout each generation, with type 1 the dominant colony morphology. Type 1 colonies from an initial type 2 colony generated all three colony types at each generation, but the proportion of type 2 colonies decreased along with reduced CFE, possibly due to their smaller size.

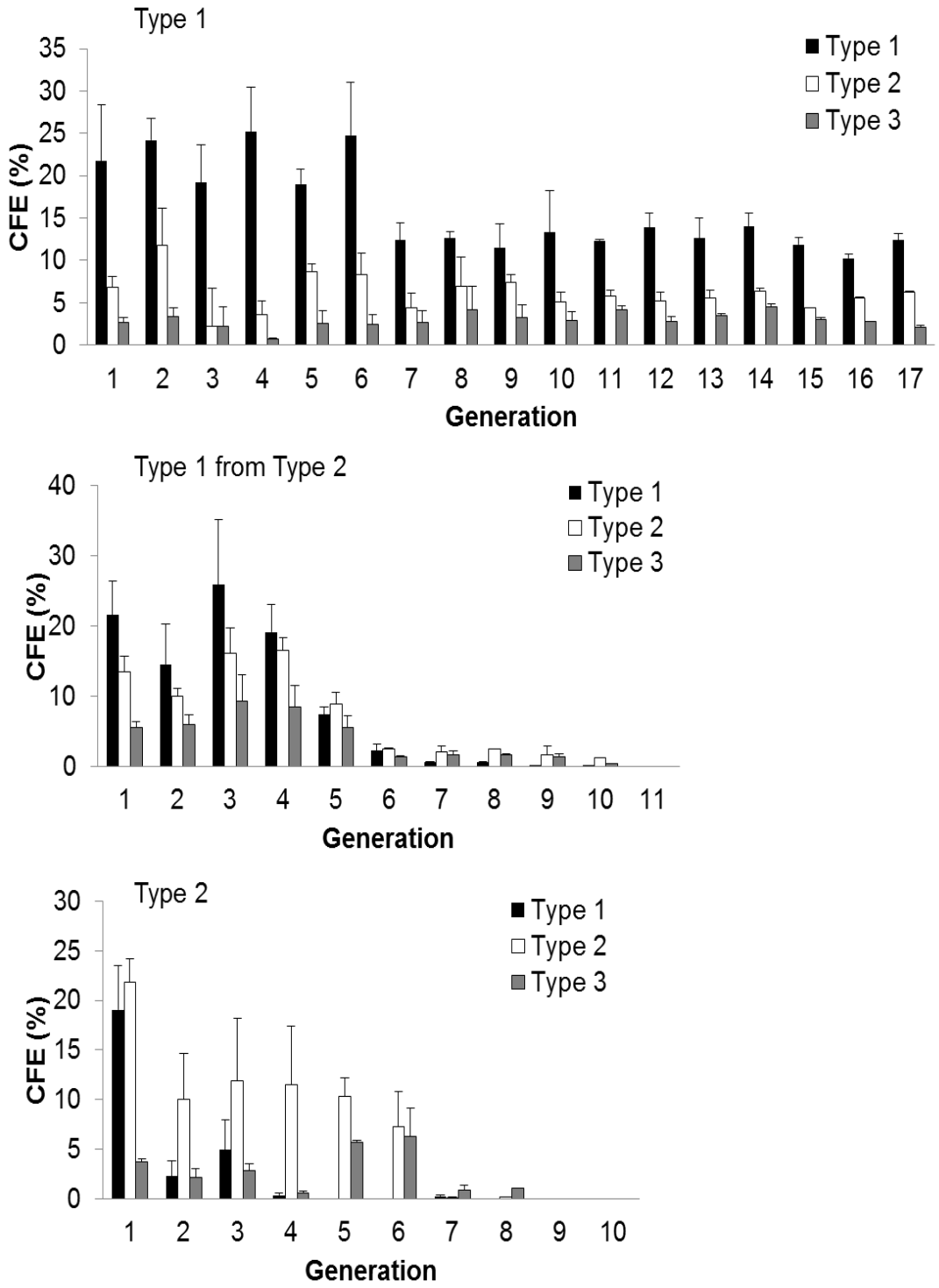

Figure 33. Serial Cloning of DU145 colonies.

Type 1, 2 and 3 DU145 colonies were serially cloned and the number and type of subsequent colonies was at each generation was observed. Mean and S.E.M of three individual experiments.

Table 16. Serial Cloning Population Doublings

Generation	Type 1	Type1 from Type 2	Type 2
1	3222 (11)	1650 (10)	1650 (10)
2	4385 (12)	2752 (11)	801 (9)
3	11700 (13)	3728 (11)	1104 (10)
4	3320 (11)	5344 (12)	1364 (10)
5	7695 (12)	3029 (11)	668 (9)
6	3521 (11)	2843 (11)	947 (9)
7	5470 (12)	1849 (10)	636 (9)
8	3029 (11)	1923 (10)	-
9	7847 (12)	2237 (11)	-
10	3728 (11)	665 (9)	-
11	12693 (13)	3222 (11)	-
12	9728 (13)	-	-
13	8789 (13)	-	-
14	9273 (13)	-	-
15	7249 (12)	-	-
16	5221 (12)	-	-
17	7889 (12)	-	-
Total Number of Divisions	**204**	**117**	**66**

Each colony type was serially cloned and the proliferative capacity of each clone determined. Colony size was used to estimate the number of cell divisions at each generation displayed as mean cell number and minimum number of cell divisions in brackets. The sum of divisions at each generation provides an estimate of how many total cell divisions the original cell which formed the original colony of each type can undergo. Results are the mean of three (type 1 and type 2) or two experiments (type 1 from type 2).

4.5.3 Serial Passage in Bulk Culture

In order to demonstrate infinite proliferative capacity at high cell density, in three separate experiments 5 holoclones and 5 meroclones were ring-cloned and transferred to T25cm flasks for serial passaging under routine maintenance conditions. The number of colonies surviving to 20 passages is shown in Table 17. 14/15 Type 1 colonies and 10/15 Type 2 colonies reconstituted the DU145 monolayer and were passaged at least 20 times. Again no type 3 cells were observed to adhere to the tissue culture flask or survived to become confluent.

Initially, cells from type 1 grew faster than those from type 2 colonies and reached confluence in an average of 23 ±10 days compared to 35 ± 12 days. However, after 4 weeks, the growth rates of cells derived from the 2 colony types were similar and each clone reverted to the typical morphology of DU145 cells grown in a monolayer.

Table 17. Proliferative Capacity of Each Colony Type.

Colony Type	Survival	Time to reach 20 passages in days (mean ± S.E.M)
1	14/15 (93%)	70 (14)
2	10/15 (67%)	82 (14)
3	0/15 (0%)	-

Number of DU145 colonies that could be passaged more than 20 times and how long it took each colony become initially confluent. Each colony type was serially passaged and the proliferative rate and time to reach confluence was monitored.

4.5.4 Sphere Formation

Non-adherent culture and the formation of spheres is frequently used as an assay for self-renewing stem cells (Reynolds and Weiss, 1992). In three separate experiments, three colonies of each type were harvested and plated at 1000 cells/well of a 6 well plate in triplicate in Matrigel. The sphere forming efficiency of each colony type was determined as a percentage of the number of cells seeded. Spheres were identified after two weeks incubation under non-adherent conditions (Figure 34). Cells that had formed misshapen aggregates which clumped and were not of a uniform shape were not counted and it was deemed that these were senescent, dead cells and debris (Schatton and Frank, 2010).

Type 1 colonies had a sphere forming efficiency of 15.3% ± 3.1% compared to 5.9% ± 2.7% for type 2 colonies ($p<0.05$). The spheres formed by type 1 colonies were also larger than those of type 2 colonies: mean diameter 105 µm ± 5.1 µm versus 63 µm ± 6.3 µm. Type 3 colonies were unable to form spheres.

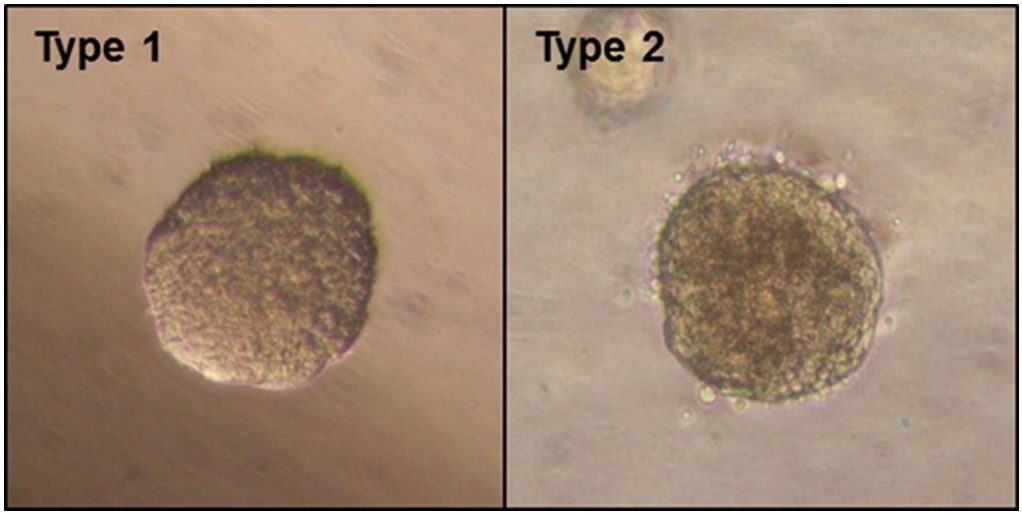

Figure 34. DU145 spheres.
Single cells derived from type 1 and 2 colonies form spheres when cultured for 2 weeks in 1:1 Matrigel^{TM}: growth medium.

4.5.5 Tumourigenicity

DU145 Colonies of each type were transplanted subcutaneously into the flanks of nude mice. The data for the type 1 colonies were based on individual colonies, whereas those for type 2 and 3 colonies were based in part on more than one colony being combined to produce the number of cells required.

Both type 1 and 2, but not type 3 colonies, were able to initiate tumor development in nude mice (Table 18), as confirmed by tumour histology (Figure 35). There was little difference between type 1 and 2 colonies in their ability to develop cancers and as few as 1000 cells from either type were able to generate tumours, shown *in situ* in Figure 35. The colonies produced fewer tumours than a monolayer, but latency and final tumour weights were comparable.

The main differences between tumours derived from type 1 and type 2 colonies were latency and final tumour weights. One average, type 2 derived tumours were palpable 10 days later than type 1 derived tumour. Tumours formed by an injection of only 1000 type 2 cells took at least 61.5 ± 3.2 days to become palpable compared to 49.5 ± 12.6 days for 1000 type 1 cells. Tumours from 1000 type 2 cells did not grow as large over the 12 week period as the type 1 derived tumours and weighed only 32 ±12 mg following dissection compared to 147 ± 78 mg for the same number of type 1 derived cells ($p<0.05$) .

Table 18. Tumorigenicity of DU145 colonies

Cell Type	No. cells injected	Tumor Incidence	Latency in days (S.E.)	Tumor Weight in mg (S.E.)
DU145 Monolayer	10000	5/6	37.8 (11)	79 (49)
	1000	4/8	41.8 (9)	194 (163)
Type 1	10000	4/9	30.5 (8)	171 (28)
	1000	4/12	49.5 (12.6)	147 (78)
Type 2	10000	2/7	47 (4)	154 (57)
	1000	4/16	61.5 (3.2)	32 (12)
Type 3	1000	0/4	-	-
VC	0	0/12	-	-

DU145 colonies were pooled and were injected subcutaneously into the flanks of nude mice in a mixture of 1:1 Matrigel^{TM} in RPMI-1640. Vehicle control (VC) animals received an injection of Matrigel^{TM} in RPMI alone. Tumour latency was determined on the basis of the first day tumours were palpable and animals sacrificed after 12 weeks and tumours weighed.

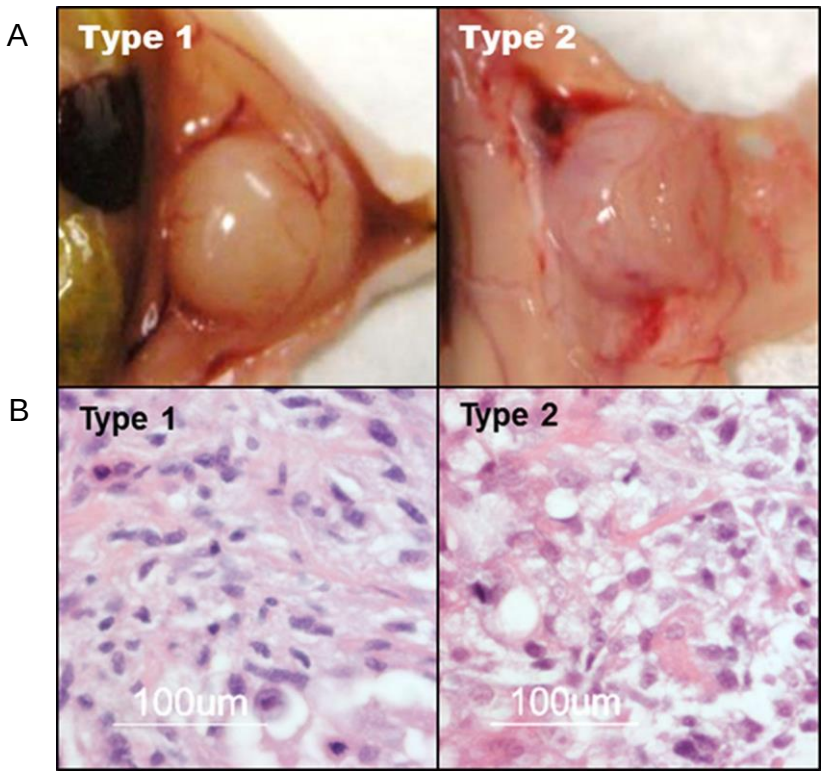

Figure 35. Tumours derived from DU145 colonies.
Cells from DU145 colonies were injected subcutaneously into the flanks of nude mice. A. Representative tumours *in situ*. B. H&E stained tumour sections.

Tumour volume was measured weekly and is plotted in Figure 36. Type 1 colonies had a shorter latency and faster growth rate than type 2 colonies or cells grown in a monolayer, when injected at a density of 10000 cells per injection site. When transplanted with 1000 cells the tumours derived from a monolayer and type 1 colonies exhibited similar growth rates which faster than those derived from type 2 colonies.

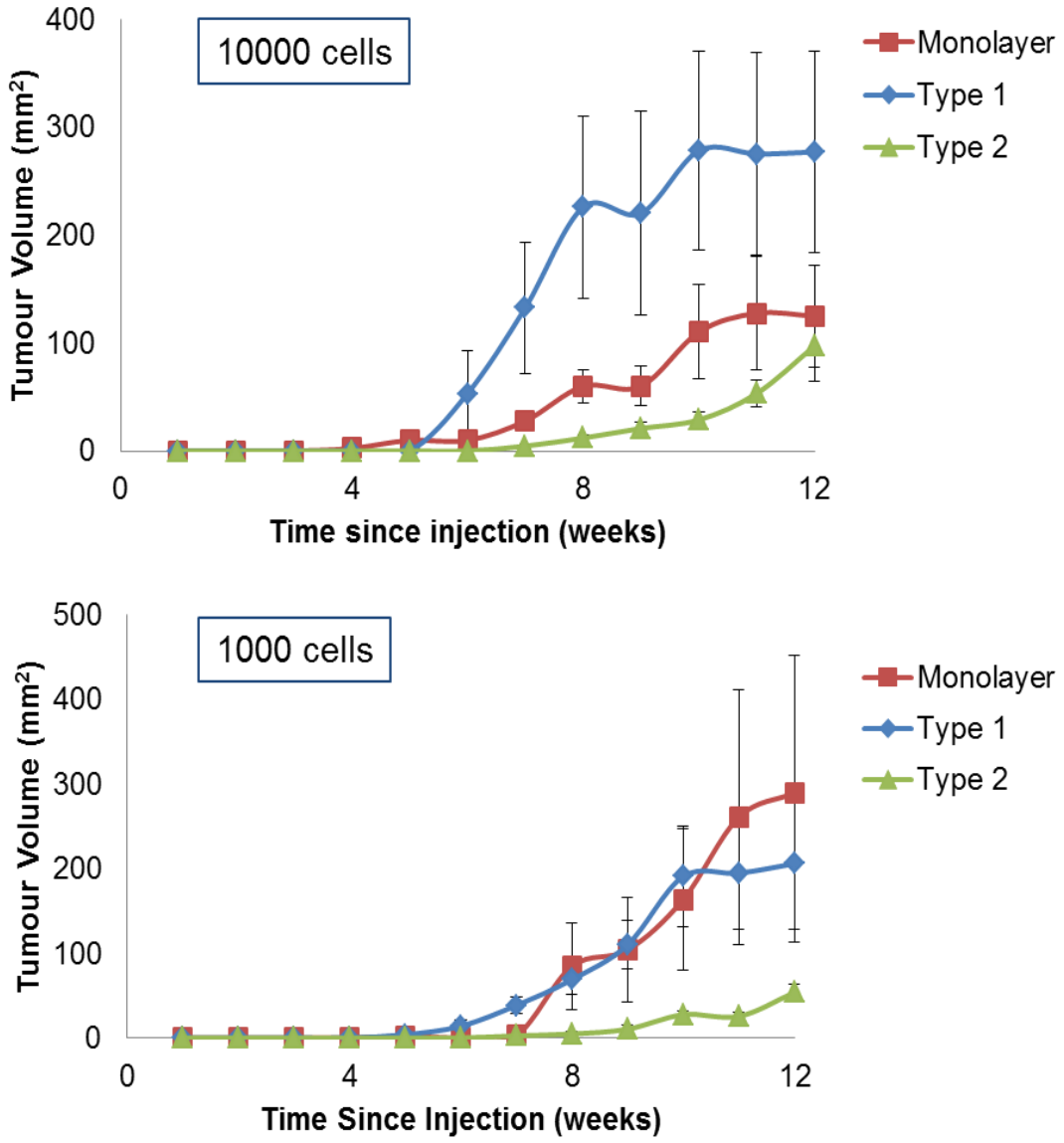

Figure 36. DU145 tumour growth rates.

10000 or 1000 DU145 cells derived from either type 1 or type 2 colonies or a monolayer were injected subcutaneously into the flanks of nude mice. The tumours were measured by digital callipers across 2 diameters at 180° weekly and tumour volume calculated (mean ± S.E.M)

Cells were isolated from the transplanted tumours and cultured in vitro in a clonogenic assay and recapitulated the three colony types in similar proportions to the original cell line (Figure 37). The overall CFE was lower than the original cell line due to high cell death during tissue digestion and obtaining a single cell suspension.

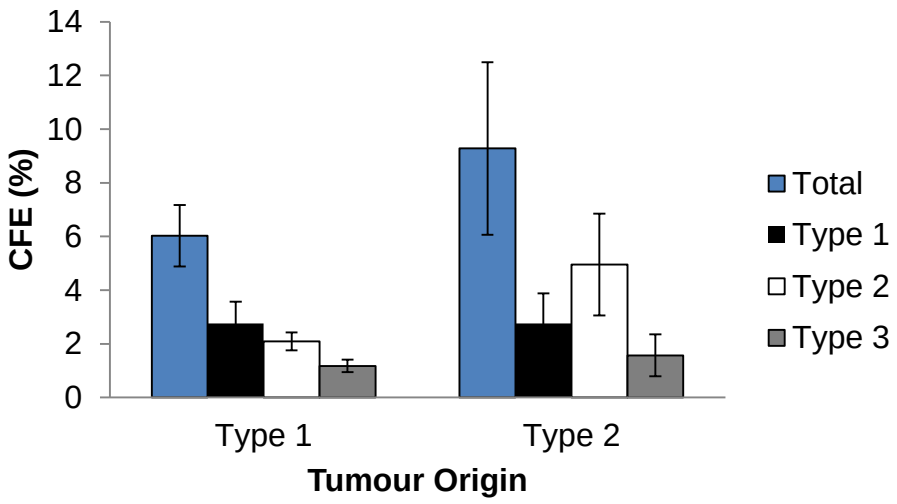

Figure 37. Clonogenicity of DU145 Derived Tumours.
Following dissection, tumours were digested in collagenase to produce a single cell suspension. 200 cells were seeded into petri dishes to determine colony forming efficiency (%) and the types of colonies formed by tumours of parent colonies. Bars represent the mean and SEM of 4 individual tumours.

4.5.5.1 *Secondary Tumourigencity*

To determine if tumours could be serially transplanted, tumours derived from type 1 and 2 colonies were digested, expanded and injected subcutaneously into the flanks of secondary mice. Both type 1 and 2 derived tumours formed secondary tumours at the same efficiency of 2/6 injections (Table 19). The latency of type 2 derived tumours was longer than tumours from type 1 colonies, but there was no difference in final tumour size.

Table 19. Secondary Tumourigenicity

Cell Type	No. cells injected	Tumor Incidence	Latency in days (S.E.M)	Tumor Weight in mg (S.E.M)
Type 1	10000	2/6	38.5 (2.4)	165.5 (73)
Type 2	10000	2/6	50 (9)	105 (45)
VC	0	0/6	-	-

Cells derived from primary DU145 tumours were injected subcutaneously into the flanks of nude mice in a mixture of 1:1 Matrigel™ in RPMI-1640. Vehicle control (VC) animals received an injection of Matrigel™ in RPMI alone. Tumour latency was determined on the basis of the first day tumours were palpable and animals sacrificed after 12 weeks and tumours weighed.

4.5.6 Marker Expression

DU145 colonies were cultured in 24 well plates, fixed with PFA and stained with antibodies against Ki67, K5, K18, $\alpha_2\beta_1$ integrin, CD44, Bmi1 and Oct4. Cells were imaged by fluorescent confocal microscopy and the number of positive cells was determined, as shown in Figure 55. All results are the mean and SE of three experiments, in which at least 10 colonies were counted.

4.5.6.1 *Ki67 – Proliferation*

Ki67 expression is a marker for proliferative cells and is absent from resting (G_0) cells. Type 1 colonies (Figure 38) contained the most (86.6 ± 3.6%) proliferating cells compared to 71.7 ± 3.3% in type 2 (Figure 39) and 58.9 ± 7.5% in type 3 (Figure 40) colonies. Ki-67 expression was spread evenly throughout the colonies with similar proportions of dividing cells in the middle and outer edges of the colony.

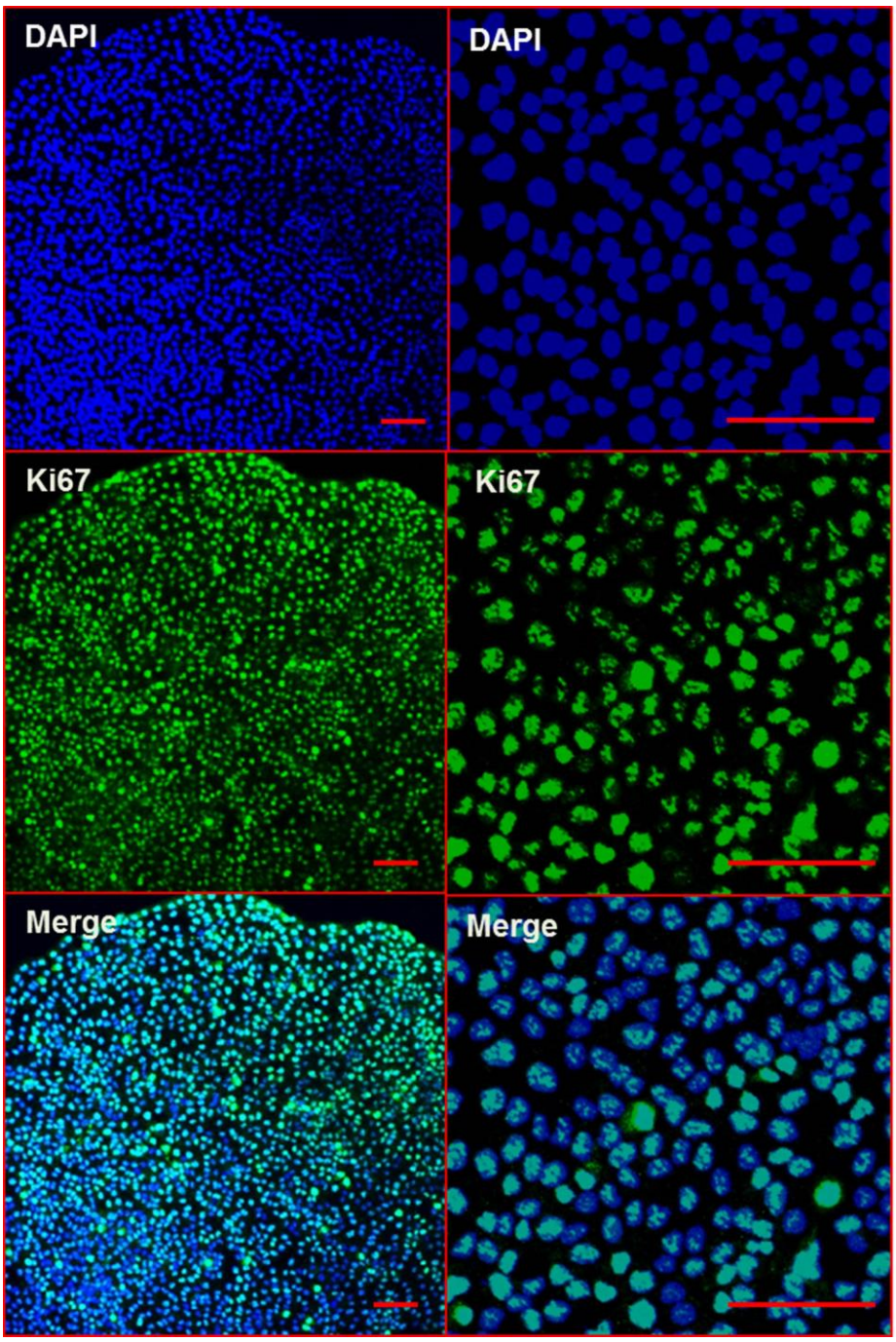

Figure 38. DU145 Type 1 Ki67 Expression

The proliferative fraction of DU145 type 1 colonies types was determined by Ki67 staining. The percentage of Ki67 positive cells was determined by counting the number of green (FITC) cells as a proportion of blue DAPI positive nuclei. Representative colonies shown. Bar = 100µm.

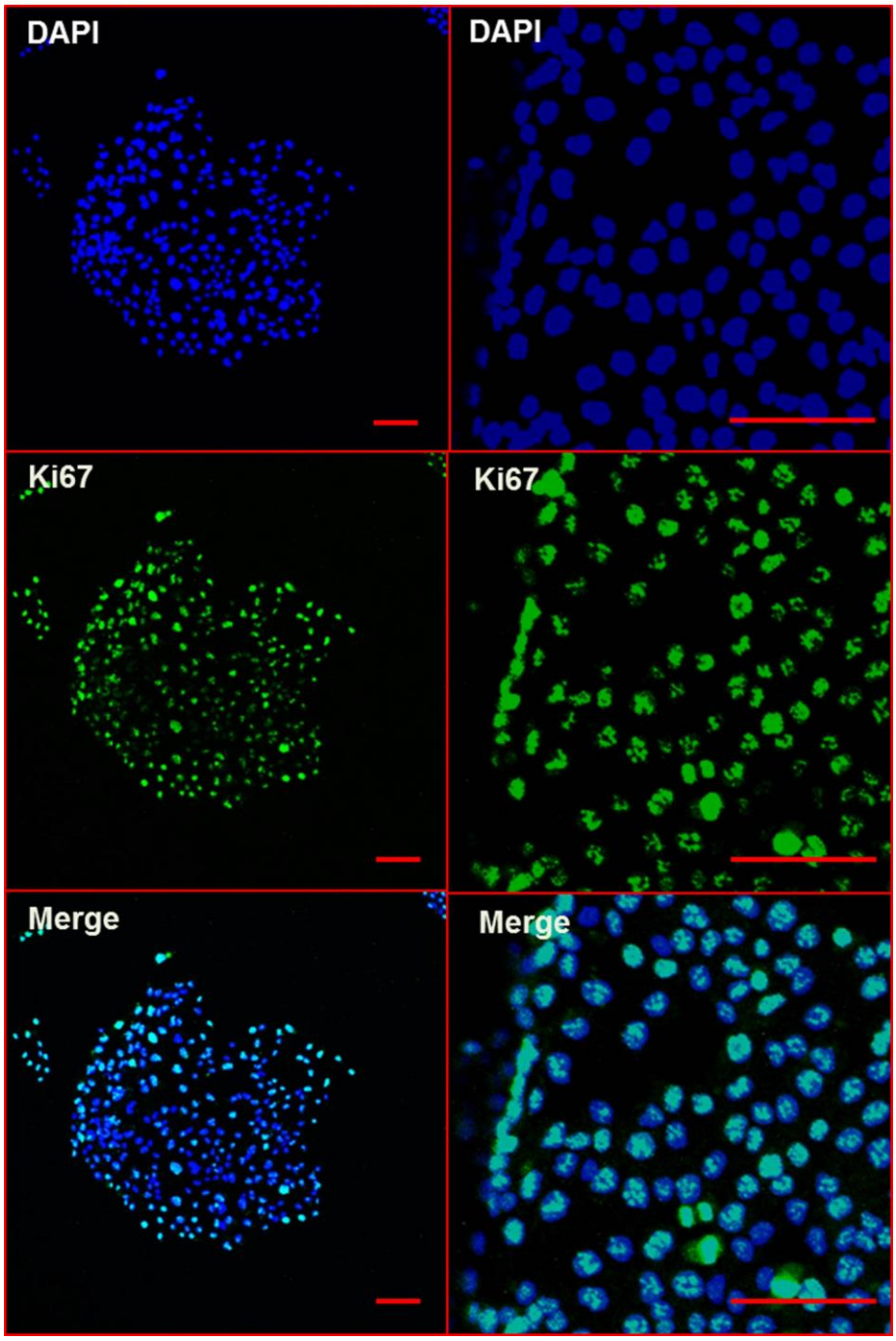

Figure 39. DU145 Type 2 Ki67 Expression

The proliferative fraction of DU145 type 2 colonies types was determined by Ki67 staining. The percentage of Ki67 positive cells was determined by counting the number of green (FITC) cells as a proportion of blue DAPI positive nuclei. Representative colonies shown.

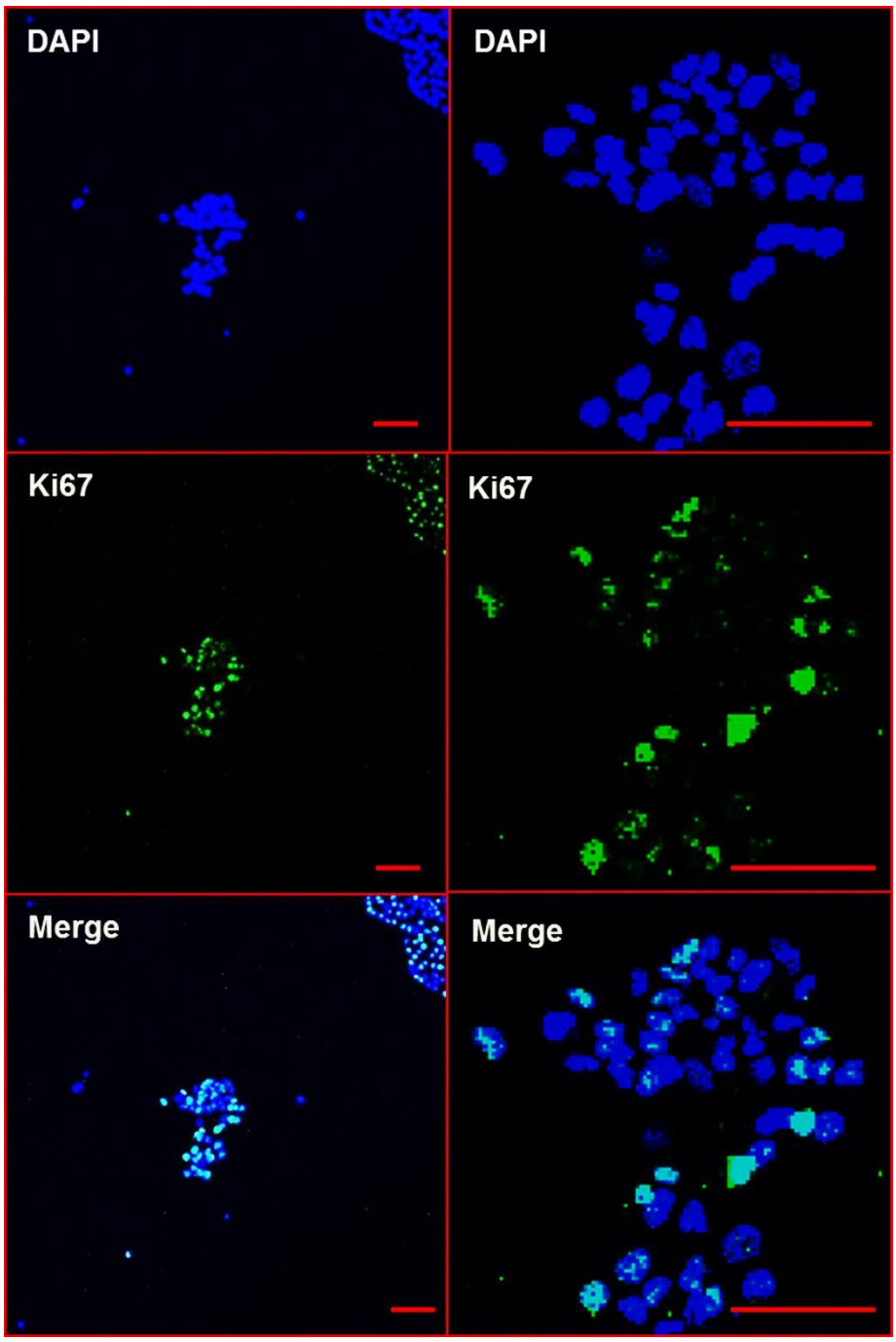

Figure 40. DU145 Type 3 Ki67 Expression

The proliferative fraction of DU145 type 3 colonies types was determined by Ki67 staining. The percentage of Ki67 positive cells was determined by counting the number of green (FITC) cells as a proportion of blue DAPI positive nuclei. Representative colonies shown. Bar = 100µm

4.5.6.2 *Cytokeratin Expression*

Colonies were stained for K5 expression, a basal epithelial marker and K18 a luminal epithelial marker in prostate cells. No K5 expression was observed in any of the three colony types (Figure 41). In contrast, all three colony types were positive for K18 which was expressed evenly throughout the colony as (Figure 42).

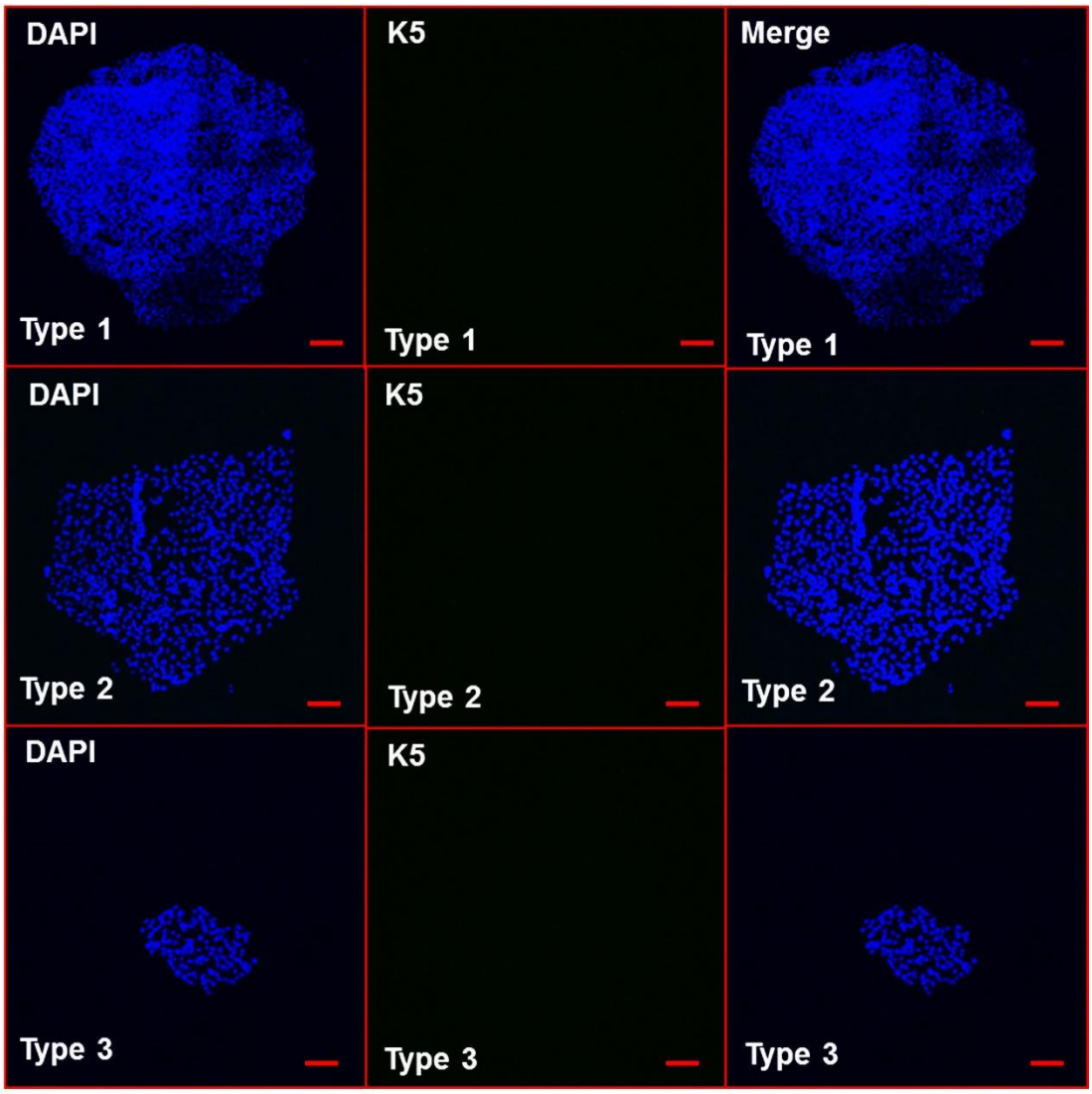

Figure 41. DU145 Cytokeratin 5 Expression

Lack of expression of the basal epithelial marker K5 by DU145 colonies. Type 1, 2 and 3 colonies were stained by immunocytochemistry with monoclonal antibodies against the target and detected with a FITC conjugated secondary antibody (green) and counter stained with DAPI (blue). Representative colonies shown. Bar = 100µm.

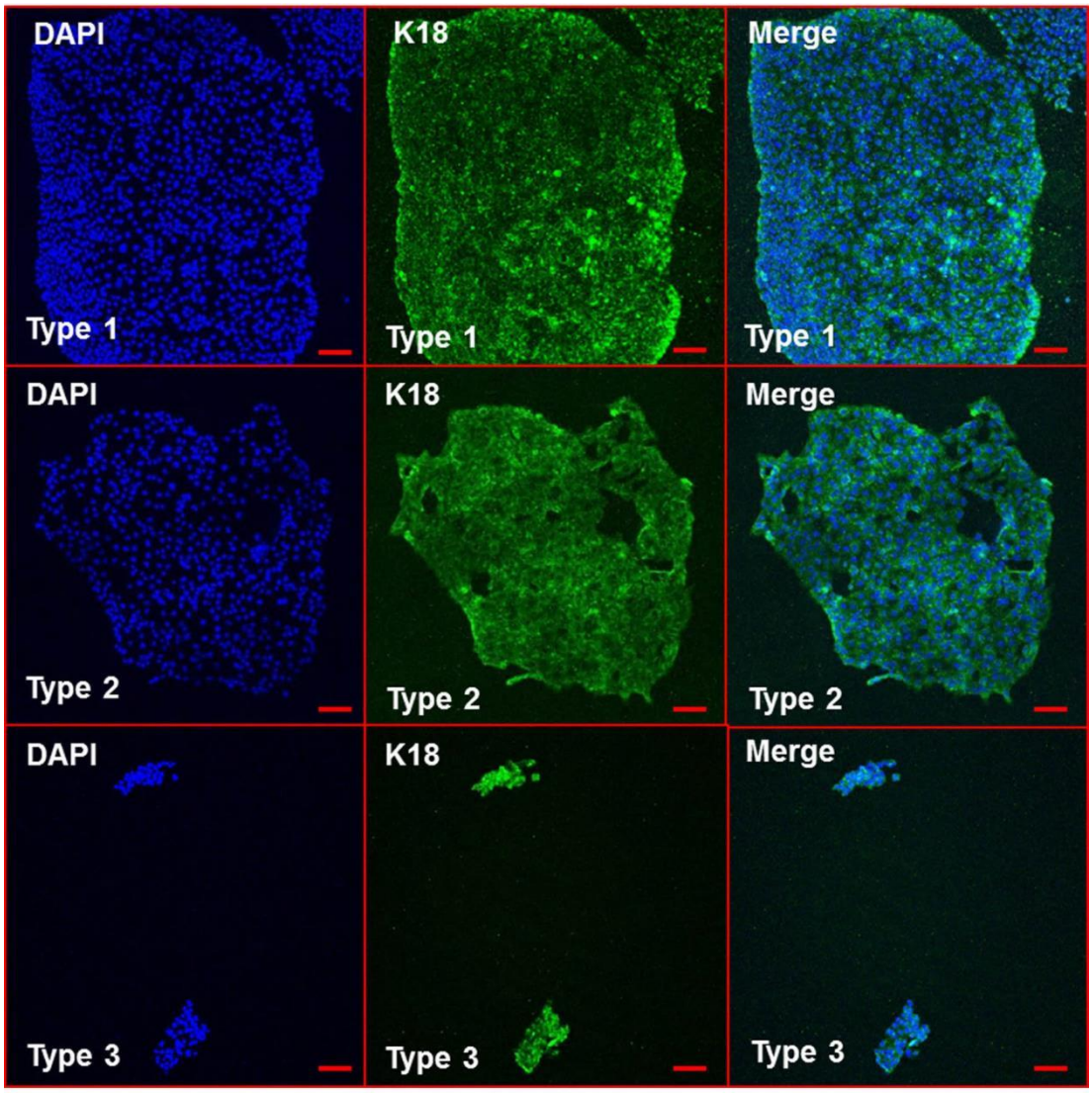

Figure 42. DU145 Cytokeratin 18 Expression

Expression of the luminal epithelial marker CK18 by DU145 colonies. Type 1, 2 and 3 colonies were stained by immunocytochemistry with monoclonal antibodies against the target and detected with a FITC conjugated secondary antibody (green) and counter stained with DAPI (blue). Representative colonies shown. Bar = 100µm.

4.5.6.3 *Putative Stem Cell Marker Expression*

DU145 colonies were stained for the putative cancer stem cell markers α2β1, CD44 Oct4 and Bmi1. Only type 1 and 2 colonies contained cells which express the cell surface integrin α2β (Figure 43 to Figure 45). Type 1 colonies stained more brightly than type 2 colonies, especially at colony edges, and contained significantly more positive cells: 76.2 ± 7.0% compared to 13.3 ± 3.0 % ($p < 0.05$). All three types of DU145 colony contained cells which expressed CD44 (Figure 46), but type 1 and 2 colonies contained more positive cells than type 3 ($p<0.05$, One-way ANOVA). Again staining tended to be brighter at the colony edge, particularly in type 1 colonies.

Oct4 and Bmi1 were expressed in the cytoplasm and nucleus of type 1 and 2, but not type 3 colonies, as shown in Figure 49 to Figure 51 and Figure 52 to Figure 54. Unlike CD44 and α2β integrin, cells staining intensity was spread evenly throughout the colony.

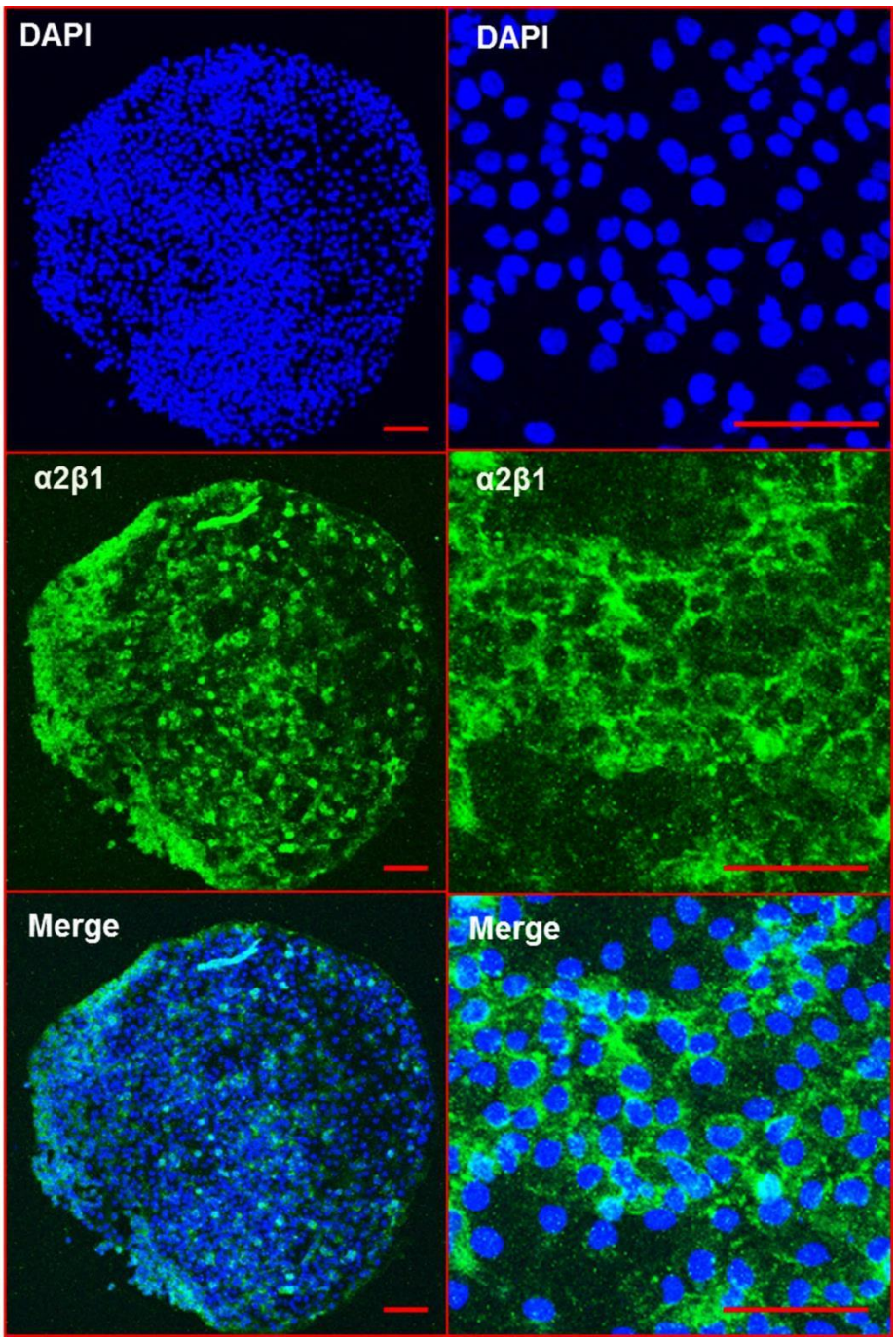

Figure 43. DU145 Type 1 α2β1 integrin Expression

Expression of the putative prostate cancer stem cell marker α2β1 integrin by DU145 colonies. Type 1 colonies were stained by immunocytochemistry with monoclonal antibodies against the target and detected with a FITC conjugated secondary antibody (green) and counter stained with DAPI (blue). Representative colonies shown. Bar = 100µm.

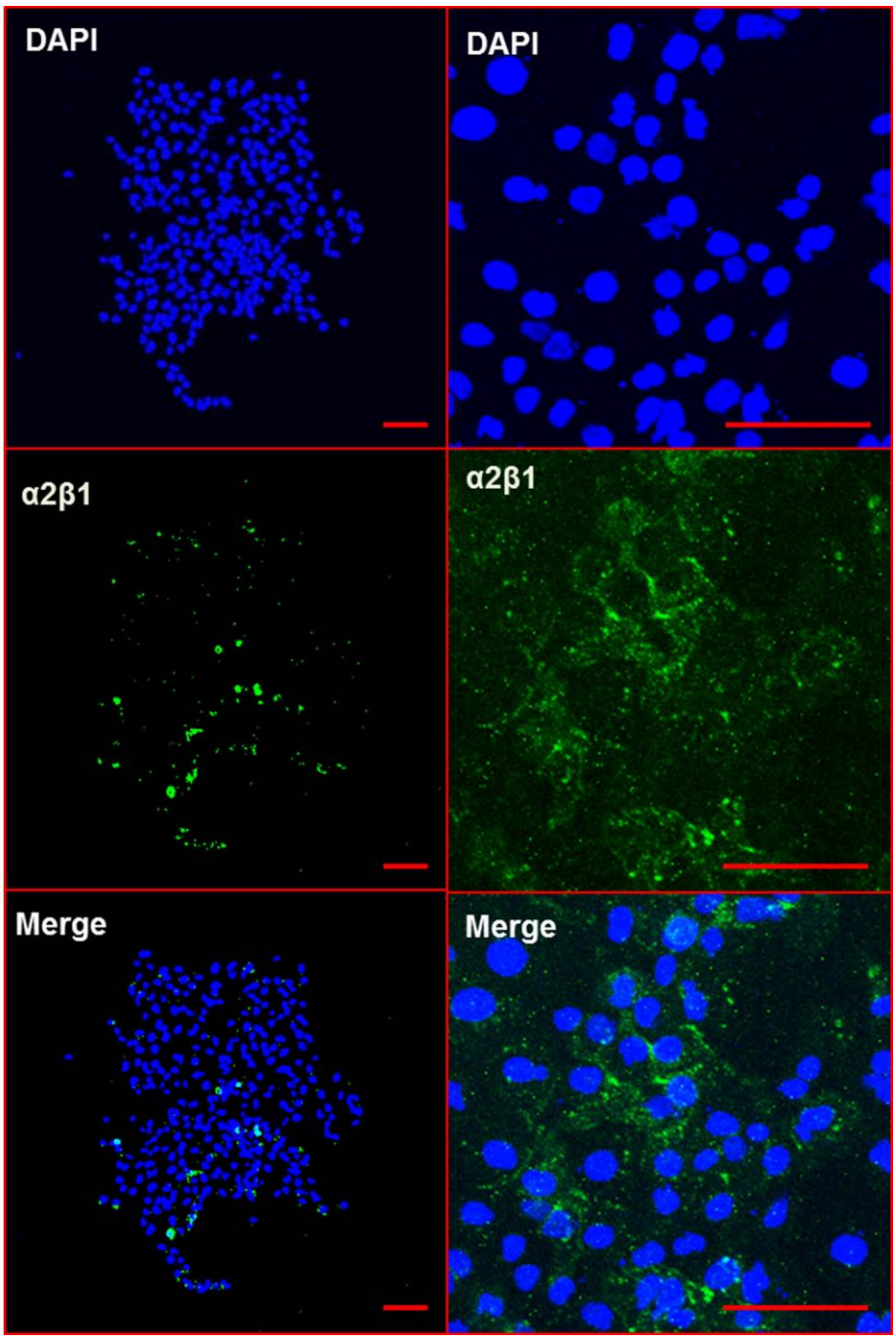

Figure 44. DU145 Type 2 α2β1 integrin Expression

Expression of the putative prostate cancer stem cell marker α2β1 integrin by DU145 colonies. Type 2 colonies were stained by immunocytochemistry with monoclonal antibodies against the target and detected with a FITC conjugated secondary antibody (green) and counter stained with DAPI (blue). Representative colonies shown. Bar = 100µm.

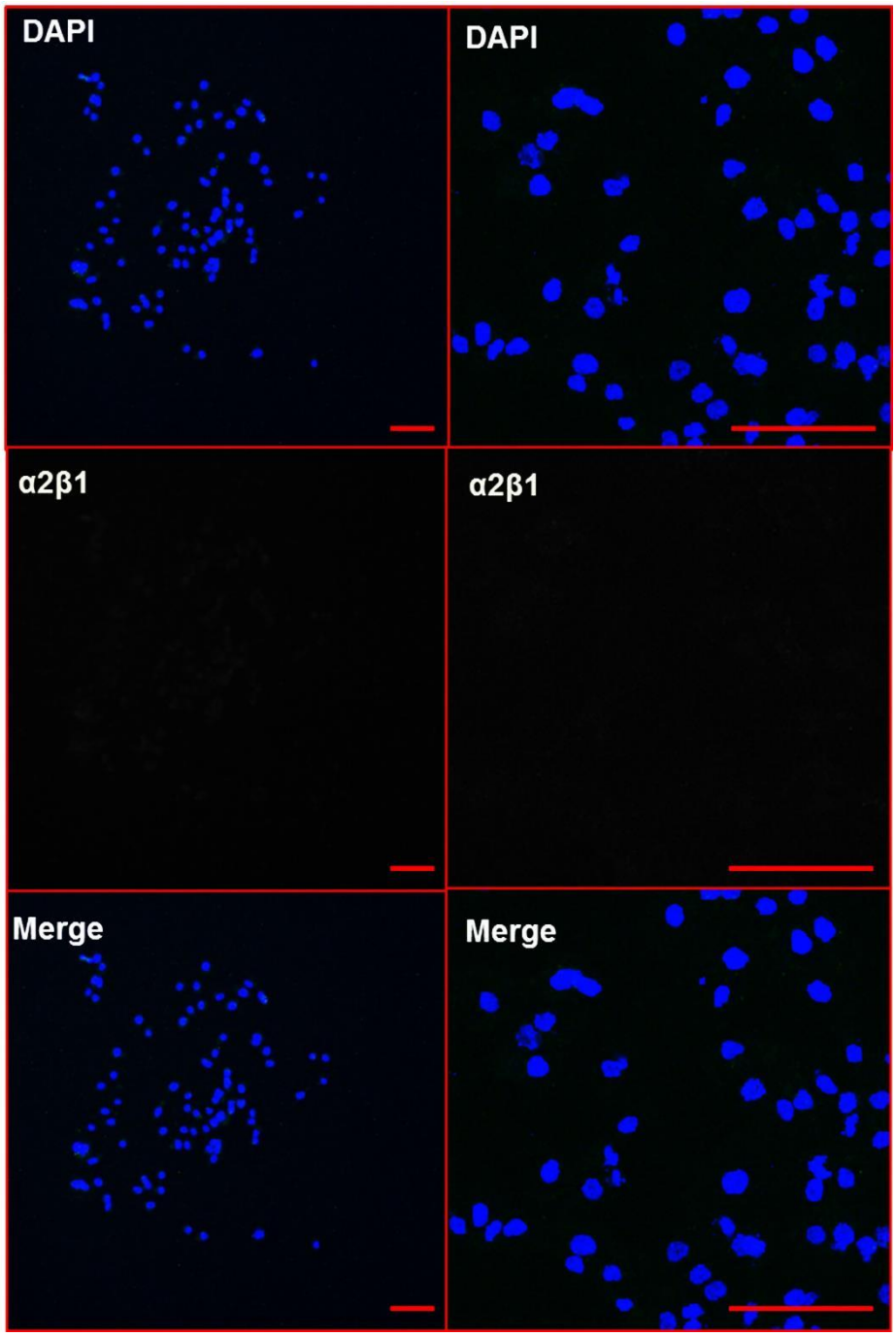

Figure 45. DU145 Type 3 α2β1 integrin Expression

Expression of the putative prostate cancer stem cell marker α2β1 integrin by DU145 colonies. Type 3 colonies were stained by immunocytochemistry with monoclonal antibodies against the target and detected with a FITC conjugated secondary antibody (green) and counter stained with DAPI (blue). Representative colonies shown. Bar = 100µm.

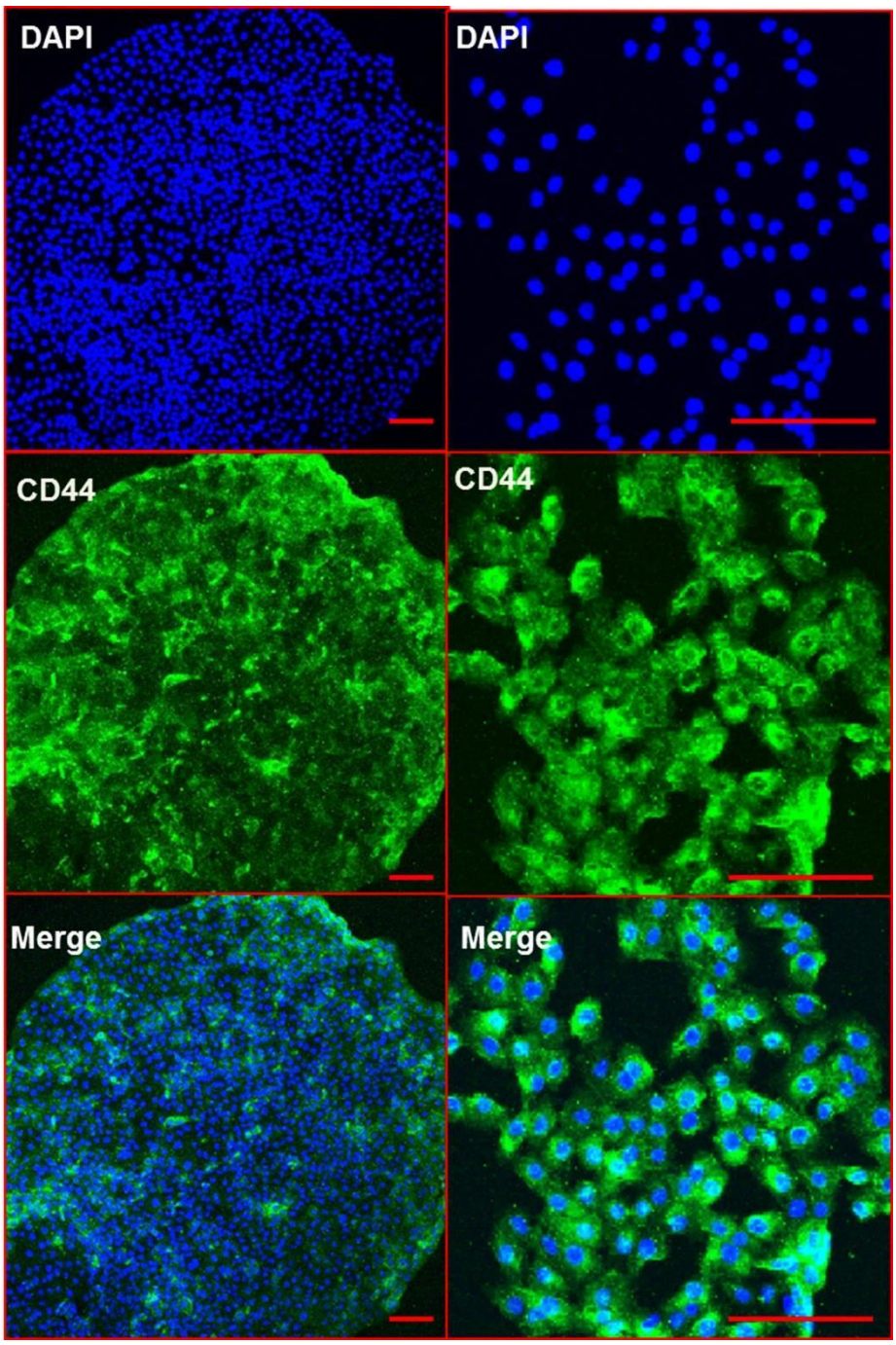

Figure 46. DU145 Type 1 CD44 Expression

Expression of the putative prostate cancer stem cell marker CD44 by DU145 colonies. Type 1 colonies were stained by immunocytochemistry with monoclonal antibodies against the target and detected with a FITC conjugated secondary antibody (green) and counter stained with DAPI (blue). Representative colonies shown. Bar = 100µm.

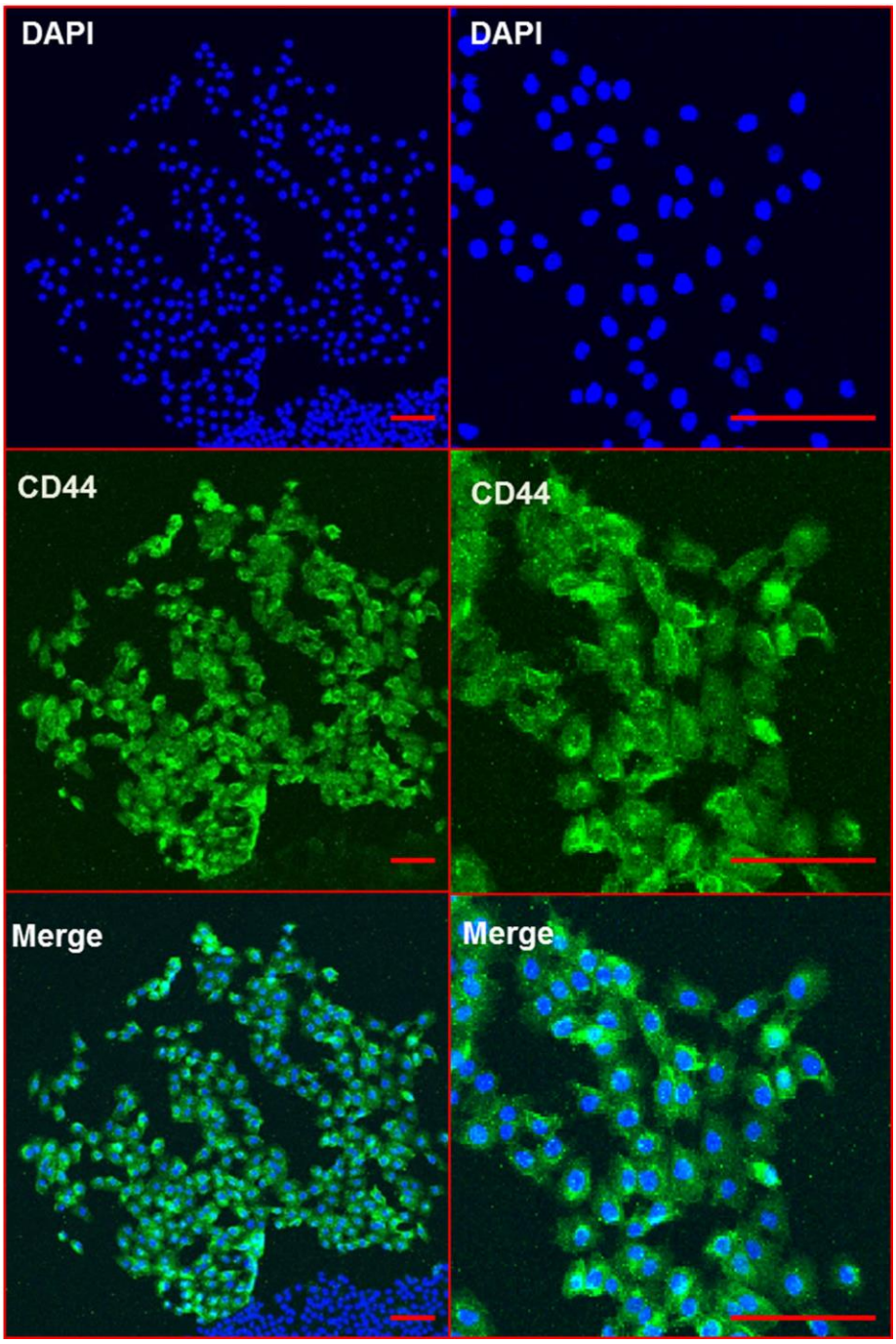

Figure 47. DU145 Type 2 CD44 Expression

Expression of the putative prostate cancer stem cell marker CD44 by DU145 colonies. Type 2 colonies were stained by immunocytochemistry with monoclonal antibodies against the target and detected with a FITC conjugated secondary antibody (green) and counter stained with DAPI (blue). Representative colonies shown. Bar = 100µm.

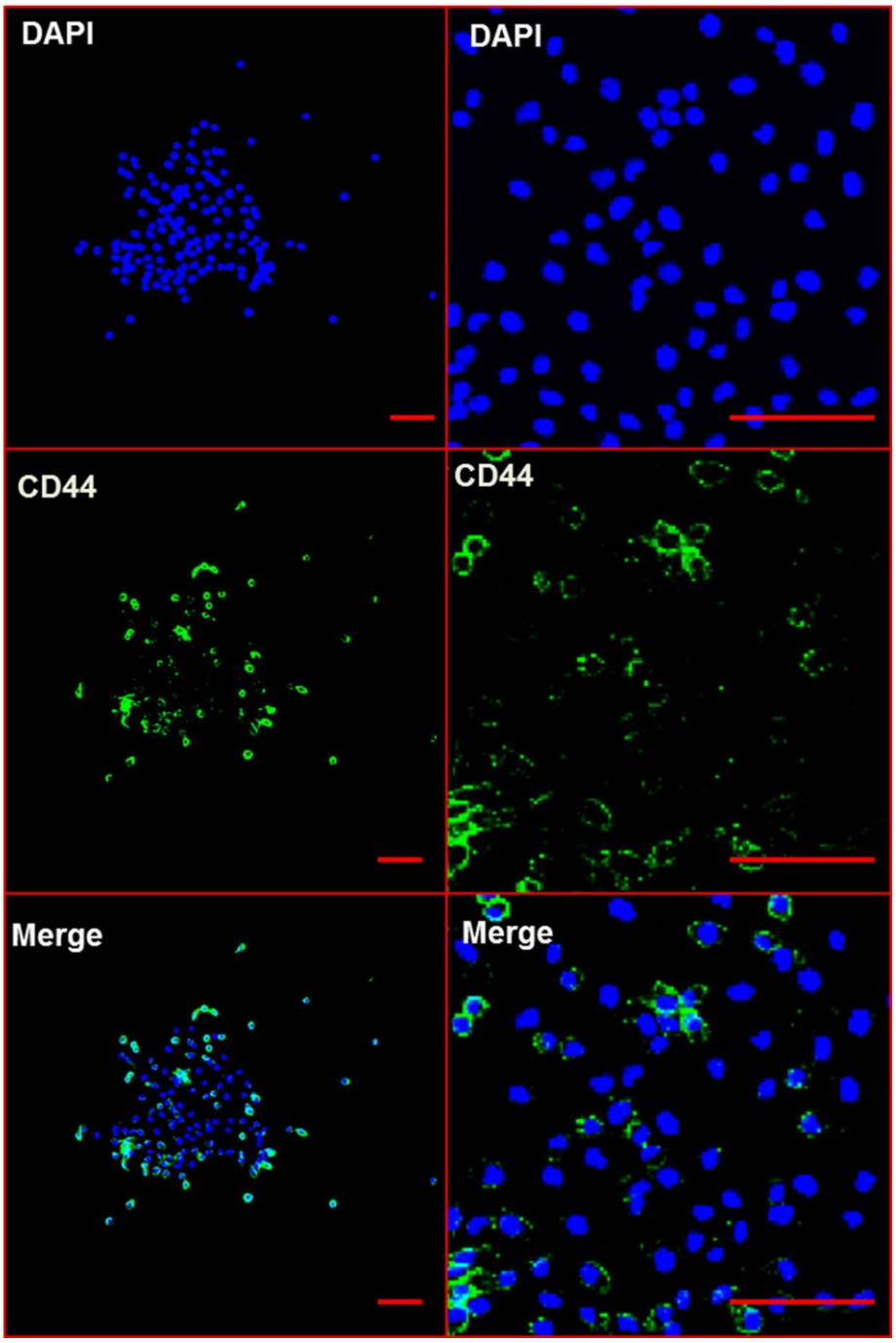

Figure 48. DU145 Type 3 CD44 Expression

Expression of the putative prostate cancer stem cell marker CD44 by DU145 colonies. Type 3 colonies were stained by immunocytochemistry with monoclonal antibodies against the target and detected with a FITC conjugated secondary antibody (green) and counter stained with DAPI (blue). Representative colonies shown. Bar = 100µm.

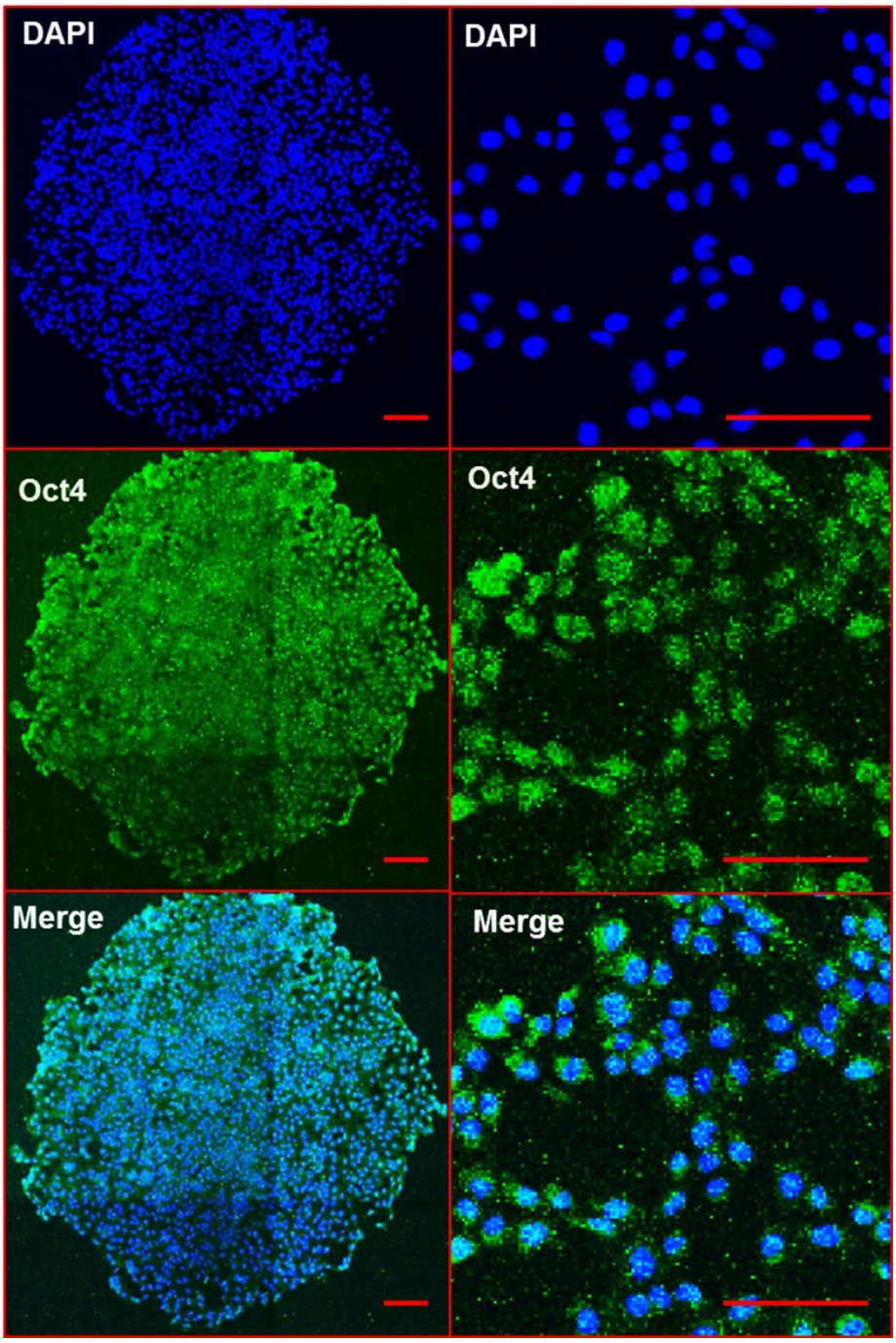

Figure 49. DU145 Type 1 Oct4 Expression

Expression of the stem cell marker Oct4 by DU145 colonies. Type 1 colonies were stained by immunocytochemistry with monoclonal antibodies against the target and detected with a FITC conjugated secondary antibody (green) and counter stained with DAPI (blue). Representative colonies shown. Bar = 100µm.

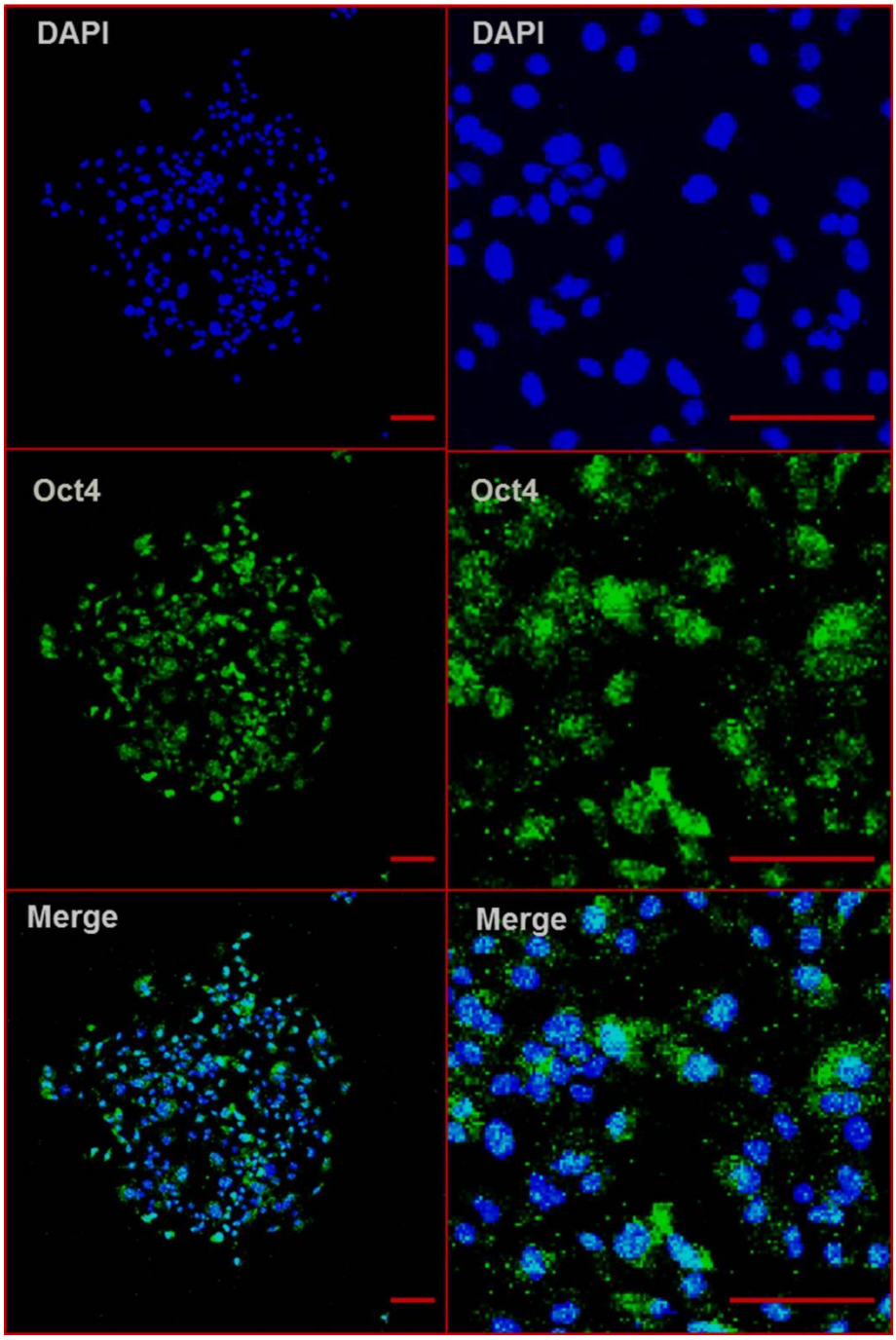

Figure 50. DU145 Type 2 Oct4 Expression

Expression of the stem cell marker Oct4 by DU145 colonies. Type 2 colonies were stained by immunocytochemistry with monoclonal antibodies against the target and detected with a FITC conjugated secondary antibody (green) and counter stained with DAPI (blue). Representative colonies shown. Bar = 100µm.

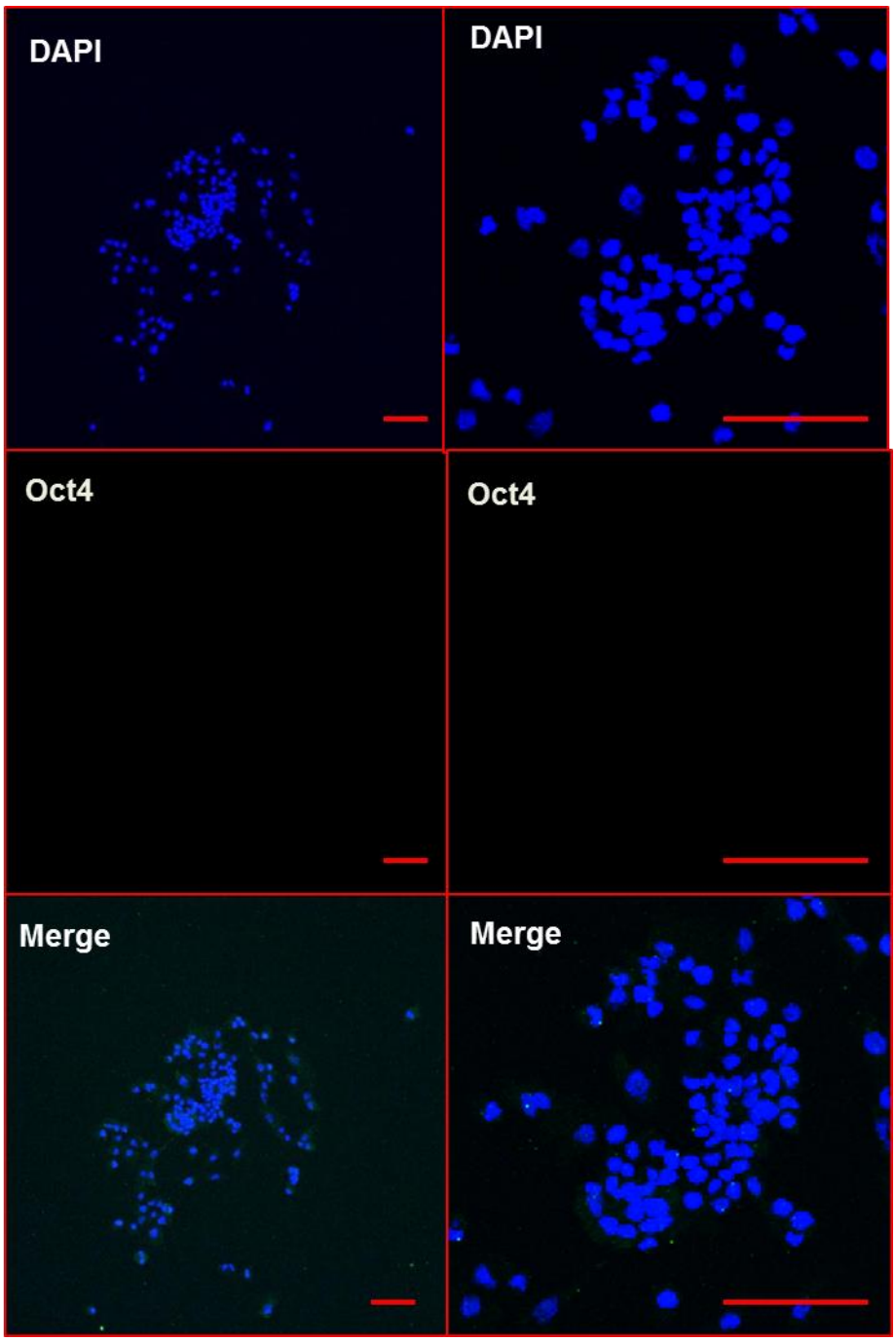

Figure 51. DU145 Type 3 Oct4 Expression

Expression of the stem cell marker Oct4 by DU145 colonies. Type 3 colonies were stained by immunocytochemistry with monoclonal antibodies against the target and detected with a FITC conjugated secondary antibody (green) and counter stained with DAPI (blue). Representative colonies shown. Bar = 100µm.

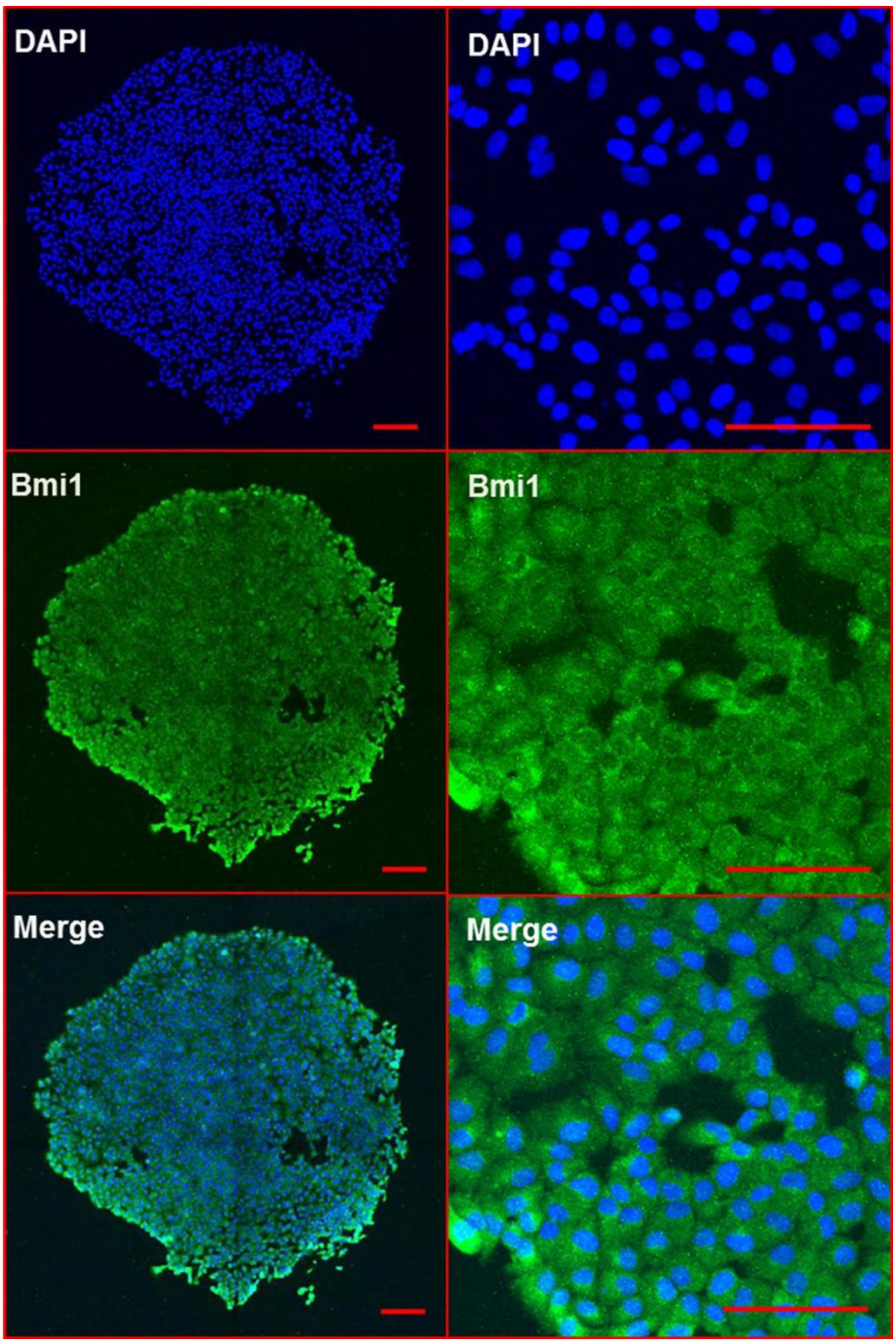

Figure 52. DU145 Type 1 Bmi1 Expression

Expression of the stem cell marker Bmi1 by DU145 colonies. Type 1 colonies were stained by immunocytochemistry with monoclonal antibodies against the target and detected with a FITC conjugated secondary antibody (green) and counter stained with DAPI (blue). Representative colonies shown. Bar = 100µm.

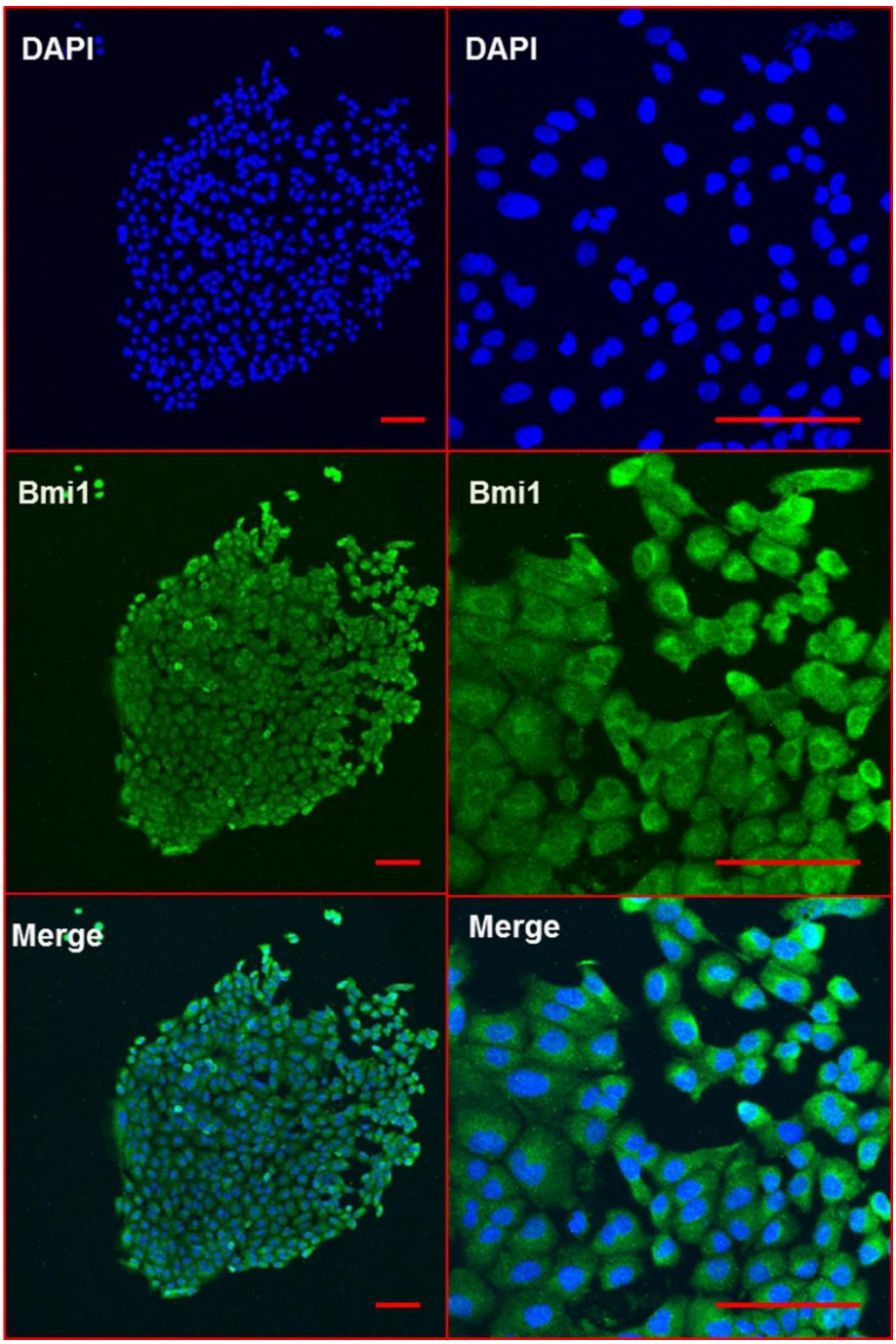

Figure 53. DU145 Type 2 Bmi1 Expression

Expression of the stem cell marker Bmi1 by DU145 colonies. Type 2 colonies were stained by immunocytochemistry with monoclonal antibodies against the target and detected with a FITC conjugated secondary antibody (green) and counter stained with DAPI (blue). Representative colonies shown. Bar = 100µm.

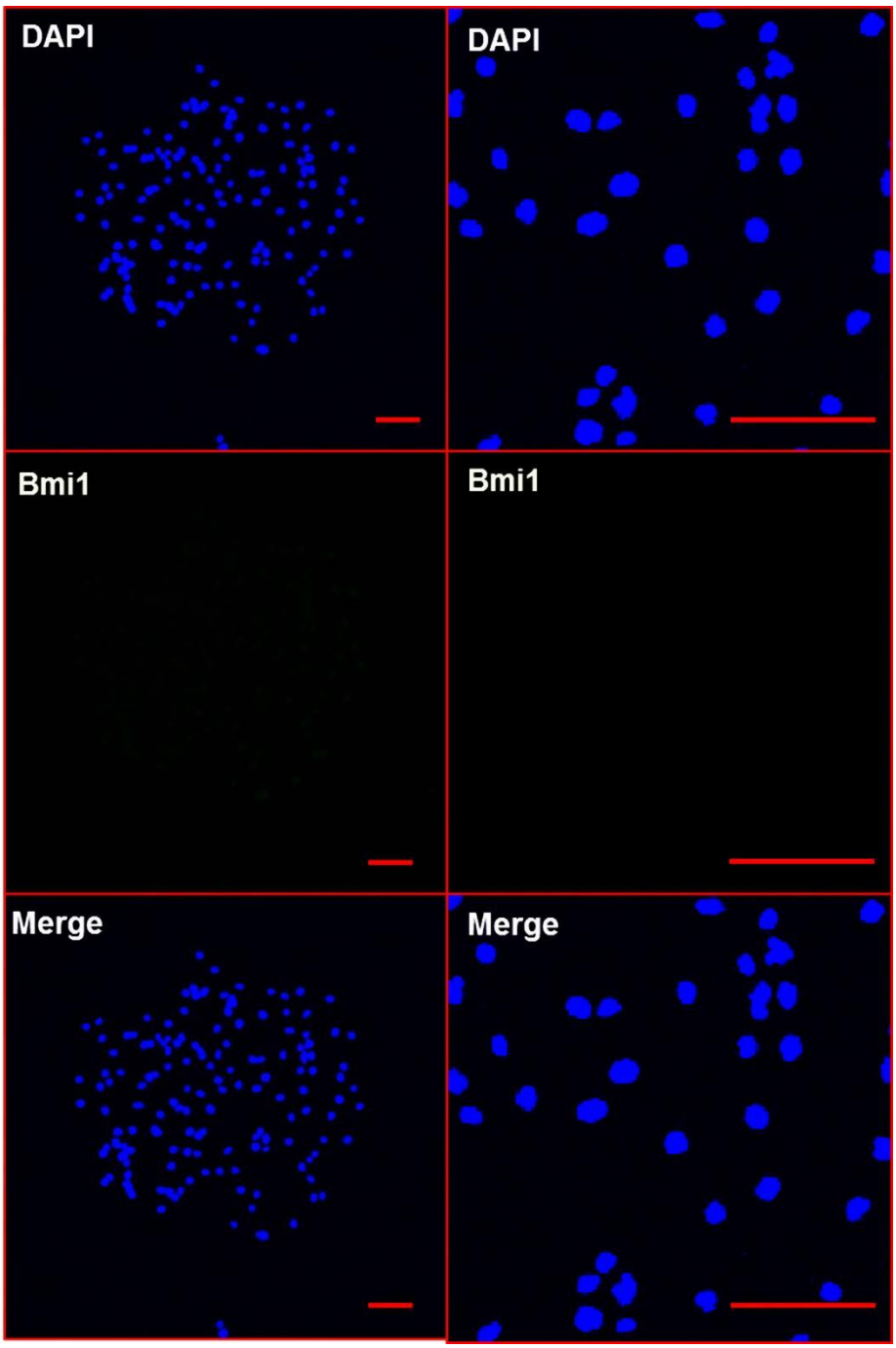

Figure 54. DU145 Type 3 Bmi1 Expression

Expression of the stem cell marker Bmi1 by DU145 colonies. Type 3 colonies were stained by immunocytochemistry with monoclonal antibodies against the target and detected with a FITC conjugated secondary antibody (green) and counter stained with DAPI (blue). Representative colonies shown. Bar = 100µm.

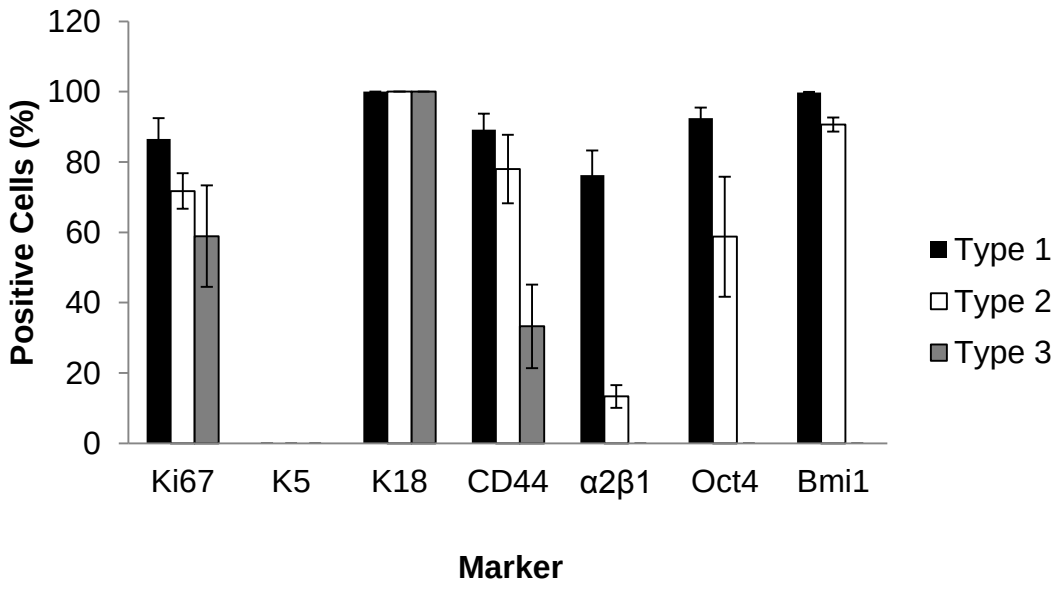

Figure 55. Heterogeneity of marker expression of DU145 colonies.

Type 1, 2 and 3 DU145 colonies were stained by immunocytochemistry with antibodies against the target and detected with a FITC conjugated secondary antibody. The proportion of cells positive for each marker was determined as a percentage of the total number of cells counted. Type 1 and 2 colonies contained more CD44 positive cells than type 3. Type 1 colonies contained more α2β1 integrin positive cells that type 2 ($p<0.05$ Oneway ANOVA). Results are the mean of 20 individual colonies ± S.E.M.

4.6 Discussion

The aim of this study initially was to validate colony forming morphology as a method of selecting stem cell colonies. Tumours are believed to contain a hierarchy of cells derived from cancer stem cells, which can self-renew and differentiate to produce the multiple cell types observed within the cancer. To be considered a CSC, a cell must be able to self-renew, differentiate and be serially tumourigenic. The results of this study show that both type 1 and 2 colonies contain cells capable of self-renewal. The evidence strongly suggests that type 1 and 2 colonies differ only in the proportions of stem cells each contains and that colony morphology of human cancer cell lines cannot be used reliably as a surrogate marker for stem cell origin.

4.6.1 Secondary Colonies

In the first experiment it was noted that both type 1 and 2 colonies were able to form all three colony types, suggesting that they both contain stem cells. Type 1 colonies formed more type 1 colonies than type 2, suggesting that they contain a higher proportion of CSCs. CFE was unaffected by colony size, which suggests that colony morphology and not size determines the proportion of CSCs. Type 3 colonies were terminal and could not be propagated by cloning. The ability of both type 1 and 2 colonies to for form secondary type 1 colonies was a surprising finding, and suggested that type 2 colonies were also the progeny of CSCs, not TA cells. These results show that the type 2 colony contains stem cells which can self-renew, are highly proliferative and can form all three colony types.

4.6.2 Self-renewal

The ability of both type 1 and 2 colonies to produce further type 1 and 2 colonies suggests they both contain cells with a capacity for self-renewal. Self-renewal was further demonstrated in both colony types by sphere formation. Sphere formation has previously been shown to enrich for prostate stem cells expressing CSC markers CD24, CD44 and α2β1integrin (Garraway et al., 2010). DU145 cells can be cultured as spheres for at least 1.5 years without loss of stemness (Rybak et al., 2011).

4.6.3 Proliferative Capacity

Both type 1 and 2 colonies contained highly proliferative cells which, when serially cloned, could be cultured for more than 100 divisions. However type 1 colonies derived from type 2 colonies were terminal after around 110 divisions. When cultured in bulk culture at higher cell seeding density, both type 1 and 2 colonies were immortal and could be cultured for at least 20 passages, had similar growth rates and regenerated the morphology of the DU145 monolayer. This suggests that although type 2 colonies contain stem cells with self-renewal capacity, there are significantly less than within type 1 colonies, and consequently are more likely to be lost when serially cloned over extended periods of time. Cells may be diluted out or lost during the ring cloning process and so the lower number of stem cells within the type 2 colonies makes the chances of loss greater than type 1 colonies.

4.6.4 Tumourigenicity

Cancer stem cells are usually considered immortal and undergo many cell divisions to drive tumour growth (Keith, 2004) and in this study both type 1 and 2 colonies were able to be serially engrafted in nude mice. Serial

xenotransplantation is considered the gold standard for the identification for CSCs (Clarke et al., 2006). Type 2 colonies had a longer latency than type 1 colonies and formed smaller tumours, again suggesting that type 1 colonies contain a higher proportion of CSCs.

4.6.5 Marker Expression

Cytokeratin staining showed that all three colony types express the luminal epithelial marker CK18, but not the basal marker CK5 (Wang et al., 2001). Because cell division is restricted mainly to the basal layer in normal prostate, it has been suggested that prostate cancer stem cells might have a basal phenotype (Maitland et al., 2011). However, DU145 cells uniformly express cytokeratins characteristic of the differentiated luminal cells and yet have stem cell capacity. Cytokeratins may be down regulated in long term *in vitro* culture (Waseem et al., 1999).

CD44 and α2β1 integrin are markers that are claimed in several studies (Lokeshwar et al., 1995, Patrawala et al., 2006) to enrich for a prostate cancer stem cell population and were expressed by the majority of the cells in DU145 colonies. α2β1 integrin was expressed at high levels in both type 1 and 2 colonies and at lower levels in type 3 colonies, whilst CD44 was only observed in type 1 and 2 colonies. CD44 has been shown to enrich for tumour initiating cells and is controlled by microRNAs such as miRNA-708 (Saini et al., 2012) and microRNA miR-34a (Liu et al., 2011). A contrasting study has shown no difference between the growth rates of PC-3 cells in high cell density culture based on CD44 and α2β1 expression (Zhang and Waxman, 2010), so these markers alone do not confirm CSC identity.

Type 1 and 2 colonies were positive for BMI-1, an oncogene suggested to play a role in stem cell self-renewal (Jiang et al., 2009) which has been shown previously to be up-regulated in pancreatic holoclones (Jeter et al., 2011). The embryonic stem cell marker Oct-4 was observed in type 1 and 2 colonies, but not in type 3 colonies, suggesting a role in self-renewal and differentiation (Trosko, 2006). Previous studies have shown that stem cell colony formation is controlled by factors involved in self-renewal, such as Nanog (Jeter et al., 2009, Jeter et al., 2011) and telomerase activity (Marian et al., 2010).

4.6.6 Comparison With Previous Studies

A number of studies using prostate (Locke et al., 2005, Li et al., 2008, Pfeiffer and Schalken, 2010, Zhang and Waxman, 2010) pancreatic (Jeter et al., 2011) colorectal (Ferrand et al., 2009), breast (Liu et al., 2012), head and neck squamous cell carcinoma (Harper et al., 2007) and uveal melanoma (Kalirai et al., 2011) cancer cell lines have tried to validate the use of colony morphology as a surrogate for colonies derived from stem cells, transit-amplifying cells and differentiating cells. The results are surprisingly disparate and are in contrast to our findings. All previous studies conclude that holoclones have a greater ability to be passaged in bulk culture (Li et al., 2008, Jeter et al., 2011) or by serial cloning (Locke et al., 2005, Pfeiffer and Schalken, 2010, Kalirai et al., 2011, Tan et al., 2011) than paraclones, and that paraclones with a differentiated morphology have a very limited proliferative potential. In these studies, meroclones were either not studied (Locke et al., 2005, Pfeiffer and Schalken, 2010) or could only be propagated for about 3 months compared to more than 6 months for holoclones (Li et al., 2008). The ability of cells derived from meroclones to generate secondary

holoclones has been observed in only one study and in that study few holoclones were formed from meroclones (Jeter et al., 2011).

Previous studies have shown that only holoclones are tumorigenic *in vivo* (Li et al., 2008, Jeter et al., 2011) or that holoclones form larger, faster growing tumours than paraclones (Ferrand et al., 2009, Miloszewska et al., 2010, Zhang and Waxman, 2010). Again, the majority of these studies only compared holoclones and paraclones. The ability of some paraclones to form tumours in some of these studies is paradoxical as it indicates that some paraclones contain stem cells. This phenomenon may be in part due to improved immune-deficient murine models. This observation has been demonstrated in melanoma where approximately 25% of all tumour cells are tumourigenic in immunocompromised NOD/SCID interleukin-2 receptor gamma chain null (Il2rg-/-) mice (Quintana et al., 2008), a much larger number than previously believed.

Holoclones formed by the prostate cancer cell line PC3 are highly tumorigenic, can be passaged long term and express the cancer stem cell markers α2β1+ CD44+ (Li et al., 2008). However, holoclones and meroclones are difficult to distinguish in cultures of PC3 (Pfeiffer and Schalken, 2010, Beaver, 2012). PC3 colonies varied in their ability to form holoclones and meroclones, with no relationship between primary and secondary colony morphology (Pfeiffer and Schalken, 2010). and therefore this cell line may not be appropriate for the study of cancer stem cells.

4.7 Chapter Conclusions

The results of this study show that the colony morphology of cancer cell lines cannot be used to distinguish an origin from stem or transit-amplifying cells. Colonies derived from the prostate cancer cell line DU145 with the morphology of holoclones and meroclones differ only in the proportion of stem cells each contains. In cancer, stem cell capacity may be shifted further down the cellular hierarchy towards differentiation, resulting in transit amplifying cells acquiring stem cell properties. These more mature stem cells are capable of self-renewal and differentiation, but require fewer cell divisions to become terminally differentiated.

5 Results: Identification and Characterisation of Prostate Epithelial Colonies

5.1 Chapter Introduction and Aims

Benign Prostatic Hyperplasia (BPH) is a frequent problem in elderly men that results from hyperplasia of the prostatic stromal and epithelial cells. Large nodules are formed in the periurethral region of the prostate which can compress the urethra to causing obstruction and interference with the flow of urine. Transurethral resection of the prostate (TURP) is a surgical procedure often used to alleviate symptoms of BPH, by creating a channel through the prostate and thus reducing constriction upon the urethra. TURP is a good source of primary prostate tissue and can be used to study non-malignant prostate cells.

Prostate epithelial cells from TURP samples form 2 types of colony which exhibit significant heterogeneity in terms of proliferation and cytokeratin expression, which were termed type I and type II (Hudson et al., 2000). Type II exhibit similar morphology to Barrandon and Green's holoclones (Barrandon and Green, 1987b), whereas type I colonies are similar to paraclones. The aim of this chapter was to further characterize the colonies formed by prostate epithelial cells from BPH samples, with a view to their use in the discovery of therapeutic targets by phage display.

5.2 Hypothesis

Prostate epithelial colony morphology is predictive of the type of founding cells. Colonies that contain stem cells have a greater proliferative potential, can self-renew, and can differentiate to form both colony types.

5.3 Objectives

The objectives were to:

1. Identify colonies derived from prostate epithelium.
2. Characterise colonies based on morphology and size.
3. Measure proliferative capacity
4. Demonstrate self-renewal by the ability to form secondary colonies with the same morphology as the primary clone and capacity to form spheres in non-adherent conditions.
5. Assess capacity for differentiation by expression of differentiation and stem cell markers.

5.4 Materials and Methods

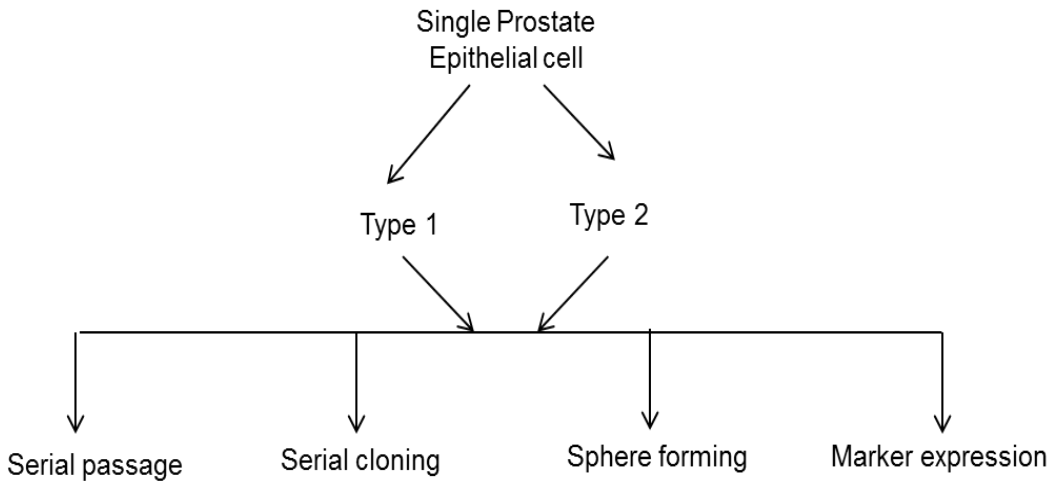

Figure 56. Characterisation of prostate epithelial colonies experimental plan. Single primary prostate epithelial cells form colonies of different types, with distinct morphologies, termed type 1, 2. The stem cell traits of self-renewal, proliferative capacity and marker expression of each colony were compared by serial passage, serial cloning, sphere formation, and immunocytochemistry.

5.5 Results

5.5.1 Colony Forming Efficiency

To study the heterogeneity of the cell population 1000 prostate epithelial cells from each of 12 patient samples were seeded as single cells into 60mm petri-dishes on a mitomycin C treated Swiss 3T3 feeder layer. Colonies were fixed and stained for counting and measurement. The CFE of prostate epithelial cells varied between 0.03% and 8.8% CFE, with a mean and S.E. of 3.7 ± 0.8 % (Table 20). The single cell origin of colonies could not be analysed due to the amount of cellular debris which affected the imaging capacity of the Incucyte system.

Table 20. CFE of Prostate Epithelial Colonies.

Patient Number	Total % CFE of All Colonies ≥ 32 cells	% CFE Type 1 Colonies	% CFE of Type 2 Colonies
1	5.3	2.6	2.7
2	4.7	1.8	2.9
3	4.9	1.4	3.5
4	8.8	2.4	6.4
5	0.4	0.2	0.2
6	7.9	2.7	5.2
7	0.1	0.0	0.1
8	4.4	1.4	3.0
9	0.3	0.1	0.2
10	0.7	0.2	0.5
11	1.8	0.3	1.5
12	5.3	2.6	2.7
Mean	**3.7**	**1.3**	**2.4**
S.E.M	**0.8**	**0.3**	**0.6**

5.5.2 Colony Morphology

Two distinct colony types were observed termed type 1 and type 2 (Figure 57). Type 1 colonies were very large with small, tightly packed cells. Type 2 colonies were smaller with flattened enlarged cells with an indistinct perimeter. There was patient to patient variability in the types of colonies formed. Generally, more type 2 colonies were observed than type 1. Between 0.1% and 2.7% of cells formed type 1 colonies and between 0.1% and 6.4% of cells formed type 2 colonies.

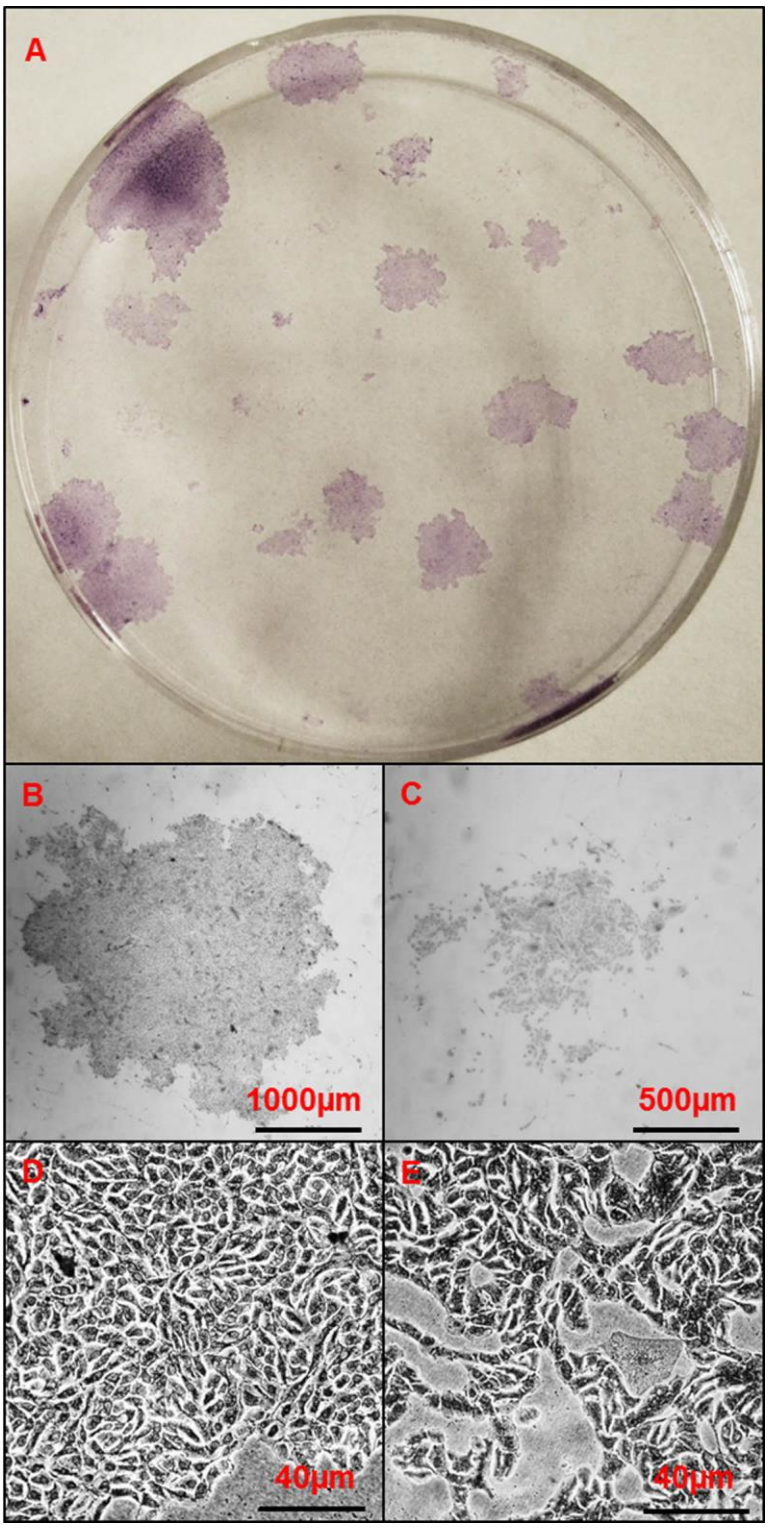

Figure 57. Prostate Epithelial Colony Morphology.

Single prostate epithelial cells were seeded at low density into 60 mm petri-dishes supported by mitomycin C treated Swiss 3t3 cells (A). Single cells formed 2 morphological types of colony termed Type 1(B), 2 (C). Type 1 colonies (D) contained small, densely packed cells with smooth edges. Type 2 colonies (E) contained a mixture of small tightly packed and larger more diffuse cells at the colony edge.

To determine the characteristics of the colony types, twenty colonies of each type were measured and the number of cells per colony was determined. Colony area, the number of cells per colony and number of cells per mm^2 are displayed in Table 20. Both type 1 and 2 colonies varied widely in terms of colony size and cell density. Type 1 colonies were very large, with a mean area of 16.5 ± 2.6 mm^2, which was much larger than type 2 colonies which were 4.3 ± 0.9 mm^2. Type 1 colonies were also more densely packed and consisted of much larger number of cells.

Table 21. Prostate Epithelial Colony Characteristics

Colony Type	Area (mm^2)	Total Number Cells	Cell Density (per mm^2)
1	16.5 (2.6)	25668 (4674)	1614 (182)
2	4.3 (0.9)	1278 (161)	372 (79)

Colonies derived from single epithelial cells were fixed, stained and measured to determine colony size and the number of cells in each colony. Results are the mean and S.E.M of twenty colonies from 3 patients.

The minimum number of cell divisions to achieve the number of cells in each colony (assuming no cell loss) can be estimated. The distribution is shown in Figure 58. Type 1 colonies underwent a minimum of 11 cell divisions, although most had divided at least 13 times within the 2 week incubation period. A small number of colonies were very fast growing and produced a 60-80,000 cells which took at least 16 cell divisions from the single founding cell. Type 2 colonies were slower growing and had undergone between 7 and 11 cell divisions in the same time period to produce a maximum of 3500 clonal daughter cells from the parent cell.

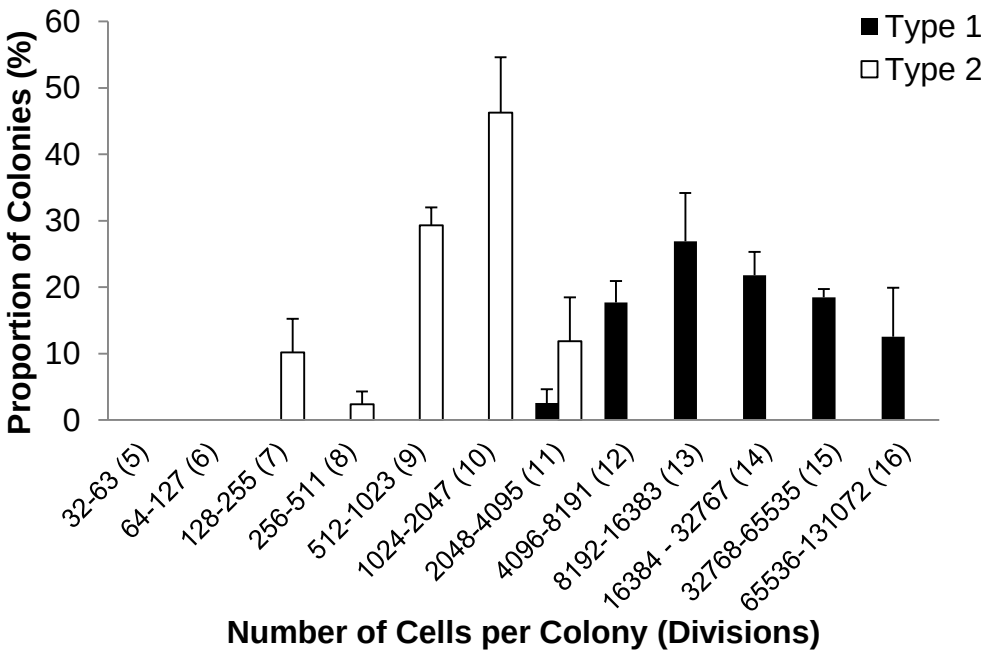

Figure 58. Distribution of Prostate Epithelial Colony Size.

Colonies formed by single prostate epithelial cells were fixed and the number of cells per colony was determined. The minimum number of cell doublings (divisions) was estimated assuming no cell loss. Results are the mean and S.E.M of 20 colonies of each type from 3 patients.

5.5.3 Secondary Cloning

In order to measure secondary CFE, 30 of each type of colony were ring cloned and plated at a density of 200-5000 cells per 6cm dish in triplicate. Neither type 1 or 2 colonies were able to form secondary colonies when seeded at low density, instead producing a sparse monolayer (Figure 59). Therefore the proliferative capacity of the colonies was measured by serial passage at high density, which supported further growth.

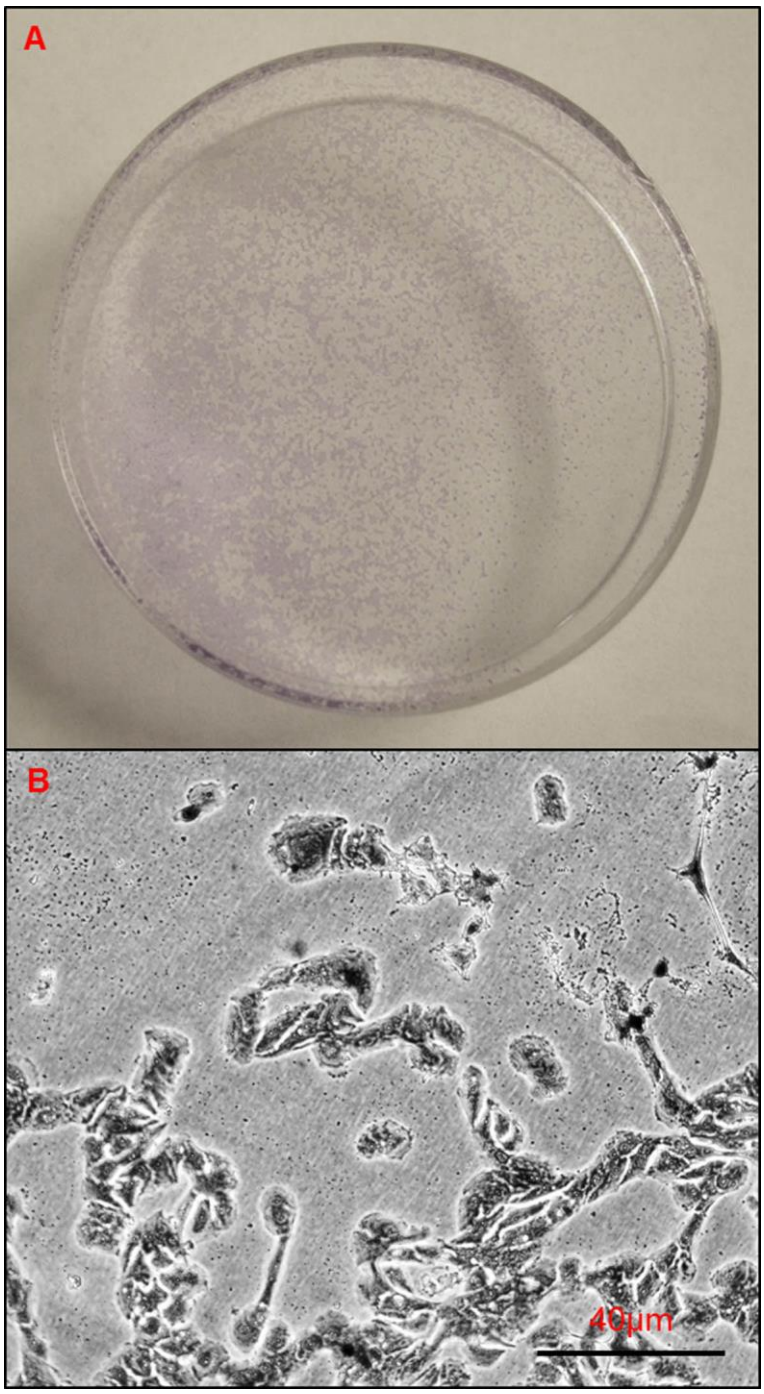

Figure 59. Secondary Cloning of Prostate Epithelial Cells.

(A) Neither Type 1 and 2 colonies were able to from distinct secondary colonies when ring cloned and seeded into collagen coated petri dishes supported by feeder cells. (B) Cells formed a sparse monolayer of enlarged cells.

5.5.4 Serial Passage

In order to demonstrate proliferative capacity in prostate epithelial colonies were bulk cultured at high cell density. Using colonies from 3 different patients, 5-6 type 1 and 2 colonies were ring-cloned and transferred to T25cm flasks for serial passaging under routine maintenance conditions. Cells were monitored daily and serially passaged until terminal.

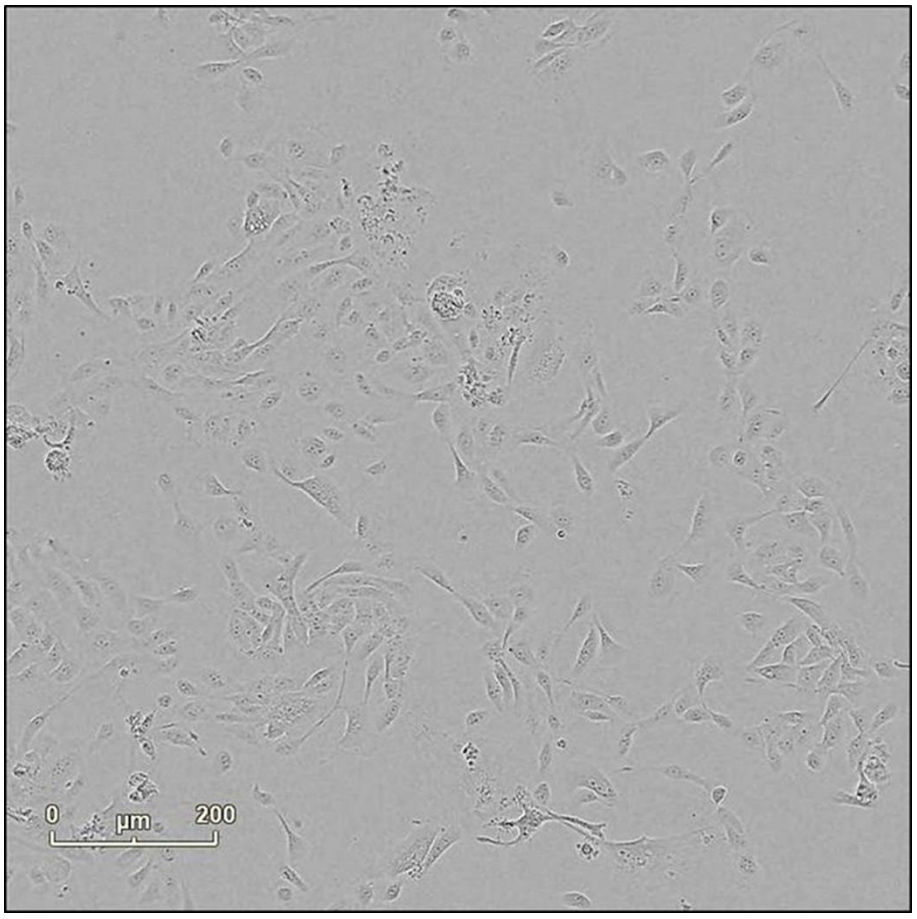

Figure 60. Primary Prostate Epithelial Cells.
Cells derived from type 1 colonies form a monolayer when cultured at high cell density. Cells from type 2 colonies failed to grow further.

When cultured at high density, 16/18 type 1 colonies compared to only 3/16 type 2 colonies survived to form a monolayer, which could be successfully passaged at least once. Type 1 colonies survived an average of 31± 2 days, which was longer than type 2 colonies which survived only 23 ± 8 days (Table 22). The majority of type 1 colonies could be passaged twice and then cells became enlarged and failed to proliferate further so were deemed senescent. The majority of type 2 cells were enlarged and senescent after only 1 passage and many became detached from the plate. The three type 2 colonies which reached confluence did not adhere to the fresh tissue culture flask when passaged.

Table 22. Proliferative Capacity of Prostate Epithelial Cells

Colony Type	Survival (%)	Passages mean ± S.E.M	Days Proliferative mean ± S.E.M
1	16/18 (89%)	2.1 (0.2)	31 (2)
2	3/16 (19%)	1.0 ± (0.0)	23 ± (8)

Colonies derived from prostate epithelial cells were ring cloned and transferred to T25cm flasks and serially passaged. Colonies which survived and to be passaged at least once and how long each colony was proliferative were determined.

5.5.5 Sphere Formation

Non-adherent culture and the formation of spheres is frequently used as an assay to measure self-renewing stem cells (Galli et al., 2003, Garraway et al., 2010). In five separate experiments, 3 each of colony type were harvested and plated at 1000 cells/well of a 6 well plate in triplicate. The sphere forming efficiency of each colony type in Matrigel^{TM} was determined as a percentage of the number of cells seeded. Spheres were identified as large rounded balls of cells which grew in the course of the two weeks incubation under non-adherent conditions. Only type 1 colonies could form spheres in non-adherent culture, at an efficiency of 13.5 ± 8.3 % with mean diameter of 63 ±3 µm, pictured in Figure 61.

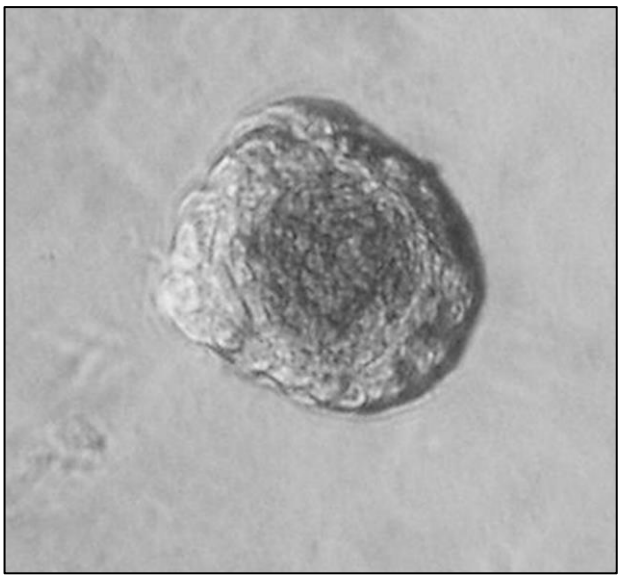

Figure 61. Prostate Epithelial Spheres.
Prostasphere formed by culture of prostate epithelial cells in Matrigel. Only type 1 colonies were able to from spheres when ring cloned and transferred to a mixture of 1:1 PrEGM: Matrigel.

5.5.6 Immunocytochemistry

Prostate epithelial colonies were cultured in 60 mm Petri-dishes, fixed with PFA and stained with antibodies against Ki67, K5, K18, $\alpha_2\beta_1$ integrin, CD44, Bmi1 and Oct4. Cells were imaged by fluorescence confocal microscopy and the number of positive cells was determined. All results are the mean and S.E.M of three experiments, from three patient samples, in which at least 20 colonies were counted.

5.5.6.1 *Ki67 staining*

Figure 63 and Figure 62 show that Type 1 colonies contain more actively proliferating cells than type 2 colonies. 87.4 ± 2.1% of type 1 compared to 38.0 ± 9.8% of type 2 cells stained positive for Ki67 (Figure 64) ($p<0.01$ unpaired t-test). Positive cells were spread evenly throughout the colony, with similar numbers observed at the centre and periphery.

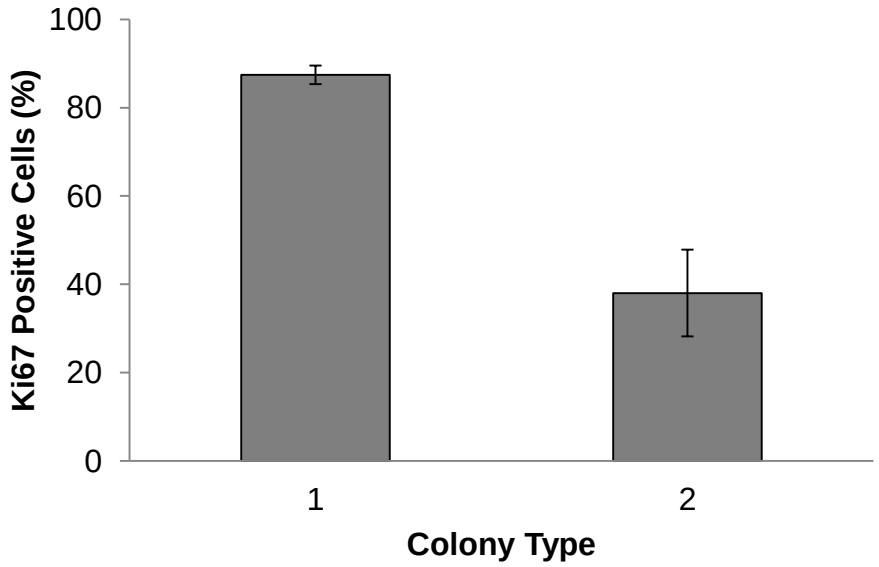

Figure 62. Ki67 Expression by Prostate Epithelial Colonies.

Colonies were stained by immunocytochemistry with antibodies against the Ki67 and detected with a FITC conjugated secondary antibody. The proportion of cells positive for each marker was determined as a percentage of the total number of cells counted. Results are the mean 20 colonies from three patients ± S.E.M.

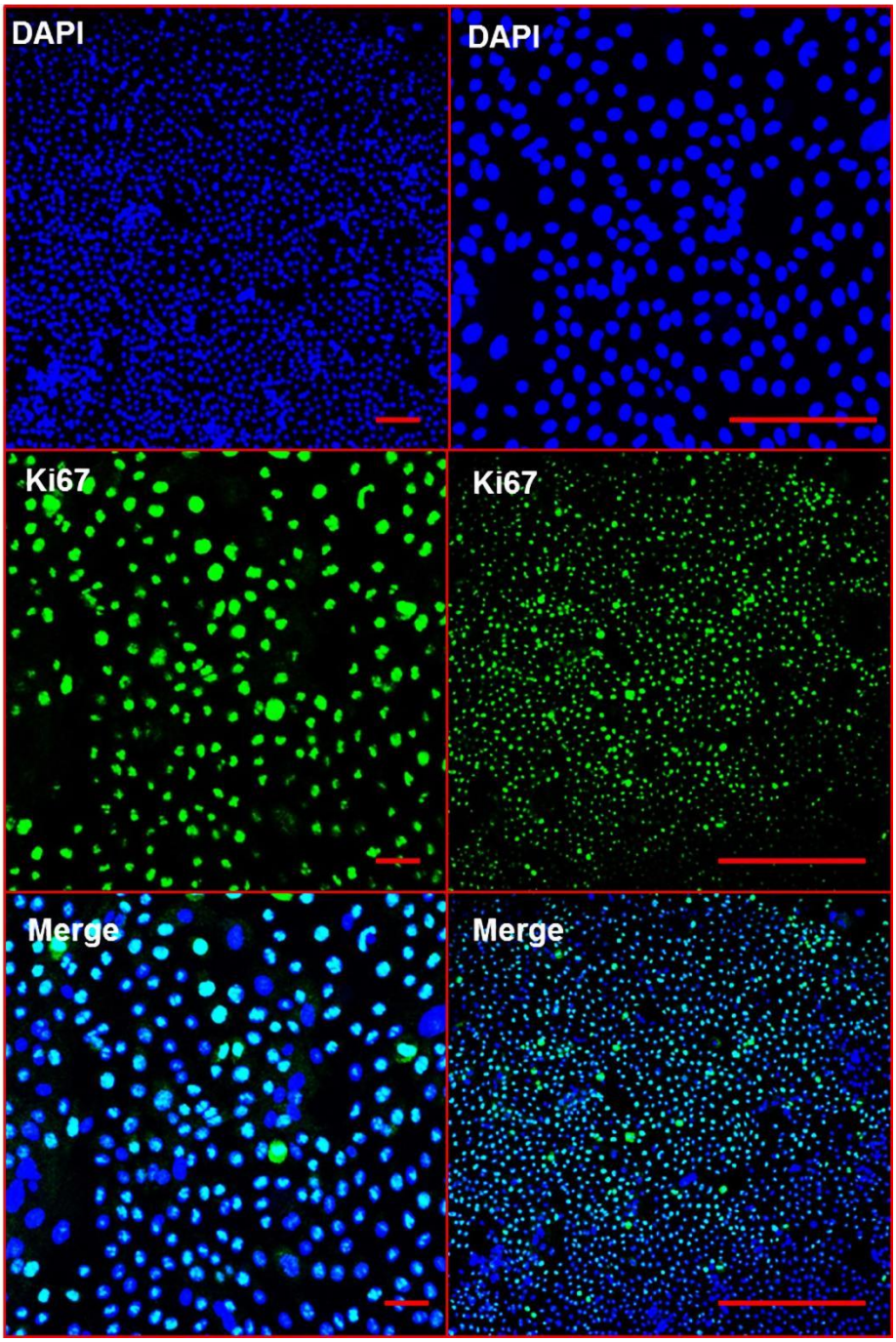

Figure 63. Prostate Epithelial Type 1 Colony Ki67 Expression

The proliferative fraction of type 1 prostate epithelial colonies was determined by Ki67 staining. Colonies were stained by immunocytochemistry with monoclonal antibodies against Ki67, detected with a FITC conjugated secondary antibody (green) and counter stained with DAPI (blue). Representative colonies shown. Bar = 100µm

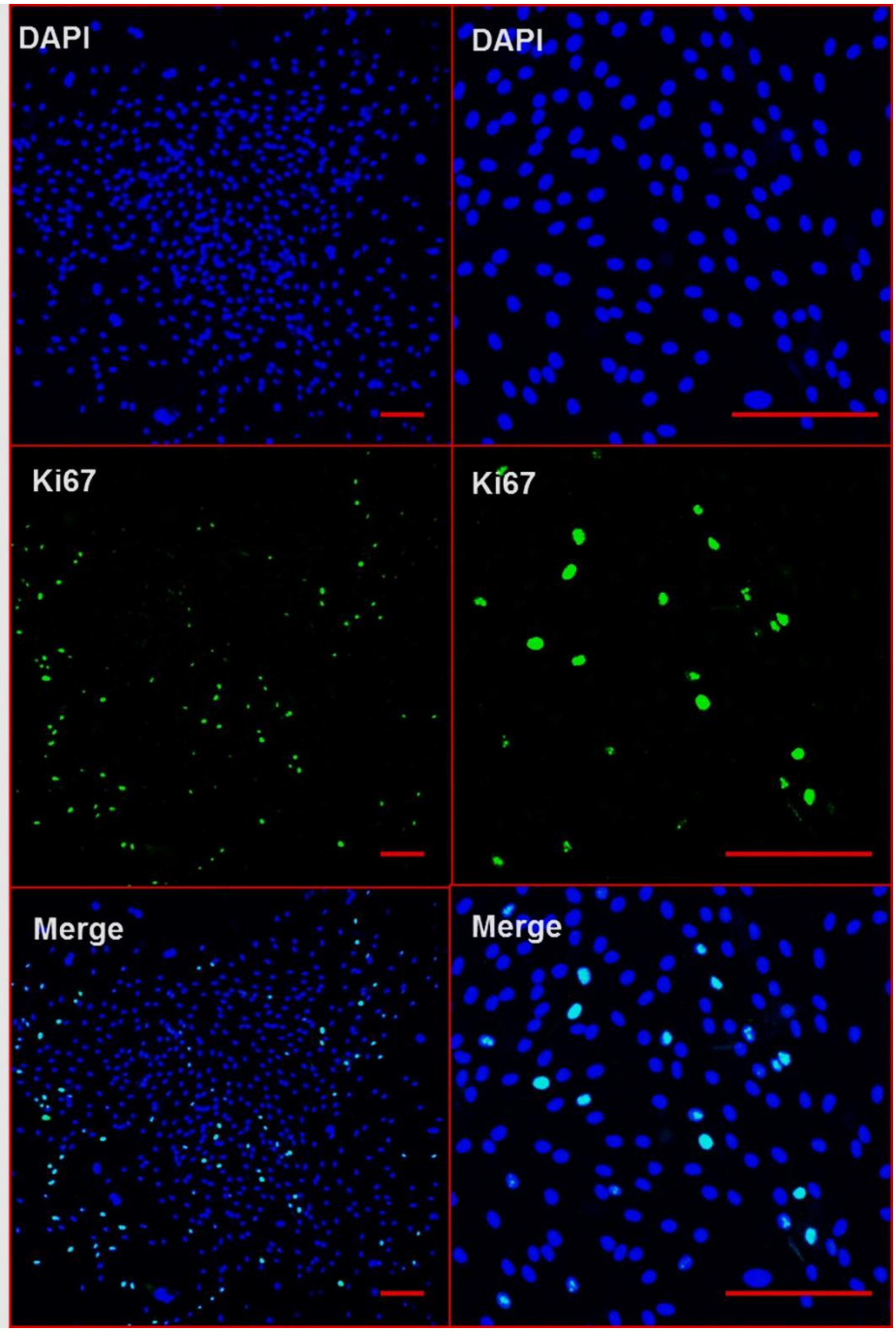

Figure 64. Prostate Epithelial Type 2 Colony Ki67 Expression

The proliferative fraction of type 2 prostate epithelial colonies was determined by Ki67 staining. Colonies were stained by immunocytochemistry with monoclonal antibodies against Ki67, detected with a FITC conjugated secondary antibody (green) and counter stained with DAPI (blue). Representative colonies shown. Bar = 100µm

5.5.6.2 *Cytokeratin Expression*

Co-staining with antibodies against K5 and K18 showed that both type1 and type 2 prostate colonies are of epithelial origin (Figure 65). Type 1 colonies (Figure 66) contained cells expressing mainly the basal epithelial marker K5, whereas type 2 colonies (Figure 67) contain a mixture of luminal and basal cells as shown by K5 and K18 staining.

Figure 65. Cytokeratin expression by Prostate Epithelial Colonies.
Colonies were stained by immunocytochemistry with antibodies against the K5 and K18 and detected with FITC and TRITC conjugated secondary antibodies. The proportion of cells positive for each marker was determined as a percentage of the total number of cells counted. Results are the mean 20 colonies from three patients ± S.E.M.

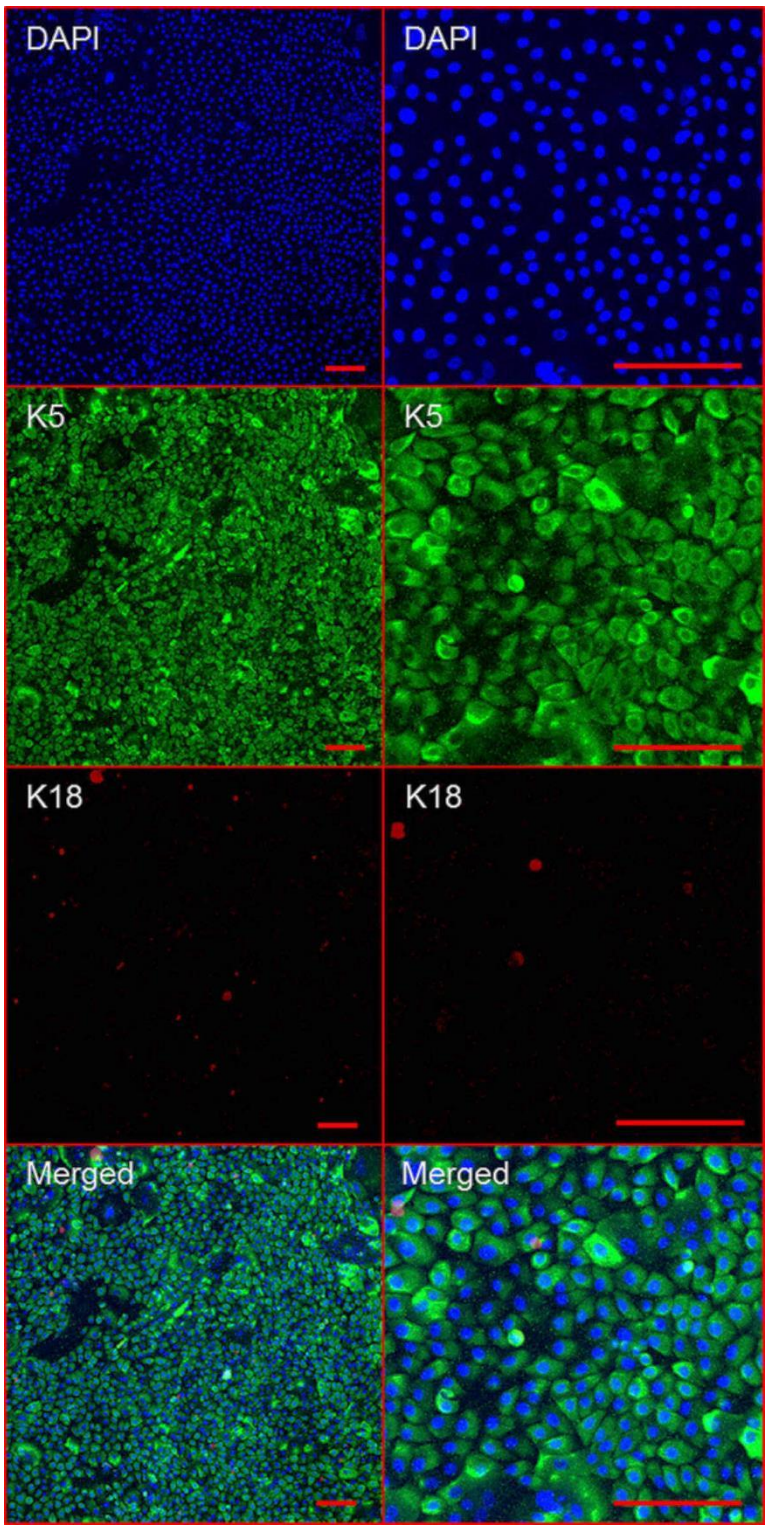

Figure 66. Prostate Epithelial Type 1 Colony Cytokeratin Expression

Expression of K5 and K18 by type 1 prostate epithelial colonies. Immunocytochemistry with monoclonal antibodies against K5, detected with a FITC conjugated secondary antibody (green) and against K18 detected by a TRICT conjugated secondary antibody (red) and counter stained with DAPI (blue). Representative colonies shown. Bar = 100µm

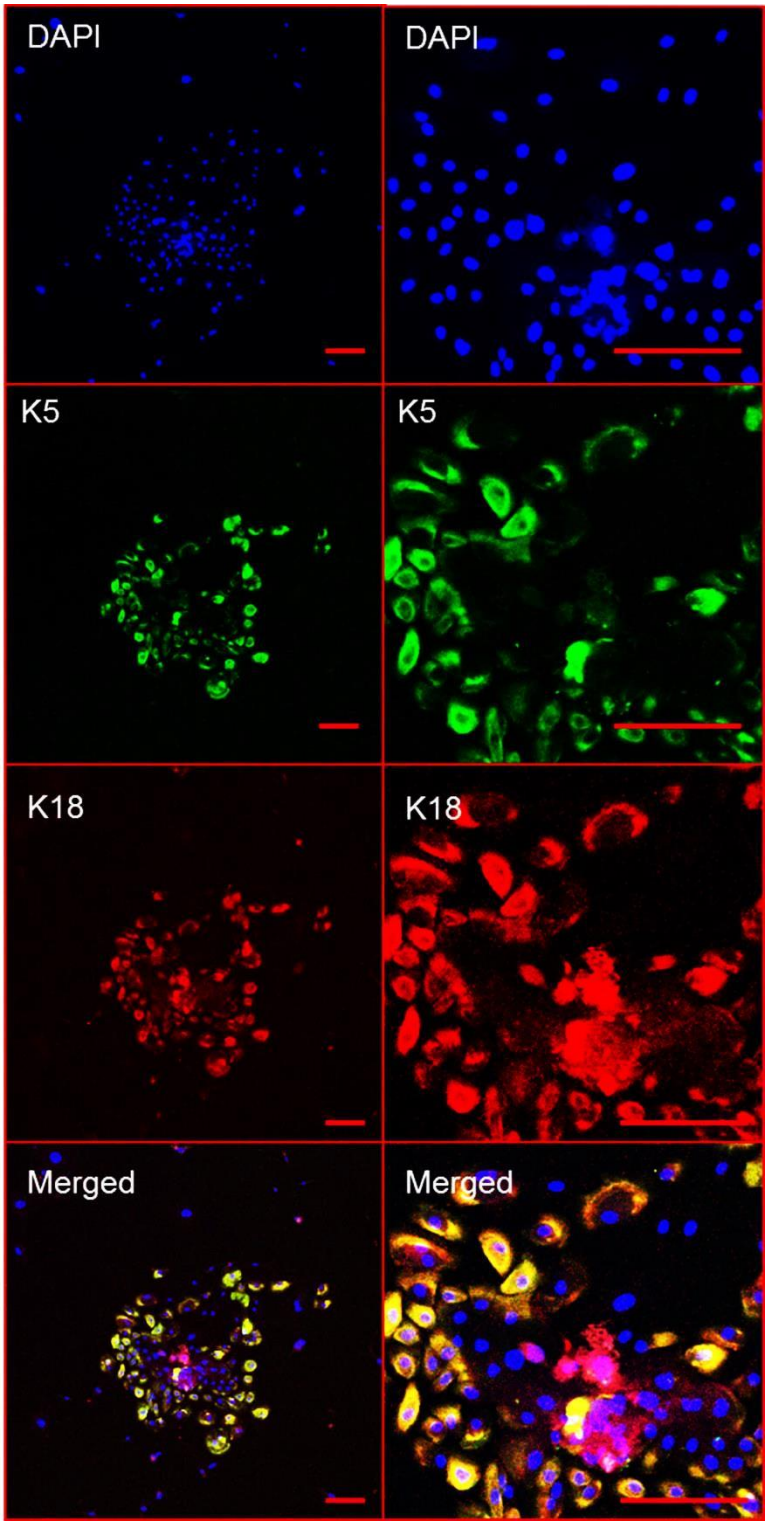

Figure 67. Prostate Epithelial Type 2 Colony Cytokeratin Expression

Expression of K5 and K18 by type 2 prostate epithelial colonies. Immunocytochemistry with monoclonal antibodies against K5, detected with a FITC conjugated secondary antibody (green) and against K18 detected by a TRICT conjugated secondary antibody (red) and counter stained with DAPI (blue). Representative colonies shown. Bar = 100µm

5.5.6.3 *Stem Cell Markers*

The number of cells expressing stem cell markers in prostate epithelial colonies was determined by immunocytochemistry and is shown as a proportion of the total number of cells in Figure 76. Type 1 prostate epithelial colonies stained brightly for the putative SC marker CD44 (Figure 68), whereas the proportion of CD44 positive cells was lower in type 2 cells (Figure 69) ($p<0.05$ unpaired t-test) and cells did not stain as brightly. In contrast, only a few type 1 and no type 2 colonies contained cells positive for the putative SC marker α2β1 integrin, which stained weakly (Figure 70 and Figure 71). Most cells in type 1 colonies were Bmi1 positive (Figure 74), and significantly more seen compared to type 2 colonies (Figure 75) ($p<0.05$). No Oct4 was observed in either colony type (Figure 72 and Figure 73).

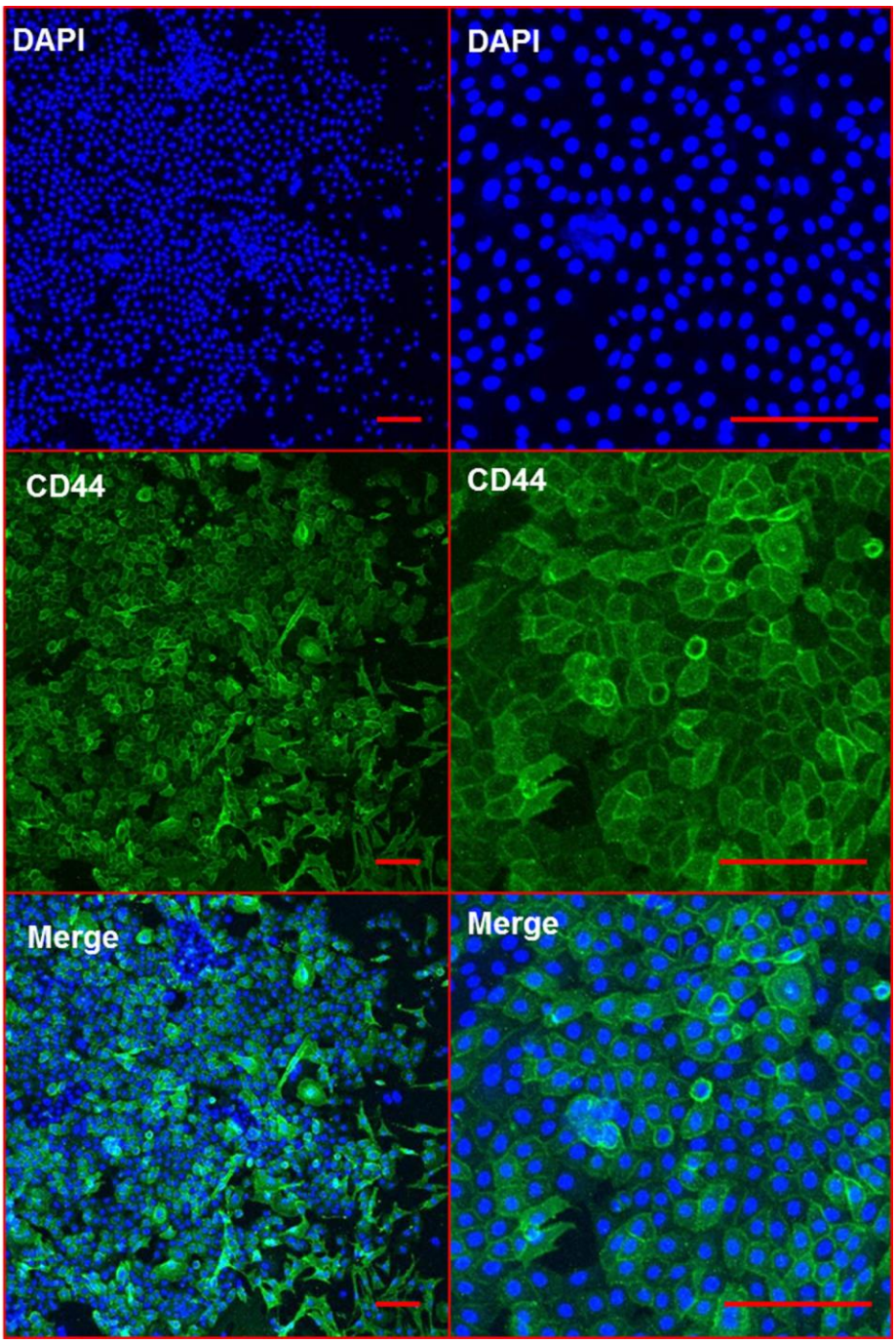

Figure 68. Prostate Epithelial Type 1 Colony CD44 Expression

Colonies were stained by immunocytochemistry with monoclonal antibodies against CD44, detected with a FITC conjugated secondary antibody (green) and counter stained with DAPI (blue). Bar = 100µm

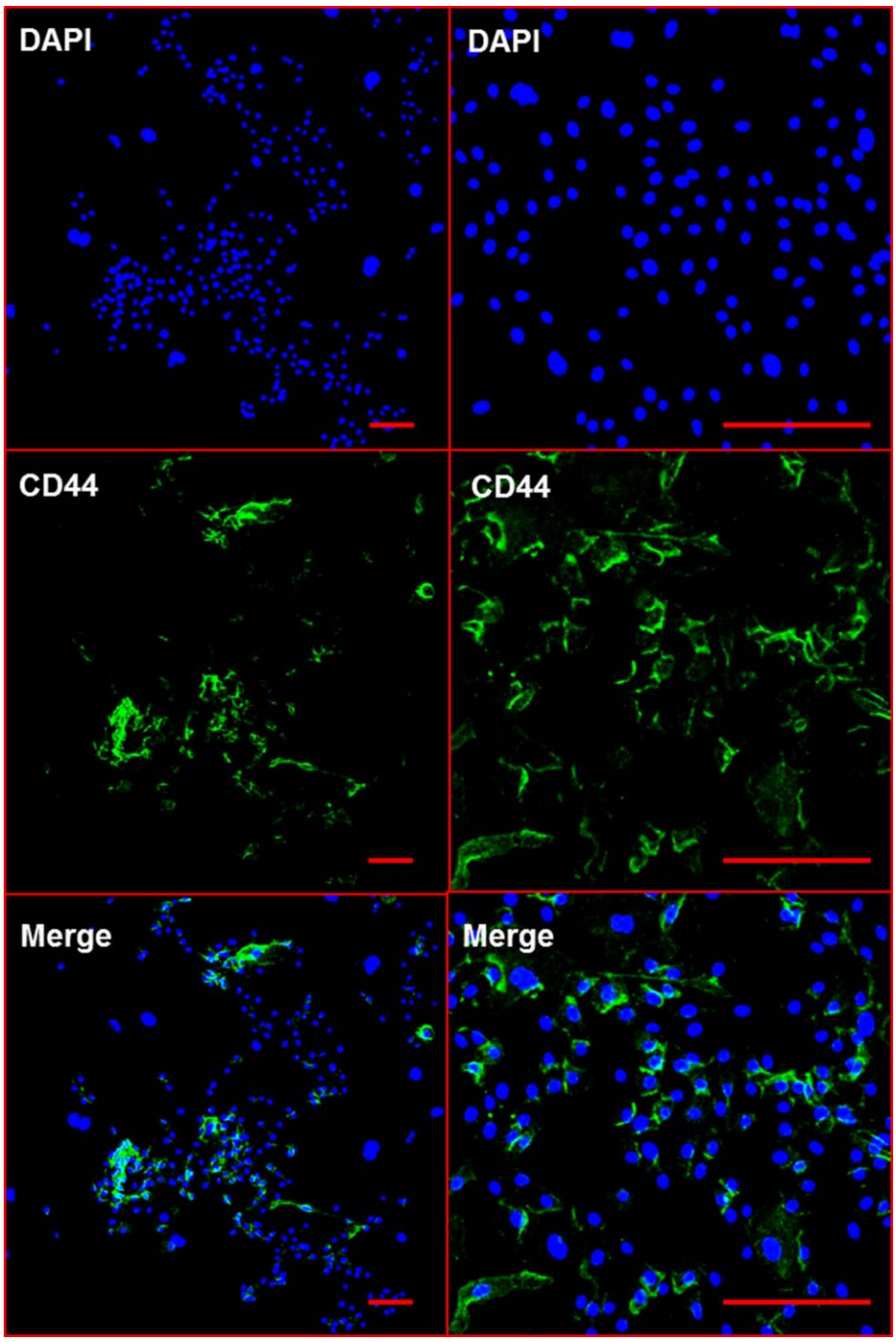

Figure 69. Prostate Epithelial Type 2 Colony CD44 Expression

Colonies were stained by immunocytochemistry with monoclonal antibodies against CD44, detected with a FITC conjugated secondary antibody (green) and counter stained with DAPI (blue). Bar = 100µm

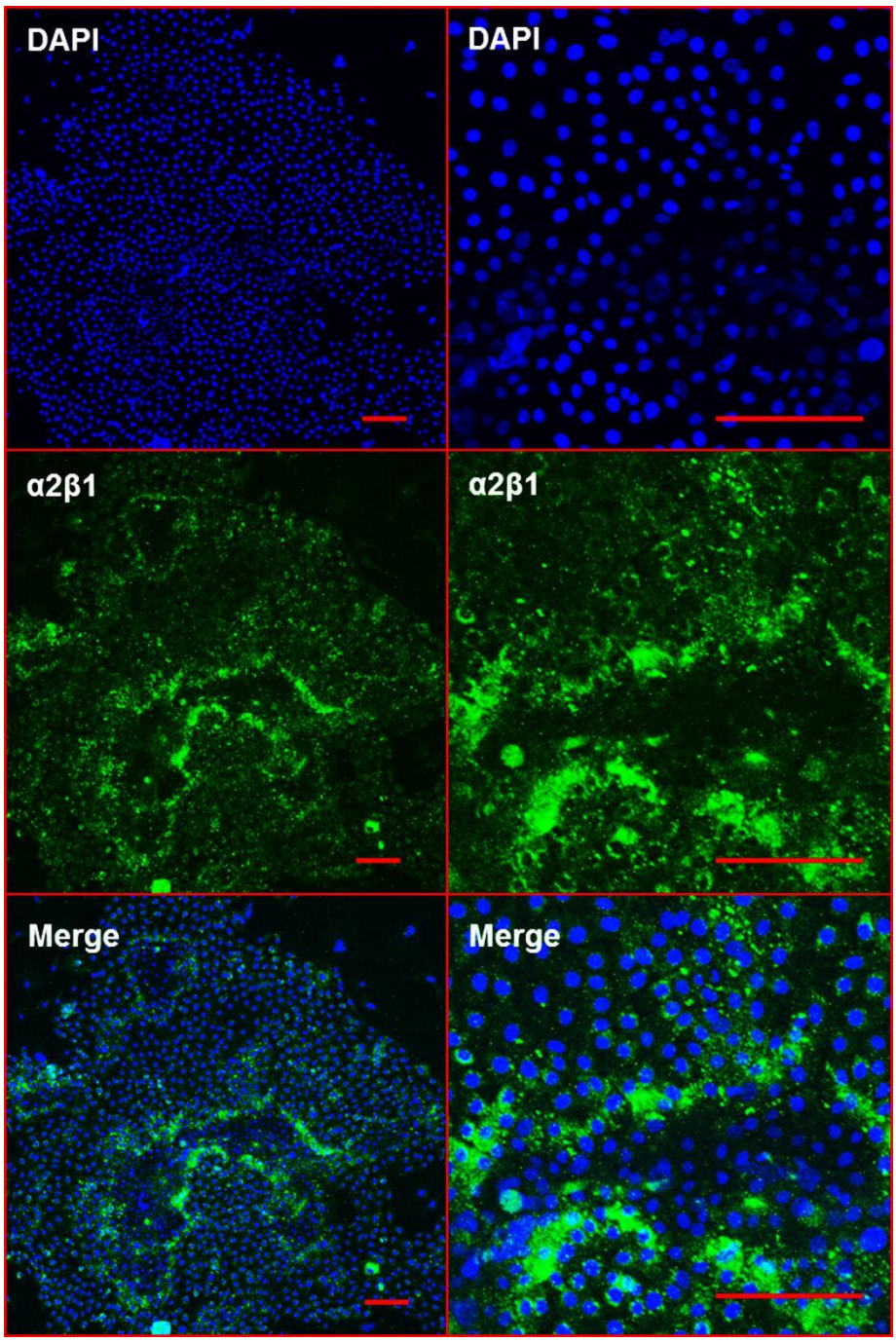

Figure 70. Prostate Epithelial Type 1 Colony α2β1 integrin Expression. Colonies were stained by immunocytochemistry with monoclonal antibodies against α2β intergin, detected with a FITC conjugated secondary antibody (green) and counter stained with DAPI (blue). Representative colonies shown. Bar = 100µm

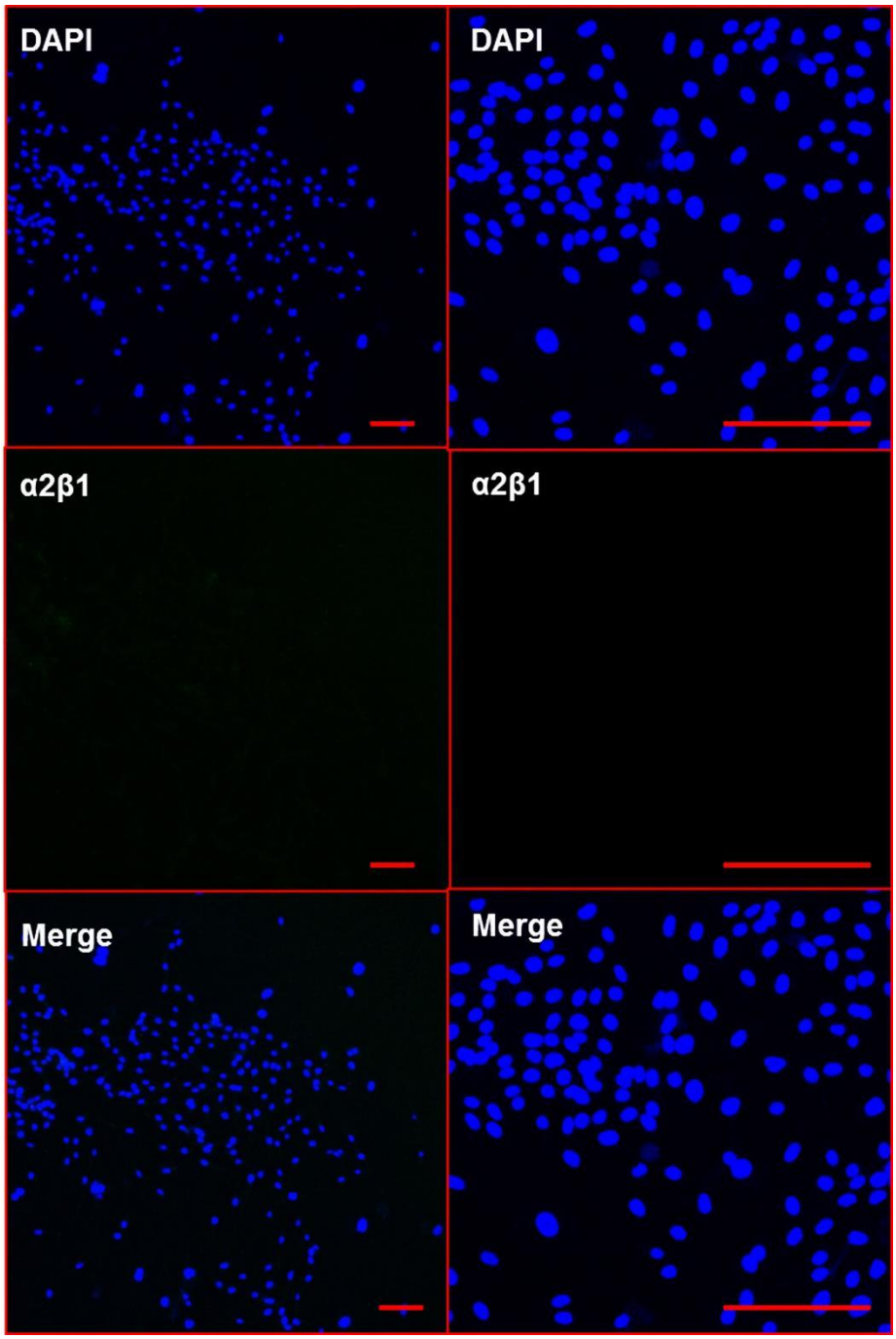

Figure 71. Prostate Epithelial Type 2 Colony α2β1 integrin Expression. Colonies were stained by immunocytochemistry with monoclonal antibodies against α2β intergin, detected with a FITC conjugated secondary antibody (green) and counter stained with DAPI (blue). Representative colonies shown. Bar = 100μm

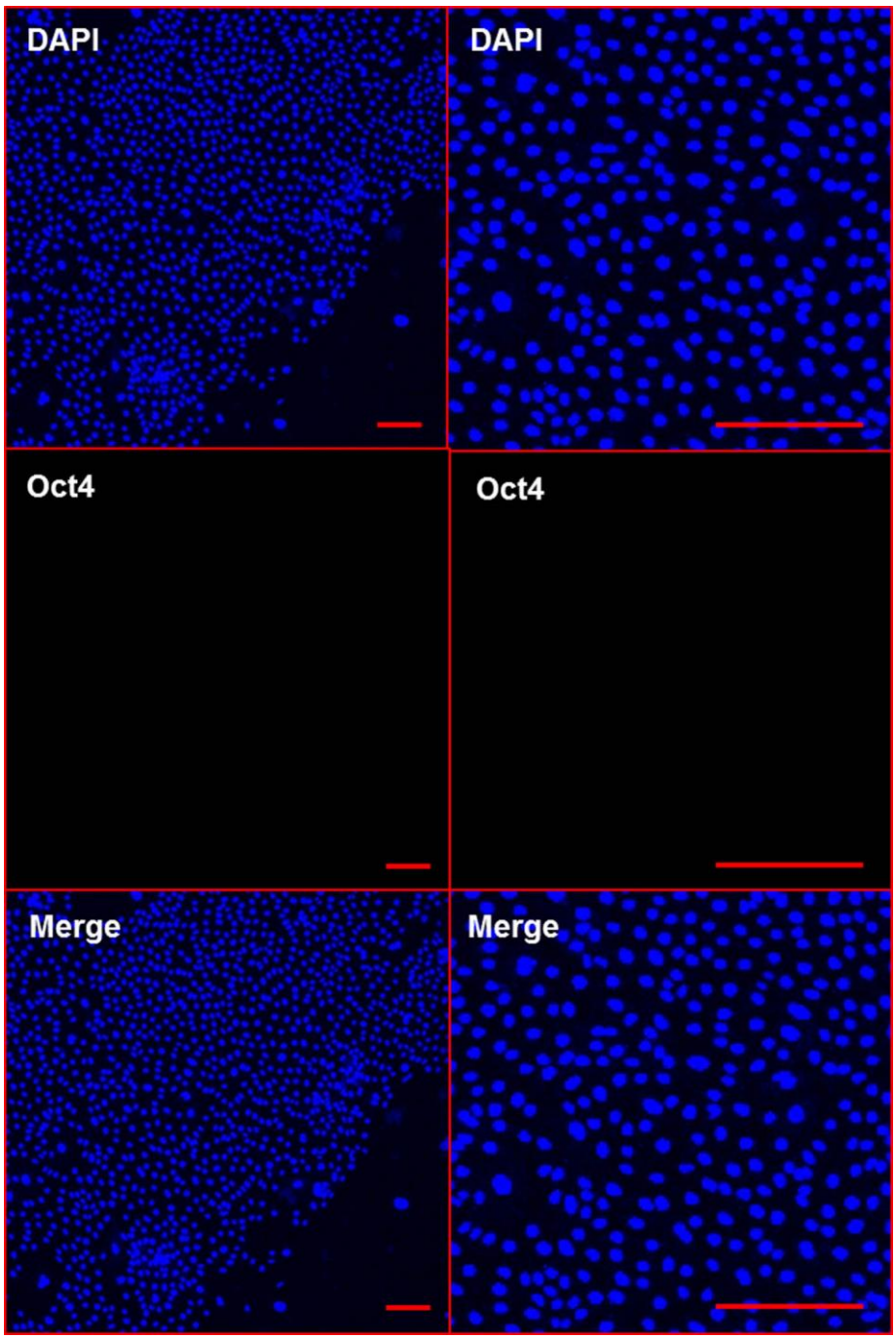

Figure 72. Prostate Epithelial Type 1 Colony Oct4 Expression.
Colonies were stained by immunocytochemistry with monoclonal antibodies against Oct4, detected with a FITC conjugated secondary antibody (green) and counter stained with DAPI (blue). Bar = 100µm

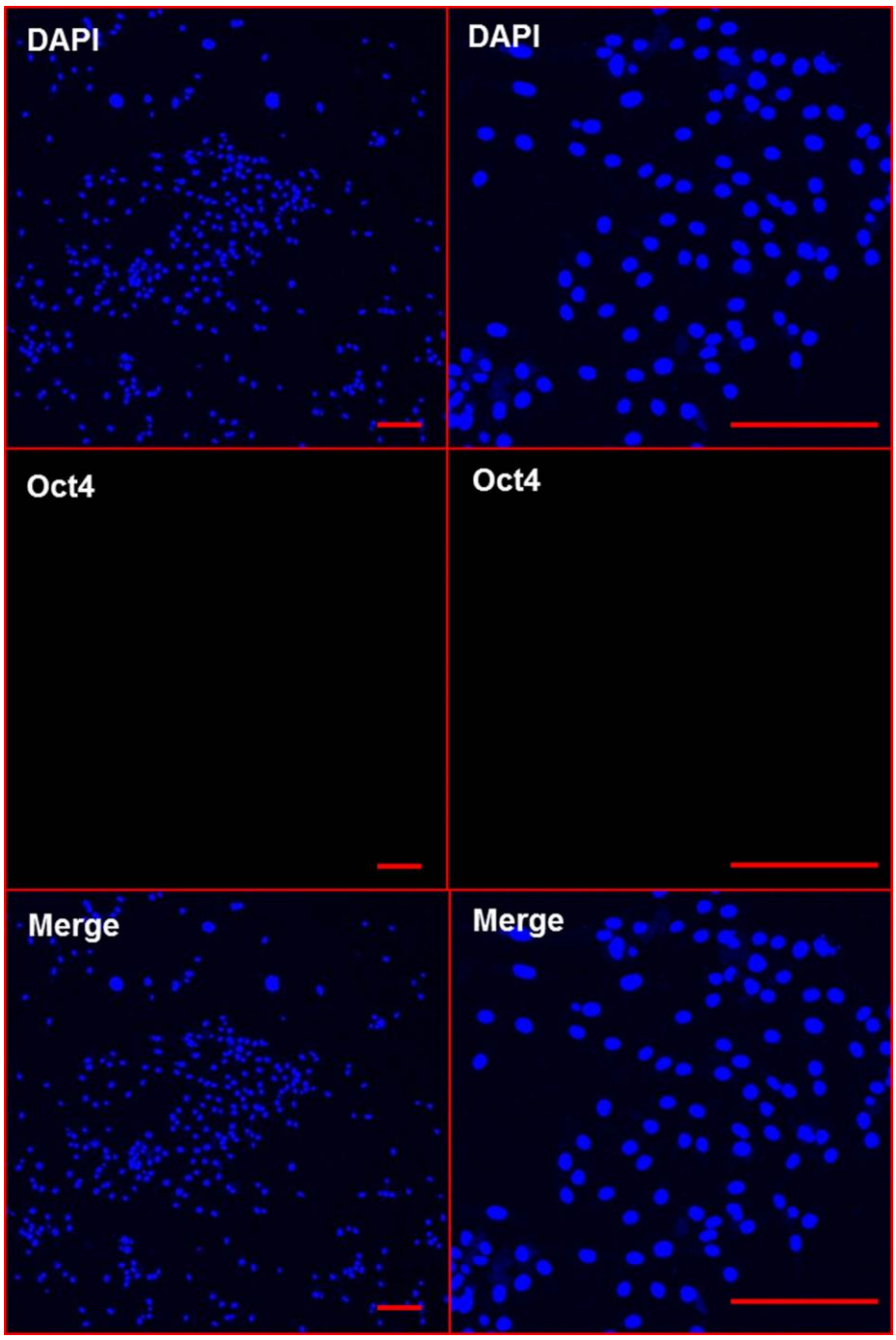

Figure 73. Prostate Epithelial Type 2 Colony Oct4 Expression.
Colonies were stained by immunocytochemistry with monoclonal antibodies against Oct4, detected with a FITC conjugated secondary antibody (green) and counter stained with DAPI (blue). Bar = 100µm

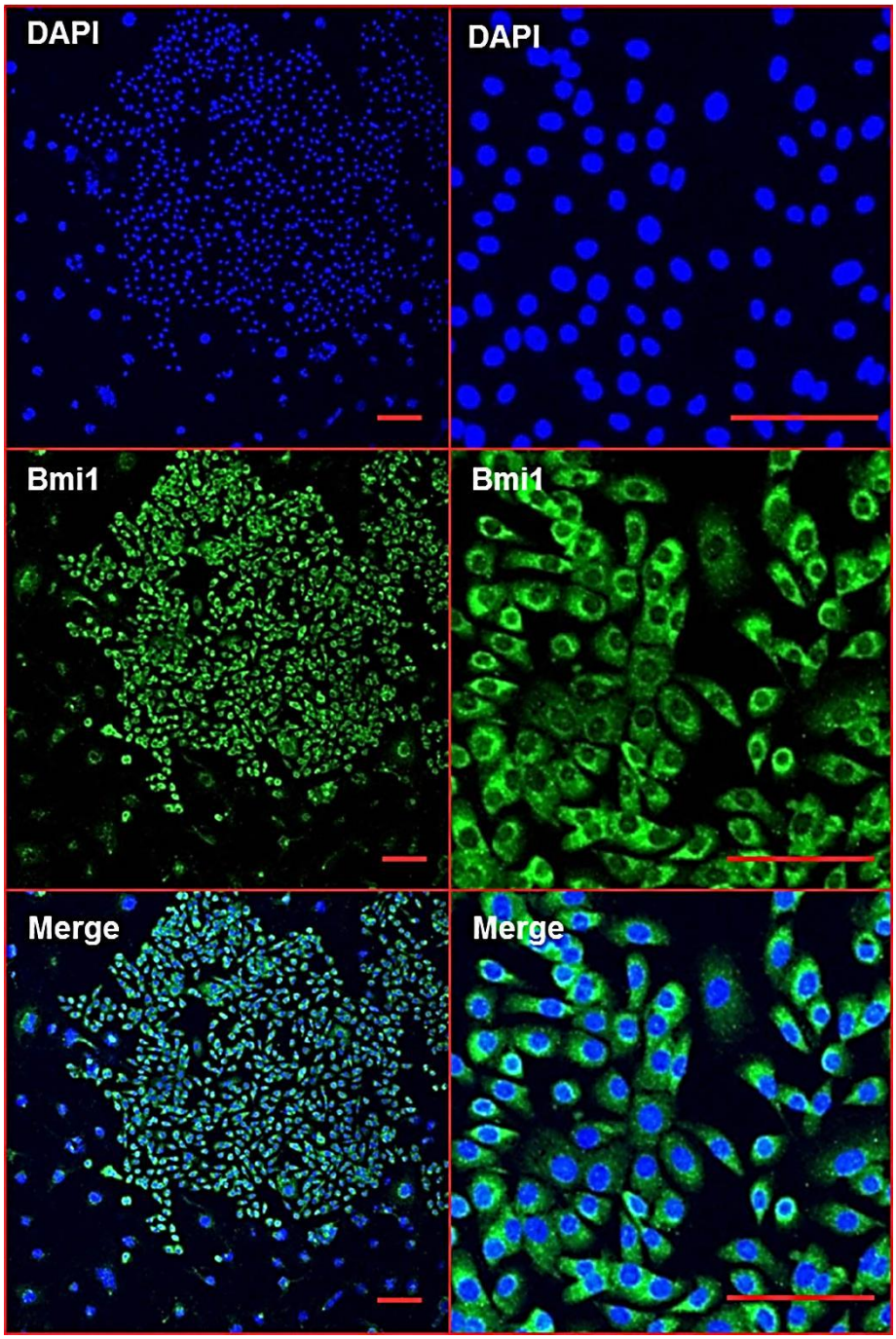

Figure 74. Prostate Epithelial Type 1 Colony Bmi1 Expression.
Colonies were stained by immunocytochemistry with monoclonal antibodies against Bmi1, detected with a FITC conjugated secondary antibody (green) and counter stained with DAPI (blue). Bar = 100µm

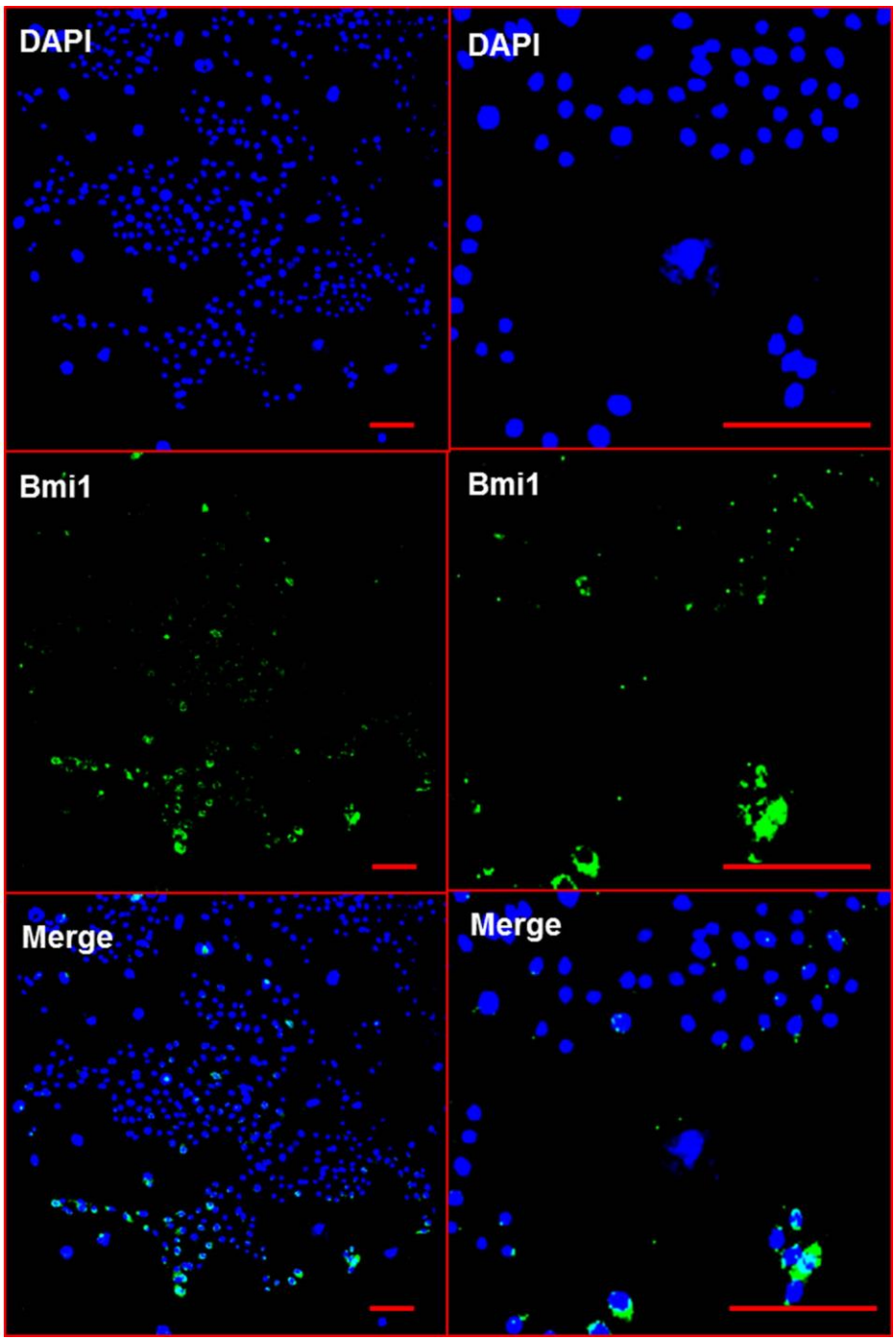

Figure 75. Prostate Epithelial Type 2 Colony Bmi1 Expression.
Colonies were stained by immunocytochemistry with monoclonal antibodies against Bmi1, detected with a FITC conjugated secondary antibody (green) and counter stained with DAPI (blue). Bar = 100µm

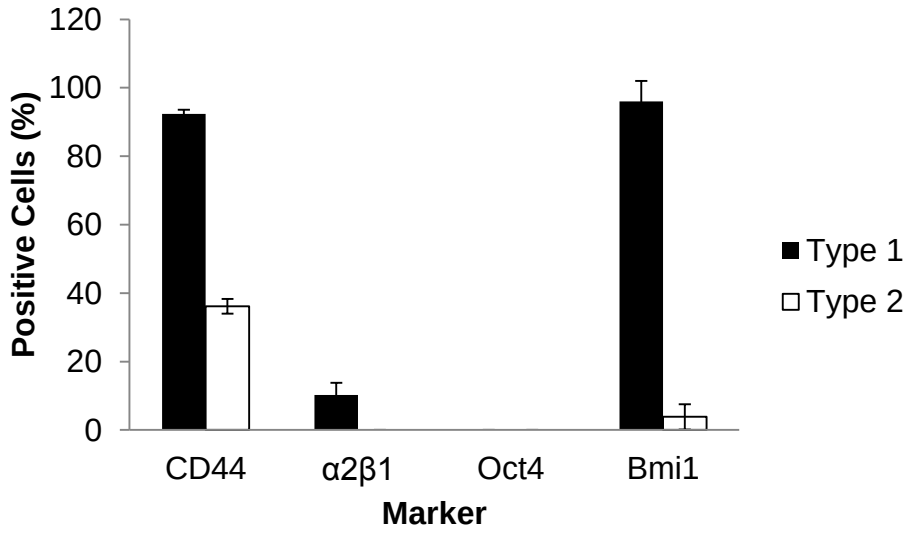

Figure 76. Prostate Epithelial Stem Cell Marker Expression.

Type 1 and 2 colonies were stained by immunocytochemistry with antibodies against each marker and detected with a FITC conjugated secondary antibody. The proportion of cells positive for each marker was expressed as a percentage of the total number of cells counted. Results are the mean of 20 colonies from each of 3 patients ± S.E.M.

5.6 Discussion

The aim of this study was to identify and characterise colonies formed by prostate epithelial cells to test their suitability as surrogates for stem cells. Two colony types were observed, which differed in proliferative and self-renewal capacity and marker expression. Type 1 colonies contained cells which could self-renew and were highly proliferative, whereas type 2 colonies contained fewer self-renewing cells and demonstrated little further proliferation. These results demonstrated a colony forming hierarchy within the prostate epithelium, of which cells with stem cell traits form large type 1 colonies. Cytokeratin staining suggests that these cells may originate from the basal compartment of the epithelium.

5.6.1 Clonogenicity and Colony Morphology

Significant heterogeneity was observed between patient samples in terms of colony forming efficiency and the morphology of colonies. The majority of cells were unable to form colonies in this *in vitro* environment and either did not attach to the collagen coated plate or failed to grow.

The colony morphology of prostate epithelial cells was similar to Barrandon and Greens holoclones and meroclones, which suggest that the larger type 1 colonies are the highly proliferative stem cell derived colonies. (Barrandon and Green, 1987b). These colony morphologies have also previously been observed by Hudson et al., 2000 in prostate derived epithelial colonies.

5.6.2 Proliferative Capacity

Size and morphology of prostate epithelial colonies reflected both their short and longer term proliferative capacity. Cells which form type 1 colonies have a greater capacity for proliferation in both short and long term culture than

type 2 colonies. Cells which formed type 1 colonies proliferated rapidly, undergoing at least 11 cell divisions in 2 weeks and contained a high proportion of actively cycling Ki67+ cells. Type 2 colonies were smaller, underwent fewer divisions and contained few actively cycling Ki67+ cells. However, within each colony type the size and number of cells per colony was highly variable, suggesting a more complex proliferative hierarchy.

In long term culture, most type 1, but only a few type 2 prostate epithelial colonies proliferated extensively to become confluent and could be further passaged. Type 2 colonies quickly became senescent, whilst type 1 colonies proliferated for longer but also senesced. These results demonstrated that the epithelial fraction of the prostate contains cells with significant clonogenic and proliferative heterogeneity. As only type 1 colonies contain cells which are capable of extensive proliferation and self-renewal, stem cell traits, this observation suggests that type 1 colonies are derived from stem cells, whereas type 2 are derived from transit amplifying cells which have a variable proliferative capacity.

Colonies became senescent too rapidly to be serially cloned. Neither type 1 or 2 colonies could form further colonies when ring cloned and cultured at low density. Although a layer of feeder cells was used, regulation of differentiation may be more affected by low density cell culture and cells differentiated and lost their self-renewal capacity at a faster rate than in high density culture (Peehl, 2005).

5.6.3 Self-renewal

Only type 1 colonies contained cells which could self-renew to form spheres in non-adherent conditions. Again this suggests that only type 1 colonies are

derived from and contain self-renewing stem cells. Prostate spheres are enriched for cells expressing prostate basal and luminal cytokeratins (34βE12 and K18) which recapitulate the basic spherical structure of the prostatic epithelium with both basal and luminal epithelial layers identified by cytokeratin expression (Garraway et al., 2010). This observation again suggests the stem cell capacity of type 1, but not type 2 colonies.

5.6.4 Marker Expression

Cytokeratin staining showed that most type 1 colonies displayed a basal phenotype (K5), whereas type 2 colonies contained a mixture of basal and luminal cells (K5 and K18) or just luminal (K18) cells. This observation suggests that type 1 colonies are derived from basal cells, whilst type 2 are from intermediate or luminal cells. As prostate epithelial stem cells are predicted to reside in the basal compartment of the prostate (Robinson et al., 1998), these results again suggest that type 1 colonies are derived from proliferative stem cells.

Expression of both the putative stem cell markers CD44 and α2β1 integrin was higher in type 1 than type 2 colonies, although type 2 colonies still contained many CD44 positive cells. CD44 and α2β1 integrin have both been used as stem cell markers in normal (Collins et al., 2001) and neoplastic prostate (Collins et al., 2005, Patrawala et al., 2006, Patrawala et al., 2007). Neither marker is a reliable stem cell marker in this setting as CD44 is expressed in both colony types and although α2β1 integrin is expressed only in type 1 colonies, staining was weak. These markers may be down-regulated when cultured *in vitro* and therefore this study does not exclude their relevance in freshly isolated tissue. Protein expression changed caused

by cell culture may also account for the lack of Oct4 staining in either colony type. However, the self-renewal marker Bmi1 was expressed strongly in type 1 colonies, suggesting other self-renewal mechanisms, unrelated to transcription factor control. These may include the role of Bmi1 in p63 and β-catenin signalling, suggesting that Bmi1 is required for activity of another self-renewal pathway (Lukacs et al., 2010).

5.6.5 Technical Issues

Overall colony forming efficiency and the proportion of each colony type varied widely between patients. This variability in CFE can be attributed to individual patient variation or tissue and cellular damage caused by the laser during surgery. Although cell isolation methods were the same for each patient, removal time of the tissue and damage caused by the laser treatment were variable due to differences in operator, laser power and size of the prostate (Das et al., 2000). Tissue digestion to achieve a single cell suspension may cause significant cell death due to harsh the enzymatic digestion (Freshney, 2005) which may kill cells already damaged by surgery (Lupold and Rodriguez, 2004). Removal of larger viable cell clumps by the cell strainer may also reduce the colony forming efficiency by reducing the proportion of epithelial cells compared to other cell types.

Although the culture of primary cells in vitro is a useful technique for studying the properties of individual cells, the cells are not immortal and can only be cultured for a finite time. The prostate epithelial cells used in this study, could only be passaged for a limited time, becoming senescent and failed to form secondary colonies. The digestion and subsequent culture of primary cells can significantly affect their gene expression, particularly cell surface

antigens (Boquest et al., 2005). The problem of senescence can be overcome by immortalisation, but this alters the cells so that they may not be representative, especially in terms of proliferative capacity (Miki et al., 2007).

5.6.6 Comparison to Previous Work

The two types of colony prostate epithelial colony in this study are similar in both morphology and proliferative capacity to holoclones and meroclones formed by keratinocytes (Barrandon and Green, 1987b). Both holoclones and type 1 prostate epithelial colonies contain a large number of cells and have an extensive proliferative capacity. Both meroclones and type 2 prostate epithelial colonies contain a smaller number of cells and a have limited proliferative capacity. However, no small paraclone type prostate epithelial colonies were observed. The morphologies of the two prostate epithelial colony types were also similar to those formed by mouse epidermis, but these colonies could be serially cloned, whereas prostate colonies could not (Tudor et al., 2004, Wolff and Mason, 2012).

In a previous study by Hudson et al, 2000, two types of colonies derived from prostate epithelium were also observed. The morphologies, proliferative capacities and cytokeratin expressions are similar in both studies. Large colonies were able to recapitulate the basic ductal structure of the prostate when cultured in Matrigel, which consisted of both basal and luminal layers determined by the expression of cytokeratins (Hudson et al., 2000). This provides further evidence that large type 1 colonies are derived from and contain stem cells which can differentiate to regenerate the prostatic duct.

Although in this study, prostate epithelial colonies have been characterised *in vitro*, their ability to reconstitute the prostatic gland *in vivo* is unclear. *In vivo*

regeneration of the prostate gland is seen as the ultimate proof of stem cell function. This has previously been shown in the mouse prostate in which Lin-Sca-1+CD133+CD44+CD117+ mouse prostate stem cells can generate a prostate after transplantation (Leong et al., 2008). Single cell transplantation of single cells derived from type 1 colonies supported by rat urogenital mesenchyme (rUGM) would demonstrate the potency of the putative stem cell fraction.

5.7 Chapter Conclusions

Prostate epithelial cells obtained from patients with BPH form two types of colony which differ in proliferative and self-renewal capacity and marker expression. Type 1 colonies have a high proliferative and self-renewal capacity and express basal epithelial and putative stem cell markers. Type 2 colonies have a limited proliferative and no self-renewal capacity, express luminal epithelial makers and contain few cells positive for putative stem cell markers. Based on these characteristics, it is likely that type 1 colonies are derived from stem cells and type 2 from transit amplifying cells, however *in vivo* regeneration data is required to confirm this conclusion.

.

6 Results: Targeting of Prostate Stem Cells By Peptide Phage Display

6.1.1 Chapter Aims

The aim of this part of the study was to identify peptides which target proliferating human primary prostate epithelial cells *in vitro* by using phage display technology. In previous chapters it was demonstrated that actively dividing clonogenic cells are tumourigenic and contain cells demonstrating CSC traits. For new therapies it is essential to target proliferative cells to cure prostate cancer. Previous studies have identified peptides which bind to prostate cancer cell lines. However, no peptides have progressed to clinical trials. The prostate is a non-essential organ therefore panning against primary human prostate epithelial cells may offer an alternative model system for target discovery.

The Ph.D.™-7 library from New England Biolabs was selected which displays a random sequence of 7 amino acids on the pIII coat protein. This library has only 7 residues therefore selects for high affinity binders compared to libraries of 12 or more residues (Shrivastava et al., 2005)., The Ph.D.™-7 library was panned initially against primary human prostate epithelial cells, in four individual experiments, which differed in the number of patient samples and stringency of the wash steps. In experiments 1 and 2 different patient samples were used in each of 4 rounds of panning, whilst in experiments 3 and 4, cells from the same patient were used in each round of panning. Either mild (experiments 1 and 3) or stringent (experiments 2 and 4) wash steps to were used to select for lower of high affinity binders. As selection of prostate specific markers was required, a negative selection step was

included to remove any phage which binds to HUVECs, collagen or tissue culture plastic. Following four rounds of panning the phage clones were sequenced and their relative binding efficiencies to prostate epithelial cells determined.

6.2 Hypothesis

Peptide phage display can be used to identify novel targets which bind specifically to proliferative prostate epithelial cells.

6.3 Objectives

1. Choose phage display library and confirm clonal diversity.
2. Pan library against primary prostate epithelial cell following a negative selection step against HUVECs to deplete non-prostate binders using the strategy in Figure 13.
3. Sequence phage clones and identify repetitive motifs.
4. Identify high affinity binders using titration and ELISA binding assays.

6.4 Results

6.4.1 Naïve Ph.D.™-7 Library Randomness

To confirm the randomness and suitability of the naive Ph.D.™-7 library, forty clones form the purchased library were isolated and sequenced (Appendix 1). No sequence was observed more than once and analysis with Pratt pattern recognition software identified no repetitive motifs of three amino acids or greater, confirming the randomness, diversity and suitability of the library for this study. However the presence of one clone coding for a stop codon was identified: clone 30, sequence QPFY*NA where * indicates the stop codon.

6.4.2 Experiment 1

6.4.2.1 *Phage Recovery*

In panning experiment 1 the number of phage particles recovered after each round of panning were titrated on IPTG / Xgal plates (Table 23). Following the first and second rounds of panning only 0.005% of the input phage were recovered. The proportion recovered increased following the third round of panning, and 0.7% of input phage were recovered following the fourth and final round. An increase in phage recovery suggested that the phage pool was being enriched, so clones from the third and fourth rounds of experiment 1 were selected for sequencing and further analysis.

Table 23. Experiment 1 Phage Recovery.

Round	Recovery (%)
1	0.005
2	0.014
3	0.400
4	0.700

The number of phage recovered as a percentage of input phage after each round of panning.

6.4.2.2 *Sequences of Third Round Clones*

Following three rounds of panning with the prostate epithelial cells the 40 phage clones were isolated and sequenced. No repeat sequences were observed more than once in the pool (Appendix 2). Sequence pattern analysis showed that although there were no repeat sequences, pattern

motifs had started to appear. There were 5 motifs of 3 amino acids WRP, TPP, LSR, LSL and PTS which appear at least twice, equating to 5% of the phage population each.

6.4.2.3 *Fourth Round Clone Sequences*

As no repeat sequences were observed after 3 rounds of panning, phage were panned against the target a fourth time. One hundred phage clones from the fourth round eluate were sequenced and analysed (Appendix 3) and out of these, the 12 sequences HAIYPRH, SILPYPY, STASYTR, KLPGWSG, LPSYHVP, STFTHPR, GETRAPL, WPTLQWA, SSLPLRK, SAPSSKN, ANTLRSP, AFPVSHN were repeated twice or more (Table 24). HAIYPRH was the most abundant clone which represented 5% of the phage pool. Interestingly, the only smaller motifs greater than 3 amino acids which appear more times than the number of whole clones were S-x-L-P which appears in 7% of the phage population, P-R-H (6%) and R-x-P and Y-x-R which both appear in 10%. The clone SAPSSKN also appeared in the third round of cloning.

Table 24. Phage Clone Patterns.

Pattern	Hits
HAIYPRH	5
SILPYPY	4
STASYTR	3
KLPGWSG	3
LPSYHVP	2
STFTHPR	2
GETRAPL	2
WPTLQWA	2
SSLPLRK	2
SAPSSKN	2
ANTLRSP	2
AFPVSHN	2
TFTH	3
PVSH	3
MPTP	2
STFT	3

Patterns identified following four rounds of panning against prostate epithelial cells. Only patterns which occur 2 more time in 100 sequenced cl9ones are shown.

6.4.3 Comparison of Clones with BLAST

Comparison of selected sequences to known human protein sequences by SWISSPROT BLAST showed that none of the 12 amino acid sequences selected had 100% homology to any known sequence. The maximum homology observed was 6/7 residues and all homologies shown are between 5/7 and 6/7 (Table 25). No homologous protein was common to more than one clone and all the clones were homologous to more than one completely different protein.

Table 25. Proteins Homologous to Experiment 1Phage Clones.

Original sequence	Homologue	Name
AFPVSHN	**AFPVSH**	Gap junction delta-3 protein
	AFPVSN**N**	Myotubularin-related protein 2
	AFPL**SHN**	Collagen alpha-2(VI) chain
	AFPI**SH**	Gap junction delta-2 protein
ANTLRSP	**ANTL**K**SP**	UHRF1 binding protein 1-like
	ANTLRS	Leucine-rich repeat and WD repeat-containing protein
	NTLRA**P**	Homeobox protein VENTX
	NTLRT**P**	Arylsulfatase D
	NTLRT**P**	Neurexin-1-alpha
	NTLRN**P**	ATP-binding cassette sub-family A member 12
	ANTA**RSP**	PHD finger protein 3
	ANTLR	Zinc finger protein 524
	TLRSP	Methyltransferase-like protein 9
	ANTLR	Phosphate carrier protein, mitochondrial
GETRAPL	**ETRAPL**	OTU domain-containing protein 7A
	GETRAP	Melanoma-associated antigen F1
	GETRV**PL**	Double C2-like domain-containing protein beta
	GETRV**PL**	Oxysterol-binding protein-related protein 3
	ETRS**PL**	DNA excision repair protein ERCC-6-like
	GETRS**P**	G patch domain and ankyrin repeat-containing protein 1
	GETRS**P**	MutS protein homolog 4
	GD**TRAP**	Sal-like protein 3
	ETRAP	Regulating synaptic membrane exocytosis protein
HAIYPRH	**HAIY-RH**	E3 ubiquitin-protein ligase Itchy homolog
	HAL**YPR**	Non-lysosomal glucosylceramidase
	AIYR**RH**	Urokinase-type plasminogen activator
	HAIYT**R**	Semaphorin-3E
	HAIYE**R**	Malonyl-CoA-acyl carrier protein transacylase, mitochondrial
KLPGWSG	**LPGWSG**	Multiple epidermal growth factor-like domains protein
	LPGWS	Integrator complex subunit 9
	LPGWT**G**	Delta-like protein 4
	LPGWS	Kin of IRRE-like protein 2
	LPGWS	Serine/threonine-protein kinase N2
	LPGWAG	Platelet endothelial aggregation receptor 1
	PGWSG	Transmembrane protein 88B
	PGWSG	Melatonin receptor type 1B
	PGWSG	ubiquitin-protein ligase NEURL1B
	PGWSG	Multiple epidermal growth factor-like domains

		protein
LPSYHVP	**LPSY**Q**VP**	R3H domain-containing protein 2
	LPSYHCPG**VP**	Egl nine homolog 2
	PSYHI**P**	Transmembrane 7 superfamily member 3
	LE**SYHVP**	Leucine-rich PPR motif-containing protein, mitochondrial
SAPSSKN	**SAPSSK**	Neuronal acetylcholine receptor subunit beta-2
	SAPSSK	Alpha-protein kinase 3
	SAPSSE**N**	Ubiquitin-associated protein 2
SILPYPY	**SILPYP**	MAX gene-associated protein
	SILQ**YPY**	Eukaryotic translation initiation factor 2-alpha kinase 3
	LPYPY	Glutathione peroxidase 2
	SILPL**PY**	Proactivator polypeptide-like 1
	SILPY	GTPase RhebL1
	SILPY	Acyl-coenzyme A thioesterase 12
SSLPLRK	**SSLPLR**	Erythrocyte membrane protein band 4.2
	SSLS**LRK**	PH domain leucine-rich repeat-containing protein phosphatase 2
	LPLRK	Metalloproteinase inhibitor 4
	LPLRK	Coiled-coil domain-containing protein 74A
	LPLRK	B-cell lymphoma 3 protein
STASYTR	**TASYTR**	Olfactory receptor 2T6
	STAQ**YTR**	Receptor-type tyrosine-protein phosphatase eta
	TAT**YTR**	zacytidine-induced protein 2
	ASYTR	Dermatan-sulfate epimerase
	TASYS**R**	ubiquitin-protein ligase TRIM37
	ASYTR	Sorbin and SH3 domain-containing protein 2
STFTHPR	**TFTHP**	Placenta-specific protein 4
	TFTHP	Taste receptor type 2 member 60
	TFTHP	Sialic acid-binding Ig-like lectin 15
	TFTHP	Zinc finger protein 398
	STFTH	Transmembrane emp24 domain-containing protein 7
	STFTH	FERM and PDZ domain-containing protein 3
	TFK**HPR**	Testis-expressed sequence 15 protein
WPTLQWA	**WPT**Q**QW**	Regulator of G-protein signaling 9
	PTLQW	Gem-associated protein 2
	WPTLQ	A/G-specific adenine DNA glycosylase
	PTLQW	Protein sidekick-1

6.4.4 Binding of Individual Clones

The 12 clone sequences identified in experiment 1 following four rounds of panning that occur 2 or more time within the 100 clones sequenced were investigated further for their binding efficiency. Individual clones were incubated with prostate epithelial cells or blank wells and the binding efficiency assessed using both a titration and whole cell ELISA assays. Results were compared to wild type phage from the unselected Ph.D.™-7 and the entire experiment 1 fourth round eluate.

As shown by the titration binding assay, (Figure 77) none of the 12 isolated phage clones or the round 4 eluate pool demonstrated increased binding efficiency to prostate epithelial cells compared to blank wells or wild type phage by binding titration assay. A large number of GETRAPL and STAYSTR phage clones were bound to patient 1 cells, but this was not observed in samples from the other 3 patients. The clones HAIYPRH, SILPYPY, KLPGWSG, ANTLRSP and SAPSSKN appear to bind specifically to the tissue culture plastic as many at least 100 - 1000 times more phage were recovered than when cultured with target cells. The low binding efficiency of pooled round 4 clones is no higher than the naive unselected library, so no increased binding efficiency is observed after 4 rounds of panning.

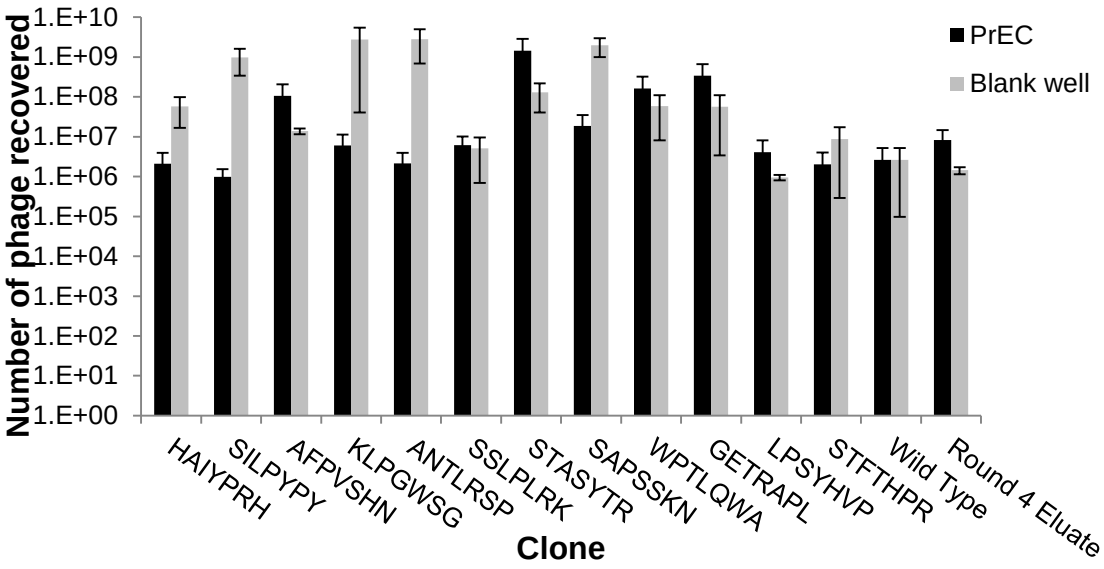

Figure 77. Titration Binding Assay.

Comparing the phage clones selected from the fourth round of panning, the whole 4th round eluate and wild type phage control number. The number of phage particles recovered after binding to the prostate epithelial cells (PrEC) and titered on IPTG / Xgal plates was compared to blank wells. Results are the mean 4 patient samples ± SEM.

Titration results were confirmed by whole cell ELISA (Figure 78). Clones were incubated with the target cells and detected using an anti-M13 antibody. The clones failed to demonstrate increased binding to the target cells compared to blank wells or wild type phage. A higher signal was observed in some of the blank wells, which was higher than in wells containing cells. Round 4 phage also did not bind more strongly than the naive library for either patient sample. The clones WPTLQWA and LSPYHVP exhibited particularly high background binding to blank wells.

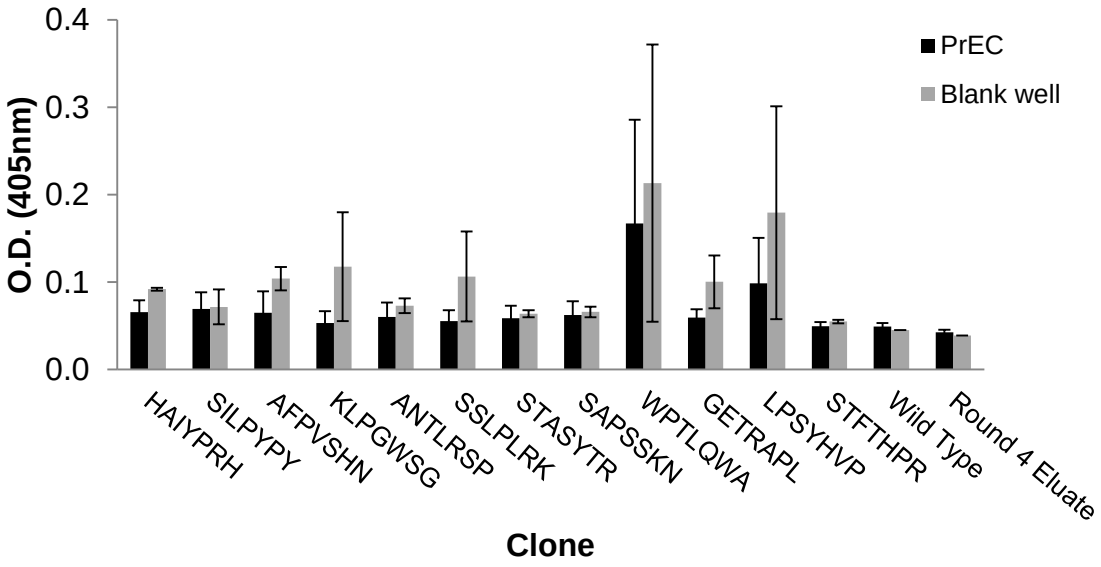

Figure 78. Whole cell ELISA.

Comparing the binding of phage clones selected from the fourth round of panning, the whole 4th round eluate and wild type control. The binding as determined by optical density at 405nm was compared to blank wells. Results are the mean 4 patient samples ± S.E.M.

6.4.5 Experiment 2, 3 and 4

As no prospective clones were identified in experiment 1, the phage panning procedure was repeated and the stringency of the wash steps increased to selecte for higher affinity binders and reduce non-specific binding (experiment 2). Increased stringency of the washing step did not reduce the number of phage recovered after the first two steps, as would be expected. There was also no increase in the number of phage recovered following panning rounds 3 and 4 (Table 26).

The panning procedure was repeated again using only 1 patient sample for all four rounds of panning to reduce the inter-patient variability and using both mild stringent washes in tandem experiments (experiment 3 and 4). Experiments 3 and 4 also failed to demonstrate an increase in phage recovery following several rounds of panning (Table 26). However, to confirm this finding, binding assays were done on the whole fourth round phage pool.

Table 26. Experiment 2, 3 and 4 Phage Recovery.

Round	4 Patient Samples	1 Patient Sample	
	Stringent (Experiment 2)	Mild (Experiment 3)	Stringent (Experiment 4)
1	0.003	0.006	0.002
2	0.001	0.001	0.012
3	0.028	0.001	0.011
4	0.003	0.001	0.013

The number of phage recovered as a percentage of input phage after each round of panning.

6.4.6 Panning Experiments 2, 3 and 4 Binding Assays

The ability of the amplified fourth round phage from experiments 2, 3 and 4 to bind to the target cells compared to tissue culture plastic and wild type phage was analysed by titration (Figure 79) and whole cell ELISA (Figure 80) assays. Again, no significant increase in binding was observed compared to wild type or phage or when cultured on tissue culture plastic. These results suggest that there no enrichment of prostate epithelial cells specific clones under these conditions therefore clones from these experiments were nor sequenced.

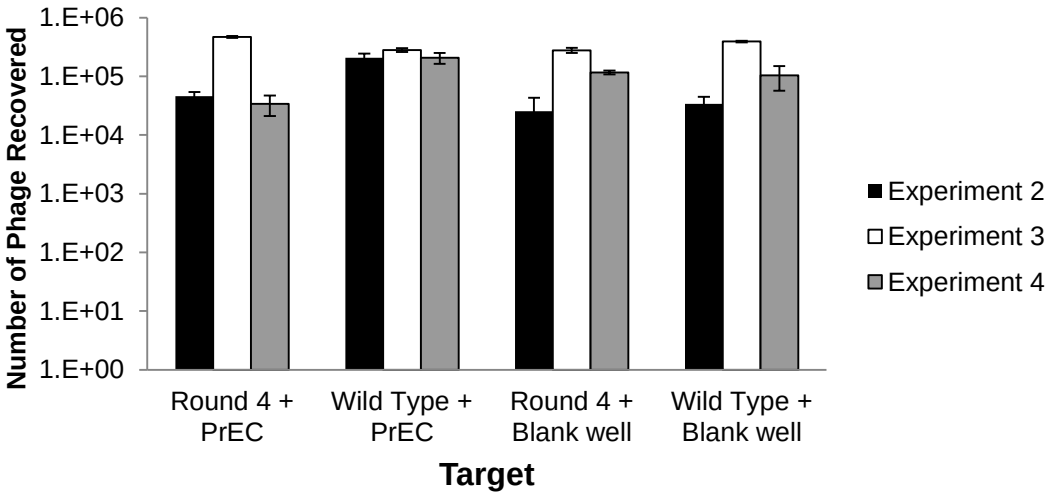

Figure 79. Phage Display Experiment 2, 3 and 4 Titration Binding Assay.
Titration binding assay comparing whole 4th round eluate and wild type phage controls. The number of phage particles recovered after binding to the prostate epithelial cells (PrEC) and titered on IPTG / Xgal plates was compared to blank wells. There was no increased binding of the panned phage clones was observed. Results are the mean 4 patient samples ± S.E.M.

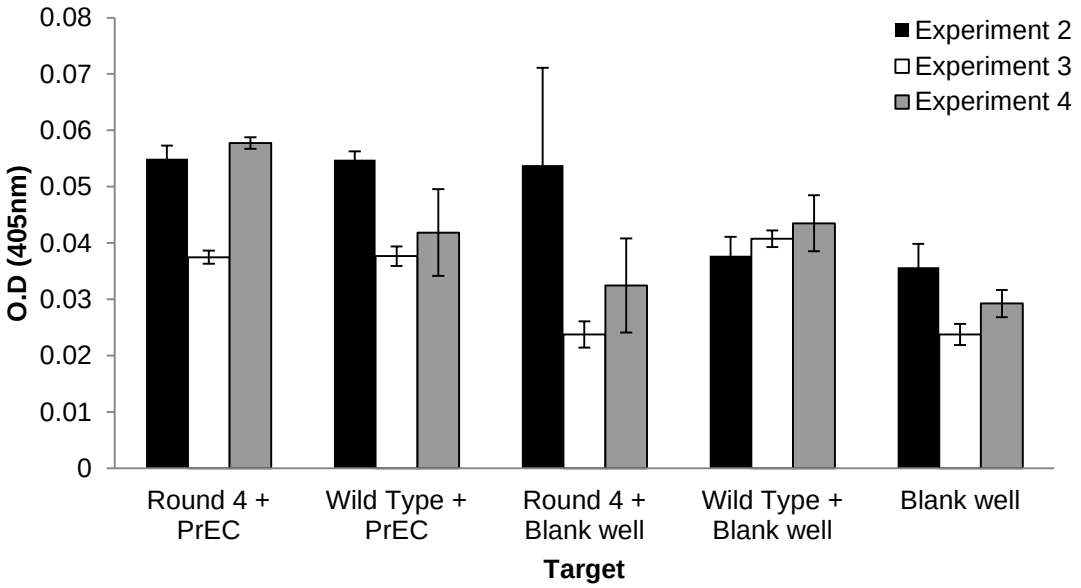

Figure 80. Phage display experiment 2, 3 and 4 whole cell ELISA.

Binding assay to compare the binding of phage panned against prostate epithelial cells against background binding to a blank well and wild type phage control. The binding as determined by optical density at 405nm was compared to blank wells. There was no increased binding of the panned phage clones. Results are the mean 4 patient samples ± SEM.

6.5 Discussion

The aim of this experiment was to identify peptides that target proliferative prostate epithelial cells. However, although initial results were promising, no potential peptides were identified. Panning of the Ph.D.™-7 peptide phage display library against adherent epithelial cells resulted in only 1 of 4 experiments demonstrating phage enrichment. Phage were sequenced and the enriched sequences were identified. However, these sequences did not show any increased binding to prostate epithelial cells.

6.5.1 Experiment 1 Clones

The 12 phage clones selected in experiment 1 showed no increased binding when analysed by either a titration assay or whole cell ELISA. The whole pool of round 4 clones also failed to demonstrate any increased affinity for prostate epithelial cells, although the increase in phage recovery during panning suggested that enrichment was taking place. It is likely that following four rounds of panning, plastic binders, phage clones with a selective advantage and clones with a low affinity for the target were enriched (Vodnik et al., 2011).

Eight of the 12 isolated clones have been previously identified, all using the Ph.D.™-7 library against a wide variety of targets (Table 27). Interestingly HAIYPRH has been identified by several previous studies (Vodnik et al., 2011), but has also been observed in amplified phage pools when not panned against a target (Brammer et al., 2008). The amplification of HAIYPRH was faster than all other clones in the Ph.D.™-7 library suggesting that it has a proliferative advantage. The ability of HAIYPRH displaying clones to out-compete other phage was traced to a mutation in G

to A the Shine–Dalgarno (SD) sequence. This sequences codes for gIIp, which is a protein involved in phage replication, imparting to the SD sequence better complementarity to the 16S ribosomal RNA (rRNA) (Brammer et al., 2008). HAIYPRH with a wild-type SD sequence was found to amplify normally. Despite this, HAIYPRH has also been shown to bind to human transferrin receptor and is a promising candidate carrier for the intracellular delivery of therapeutics (Lee et al., 2001).

The sequences STFTHPR and SSLPLRK were both shown in the same study to bind to human immunodeficiency virus type 1 integrase (Desjobert et al., 2004). However, their target affinity was significantly lower than other clones selected, suggesting a proliferative advantage or binding to plastic or BSA. The sequence SILPYPY appears in two studies panning the phd7 library against ribosomal idiosyncratic pseudoknot structure (h18) (Llano-Sotelo et al., 2009) and 8C11 and 8H3 mAbs, which bind to neutralizing epitopes of hepatitis E virus (Gu et al., 2004), although the study lacks binding assays so a full comparison is not possible.

Other sequences that have been previously identified all have low affinity to the target in competition and gene delivery assays (Work et al., 2004, Matsuno et al., 2008, Sawada and Mihara, 2012), With the exception of SAPSSKN which showed great affinity for the anti-hepatitis C virus mAb target (Barban et al., 2000). The sequences KLPGWSG, LPSYHVP, AFPVSHN and WPTLQWA have not been previously identified.

Table 27. Previously Identified Phage Clones.

Sequence	Target
ANTLRSP	poly(l-lactide) (PLLA) crystalline films (Matsuno et al., 2008)
GETRAPL	Vascular smooth muscle cell (Work et al., 2004)
HAIYPRH	No target (Brammer et al., 2008)
	Human transferrin receptor (Lee et al., 2001)
SAPSSKN	Antibody against Hepatitis C Virus (Barban et al., 2000)
SILPYPY	Ribosomal idiosyncratic pseudoknot structure (h18) (Llano-Sotelo et al., 2009)
	8C11 and 8H3 mAbs, which could conformationally bind to neutralizing epitopes of HEV. (Gu et al., 2004)
SSLPLRK STFTHPR	Human immunodeficiency virus type 1 integrase (Desjobert et al., 2004)
STASYTR	Nanofibers constructed of β-sheet peptides (Sawada and Mihara, 2012)
AFPVSHN KLPGWSG, LPSYHVP WPTLQWA	Not previously identified

Clones isolated in this study which have been identified previously by the Ph.D.™-7 library against a range of targets .

6.5.2 Target unrelated phage

Panned phage pools are thought to consist of 3 possible types: high affinity target specific binders, lower affinity target specific binders and a population of ‘‘target-unrelated phage’’ displaying ‘‘target-unrelated peptides’’ (TUP). The latter may react with components of the screening system, such as the solid phase BSA or tissue culture vessels (Menendez and Scott, 2005). Several sequences are known to bind to plastic, including FHWTWYW and WHWRLPS and binders to BSA including FHEFWPT and FHENWPS (Menendez and Scott, 2005, Brammer et al., 2008). Known plastic and BSA binders were not identified in this study. Binders to plastic tend to have an abundance of aromatic amino acid residues (usually W) which are crucial to hydrophobic interactions. Two W residues separated by one, two or three random amino acids frequently bind to plastic (Adey et al., 1995). The peptides selected in this study are unlikely to be selected by binding to plastic or BSA as the blank wells in the binding assays show no higher binding than the insert-less phage. The subtractive panning step should have removed the majority of plastic binders along with those that bound to HUVECs.

Other clones that were recovered independently of their affinity could be selected by an advantage in replication enabling them to remain in the phage pool. Faster propagation of certain phage clones may be an intrinsic property of the displayed peptide itself, without any causative mutation, which increases infectivity. Alternatively the phenomenon may be the result of a mutation in the phage genome, as seen in HAIYPRH, which influences the ability of the virus to infect host bacteria or accelerates the process of phage particle assembly (Vodnik et al., 2011). It is suggested that selection of rapidly propagating target-unrelated peptides is favoured when only low

affinity ligands for a specific target are present in a phage display library (Vodnik et al., 2011).

6.5.3 Patient Samples

The failure of this experiment to find any potential targets to prostate epithelial cells may be due to the patient samples which the library was panned against. Two selection strategies were attempted: panning against a different patient sample at every round and panning against only one patient sample for four rounds. Both methods have issues which may be detrimental to selection efficacy.

In the first and second experiments 4 patient samples were used. Patient to patient variability may result in a range of ways in which clones were lost including the proteins expressed, level of expression, cell viability, cellular damage and differentiation state. Gene and protein expression in BPH tissue can vary between patients (Luo et al., 2001) and the histopathology of BPH can vary widely (Di Silverio et al., 2003). Cellular damage during tissue processing may also results in sample variability. Cell damage may cause up or down-regulation of potential targets, a phenomenon known *in vivo* for heat shock protein (Rylander et al., 2006). Target expression in only 3 out of 4 samples would significantly affect subsequent rounds of panning as many of the target binders would be lost. One way to counteract this anomaly would be to pan against several mixed patient samples within the same well, although this is approach made difficult by the limited availability of fresh tissue.

Long term cell culture of primary cells results in their differentiation and eventual senescence. Additionally, although there are likely to be differences between in situ and cultured cells, isolation and culture of cells in vitro may also down-regulate possible targets (Peehl, 2005). The stage of cell differentiation would be an increased problem for the 3rd and 4th experiments which involved panning against 1 patient sample only. Although patient to patient variation was eliminated by this design, the longer the cells were cultured for is a limitation of this method. Time from initial cell digestion and seeding to the fourth round of panning was nearly four weeks, although in this time cell morphology was unchanged. Prostate epithelial cells have a limited proliferative lifespan of approximately 30 cell divisions over 6 weeks *in vitro* (Peehl, 2005) (see chapter 3) before becoming terminally differentiated and senescent. In this time cells may undergo many phenotypic changes influenced by genetic instability and selective culture conditions (Rhee et al., 2001). Any useful targets that were present in the first rounds of panning may have been down-regulated by the fourth round and the binding clones lost. Although cryopreservation of primary cell samples at an early stage may, to some extent, counteract this problem, cryopreservation itself can change cell characteristics, and cause cell damage and loss (Karlsson and Toner, 1996).

6.5.4 Assay Improvement

Several methods could be used to improve this assay, including modification of panning conditions, immobilisation of target at higher density (increased seeding density) and use of different peptide libraries such as T7 lytic phage-displayed peptide libraries, which exhibit less sequence bias in comparison to M13 phage-displayed peptide libraries (Krumpe et al., 2006).

Panning conditions in previously published work vary widely. The conditions in this study closely follow the New England Bioscience protocol specific for the Ph.D.-7 library. Further optimisation of the protocol may result the identification of prostate specific clones. Different incubation temperatures, particularly at either room temperature or 4°C, may prevent internalisation of the phage peptide or increase or reduce binding times. Blocking is an important step in the panning protocol to reduce non-specific binding. In this study samples were blocked with 2% BSA, but this may not efficiently prevent non-specific binding (Xiao and Isaacs, 2012). Therefore some other studies have used 'Marvel' powdered milk, as it contains a wider mix of proteins. Elution and phage recovery could be further optimised. In this study, phage were eluted by chemical disturbance of target-phage bonds which were disrupted by a low pH solution, although there is evidence that this may be inefficient (Yu et al., 2004). Therefore other methods may be needed to elute and collect all binding phage. Additionally, the number of rounds of phage panning could be reduced, to reduce the number of amplification of phage with a replicative advantage (Vodnik et al., 2011). However, following only 3 rounds of panning in this study, no or only a minimal increase in phage recovery was observed.

6.5.5 Alternative Systems

Advancements in phage display techniques have allowed Fab, Fv or a linker stabilised single chain scFv antibody fragments to be displayed on outer phage coat proteins, creating antibody phage display libraries (Clackson et al., 1991, Carmen and Jermutus, 2002) . Synthetic (Silacci et al., 2005), naïve (de Haard et al., 1999) and immune (Sommavilla et al., 2010) libraries

are panned in a similar way to peptide libraries and have been used to generate antibody fragments to a range of antigens.

An advantage of displaying human antibody fragments is their reduced risk of an immune response in patients. Antibody phage display technology has successfully lead to the development of the drug several drugs including HUMIRA (Human Monoclonal Antibody in Rheumatoid Arthritis) a human anti-TNF alpha monoclonal antibody (also known as adalimumab and D2E7) (Kempeni, 1999) used for the treatment of multiple autoimmune diseases including rheumatoid arthritis, Crohn's disease, psoriasis and psoriatic arthritis (Leonardi et al., 2011, Rubin et al., 2011). Panitumumab (formerly ABX-EGF) is another phage display developed human monoclonal antibody specific to EGFR (Yang et al., 2001) used in the treatment of EGFR expressing metastatic colo-rectal cancer of patients with wild type KRAS (Peeters et al., 2008). Several other phage mAbs have progress to pre-clinical and clinical trial, with the majority targeting growth factors implicated in immune dysfunction and cancer progression (Ronca et al., 2012). In this study, using antibody phage display would have the same drawbacks as peptide phage display and it is also harder to identify the targets as direct sequencing is difficult.

In vivo panning of peptide and antibody phage display libraries can be utilised to identify tissue and organ specific sequences by injecting intravenously into mice and harvesting the organs. It has been utilised particularly in the area of gene therapy. The drawback of this technique is that some organs capture too many phages (Pasqualini and Ruoslahti, 1996). Also, when panned against a murine model, the difference between

mouse and human expression is not accounted for. In vivo panning has been performed in humans with appropriate ethical approval in one patient with a B cell tumour who had an intracranial bleed and was pronounced brainstem dead (Arap et al., 2002). Although some interesting motifs were identified, including a known mimotope of interleukin-11, this experiment is not easily repeatable due to the ethical issues (George et al., 2003). An alternative approach is to grow human tissue in immunocompromised animals. *In vivo* panning against human tumour xenografts has identified potential breast (Passarella et al., 2009) and prostate cancer biomarkers (Newton et al., 2006) and functional adhesion molecules related to metastasis (Sadanandam et al., 2007). Peptides that home specifically to tumour blood vessels have been coupled to anticancer drugs such as doxorubicin to increase drug efficacy (Arap et al., 1998, Li et al., 2006). However, no molecules identified by peptide phage display have gone into clinical trials.

6.5.6 Alternative System: Non-phage based systems

Alternative systems have been developed which are similar to the phage display system. These include a peptide displaying Bacterial FliTrx System in which a phagemid vector allows the display of peptides directly on the surface of E.coli using major bacterial flagellar protein and thioredoxin (Zitzmann et al., 2005). This technique has been used to identify potential prostate cancer specific peptides. However, bacterial display systems have proven to be inferior to conventional phage systems (Lunder et al., 2005b).

RNA and DNA aptamers are a recent technology and have shown promise (Baines and Colas, 2006). This technique involves the systematic evolution of ligands by exponential enrichment (SELEX) using a oligonucleotide library.

The process is based on an *in vitro* selection approach, similar to phage display, in which DNA or RNA molecules are selected by their ability to bind their targets with high affinity and specificity (Ulrich et al., 2006). Several aptamers are currently being tested in preclinical and clinical trials and the anti-VEGF aptamer pegaptanib received FDA approval for the treatment of human ocular vascular disease (Ulrich et al., 2006). This system has an advantage over traditional phage display system as it does not require amplification in a bacterial host, which can lead to the selection of clones with a reproductive, infective or proliferative advantage.

6.6 Chapter Conclusions

Although the Ph.D-7 peptide phage display system identified some potential candidate clones, which were enriched for by multiple rounds of panning, these clones did not specifically bind to prostate epithelial cells strongly enough to be considered as potential therapeutic or diagnostic targets. An alternative approach is required to identify new ways to target and deliver therapies which specifically target stem cells within the prostate.

7 Discussion and Conclusions

7.1 Summary of Findings

- Two out of three prostate cancer cell lines form colonies with three morphologies.
- The number of colonies is minimally altered by changing culture conditions.
- Two types of DU145 colonies contain cells with stem cell traits of high proliferative and self-renewal and tumourigenicity.
- Prostate epithelial colonies from patients with BPH form two types of morphological colony.
- Only large holoclone type prostate epithelial colonies are capable of extensive proliferation and self-renewal.
- Phage display panning against larger prostate epithelial colonies failed to yield potential therapeutic targets.

7.2 Relationship between Stem Cells and Clonogenicity

The aim of this study was to explore the relationship between clonogenicity and stem cells. Both somatic and cancer stem cells are defined by the traits of self-renewal and potency. During homeostasis or in response to injury somatic SCs must be able to regenerate all types of cell observed within the tissue. CSCs are believed to escape killing by conventional therapies and proliferate extensively to regenerate the tumour (Clarke et al., 2006)

The clonogenic assay is frequently used as a surrogate assay to identify the progeny of SCs in normal epithelial (Pellegrini et al., 2001) and cancer (Patrawala et al., 2006) populations. However the relationship between clonogenicity and stem cells is not fully understood. From the results of this study, it is clear that clonogenic cells are derived from cells with different *in vitro* proliferative capacities. Further analysis shows that colony morphology and colony size is predictive of stem cell function. Larger colonies formed by both normal and cancer cells have the greatest proliferative and self-renewal potential, whereas the smallest colonies have limited self-renewal potential and cannot self-renew. However, intermediate type 2 cancer colonies also contained cells with stem cell traits. Serial xenografting of type 1 and 2 cancer colonies further established their stem cell traits. This result suggests that the relationship between clonogenicity and SCs differs in normal and cancer populations.

The differences in self-renewal capacity suggest that cancer cells may be capable of aberrant self-renewal. The ability of some cells in type 2 (meroclone) colonies to form secondary type 1 colonies (holoclones) and proliferate indefinitely suggests that some cancer cells maintain the capacity

for self-renewal further down their cellular hierarchy, as shown in Figure 81. Early transit amplifying cancer cells may undergo either symmetrical or asymmetrical divisions to produce one or more daughter cells with the same proliferative and self-renewal potential as the parent cell. Upon differentiation self-renewing transitional cells can undergo fewer cell divisions before termination. Alternatively there may be a hierarchy of CSCs which maintain self-renewal capacity but become fully differentiated in fewer cell divisions. In contrast only stem cells in prostatic epithelium can self-renew, a property that is quickly lost during differentiation in adherent cell culture. The cause of abnormal self-renewal and differentiation of cancer stem cells is unknown, although increased expression of Bmi1 and Oct4 in cancer colonies suggests that alterations in self-renewal pathways may be involved.

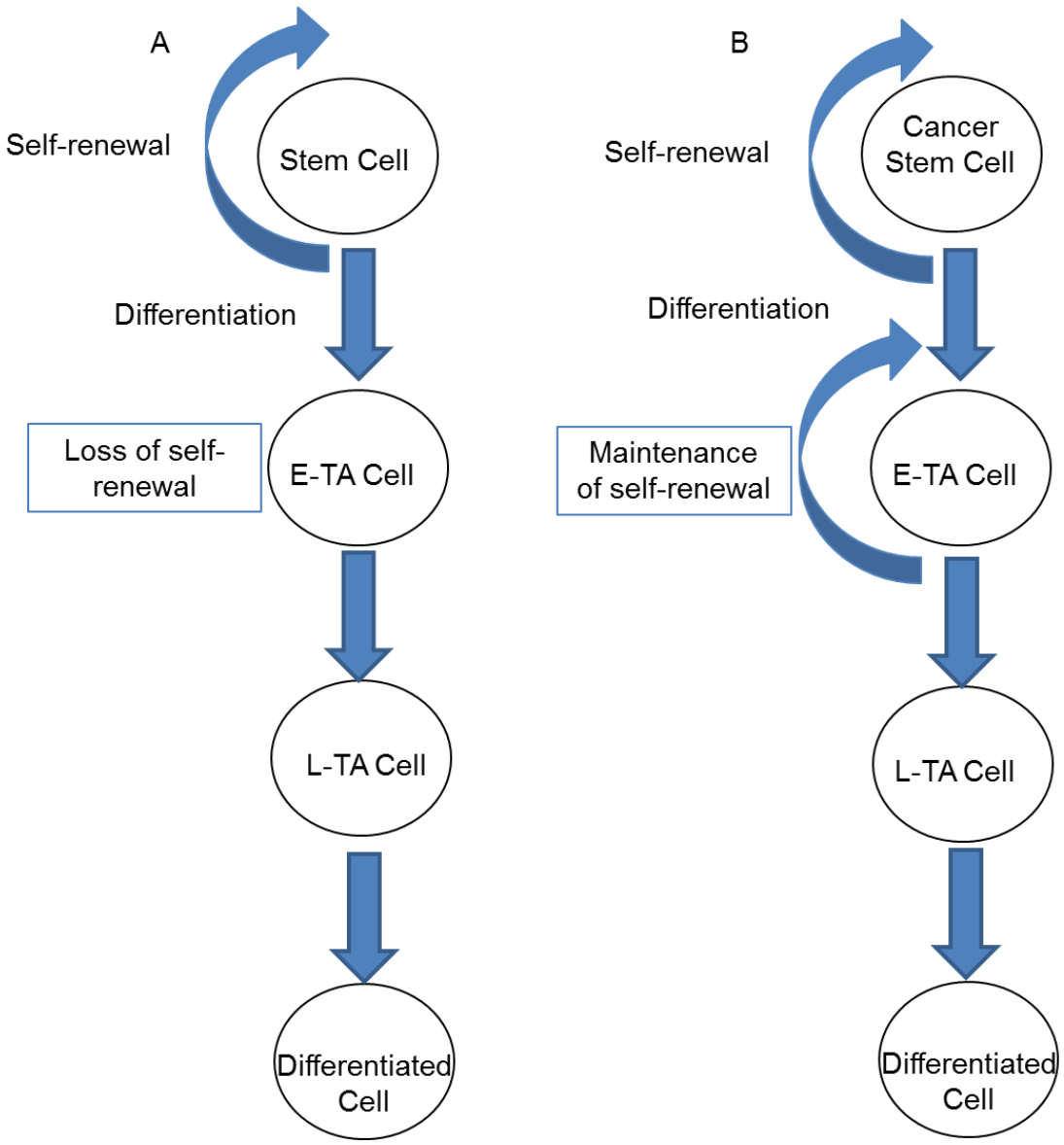

Figure 81. Comparison of Self-renewal in Normal and Cancer Cells.

A) Normal prostate epithelial cells following the traditional cellular hierarchy and differentiation model. Only stem cells can self-renewal to form daughter stem cells or differentiate to form early transit amplifying (E-TA) cells and late transit amplifying cells (L-TA). Transit amplifying cells have a limited proliferative potential and become terminally differentiated. B) Both prostate cancer stem cells and E-TA cells maintain a self-renewal capacity to form daughter cells identical to the parent cells with an infinite proliferative potential. Further differentiation to L-TA results in the loss of self-renewal capacity, and the cells undergoes proliferation and terminal differentiation.

Extensive proliferation is viewed as a hallmark of SCs in both normal and cancer tissues. The clonogenic assay measures short term proliferative potential, whilst serial cloning enables the study of clonal proliferation over many generations. In this study prostate epithelial cells became senescent after approximately one month of culture *in vitro*. In contrast putative stem cells in the DU145 prostate cancer cell line were able to undergo at least 200 cell divisions any without loss of self-renewal capacity and were deemed immortal. Somatic stem cells must be able to maintain and regenerate the organ for life, therefore must have a high proliferative capacity (Ichim and Wells, 2006). However, in many tissues ageing is accompanied by a progressive decline in stem cell function, resulting in reduced proliferative and regeneration ability (Jones and Rando, 2011). The prostate epithelial cells in this study were obtained from elderly patient samples which may demonstrate reduced stem cell function and lower proliferative capacity. Culture *in vitro* may also affect their proliferative capacity by driving differentiation. In many studies CSC are viewed as immortal as tested by their ability to serially regenerate tumours over many months (Dalerba et al., 2007). CSCs clearly have a high proliferative capacity, but cancer cell lines may not be representative of primary cancer cells *in vitro*, increasing the differences observed between SCs and CSCs.

It is clear that both SCs and non-SCs can form colonies, as observed by their proliferative heterogeneity. However, it is not known whether all stem cells are able to form colonies. The cancer cell lines in this study were assayed in several different conditions, but little improvement in CFE was observed. This suggests that the number of SCs or the ability of SCs to form colonies is intrinsically regulated by cell population. Unlike cancer cell lines, primary

prostate epithelial cells are not ‘acclimatised’ to *in vitro* cell culture and it is unlikely that all stem cells form colonies under these conditions. Cells may be damaged during the tissue digestion process or act differently once removed from the regulation of the stem cell niche. Some stem cells are also quiescent and may not proliferate in response to low density *in vitro* cell culture.

7.2.1 Quiescence and the Stem Cell Niche

The colony forming assay may not account for the number of quiescent stem cells in a population. In slowly regenerating tissue, such as the prostate and brain, stem cells are usually located in a niche where proliferation and differentiation is controlled by intrinsic regulatory mechanisms and extrinsic signals from the microenvironment (Moore and Lemischka, 2006, Li and Bhatia, 2011). These stem cells are often quiescent and proliferate either slowly or in response to damage (Tsujimura et al., 2002). Stem cells in the normal prostate are believed to be maintained in a quiescent state by transforming growth factor beta (TGF-β) (Salm et al., 2005) and Wnt signalling (Li and Bhatia, 2011) from the niche.

When the stem cell is removed from its natural niche by digestion and tissue culture it is unknown how differently it behaves. Cells may not proliferate in response to *in vitro* culture conditions, therefore underestimating the number of stem cells in the prostate epithelium in this study. This phenomenon has previously been demonstrated in neurospheres in which quiescent stem cells, expressing minichromosome maintenance 2 which labels cells at the initiation of DNA replication, fail to form spheres whereas activated stem cells do (Pastrana et al., 2009),.

Quiescent stem cells have also been observed in cancers and quiescence is predicted to be one of the mechanisms by which CSCs are resistant to chemotherapy (Reya et al., 2001, Dick, 2008). In this study, cancer cells had been growing *in vitro* for many generations and therefore were adapted to their microenvironment. Ki67 staining showed that most cells in DU145 colonies were actively proliferating, although all colonies contained at least a few cells which were in G_0 phase. This suggests that some cells within the cell line may be quiescent and therefore the cell–cell signalling may provide a substitue niche for these cells. The cancer cell micro-environment may also play a role and control cell plasticity (Tang, 2012). The basic micro-environment of the tissue culture dish may not provide the normal controls and influences observed within a tumour *in situ,* leading to altered clonal behaviour.

The different CFE of cancer cell lines, both in this study and previous work suggests that there a large variation in the number of CSCs in different cancers. Previously, increased clonogenicity has been linked to more aggressive disease (Bapat et al., 2005). Characterisation of self-renewal, proliferation and tumour formation potential of colonies formed by each cell type is essential to avoid inaccurate interpretation and underestimation of the number of cells with stem cell traits. Characterised cancer colonies which are known to contain cells with stem cell traits can be utilised to allow rapid evaluation of new therapeutics and the study of gene mutations and signalling pathways involved in tumour initiation and progression.

7.2.2 Targeting Self-Renewal

The increased capacity for self-renewal observed in prostate cancer colonies suggests that factors controlling self-renewal pathways may be targets for therapy. Signalling pathways such as Wnt/β- catenin (Reya and Clevers, 2005), Notch (Sikandar et al., 2010), Hedgehog (Hh) and Bmi1 (Liu et al., 2006b) have been implicated in the control of self-renewal of CSCs. These pathways are also involved in self-renewal in embryonic and somatic stem cells. Inhibition of these pathways using small molecules and monoclonal antibodies has resulted in a reduction in self-renewal and CSC capacity (Takebe et al., 2011) (Rudin et al., 2009, Yauch et al., 2009) (Wu et al., 2010). Wnt is also thought to be linked to CD44 variant isoforms which act downstream of Wnt signalling (Zeilstra et al., 2013) and may be related to the increased CD44 expression observed in type 1 DU145 colonies.

Bmi1 is a 37 kDa polycomb group protein (PcG) which plays a role in stem cell renewal and maintenance, which when deficient leads to compromised adult stem cell function. There is increasing evidence that polycomb group (PcG) proteins play a crucial role in cancer development and recurrence. Bmi1 is associated with a number of human malignancies including prostate cancer (Lukacs et al., 2010) which suggests that it plays a role in CSC maintenance (Cao et al., 2011), which is supported by the increase in Bmi1 expression observed in both cancer and normal prostate type 1 colonies. Loss-of-function of Bmi1 induced by RNA interference (RNAi) in both normal and malignant human cells has shown that Bmi1 is crucial for the short-term survival of cancer cells but not of normal cells and abolishes chemo resistance in prostate cancer cells (Liu et al., 2006a), but had no effect on the proliferation of LNCaP or DU145 cells (Crea et al., 2011).

There may be significant cross talk and intersection between these pathways and, therefore their relationship requires further exploration and combination of pathway inhibitors maybe required. Colony morphology may allow the study of these interactions on self-renewal. A significant reduction in the self-renewal capacity of CSCs would result in a reduction in the number of holoclones and meroclones and diminish their long term proliferative capacity.

7.2.3 Cell Surface Marker Expression

During recent years, efforts to identify and enrich for stem cell populations have concentrated on cell surface marker selection. In this study, colonies were stained with antibodies against the cell surface antigens CD44 and α2β1 integrin. Expression was heterogeneous within both normal and cancer colonies in terms of positive cell numbers and brightness of staining. Although these markers tended to be more highly expressed in stem cell colonies their expression does not in itself confirm stem cell identity.

In previous studies CD44 and α2β1intergin alone and in combination with CD133 have been used to enrich populations of both normal and neoplastic SCs. Other markers which have been used to identify SCs in normal and neoplastic prostate are CD133 (Richardson et al., 2004), Epcam, CD49f (Guo et al., 2012), CD166 (Jiao et al., 2012). However CD133 has been shown to be a poor marker for clonogenicity and sphere formation, in contrast to CD49f (Yamamoto et al., 2012). There is unlikely to be one single marker that is specific for either normal or cancer stem cells, and many markers select both normal and cancer SCs, meaning new markers are required. In this study, phage display did not successfully identify new targets

to cell surface antigens. This lack of potential targets was possibly due to changes in marker expression during culture of primary cells *in vitro*.

It is largely unknown whether CSC-marker expression is static or continuously shifting during differentiation or as an environmental response (Keysar and Jimeno, 2010, Roesch et al., 2010). There is evidence to suggest that the populations responsible for driving tumour progression are actually in a transient phase of altered cell cycling, gene expression, and drug sensitivity, likely because of alteration in chromatin structure resulting in changes in gene expression (Keysar and Jimeno, 2010). Cellular activities, such as the efflux of Hoechst dye or aldehyde dehydrogenase activity are also likely to be affected by cell cycle state. These markers can also be altered by exposure to anticancer therapeutics suggesting their role in protecting the SCs from toxicity (Keysar and Jimeno, 2010).

Cancer cells lack some of the normal genetic and environmental controls that are present in healthy tissues and therefore may have greater plasticity (Tang, 2012). It has been suggested that non-CSCs can dedifferentiate into CSCs which have a more stem-like phenotype (Chaffer et al., 2011, Gupta et al., 2011), which has been demonstrated, to some extent, by inter-conversion of ABCG2+ and ABGG2- prostate and breast cancer cells (Patrawala et al., 2005) and CD44+ and CD44- prostate cancer cells (Patrawala et al., 2006). In these studies cells the negative cell fractions were able to generate numbers of positive cells in similar proportions to those observed in the original cell line. However, this is not conclusive evidence as there may be overlap between marker expression of CSCs and non-CSCs and inadequate enrichment of unselected populations.

7.3 Further Research

7.3.1 Clonal Origin

The ability to track colony formation using time lapse photography confirmed the single cell origin of cancer colonies. However it is still unclear whether all cells are dividing equally throughout the colony or whether some cells are cycling more rapidly than others. Ki67 staining showed that all colonies contained a mixture of cycling and resting cells. This does not give any indication of the history of proliferation in each cell or cell cycling times. Some cells may be rapidly cycling whilst others are slower. There are several methods which could be used to study this. Bromodeoxyuridine (BrdU) is a synthetic nucleoside that is an analogue of thymidine which can be incorporated into the DNA of dividing cells, by substitution with thymidine, during S phase (Hardonk and Harms, 1990). Pulsing colonies with BrdU at different time points would allow detection of actively diving and resting cells over a longer period than Ki67 staining. Alternatively cells can be tracked by simultaneous transduction of cells with three lentiviral gene ontology (LeGO) vectors encoding red, green or blue fluorescent proteins (Weber et al., 2012). The unique and random combination of colours expressed by each cell enables tracking of their progeny by fluorescent microscopy. In this way the cell cycle time and proliferative heterogeneity within the colonies could be traced.

Long term culture of cancer cells, which are genetically unstable, may result in an increase in dominant clones, a type of *in vitro* clonal evolution (Duesberg et al., 1998). This instability has been shown *in vivo* in many tissues including prostate. In human samples, cancer progression is

concordant with PTEN gene deletions and TMPRSS2:ERG fusion breakpoints which confirm clonal origin (Sowalsky et al., 2013). The accumulation of genetic variations may give the cancer cells enhanced proliferative and stem cell capacity. However, in this study, no increase in CFE or the number of stem cells was observed over 17 serial clonings, suggesting clonal evolution is not taking place. Comparison of the whole cell genome of low and high passage cells to compare mutations would confirm that genetic mutations are not responsible for the loss of function in type 2 and 3 colonies. Studying any mutations which predominately give rise to highly proliferative colonies may give further insight into the mechanisms behind clonogenicity.

7.3.2 Microarray

This study clearly suggests that type 1 and 2 colonies DU145 are derived from and contain CSCs, but the mechanisms that control the CFE and maiantain a constant number of stem cells are unknown. Gene expression array would compare levels of genes in type 1, 2 and 3 colonies. Gene sets overexpressed in type 1 colonies could provide insight into the pathways involved in CSC maintenance, including self-renewal. Previously, analysis of gene expression of PC-3 holocones has shown an increase in *FAM65B* expression, which is a transcriptional target of FOXO1 that regulates RhoA activity (Rougerie et al., 2013), compared to the original monolayer (Zhang and Waxman, 2010). However, many of the gene sets studied were actually down-regulated in PC-3 holoclones compared to the whole cell population. The differences observed CFE between cancer cell lines may mean that different genes are involved, therefore analysis of several different cell lines may be required to study differences in gene expression in-depth.

7.3.3 Gene Silencing

In this study phage display failed to identify a target to proliferative prostate cells. More knowledge about the genetic mechanisms behind CSC progression is required to understand cancer progression and identify new targets. Expression of CD44, α2β1 integrin, Bmi1 and Oct4 were increased in type 1 DU145 colonies and also observed in lower numbers in type 2 colonies. To further study their effects on prostate CSCs, each of these genes could be knocked down using RNAi. If Bmi1 and Oct4 are involved in the increased self-renewal capacity of CSCs, knocking down these genes should significantly decrease the number of type 1 and 2 colonies observed. Alternatively, RNAi libraries could be used to test the loss of function of genes from either the entire genome or specific gene sets involved in specific cellular processes (Hannon and Rossi, 2004, Boutros and Ahringer, 2008). Genes that significantly affect clonogenicity can then be further studied to explore their role in CSC self-renewal and differentiation.

7.4 Conclusions

This study explored the relationship between clonogenicity, colony morphology and stem cells within both normal and cancerous prostate cells. In normal prostate two types of colonies are formed which corresponded to stem and transit amplifying colonies. Cancer cells contain a larger proportion of cells with self-renewal capacity and therefore both type 1 and 2 colonies contain cells with stem cell traits. This is contrary to previous studies which have shown that only cancer holoclones contain stem cells. The mechanisms which control self-renewal and colony formation in prostate cancer cells are still unknown. Further investigation into these mechanisms may identify pathways which can be targeted therapeutically. Targeting of self-renewal would prevent the maintenance of the CSC pool and would lead to cancer regression.

8 Appendix

Appendix 1. Naïve PhD-7 Library sequences

Clone	Peptide	Amino Acid Sequence
1	CGGACGAATATTGTGCTGGAT	RTNIVLD
2	TCTACTTTTCCGAGGAATTGGG	STFPRNW
3	TTTACTAGTTCTACGGTGCCT	FTSSTVP
4	CTGAAGCTGCCGCCTAAGTTG	LKLPPKL
5	GTGACTCCTCTGGTGCGGCTG	VTPLVRL
6	GCTAATCCTGCGCCTCCGAAT	ANPAPPN
7	CAGGTTACTCCGTCGGCTGGT	QVTPSAG
8	AGTGATCTTGGTAGTAATGAG	SDLGSNE
9	TCTGCGCAGAAGGCTCATTCT	SAQKAHS
10	GTTTCTAATGCTGAGCAGGAG	VSNAEQE
11	TCGCCGAAGTCGCATACTATT	SPKSHTI
12	ACGTCGTCTCCTTCTACTACG	TSSPSTT
13	GCTCCGGTTAGTAATATTCGT	APVSNIR
14	CAGCTTGGTGCGGCTGCGTCG	QLGAAAS
15	TCTCCGACTCTGCCGGTGACG	SPTLPVT
16	ACGACTTCTCATTTTAGTAAG	TTSHFSK
17	TTGATTCCTAATTCTAAGTCT	LIPNSKS
18	TTTTCGGCGCCGCTTCCGTAT	FSAPLPY
19	AATCTGAAGCATACTCCTCCG	NLKHTPP
20	GTGCCTACTAAGCATATGCTT	VPTKHML
21	GTTCATTTTCAGTTTCATATG	VHFQFHM
22	ACTGTTCCTTTGCCTATGATT	TVPLPMI
23	CAGTGGTCTCATCGTGAGCGG	QWSHRER
24	TCTCCTATGCTTCATACGTTG	SPMLHTL
25	GATGATTATACGCTTCATCTT	DDYTLHL
26	AGTCCTCGTTTGTGGCCTCTG	SPRLWPL
27	CAGCCGGCTAATCAGACTCTG	QPANQTL
28	AATCCGCGTGCTCCGCTGGCT	NPRAPLA
29	CTGCCTCATTCTGCGCGGCCT	LPHSARP
30	CAGCCTTTTTATTAGAATGCG	QPFY*NA
31	AGTACGTCTTCTCTTGCGCCT	STSSLAP
32	AAGCTTAGTGCCGAGTGTGCCT	KLSAECA
33	CAGATTACTTCGGATTATTCT	QITSDYS
34	TCTGATACGGTGTAGATTGAT	SDTVLID
35	CATGATAATACTCTTCCGACT	HDNTLPT
36	AGTCTGCCGATTGCGGCTGTG	SLPIAAV
37	ACGCCTCCGCCGGCTCATATG	TPPPAHM
38	TCGCCTACTATGACTACTCCG	SPTMTTP
39	GCTTCGCCTAGGGCTCCGATG	ASPRAPM
40	ACGCCTCATTTTCTTAATCCT	TPHFLNP

Appendix 2. Sequences of third round phage clones

Clone Number	Peptides	Amino acids
1	TATCTTACGATGCCGACGCCT	YLTMPTP
2	GATAGGATGTCTGTTCGTACT	DRMSVRT
3	CATCCTACTGGGGCTGTTCTT	HPTGAVL
4	GTTTTGAAGCCTCCGAAGCAT	VLKPPKH
5	GGGAAGTGGAGTGTGTATGGT	GKWSVYG
6	GGTTCTATGCCTCGTACTCCT	GSMPRTP
7	AATAATCATCGTCCGATTTAT	NNHRPIY
8	CATCAGGCTTCTTATAAGCCG	HQASYKP
9	ACGAAGTTTGGGCGGCATCCG	TKFGRHP
10	ACGCCGTTTATGGCGTATCAT	TPFMAYH
11	TCTTATTTGAATCGGGCTCTG	SYLNRAL
12	TTTTGGCGTCCTCCGATGTTT	FWRPPMF
13	CATGTGCCTGCGACTGCGCGG	HVPATAR
14	TCTAATTTGAGGACGCATCCT	SNLRTHP
15	TCGCTGCTGTCTCTTCATTCG	SLLSLHS
16	ACGGCGCTTTCTGCTCGGACT	TALSART
17	CATACTGCGCCTAATTTTGCT	HTAPNFA
18	GCGTCTGTTCATTTGCCTCCT	ASVHLPP
19	ACTCATGTGATGCAGACTCTT	THVMQTL
20	TTTCCTTCGACGATTACTCCG	FPSTITP
21	GTTCAGACTTATGCTCGTGTT	VQTYARV
22	TATCTTACGATGCCGACGCCT	YLTMPTP
23	GATAGGATGTCTGTTCGTACT	DRMSVRT
24	CATCCTACTGGGGCTGTTCTT	HPTGAVL
25	GAGCTGCAGCCTATGCTGCAG	ELQPMLQ
26	AGTGCGCTTTATCGGCATTCT	SALYRHS
27	ACTACGCCGCCGTGGCGTACT	TTPPWRT
28	GAGGGTCCGCCTCTTTCGCGT	EGPPLSR
29	CAGCCTTGGCCGACGAGTATT	QPWPTSI
30	GCTCCGCCTACGTCTGGTACG	APPTSGT
31	TCTTTGTCGCTTATTCAGACG	SLSLIQT
32	GCGCATCATCCTGCGGTGAAG	AHHPAVK
33	CAGAATTCGCAGCTGAGTCGT	QNSQLSR
34	GAGCTGCAGCCTATGCTGCAG	ELQPMLQ
35	AGTGCGCTTTATCGGCATTCT	SALYRHS
36	ACTACGCCGCCGTGGCGTACT	TTPPWRT
37	TCTGCGCCGTCGTCTAAGAAT	SAPSSKN
38	TCGAGTCCTCTTACTCCTCCG	SSPLTPP
39	GAGCTTTGGCGGCCTACTCGG	ELWRPTR
40	ACTGATACTGAGTCTAAGCGG	TDTESKR

Appendix 3.Sequences of Clones from the Fourth round panning of experiment 1. Sequences which are repeated are displayed in bold

Clone Number	Peptide Sequence	Amino acid Sequence
1	GCGTGTGCTAGTAATAAGTCG	ACASNKS
2	CATGCTATTTATCCGCGTCAT	**HAIYPRH**
3	TATGCTGGTCCTTATCAGCAT	YAGPYQH
4	TCTATTCTGCCGTATCCTTAT	**SILPYPY**
5	GCTTTTCCGGTTTCTCATAAT	**AFPVSHN**
6	AAGTGGCCGTTGTCGCATCCT	KWPLSHP
7	GTTGCGCTGTCGGCGCCTTAT	VALSAPY
8	GGGAAGCCTATGCCTCCGATG	GKPMPPM
9	GCTCTTTATAAGAATACTTCT	ALYKNTS
10	TCTACGTTTACTAAGTCTCCT	STFTKSP
11	CATCCGATGTCGATTCGGGTT	HPMSIRV
12	TTTGCGACTCATTTTGCGCCG	FATHFAP
13	TCGGTGGAGTCGGCGTGGAGG	SVESAWR
14	TCTTATTTGAATCGGGCTCTG	SYLNRAL
15	AGTCCGACGCAGCCTAAGTCG	SPTQPKS
16	GCGCTGAATTCTCTGACGAA	ALNSLT
17	GCTTTTCCGGTTTCTCATAAT	**AFPVSHN**
18	AGTTCTACGAAGCTTTCGTTG	SSTKLSL
19	GTGAGGCCTCATACTTCTTCG	VRPHTSS
20	ACTTCTGAGCCGCCTACGAAG	TSEPPTK
21	TGGCCGCAGAAGGCTCAGCCT	WPQKAQP
22	AAGCTTCCTGGGTGGTCGGGG	**KLPGWSG**
23	AAGCATTATCATTCTATTAAT	KHYHSIN
24	GCGCTGATTCCGAAGCCTAGG	ALIPKPR
25	GCTTCTTATTCGGGGACTGCG	ASYSGTA
26	TCTATTCTGCCGTATCCTTAT	**SILPYPY**
27	GATTCGCATACTCCGCAGAGG	DSHTPQR
28	ATGTCTCTTCAGCAGGAGCAT	MSLQQEH
29	GTGATTCGTATGCCGACTCCG	VIRMPTP
30	TTTCATCAGCATACGTCTAAG	FHQHTSK
31	GCGAATACTCTGCGTTCTCCG	**ANTLRSP**
32	CAGTTTCTGTCTATTAATATG	QFLSINM
33	GGGATTCGGCATACTAATCCT	GIRHTNP
34	CAGCCTTGGCCGACGAGTATT	QPWPTSI
35	TATCTTACGATGCCGACGCCT	YLTMPTP
36	ACGCGGGCTGGTCTGGATTTT	TRAGLDF
37	ACGGATTCGCTTCGGCTGCTG	TDSLRLL
38	TCGTCTCTTCCTCTGCGGAAG	**SSLPLRK**
39	TCGACGGCGTCTTATACTCGT	**STASYTR**
40	TCTATTCTGCCGTATCCTTAT	**SILPYPY**
41	TCTATTCTGCCGTATCCTTAT	**SILPYPY**
42	GCGAATACTCTGCGTTCTCCG	**ANTLRSP**

43	GCGCTTTGGGGGCCGACGAGT	ALWGPTS
44	TATAGGGCTCCTTGGCCGCCT	YRAPWPP
45	TCTGCGCCGTCGTCTAAGAAT	**SAPSSKN**
46	TGGCCTACGCTGCAGTGGGCG	**WPTLQWA**
47	GGGGAGACTCGTGCGCCGCTT	**GETRAPL**
48	GCGAAGATTGATGCTCGTACTG	AKIDART
49	TCTGCGCCGTCGTCTAAGAAT	**SAPSSKN**
50	CTTCCTAGTGTGGATCGTCCT	LPSVDRP
51	CATGCTATTTATCCGCGTCAT	**HAIYPRH**
52	GGTGTTCAGATTATGGGGCGT	GVQIMGR
53	ACGGCGCCTACGTCTCCGTCT	TAPTSPS
54	TGGCAGACTTCTCCGCCTTTT	WQTSPPF
55	ACGCCTATTACGCAGCTGCTG	TPITQLL
56	GCTCTGCATTCTGCTCGTGTG	ALHSARV
57	CATGCTATTTATCCGCGTCAT	**HAIYPRH**
58	TCGTCTCTTCCTCTGCGGAAG	**SSLPLRK**
59	TCGTATGTTAGTCATCATTCT	SYVSHHS
60	ACGATTCCTTCTCGGGTTCTT	TIPSRVL
61	AAGCTTCCTGGGTGGTCGGGG	**KLPGWSG**
62	CAGCCGCTGTCTAATGCTTCT	QPLSNAS
63	CTGAATAATAATCTGCCGTCT	LNNNLPS
64	CTACCTTCATATCATGTGCCT	**LPSYHVP**
65	CATGCTATTTATCCGCGTCAT	**HAIYPRH**
66	AGTAATCAGTGGTATGCTTCG	SNQWYAS
67	CATGCTATTTATCCGCGTCAT	**HAIYPRH**
68	ACGTTGACTACGCTGACGAAT	TLTTLTN
69	AGTCTTCCTACTCTGACTCTG	SLPTLTL
70	CATTGGCCTGTTAGGTCTCTT	HWPVRSL
71	TTTGCTCCTGTTAGTCATACT	FAPVSHT
72	TGGAATCCGAATCTTCCTACT	WNPNLPT
73	AGTACGTTTACGCATCCGAGG	**STFTHPR**
74	GTTCAGACTTATGCTCGTGTT	VQTYARV
75	AAGCTTCCTGGGTGGTCGGGG	**KLPGWSG**
76	TGGGCTTTGGATAGGGGTGCG	WALDRGA
77	AGTGCGCTTTATCGGCATTCT	SALYRHS
78	GGGGTGAAGGCTCTGTCGACT	GVKALST
79	TCGACGGCGTCTTATACTCGT	**STASYTR**
80	TCTCATTATCCTAATTATGGG	SHYPNYG
81	TGGCCTACGCTGCAGTGGGCG	**WPTLQWA**
82	TCGACGTCTGGGCGGCTTCCT	STSGRLP
83	ACGATTAAGTCTCCTCTGCAT	TIKSPLH
84	TCGACGGCGTCTTATACTCGT	**STASYTR**
85	GCTAATACTACTCCGAGGCAT	ANTTPRH
86	GGGGAGACTCGTGCGCCGCTT	**GETRAPL**
87	AGTACGTTTACGCATCCGAGG	**STFTHPR**
88	TCGGAGCGGGCGTCGTCGCCT	SERASSP

89	ACTGTGACGTCTCGGTTGCCG	TVTSRLP
90	ACGCGGGCGATTTCTCAGCCT	TRAISQP
91	CATAGTCGTCTTGTGTTTCCG	HSRLVFP
92	GGGGGGTTTAATGGGCCTTTT	GGFNGPF
93	GCGACTCCGCTTTGGCTTAAG	ATPLWLK
94	GCTACTTTTACTCATTATAAG	ATFTHYK
95	GCTATGTCGTCTCGTTCGCTT	AMSSRSL
96	CTACCTTCATATCATGTGCCT	**LPSYHVP**
97	ACGCCGTTTATGGCGTATCAT	TPFMAYH
98	GTGTCGTTTACTCCGTCGTTT	VSFTPSF
99	GCTATTACTAGGTCGCCTGCG	AITRSPA
100	ACTCATCTTCCGTGGCAGACG	THLPWQT

9 References

Adey NB, Mataragnon, AH, Rider, JE, Carter, JM & Kay, BK. Characterization of phage that bind plastic from phage-displayed random peptide libraries. Gene.1995; 156: 27-31.

Al-Hajj M, Wicha, MS, Benito-Hernandez, A, Morrison, SJ & Clarke, MF. Prospective identification of tumorigenic breast cancer cells. Proceedings of the National Academy of Sciences of the United States of America.2003; 100: 3983-8.

Ali-Osman F & Beltz, PA. Optimization and characterization of the capillary human tumor clonogenic cell assay. Cancer research.1988; 48: 715-24.

Alison MR & Islam, S. Attributes of adult stem cells. J Pathol.2009; 217: 144-60.

Arap W, Kolonin, MG, Trepel, M, Lahdenranta, J, Cardo-Vila, M, Giordano, RJ, Mintz, PJ, Ardelt, PU, Yao, VJ, Vidal, CI, Chen, L, Flamm, A, Valtanen, H, Weavind, LM, Hicks, ME, Pollock, RE, Botz, GH, Bucana, CD, Koivunen, E, Cahill, D, Troncoso, P, Baggerly, KA, Pentz, RD, Do, KA, Logothetis, CJ & Pasqualini, R. Steps toward mapping the human vasculature by phage display. Nat Med.2002; 8: 121-7.

Arap W, Pasqualini, R & Ruoslahti, E. Cancer treatment by targeted drug delivery to tumor vasculature in a mouse model. Science.1998; 279: 377-80.

Argani P, Walsh, PC & Epstein, JI. Analysis of the prostatic central zone in patients with unilateral absence of wolffian duct structures: further evidence of the mesodermal origin of the prostatic central zone. J Urol.1998; 160: 2126-9.

Asano S & Riglar, C. Colony growth in agar by human melanoma cells. Cancer research.1981; 41: 1199-204.

Bagley R.G. TBA (ed.) 2009. *Cancer Drug Discovery and Development: Stem Cells and Cancer*: Humana Press.

Baines IC & Colas, P. Peptide aptamers as guides for small-molecule drug discovery. Drug Discov Today.2006; 11: 334-41.

Baker FL, Ajani, J, Spitzer, G, Tomasovic, BJ, Williams, M, Finders, M & Brock, WA. High colony-forming efficiency of primary human tumor cells cultured in the adhesive-tumor-cell culture system: improvements with medium and serum alterations. Int J Cell Cloning.1988; 6: 95-105.

Bannuru RR, Dvorak, T, Obadan, N, Yu, WW, Patel, K, Chung, M & Ip, S. Comparative evaluation of radiation treatments for clinically localized prostate cancer: an updated systematic review. Ann Intern Med.2011; 155: 171-8.

Bapat SA, Mali, AM, Koppikar, CB & Kurrey, NK. Stem and progenitor-like cells contribute to the aggressive behavior of human epithelial ovarian cancer. Cancer research.2005; 65: 3025-9.

Barban V, Fraysse-Corgier, S, Paranhos-Baccala, G, Petit, M, Manin, C, Berard, Y, Prince, AM, Mandrand, B & Meulien, P. Identification of a human epitope in hepatitis C virus (HCV) core protein using a molecularly cloned antibody repertoire from a non-symptomatic, anti-HCV-positive patient. J Gen Virol.2000; 81: 461-9.

Barker N, Van Es, JH, Kuipers, J, Kujala, P, Van Den Born, M, Cozijnsen, M, Haegebarth, A, Korving, J, Begthel, H, Peters, PJ & Clevers, H. Identification of stem cells in small intestine and colon by marker gene Lgr5. Nature.2007; 449: 1003-7.

Barrandon Y & Green, H. Cell migration is essential for sustained growth of keratinocyte colonies: the roles of transforming growth factor-alpha and epidermal growth factor. Cell.1987a; 50: 1131-7.

Barrandon Y & Green, H. Three clonal types of keratinocyte with different capacities for multiplication. Proceedings of the National Academy of Sciences of the United States of America.1987b; 84: 2302-6.

Barrie SE, Potter, GA, Goddard, PM, Haynes, BP, Dowsett, M & Jarman, M. Pharmacology of novel steroidal inhibitors of cytochrome P450(17) alpha (17 alpha-hydroxylase/C17-20 lyase). J Steroid Biochem Mol Biol.1994; 50: 267-73.

Baylin SB & Jones, PA. A decade of exploring the cancer epigenome - biological and translational implications. Nat Rev Cancer.2011; 11: 726-34.

Beaver CM. The effect of culture conditions on colony morphology and proliferative capacity in human prostate cancer cell lines. Cell Biol Toxicol.2012.

Becker AJ, Mc, CE & Till, JE. Cytological demonstration of the clonal nature of spleen colonies derived from transplanted mouse marrow cells. Nature.1963; 197: 452-4.

Belanger LF & Leblond, CP. A Method for Locating Radioactive Elements in Tissues by Covering Histological Sections with a Photographic Emulsion. Endocrinology.1946; 39: 8-13.

Beltrami AP, Barlucchi, L, Torella, D, Baker, M, Limana, F, Chimenti, S, Kasahara, H, Rota, M, Musso, E, Urbanek, K, Leri, A, Kajstura, J, Nadal-Ginard, B & Anversa, P. Adult cardiac stem cells are multipotent and support myocardial regeneration. Cell.2003; 114: 763-76.

Bhatia M. AC133 expression in human stem cells. Leukemia.2001; 15: 1685-8.

Blanpain C, Lowry, WE, Geoghegan, A, Polak, L & Fuchs, E. Self-renewal, multipotency, and the existence of two cell populations within an epithelial stem cell niche. Cell.2004; 118: 635-48.

Bonnet D & Dick, JE. Human acute myeloid leukemia is organized as a hierarchy that originates from a primitive hematopoietic cell. Nat Med.1997; 3: 730-7.

Boquest AC, Shahdadfar, A, Fronsdal, K, Sigurjonsson, O, Tunheim, SH, Collas, P & Brinchmann, JE. Isolation and transcription profiling of purified uncultured human stromal stem cells: alteration of gene expression after in vitro cell culture. Mol Biol Cell.2005; 16: 1131-41.

Boutros M & Ahringer, J. The art and design of genetic screens: RNA interference. Nat Rev Genet.2008; 9: 554-66.

Brammer LA, Bolduc, B, Kass, JL, Felice, KM, Noren, CJ & Hall, MF. A target-unrelated peptide in an M13 phage display library traced to an advantageous mutation in the gene II ribosome-binding site. Anal Biochem.2008; 373: 88-98.

Brazelton TR, Rossi, FM, Keshet, GI & Blau, HM. From marrow to brain: expression of neuronal phenotypes in adult mice. Science.2000; 290: 1775-9.

Brehm MA, Shultz, LD & Greiner, DL. Humanized mouse models to study human diseases. Curr Opin Endocrinol Diabetes Obes.2010; 17: 120-5.

Brown MD, Gilmore, PE, Hart, CA, Samuel, JD, Ramani, VaC, George, NJ & Clarke, NW. Characterization of benign and malignant prostate epithelial Hoechst 33342 side populations. Prostate.2007; 67: 1384-96.

Bruce WR & Mcculloch, EA. The Effect of Erythropoietic Stimulation on the Hemopoietic Colony-Forming Cells of Mice. Blood.1964; 23: 216-32.

Bussolati B, Bruno, S, Grange, C, Buttiglieri, S, Deregibus, MC, Cantino, D & Camussi, G. Isolation of renal progenitor cells from adult human kidney. The American journal of pathology.2005; 166: 545-55.

Cao L, Bombard, J, Cintron, K, Sheedy, J, Weetall, ML & Davis, TW. BMI1 as a novel target for drug discovery in cancer. J Cell Biochem.2011; 112: 2729-41.

Cardo-Vila M, Giordano, RJ, Sidman, RL, Bronk, LF, Fan, Z, Mendelsohn, J, Arap, W & Pasqualini, R. From combinatorial peptide selection to drug prototype (II): targeting the epidermal growth factor receptor pathway. Proceedings of the National Academy of Sciences of the United States of America.2010; 107: 5118-23.

Carmen S & Jermutus, L. Concepts in antibody phage display. Brief Funct Genomic Proteomic.2002; 1: 189-203.

Chaffer CL, Brueckmann, I, Scheel, C, Kaestli, AJ, Wiggins, PA, Rodrigues, LO, Brooks, M, Reinhardt, F, Su, Y, Polyak, K, Arendt, LM, Kuperwasser, C, Bierie, B & Weinberg, RA. Normal and neoplastic nonstem cells can spontaneously convert to a stem-like state. Proceedings of the National Academy of Sciences of the United States of America.2011; 108: 7950-5.

Cheshier SH, Morrison, SJ, Liao, X & Weissman, IL. In vivo proliferation and cell cycle kinetics of long-term self-renewing hematopoietic stem cells. Proceedings of the National Academy of Sciences of the United States of America.1999; 96: 3120-5.

Clackson T, Hoogenboom, HR, Griffiths, AD & Winter, G. Making antibody fragments using phage display libraries. Nature.1991; 352: 624-8.

Clarke MF, Dick, JE, Dirks, PB, Eaves, CJ, Jamieson, CH, Jones, DL, Visvader, J, Weissman, IL & Wahl, GM. Cancer stem cells--perspectives on current status and future directions: AACR Workshop on cancer stem cells. Cancer research.2006; 66: 9339-44.

Clarke RB, Spence, K, Anderson, E, Howell, A, Okano, H & Potten, CS. A putative human breast stem cell population is enriched for steroid receptor-positive cells. Dev Biol.2005; 277: 443-56.

Clarkson B, Fried, J, Strife, A, Sakai, Y, Ota, K & Okita, T. Studies of cellular proliferation in human leukemia. 3. Behavior of leukemic cells in three adults with acute leukemia given continuous infusions of 3H-thymidine for 8 or 10 days. Cancer.1970; 25: 1237-60.

Clarkson BD, Dowling, MD, Gee, TS, Cunningham, IB & Burchenal, JH. Treatment of acute leukemia in adults. Cancer.1975; 36: 775-95.

Claudinot S, Nicolas, M, Oshima, H, Rochat, A & Barrandon, Y. Long-term renewal of hair follicles from clonogenic multipotent stem cells. Proceedings of the National Academy of Sciences of the United States of America.2005; 102: 14677-82.

Collins AT, Berry, PA, Hyde, C, Stower, MJ & Maitland, NJ. Prospective identification of tumorigenic prostate cancer stem cells. Cancer research.2005; 65: 10946-51.

Collins AT, Habib, FK, Maitland, NJ & Neal, DE. Identification and isolation of human prostate epithelial stem cells based on alpha(2)beta(1)-integrin expression. J Cell Sci.2001; 114: 3865-72.

Cox RP & Gesner, BM. Studies on the effects of simple sugars on mammalian cells in culture and characterization of the inhibition of 3T3 fibroblasts by L-fucose. Cancer research.1968; 28: 1162-72.

Crea F, Duhagon Serrat, MA, Hurt, EM, Thomas, SB, Danesi, R & Farrar, WL. BMI1 silencing enhances docetaxel activity and impairs antioxidant response in prostate cancer. International journal of cancer. Journal international du cancer.2011; 128: 1946-54.

Cronkite EP. Acute leukemia: is there a relationship between cell growth kinetics and response to chemotherapy? Proc Natl Cancer Conf.1970; 6: 113-7.

Dalerba P, Cho, RW & Clarke, MF. Cancer stem cells: models and concepts. Annu Rev Med.2007; 58: 267-84.

Daniels JT, Kearney, JN & Ingham, E. An investigation into the potential of extracellular matrix factors for attachment and proliferation of human keratinocytes on skin substitutes. Burns.1997; 23: 26-31.

Das A, Kennett, KM, Sutton, T, Fraundorfer, MR & Gilling, PJ. Histologic effects of holmium:YAG laser resection versus transurethral resection of the prostate. J Endourol.2000; 14: 459-62.

De Haard HJ, Van Neer, N, Reurs, A, Hufton, SE, Roovers, RC, Henderikx, P, De Bruine, AP, Arends, JW & Hoogenboom, HR. A large non-immunized human Fab fragment phage library that permits rapid isolation and kinetic analysis of high affinity antibodies. J Biol Chem.1999; 274: 18218-30.

Desjobert C, De Soultrait, VR, Faure, A, Parissi, V, Litvak, S, Tarrago-Litvak, L & Fournier, M. Identification by phage display selection of a short peptide able to inhibit only the strand transfer reaction catalyzed by human immunodeficiency virus type 1 integrase. Biochemistry.2004; 43: 13097-105.

Di Silverio F, Gentile, V, De Matteis, A, Mariotti, G, Giuseppe, V, Luigi, PA & Sciarra, A. Distribution of inflammation, pre-malignant lesions, incidental carcinoma in histologically confirmed benign prostatic hyperplasia: a retrospective analysis. Eur Urol.2003; 43: 164-75.

Dick JE. Stem cell concepts renew cancer research. Blood.2008; 112: 4793-807.

Doherty RE, Haywood-Small, SL, Sisley, K & Cross, NA. Aldehyde dehydrogenase activity selects for the holoclone phenotype in prostate cancer cells. Biochem Biophys Res Commun.2011; 414: 801-7.

Dominici M, Le Blanc, K, Mueller, I, Slaper-Cortenbach, I, Marini, F, Krause, D, Deans, R, Keating, A, Prockop, D & Horwitz, E. Minimal criteria for defining multipotent mesenchymal stromal cells. The International Society for Cellular Therapy position statement. Cytotherapy.2006; 8: 315-7.

Dontu G, Abdallah, WM, Foley, JM, Jackson, KW, Clarke, MF, Kawamura, MJ & Wicha, MS. In vitro propagation and transcriptional profiling of human mammary stem/progenitor cells. Genes Dev.2003a; 17: 1253-70.

Dontu G, Al-Hajj, M, Abdallah, WM, Clarke, MF & Wicha, MS. Stem cells in normal breast development and breast cancer. Cell Prolif.2003b; 36 Suppl 1: 59-72.

Dontu G & Wicha, MS. Survival of mammary stem cells in suspension culture: implications for stem cell biology and neoplasia. J Mammary Gland Biol Neoplasia.2005; 10: 75-86.

Du B, Han, H, Wang, Z, Kuang, L, Wang, L, Yu, L, Wu, M, Zhou, Z & Qian, M. targeted drug delivery to hepatocarcinoma in vivo by phage-displayed specific binding peptide. Mol Cancer Res.2010; 8: 135-44.

Duesberg P, Rausch, C, Rasnick, D & Hehlmann, R. Genetic instability of cancer cells is proportional to their degree of aneuploidy. Proceedings of the National Academy of Sciences of the United States of America.1998; 95: 13692-7.

Eglitis MA & Mezey, E. Hematopoietic cells differentiate into both microglia and macroglia in the brains of adult mice. Proceedings of the National Academy of Sciences of the United States of America.1997; 94: 4080-5.

Engler AJ, Sen, S, Sweeney, HL & Discher, DE. Matrix elasticity directs stem cell lineage specification. Cell.2006; 126: 677-89.

English HF, Santen, RJ & Isaacs, JT. Response of glandular versus basal rat ventral prostatic epithelial cells to androgen withdrawal and replacement. Prostate.1987; 11: 229-42.

Epstein JI, Allsbrook, WC, Jr., Amin, MB & Egevad, LL. The 2005 International Society of Urological Pathology (ISUP) Consensus Conference on Gleason Grading of Prostatic Carcinoma. The American journal of surgical pathology.2005; 29: 1228-42.

Evans GS & Chandler, JA. Cell proliferation studies in the rat prostate: II. The effects of castration and androgen-induced regeneration upon basal and secretory cell proliferation. Prostate.1987; 11: 339-51.

Ferrand A, Sandrin, MS, Shulkes, A & Baldwin, GS. Expression of gastrin precursors by CD133-positive colorectal cancer cells is crucial for tumour growth. Biochimica et biophysica acta.2009; 1793: 477-88.

Ferrari G, Cusella-De Angelis, G, Coletta, M, Paolucci, E, Stornaiuolo, A, Cossu, G & Mavilio, F. Muscle regeneration by bone marrow-derived myogenic progenitors. Science.1998; 279: 1528-30.

Ferrieu-Weisbuch C, Michel, S, Collomb-Clerc, E, Pothion, C, Deleage, G & Jolivet-Reynaud, C. Characterization of prostate-specific antigen binding peptides selected by phage display technology. J Mol Recognit.2006; 19: 10-20.

Fong S, Doyle, MV, Goodson, RJ, Drummond, RJ, Stratton, JR, Mcguire, L, Doyle, LV, Chapman, HA & Rosenberg, S. Random peptide bacteriophage display as a probe for urokinase receptor ligands. Biol Chem.2002; 383: 149-58.

Frank NY, Schatton, T & Frank, MH. The therapeutic promise of the cancer stem cell concept. J Clin Invest.120: 41-50.

Franken NA, Rodermond, HM, Stap, J, Haveman, J & Van Bree, C. Clonogenic assay of cells in vitro. Nat Protoc.2006; 1: 2315-9.

Freshney RI 2005. Culture of Specific Cell Types. *Culture of Animal Cells.* John Wiley & Sons, Inc.

Friedman HM & Glaubiger, DL. Assessment of in vitro drug sensitivity of human tumor cells using [3H]thymidine incorporation in a modified human tumor stem cell assay. Cancer research.1982; 42: 4683-9.

Fukuchi K, Steiniger, SC, Deryugina, E, Liu, Y, Lowery, CA, Gloeckner, C, Zhou, B, Kaufmann, GF, Quigley, JP & Janda, KD. Inhibition of tumor metastasis: functional immune modulation of the CUB domain containing protein 1. Mol Pharm.2010; 7: 245-53.

Galli R, Gritti, A, Bonfanti, L & Vescovi, AL. Neural stem cells: an overview. Circ Res.2003; 92: 598-608.

Gao Q, Geng, L, Kvalheim, G, Gaudernack, G & Suo, Z. Identification of cancer stem-like side population cells in ovarian cancer cell line OVCAR-3. Ultrastruct Pathol.2009; 33: 175-81.

Garraway IP, Sun, W, Tran, CP, Perner, S, Zhang, B, Goldstein, AS, Hahm, SA, Haider, M, Head, CS, Reiter, RE, Rubin, MA & Witte, ON. Human prostate sphere-forming cells represent a subset of basal epithelial cells capable of glandular regeneration in vivo. Prostate.2010; 70: 491-501.

George AJ, Lee, L & Pitzalis, C. Isolating ligands specific for human vasculature using in vivo phage selection. Trends Biotechnol.2003; 21: 199-203.

Ghotra VP, Puigvert, JC & Danen, EH. The cancer stem cell microenvironment and anti-cancer therapy. Int J Radiat Biol.2009; 85: 955-62.

Goldstein AS, Huang, J, Guo, C, Garraway, IP & Witte, ON. Identification of a cell of origin for human prostate cancer. Science.2010; 329: 568-71.

Goodson RJ, Doyle, MV, Kaufman, SE & Rosenberg, S. High-affinity urokinase receptor antagonists identified with bacteriophage peptide display. Proceedings of the National Academy of Sciences of the United States of America.1994; 91: 7129-33.

Greaves M & Maley, CC. Clonal evolution in cancer. Nature.2012; 481: 306-13.

Grenman R, Burk, D, Virolainen, E, Buick, RN, Church, J, Schwartz, DR & Carey, TE. Clonogenic cell assay for anchorage-dependent squamous carcinoma cell lines using limiting dilution. International journal of cancer. Journal international du cancer.1989; 44: 131-6.

Griffin JD & Lowenberg, B. Clonogenic cells in acute myeloblastic leukemia. Blood.1986; 68: 1185-95.

Griffiths AD, Williams, SC, Hartley, O, Tomlinson, IM, Waterhouse, P, Crosby, WL, Kontermann, RE, Jones, PT, Low, NM, Allison, TJ & Et Al. Isolation of high affinity human antibodies directly from large synthetic repertoires. Embo J.1994; 13: 3245-60.

Gu GY, Yuan, JL, Wils, M & Kasper, S. Prostate cancer cells with stem cell characteristics reconstitute the original human tumor in vivo. Cancer research.2007; 67: 4807-15.

Gu Y, Zhang, J, Wang, YB, Li, SW, Yang, HJ, Luo, WX & Xia, NS. Selection of a peptide mimicking neutralization epitope of hepatitis E virus with phage peptide display technology. World J Gastroenterol.2004; 10: 1583-8.

Guo C, Liu, H, Zhang, BH, Cadaneanu, RM, Mayle, AM & Garraway, IP. Epcam, CD44, and CD49f distinguish sphere-forming human prostate basal cells from a subpopulation with predominant tubule initiation capability. PLoS One.2012; 7: e34219.

Gupta PB, Fillmore, CM, Jiang, G, Shapira, SD, Tao, K, Kuperwasser, C & Lander, ES. Stochastic state transitions give rise to phenotypic equilibrium in populations of cancer cells. Cell.2011; 146: 633-44.

Gur D, Liu, S, Shukla, A, Pero, SC, Wicha, MS & Krag, DN. Identification of single chain antibodies to breast cancer stem cells using phage display. Biotechnol Prog.2009; 25: 1780-7.

Hamburger AW & Salmon, SE. Primary bioassay of human tumor stem cells. Science.1977; 197: 461-3.

Hannon GJ & Rossi, JJ. Unlocking the potential of the human genome with RNA interference. Nature.2004; 431: 371-8.

Hardonk MJ & Harms, G. The use of 5'-bromodeoxyuridine in the study of cell proliferation. Acta Histochem Suppl.1990; 39: 99-108.

Harper LJ, Piper, K, Common, J, Fortune, F & Mackenzie, IC. Stem cell patterns in cell lines derived from head and neck squamous cell carcinoma. J Oral Pathol Med.2007; 36: 594-603.

Hermann PC, Huber, SL, Herrler, T, Aicher, A, Ellwart, JW, Guba, M, Bruns, CJ & Heeschen, C. Distinct populations of cancer stem cells determine tumor growth and metastatic activity in human pancreatic cancer. Cell Stem Cell.2007; 1: 313-23.

Herrera MB, Bruno, S, Buttiglieri, S, Tetta, C, Gatti, S, Deregibus, MC, Bussolati, B & Camussi, G. Isolation and characterization of a stem cell population from adult human liver. Stem Cells.2006; 24: 2840-50.

Hirschmann-Jax C, Foster, AE, Wulf, GG, Nuchtern, JG, Jax, TW, Gobel, U, Goodell, MA & Brenner, MK. A distinct "side population" of cells with

high drug efflux capacity in human tumor cells. Proceedings of the National Academy of Sciences of the United States of America.2004; 101: 14228-33.

Horoszewicz JS, Leong, SS, Kawinski, E, Karr, JP, Rosenthal, H, Chu, TM, Mirand, EA & Murphy, GP. LNCaP model of human prostatic carcinoma. Cancer research.1983; 43: 1809-18.

Hudson DL. Epithelial stem cells in human prostate growth and disease. Prostate Cancer Prostatic Dis.2004; 7: 188-94.

Hudson DL, O'hare, M, Watt, FM & Masters, JR. Proliferative heterogeneity in the human prostate: evidence for epithelial stem cells. Lab Invest.2000; 80: 1243-50.

Hug V, Thames, H, Johnston, D, Blumenschein, G, Drewinko, B & Spitzer, G. The true predictive value of the human tumor stem cell assay: does a workable assay select for treatment responders? Journal of clinical oncology : official journal of the American Society of Clinical Oncology.1984; 2: 42-5.

Ichim CV & Wells, RA. First among equals: the cancer cell hierarchy. Leuk Lymphoma.2006; 47: 2017-27.

Isaacs JT & Coffey, DS. Etiology and disease process of benign prostatic hyperplasia. Prostate Suppl.1989; 2: 33-50.

Jager S, Jahnke, A, Wilmes, T, Adebahr, S, Vogtle, FN, Delima-Hahn, E, Pfeifer, D, Berg, T, Lubbert, M & Trepel, M. Leukemia-targeting ligands isolated from phage-display peptide libraries. Leukemia : official journal of the Leukemia Society of America, Leukemia Research Fund, U.K.2007; 21: 411-20.

Jakobsen CG, Rasmussen, N, Laenkholm, AV & Ditzel, HJ. Phage display derived human monoclonal antibodies isolated by binding to the surface of live primary breast cancer cells recognize GRP78. Cancer research.2007; 67: 9507-17.

Jayanna PK, Bedi, D, Deinnocentes, P, Bird, RC & Petrenko, VA. Landscape phage ligands for PC3 prostate carcinoma cells. Protein Eng Des Sel.2010; 23: 423-30.

Jensen KB, Jensen, ON, Ravn, P, Clark, BF & Kristensen, P. Identification of keratinocyte-specific markers using phage display and mass spectrometry. Mol Cell Proteomics.2003; 2: 61-9.

Jeter CR, Badeaux, M, Choy, G, Chandra, D, Patrawala, L, Liu, C, Calhoun-Davis, T, Zaehres, H, Daley, GQ & Tang, DG. Functional evidence that the self-renewal gene NANOG regulates human tumor development. Stem Cells.2009; 27: 993-1005.

Jeter CR, Liu, B, Liu, X, Chen, X, Liu, C, Calhoun-Davis, T, Repass, J, Zaehres, H, Shen, JJ & Tang, DG. NANOG promotes cancer stem cell

characteristics and prostate cancer resistance to androgen deprivation. Oncogene.2011; 30: 3833-45.

Jiang LL, Li, J & Song, LB. Bmi-1, stem cells and cancer. Acta Bioch Bioph Sin.2009; 41: 527-34.

Jiao J, Hindoyan, A, Wang, S, Tran, LM, Goldstein, AS, Lawson, D, Chen, D, Li, Y, Guo, C, Zhang, B, Fazli, L, Gleave, M, Witte, ON, Garraway, IP & Wu, H. Identification of CD166 as a surface marker for enriching prostate stem/progenitor and cancer initiating cells. PLoS One.2012; 7: e42564.

Jonassen I, Collins, JF & Higgins, DG. Finding flexible patterns in unaligned protein sequences. Protein Sci.1995; 4: 1587-95.

Jones DL & Rando, TA. Emerging models and paradigms for stem cell ageing. Nat Cell Biol.2011; 13: 506-12.

Kaighn ME, Narayan, KS, Ohnuki, Y, Lechner, JF & Jones, LW. Establishment and characterization of a human prostatic carcinoma cell line (PC-3). Invest Urol.1979; 17: 16-23.

Kalirai H, Damato, BE & Coupland, SE. Uveal melanoma cell lines contain stem-like cells that self-renew, produce differentiated progeny, and survive chemotherapy. Invest Ophthalmol Vis Sci.2011; 52: 8458-66.

Karasseva NG, Glinsky, VV, Chen, NX, Komatireddy, R & Quinn, TP. Identification and characterization of peptides that bind human ErbB-2 selected from a bacteriophage display library. J Protein Chem.2002; 21: 287-96.

Karlsson JO & Toner, M. Long-term storage of tissues by cryopreservation: critical issues. Biomaterials.1996; 17: 243-56.

Kasper S. Exploring the origins of the normal prostate and prostate cancer stem cell. Stem Cell Rev.2008; 4: 193-201.

Keith WN. From stem cells to cancer: balancing immortality and neoplasia. Oncogene.2004; 23: 5092-4.

Kempeni J. Preliminary results of early clinical trials with the fully human anti-TNFalpha monoclonal antibody D2E7. Ann Rheum Dis.1999; 58 Suppl 1: I70-2.

Keysar SB & Jimeno, A. More than markers: biological significance of cancer stem cell-defining molecules. Mol Cancer Ther.2010; 9: 2450-7.

Kirby R 2003. *An Atlas of Prostatic Diseases,* London, Parthenon Publishing Group.

Kirby R & Madhavan, SG. Prostate cancer. Surgery (Oxford).2010; 28: 594-98.

Kirkels WJ, Pelgrim, OE, Hoogenboom, AM, Aalders, MW, Debruyne, FM, Vooijs, GP & Herman, CJ. Patterns of tumor colony development over time in soft-agar culture. International journal of cancer. Journal international du cancer.1983; 32: 399-406.

Klarmann GJ, Hurt, EM, Mathews, LA, Zhang, X, Duhagon, MA, Mistree, T, Thomas, SB & Farrar, WL. Invasive prostate cancer cells are tumor initiating cells that have a stem cell-like genomic signature. Clin Exp Metastasis.2009; 26: 433-46.

Klein WM, Wu, BP, Zhao, SP, Wu, H, Klein-Szanto, AJP & Tahan, SR. Increased expression of stem cell markers in malignant melanoma. Modern Pathol.2007; 20: 102-07.

Kolonin MG, Bover, L, Sun, J, Zurita, AJ, Do, KA, Lahdenranta, J, Cardo-Vila, M, Giordano, RJ, Jaalouk, DE, Ozawa, MG, Moya, CA, Souza, GR, Staquicini, FI, Kunyiasu, A, Scudiero, DA, Holbeck, SL, Sausville, EA, Arap, W & Pasqualini, R. Ligand-directed surface profiling of human cancer cells with combinatorial peptide libraries. Cancer research.2006; 66: 34-40.

Kuczek T & Axelrod, DE. Tumor-Cell Heterogeneity - Divided-Colony Assay for Measuring Drug Response. Proceedings of the National Academy of Sciences of the United States of America.1987; 84: 4490-94.

Lapidot T, Sirard, C, Vormoor, J, Murdoch, B, Hoang, T, Caceres-Cortes, J, Minden, M, Paterson, B, Caligiuri, MA & Dick, JE. A cell initiating human acute myeloid leukaemia after transplantation into SCID mice. Nature.1994; 367: 645-8.

Lee A, Kessler, JD, Read, TA, Kaiser, C, Corbeil, D, Huttner, WB, Johnson, JE & Wechsler-Reya, RJ. Isolation of neural stem cells from the postnatal cerebellum. Nat Neurosci.2005; 8: 723-9.

Lee JH, Engler, JA, Collawn, JF & Moore, BA. Receptor mediated uptake of peptides that bind the human transferrin receptor. Eur J Biochem.2001; 268: 2004-12.

Leonardi C, Papp, K, Strober, B, Reich, K, Asahina, A, Gu, Y, Beason, J, Rozzo, S & Tyring, S. The long-term safety of adalimumab treatment in moderate to severe psoriasis: a comprehensive analysis of all adalimumab exposure in all clinical trials. Am J Clin Dermatol.2011; 12: 321-37.

Leong KG, Wang, BE, Johnson, L & Gao, WQ. Generation of a prostate from a single adult stem cell. Nature.2008; 456: 804-8.

Li CW, Heidt, DG, Dalerba, P, Burant, CF, Zhang, LJ, Adsay, V, Wicha, M, Clarke, MF & Simeone, DM. Identification of pancreatic cancer stem cells. Cancer research.2007; 67: 1030-37.

Li H, Chen, X, Calhoun-Davis, T, Claypool, K & Tang, DG. PC3 human prostate carcinoma cell holoclones contain self-renewing tumor-initiating cells. Cancer research.2008; 68: 1820-5.

Li L & Bhatia, R. Stem cell quiescence. Clinical cancer research : an official journal of the American Association for Cancer Research.2011; 17: 4936-41.

Li XB, Schluesener, HJ & Xu, SQ. Molecular addresses of tumors: selection by in vivo phage display. Arch Immunol Ther Exp (Warsz).2006; 54: 177-81.

Lindner T, Kolmar, H, Haberkorn, U & Mier, W. DNA libraries for the construction of phage libraries: statistical and structural requirements and synthetic methods. Molecules.2012; 16: 1625-41.

Liu C, Kelnar, K, Liu, B, Chen, X, Calhoun-Davis, T, Li, H, Patrawala, L, Yan, H, Jeter, C, Honorio, S, Wiggins, JF, Bader, AG, Fagin, R, Brown, D & Tang, DG. The microRNA miR-34a inhibits prostate cancer stem cells and metastasis by directly repressing CD44. Nat Med.2011; 17: 211-5.

Liu L, Andrews, LG & Tollefsbol, TO. Loss of the human polycomb group protein BMI1 promotes cancer-specific cell death. Oncogene.2006a; 25: 4370-5.

Liu S, Dontu, G, Mantle, ID, Patel, S, Ahn, NS, Jackson, KW, Suri, P & Wicha, MS. Hedgehog signaling and Bmi-1 regulate self-renewal of normal and malignant human mammary stem cells. Cancer research.2006b; 66: 6063-71.

Liu TJ, Sun, BC, Zhao, XL, Zhao, XM, Sun, T, Gu, Q, Yao, Z, Dong, XY, Zhao, N & Liu, N. CD133(+) cells with cancer stem cell characteristics associates with vasculogenic mimicry in triple-negative breast cancer. Oncogene.2012.

Llano-Sotelo B, Klepacki, D & Mankin, AS. Selection of small peptides, inhibitors of translation. J Mol Biol.2009; 391: 813-9.

Locke M, Heywood, M, Fawell, S & Mackenzie, IC. Retention of intrinsic stem cell hierarchies in carcinoma-derived cell lines. Cancer research.2005; 65: 8944-50.

Lokeshwar BL, Lokeshwar, VB & Block, NL. Expression of CD44 in prostate cancer cells: association with cell proliferation and invasive potential. Anticancer Res.1995; 15: 1191-8.

Lukacs RU, Memarzadeh, S, Wu, H & Witte, ON. Bmi-1 is a crucial regulator of prostate stem cell self-renewal and malignant transformation. Cell Stem Cell.2010; 7: 682-93.

Lunder M, Bratkovic, T, Doljak, B, Kreft, S, Urleb, U, Strukelj, B & Plazar, N. Comparison of bacterial and phage display peptide libraries in search of target-binding motif. Appl Biochem Biotechnol.2005; 127: 125-31.

Luo J, Duggan, DJ, Chen, Y, Sauvageot, J, Ewing, CM, Bittner, ML, Trent, JM & Isaacs, WB. Human prostate cancer and benign prostatic hyperplasia: molecular dissection by gene expression profiling. Cancer research.2001; 61: 4683-8.

Lupold SE & Rodriguez, R. Disulfide-constrained peptides that bind to the extracellular portion of the prostate-specific membrane antigen. Mol Cancer Ther.2004; 3: 597-603.

Mackenzie CG, Mackenzie, JB & Beck, P. The effect of pH on growth, protein synthesis, and lipid-rich particles of cultured mammalian cells. J Biophys Biochem Cytol.1961; 9: 141-56.

Mackillop WJ, Bizarri, JP & Ward, GK. Cellular heterogeneity in normal and neoplastic human urothelium. Cancer research.1985; 45: 4360-5.

Mackillop WJ, Ciampi, A, Till, JE & Buick, RN. A stem cell model of human tumor growth: implications for tumor cell clonogenic assays. J Natl Cancer Inst.1983; 70: 9-16.

Magee JA, Piskounova, E & Morrison, SJ. Cancer stem cells: impact, heterogeneity, and uncertainty. Cancer Cell.2012; 21: 283-96.

Maitland NJ, Frame, FM, Polson, ES, Lewis, JL & Collins, AT. Prostate cancer stem cells: do they have a basal or luminal phenotype? Horm Cancer.2011; 2: 47-61.

Marian CO, Wright, WE & Shay, JW. The effects of telomerase inhibition on prostate tumor-initiating cells. International journal of cancer. Journal international du cancer.2010; 127: 321-31.

Maruta F, Parker, AL, Fisher, KD, Murray, PG, Kerr, DJ & Seymour, LW. Use of a phage display library to identify oligopeptides binding to the lumenal surface of polarized endothelium by ex vivo perfusion of human umbilical veins. J Drug Target.2003; 11: 53-9.

Matsuno H, Sekine, J, Yajima, H & Serizawa, T. Biological selection of peptides for poly(l-lactide) substrates. Langmuir.2008; 24: 6399-403.

Mavilio F, Pellegrini, G, Ferrari, S, Di Nunzio, F, Di Iorio, E, Recchia, A, Maruggi, G, Ferrari, G, Provasi, E, Bonini, C, Capurro, S, Conti, A, Magnoni, C, Giannetti, A & De Luca, M. Correction of junctional epidermolysis bullosa by transplantation of genetically modified epidermal stem cells. Nat Med.2006; 12: 1397-402.

Mcculloch EA. Stem cells in normal and leukemic hemopoiesis (Henry Stratton Lecture, 1982). Blood.1983; 62: 1-13.

Mcculloch EA, Buick, RN, Curtis, JE, Messner, HA & Senn, JS. The heritable nature of clonal characteristics in acute myeloblastic leukemia. Blood.1981; 58: 105-9.

Mcculloch EA & Till, JE. The sensitivity of cells from normal mouse bone marrow to gamma radiation in vitro and in vivo. Radiat Res.1962; 16: 822-32.

Mcneal JE. Normal and pathologic anatomy of prostate. Urology.1981; 17: 11-6.

Mcneal JE. Normal histology of the prostate. Am J Surg Pathol.1988; 12: 619-33.

Mcneal JE. Anatomy of the prostate: an historical survey of divergent views. Prostate.2006; 1: 3-13.

Menendez A & Scott, JK. The nature of target-unrelated peptides recovered in the screening of phage-displayed random peptide libraries with antibodies. Anal Biochem.2005; 336: 145-57.

Meyskens FL, Jr., Thomson, SP & Moon, TE. Similar self-renewal properties for different sizes of human primary melanoma colonies replated in agar. Cancer research.1985; 45: 1101-7.

Mezey E, Chandross, KJ, Harta, G, Maki, RA & Mckercher, SR. Turning blood into brain: cells bearing neuronal antigens generated in vivo from bone marrow. Science.2000; 290: 1779-82.

Michel M, Torok, N, Godbout, MJ, Lussier, M, Gaudreau, P, Royal, A & Germain, L. Keratin 19 as a biochemical marker of skin stem cells in vivo and in vitro: keratin 19 expressing cells are differentially localized in function of anatomic sites, and their number varies with donor age and culture stage. J Cell Sci.1996; 109 (Pt 5): 1017-28.

Miki J, Furusato, B, Li, H, Gu, Y, Takahashi, H, Egawa, S, Sesterhenn, IA, Mcleod, DG, Srivastava, S & Rhim, JS. Identification of putative stem cell markers, CD133 and CXCR4, in hTERT-immortalized primary nonmalignant and malignant tumor-derived human prostate epithelial cell lines and in prostate cancer specimens. Cancer research.2007; 67: 3153-61.

Miller SJ, Lavker, RM & Sun, TT. Interpreting epithelial cancer biology in the context of stem cells: tumor properties and therapeutic implications. Biochimica et biophysica acta.2005; 1756: 25-52.

Mills JC, Andersson, N, Hong, CV, Stappenbeck, TS & Gordon, JI. Molecular characterization of mouse gastric epithelial progenitor cells. Proceedings of the National Academy of Sciences of the United States of America.2002; 99: 14819-24.

Miloszewska J, Gos, M, Przybyszewska, M, Trembacz, H, Koronkiewicz, M & Janik, P. Mouse sarcoma L1 cell line holoclones have a stemness signature. Cell Prolif.2010; 43: 229-34.

Mittal S, Mifflin, R & Powell, DW. Cancer stem cells: the other face of Janus. Am J Med Sci.2009; 338: 107-12.

Miyamoto H, Messing, EM & Chang, C. Androgen deprivation therapy for prostate cancer: current status and future prospects. Prostate.2004; 61: 332-53.

Moore KA & Lemischka, IR. Stem cells and their niches. Science.2006; 311: 1880-5.

Mori S, Chang, JT, Andrechek, ER, Matsumura, N, Baba, T, Yao, G, Kim, JW, Gatza, M, Murphy, S & Nevins, JR. Anchorage-independent cell growth signature identifies tumors with metastatic potential. Oncogene.2009; 28: 2796-805.

Morton RA, Ewing, CM, Nagafuchi, A, Tsukita, S & Isaacs, WB. Reduction of E-cadherin levels and deletion of the alpha-catenin gene in human prostate cancer cells. Cancer research.1993; 53: 3585-90.

Murayama K, Kimura, T, Tarutani, M, Tomooka, M, Hayashi, R, Okabe, M, Nishida, K, Itami, S, Katayama, I & Nakano, T. Akt activation induces epidermal hyperplasia and proliferation of epidermal progenitors. Oncogene.2007; 26: 4882-8.

Newton JR, Kelly, KA, Mahmood, U, Weissleder, R & Deutscher, SL. In vivo selection of phage for the optical imaging of PC-3 human prostate carcinoma in mice. Neoplasia.2006; 8: 772-80.

Nowell PC. The clonal evolution of tumor cell populations. Science.1976; 194: 23-8.

Nowell PC. Mechanisms of tumor progression. Cancer research.1986; 46: 2203-7.

O'brien CA, Kreso, A & Jamieson, CHM. Cancer Stem Cells and Self-renewal. Clin Cancer Res.2010; 16: 3113-20.

O'brien CA, Pollett, A, Gallinger, S & Dick, JE. A human colon cancer cell capable of initiating tumour growth in immunodeficient mice. Nature.2007; 445: 106-10.

Okada H, Tsubura, A, Okamura, A, Senzaki, H, Naka, Y, Komatz, Y & Morii, S. Keratin profiles in normal/hyperplastic prostates and prostate carcinoma. Virchows Arch A Pathol Anat Histopathol.1992; 421: 157-61.

Panasci LC, Dufour, M, Chevalier, L, Isabel, G, Lazarus, P, Mcquillan, A, Arbit, E, Brem, S & Feindel, W. Utilization of the HTSCA and CFU-C assay to identify two new 2-chloroethylnitrosourea congeners of amino acid amides with increased in vitro activity against human glioma compared with BCNU. Cancer Chemother Pharmacol.1985; 14: 156-9.

Park HY, Lee, KJ, Lee, SJ & Yoon, MY. Screening of Peptides Bound to Breast Cancer Stem Cell Specific Surface Marker CD44 by Phage Display. Mol Biotechnol.2011.

Pasqualini R & Ruoslahti, E. Organ targeting in vivo using phage display peptide libraries. Nature.1996; 380: 364-6.

Passarella RJ, Zhou, L, Phillips, JG, Wu, H, Hallahan, DE & Diaz, R. Recombinant peptides as biomarkers for tumor response to molecular targeted therapy. Clinical cancer research : an official journal of the American Association for Cancer Research.2009; 15: 6421-9.

Pastrana E, Cheng, LC & Doetsch, F. Simultaneous prospective purification of adult subventricular zone neural stem cells and their progeny. Proceedings of the National Academy of Sciences of the United States of America.2009; 106: 6387-92.

Pastrana E, Silva-Vargas, V & Doetsch, F. Eyes Wide Open: A Critical Review of Sphere-Formation as an Assay for Stem Cells. Cell Stem Cell.2011; 8: 486-98.

Patrawala L, Calhoun-Davis, T, Schneider-Broussard, R & Tang, DG. Hierarchical organization of prostate cancer cells in xenograft tumors: the CD44(+)alpha 2 beta 1(+) cell population is enriched in tumor-initiating cells. (vol 67, pg 6796, 2007). Cancer research.2007; 67: 8973-73.

Patrawala L, Calhoun, T, Schneider-Broussard, R, Li, H, Bhatia, B, Tang, S, Reilly, JG, Chandra, D, Zhou, J, Claypool, K, Coghlan, L & Tang, DG. Highly purified CD44+ prostate cancer cells from xenograft human tumors are enriched in tumorigenic and metastatic progenitor cells. Oncogene.2006; 25: 1696-708.

Patrawala L, Calhoun, T, Schneider-Broussard, R, Zhou, J, Claypool, K & Tang, DG. Side population is enriched in tumorigenic, stem-like cancer cells, whereas ABCG2+ and ABCG2- cancer cells are similarly tumorigenic. Cancer research.2005; 65: 6207-19.

Peehl DM. Primary cell cultures as models of prostate cancer development. Endocr Relat Cancer.2005; 12: 19-47.

Peeters M, Balfour, J & Arnold, D. Review article: panitumumab--a fully human anti-EGFR monoclonal antibody for treatment of metastatic colorectal cancer. Aliment Pharmacol Ther.2008; 28: 269-81.

Pellegrini G, Dellambra, E, Golisano, O, Martinelli, E, Fantozzi, I, Bondanza, S, Ponzin, D, Mckeon, F & De Luca, M. p63 identifies keratinocyte stem cells. Proceedings of the National Academy of Sciences of the United States of America.2001; 98: 3156-61.

Pellegrini G, Golisano, O, Paterna, P, Lambiase, A, Bonini, S, Rama, P & De Luca, M. Location and clonal analysis of stem cells and their differentiated progeny in the human ocular surface. J Cell Biol.1999; 145: 769-82.

Petersen BE, Bowen, WC, Patrene, KD, Mars, WM, Sullivan, AK, Murase, N, Boggs, SS, Greenberger, JS & Goff, JP. Bone marrow as a potential source of hepatic oval cells. Science.1999; 284: 1168-70.

Pfeiffer MJ & Schalken, JA. Stem cell characteristics in prostate cancer cell lines. Eur Urol.2010; 57: 246-54.

Pierce GB & Speers, WC. Tumors as caricatures of the process of tissue renewal: prospects for therapy by directing differentiation. Cancer research.1988; 48: 1996-2004.

Popkov M, Rader, C & Barbas, CF, 3rd. Isolation of human prostate cancer cell reactive antibodies using phage display technology. J Immunol Methods.2004; 291: 137-51.

Potter KC, Evans, H & Patel, U. Clinically orientated imaging of the prostate gland. Imaging.2005; 17: 122-29.

Qin J, Liu, X, Laffin, B, Chen, X, Choy, G, Jeter, CR, Calhoun-Davis, T, Li, H, Palapattu, GS, Pang, S, Lin, K, Huang, J, Ivanov, I, Li, W, Suraneni, MV & Tang, DG. The PSA(-/lo) prostate cancer cell population harbors self-renewing long-term tumor-propagating cells that resist castration. Cell Stem Cell.2012; 10: 556-69.

Quintana E, Shackleton, M, Sabel, MS, Fullen, DR, Johnson, TM & Morrison, SJ. Efficient tumour formation by single human melanoma cells. Nature.2008; 456: 593-8.

Rajasekhar VK, Studer, L, Gerald, W, Socci, ND & Scher, HI. Tumour-initiating stem-like cells in human prostate cancer exhibit increased NF-kappaB signalling. Nat Commun.2011; 2: 162.

Rajotte D, Arap, W, Hagedorn, M, Koivunen, E, Pasqualini, R & Ruoslahti, E. Molecular heterogeneity of the vascular endothelium revealed by in vivo phage display. The Journal of clinical investigation.1998; 102: 430-7.

Rasmussen UB, Schreiber, V, Schultz, H, Mischler, F & Schughart, K. Tumor cell-targeting by phage-displayed peptides. Cancer Gene Ther.2002; 9: 606-12.

Reya T & Clevers, H. Wnt signalling in stem cells and cancer. Nature.2005; 434: 843-50.

Reya T, Morrison, SJ, Clarke, MF & Weissman, IL. Stem cells, cancer, and cancer stem cells. Nature.2001; 414: 105-11.

Reynolds BA & Weiss, S. Generation of neurons and astrocytes from isolated cells of the adult mammalian central nervous system. Science.1992; 255: 1707-10.

Reynolds JC & Putnam, PE. Prokinetic agents. Gastroenterol Clin North Am.1992; 21: 567-96.

Reynolds RD. The Norplant contraceptive. J Fam Pract.1992; 35: 249; author reply 49, 52-3.

Rhee HW, Zhau, HE, Pathak, S, Multani, AS, Pennanen, S, Visakorpi, T & Chung, LW. Permanent phenotypic and genotypic changes of prostate cancer cells cultured in a three-dimensional rotating-wall vessel. In Vitro Cell Dev Biol Anim.2001; 37: 127-40.

Ricci-Vitiani L, Lombardi, DG, Pilozzi, E, Biffoni, M, Todaro, M, Peschle, C & De Maria, R. Identification and expansion of human colon-cancer-initiating cells. Nature.2007; 445: 111-15.

Richardson GD, Robson, CN, Lang, SH, Neal, DE, Maitland, NJ & Collins, AT. CD133, a novel marker for human prostatic epithelial stem cells. J Cell Sci.2004; 117: 3539-45.

Robinson EJ, Neal, DE & Collins, AT. Basal cells are progenitors of luminal cells in primary cultures of differentiating human prostatic epithelium. Prostate.1998; 37: 149-60.

Rochat A, Kobayashi, K & Barrandon, Y. Location of stem cells of human hair follicles by clonal analysis. Cell.1994; 76: 1063-73.

Roesch A, Fukunaga-Kalabis, M, Schmidt, EC, Zabierowski, SE, Brafford, PA, Vultur, A, Basu, D, Gimotty, P, Vogt, T & Herlyn, M. A temporarily distinct subpopulation of slow-cycling melanoma cells is required for continuous tumor growth. Cell.2010; 141: 583-94.

Romanov VI, Durand, DB & Petrenko, VA. Phage display selection of peptides that affect prostate carcinoma cells attachment and invasion. Prostate.2001; 47: 239-51.

Ronca R, Benzoni, P, De Luca, A, Crescini, E & Dell'era, P. Phage displayed peptides/antibodies recognizing growth factors and their tyrosine kinase receptors as tools for anti-cancer therapeutics. Int J Mol Sci.2012; 13: 5254-77.

Rougerie P, Largeteau, Q, Megrelis, L, Carrette, F, Lejeune, T, Toffali, L, Rossi, B, Zeghouf, M, Cherfils, J, Constantin, G, Laudanna, C, Bismuth, G, Mangeney, M & Delon, J. Fam65b is a new transcriptional target of FOXO1 that regulates RhoA signaling for T lymphocyte migration. J Immunol.2013; 190: 748-55.

Rubin DT, Panaccione, R, Chao, J & Robinson, AM. A practical, evidence-based guide to the use of adalimumab in Crohn's disease. Curr Med Res Opin.2011; 27: 1803-13.

Rudin CM, Hann, CL, Laterra, J, Yauch, RL, Callahan, CA, Fu, L, Holcomb, T, Stinson, J, Gould, SE, Coleman, B, Lorusso, PM, Von Hoff, DD, De Sauvage, FJ & Low, JA. Treatment of medulloblastoma with hedgehog pathway inhibitor GDC-0449. N Engl J Med.2009; 361: 1173-8.

Rybak AP, He, L, Kapoor, A, Cutz, JC & Tang, D. Characterization of sphere-propagating cells with stem-like properties from DU145 prostate cancer cells. Biochimica et biophysica acta.2011; 1813: 683-94.

Rylander MN, Feng, YS, Zhang, YJ, Bass, J, Stafford, RJ, Volgin, A, Hazle, JD & Diller, KR. Optimizing heat shock protein expression induced by prostate cancer laser therapy through predictive computational models. J Biomed Opt.2006; 11.

Sadanandam A, Varney, ML, Kinarsky, L, Ali, H, Mosley, RL & Singh, RK. Identification of functional cell adhesion molecules with a potential role in metastasis by a combination of in vivo phage display and in silico analysis. Omics.2007; 11: 41-57.

Saini S, Majid, S, Shahryari, V, Arora, S, Yamamura, S, Chang, I, Zaman, MS, Deng, G, Tanaka, Y & Dahiya, R. miRNA-708 control of CD44(+) prostate cancer-initiating cells. Cancer research.2012; 72: 3618-30.

Salm SN, Burger, PE, Coetzee, S, Goto, K, Moscatelli, D & Wilson, EL. TGF-{beta} maintains dormancy of prostatic stem cells in the proximal region of ducts. J Cell Biol.2005; 170: 81-90.

Santini V, Bernabei, PA, Silvestro, L, Dal Pozzo, O, Bezzini, R, Viano, I, Gattei, V, Saccardi, R & Ferrini, PR. In vitro chemosensitivity testing of leukemic cells: prediction of response to chemotherapy in patients with acute non-lymphocytic leukemia. Hematol Oncol.1989; 7: 287-93.

Sawada T & Mihara, H. Dense surface functionalization using peptides that recognize differences in organized structures of self-assembling nanomaterials. Mol Biosyst.2012; 8: 1264-74.

Schatton T & Frank, MH. The in vitro spheroid melanoma cell culture assay: cues on tumor initiation? The Journal of investigative dermatology.2010; 130: 1769-71.

Schatton T, Murphy, GF, Yamaura, K, Waaga-Gasser, A, Gasser, M, Zhan, Q, Jordan, S, Duncan, IM, Weishaupt, C, Fuhlbrigge, RC, Kupper, TS, Sayegh, MH & Frank, MH. Identification of cells initiating human melanomas. J Invest Dermatol.2008; 128: S213-S13.

Schatzl G, Madersbacher, S, Djavan, B, Lang, T & Marberger, M. Two-year results of transurethral resection of the prostate versus four 'less invasive' treatment options. Eur Urol.2000; 37: 695-701.

Scher HI, Fizazi, K, Saad, F, Taplin, ME, Sternberg, CN, Miller, K, De Wit, R, Mulders, P, Chi, KN, Shore, ND, Armstrong, AJ, Flaig, TW, Flechon, A, Mainwaring, P, Fleming, M, Hainsworth, JD, Hirmand, M, Selby, B, Seely, L & De Bono, JS. Increased survival with enzalutamide in prostate cancer after chemotherapy. N Engl J Med.2012; 367: 1187-97.

Selby P, Buick, RN & Tannock, I. A critical appraisal of the "human tumor stem-cell assay". N Engl J Med.1983; 308: 129-34.

Setoguchi T, Taga, T & Kondo, T. Cancer stem cells persist in many cancer cell lines. Cell Cycle.2004; 3: 414-5.

Shackleton M, Quintana, E, Fearon, ER & Morrison, SJ. Heterogeneity in cancer: cancer stem cells versus clonal evolution. Cell.2009; 138: 822-9.

Shanmugam A, Suriano, R, Chaudhuri, D, Rajoria, S, George, A, Mittelman, A & Tiwari, RK. Identification of PSA peptide mimotopes using phage display peptide library. Peptides.2011; 32: 1097-102.

Shortt AJ, Secker, GA, Munro, PM, Khaw, PT, Tuft, SJ & Daniels, JT. Characterization of the limbal epithelial stem cell niche: novel imaging techniques permit in vivo observation and targeted biopsy of limbal epithelial stem cells. Stem Cells.2007; 25: 1402-9.

Shrivastava A, Von Wronski, MA, Sato, AK, Dransfield, DT, Sexton, D, Bogdan, N, Pillai, R, Nanjappan, P, Song, B, Marinelli, E, Deoliveira, D, Luneau, C, Devlin, M, Muruganandam, A, Abujoub, A, Connelly, G, Wu, QL, Conley, G, Chang, Q, Tweedle, MF, Ladner, RC, Swenson, RE & Nunn, AD. A distinct strategy to generate high-affinity peptide binders to receptor tyrosine kinases. Protein Eng Des Sel.2005; 18: 417-24.

Sidhu SS. Engineering M13 for phage display. Biomol Eng.2001; 18: 57-63.

Sikandar SS, Pate, KT, Anderson, S, Dizon, D, Edwards, RA, Waterman, ML & Lipkin, SM. NOTCH signaling is required for formation and self-renewal of tumor-initiating cells and for repression of secretory cell differentiation in colon cancer. Cancer research.2010; 70: 1469-78.

Silacci M, Brack, S, Schirru, G, Marlind, J, Ettorre, A, Merlo, A, Viti, F & Neri, D. Design, construction, and characterization of a large synthetic human antibody phage display library. Proteomics.2005; 5: 2340-50.

Singh SK, Hawkins, C, Clarke, ID, Squire, JA, Bayani, J, Hide, T, Henkelman, RM, Cusimano, MD & Dirks, PB. Identification of human brain tumour initiating cells. Nature.2004; 432: 396-401.

Smith GP. Filamentous fusion phage: novel expression vectors that display cloned antigens on the virion surface. Science.1985; 228: 1315-7.

Smith GP & Petrenko, VA. Phage Display. Chem Rev.1997; 97: 391-410.

Snippert HJ, Haegebarth, A, Kasper, M, Jaks, V, Van Es, JH, Barker, N, Van De Wetering, M, Van Den Born, M, Begthel, H, Vries, RG, Stange, DE, Toftgard, R & Clevers, H. Lgr6 marks stem cells in the hair follicle that generate all cell lineages of the skin. Science.2010; 327: 1385-9.

Sommavilla R, Lovato, V, Villa, A, Sgier, D & Neri, D. Design and construction of a naive mouse antibody phage display library. J Immunol Methods.2010; 353: 31-43.

Sowalsky AG, Ye, H, Bubley, GJ & Balk, SP. Clonal progression of prostate cancers from Gleason grade 3 to grade 4. Cancer research.2013; 73: 1050-5.

Stone KR, Mickey, DD, Wunderli, H, Mickey, GH & Paulson, DF. Isolation of a Human Prostate Carcinoma Cell Line (Du 145). Int J Cancer.1978; 21: 274-81.

Szabo AZ, Fong, S, Yue, L, Zhang, K, Strachan, LR, Scalapino, K, Mancianti, ML & Ghadially, R. The CD44(+) ALDH(+) Population of Human Keratinocytes is Enriched for Epidermal Stem Cells with Long Term Repopulating Ability. Stem Cells.2013.

Takebe N, Harris, PJ, Warren, RQ & Ivy, SP. Targeting cancer stem cells by inhibiting Wnt, Notch, and Hedgehog pathways. Nat Rev Clin Oncol.2011; 8: 97-106.

Talbot NC, Powell, AM & Caperna, TJ. Comparison of colony-formation efficiency of bovine fetal fibroblast cell lines cultured with low oxygen, hydrocortisone, L-carnosine, bFGF, or different levels of FBS. Cloning Stem Cells.2004; 6: 37-47.

Tammela T. Benign prostatic hyperplasia. Practical treatment guidelines. Drugs Aging.1997; 10: 349-66.

Tan L, Sui, X, Deng, H & Ding, M. Holoclone forming cells from pancreatic cancer cells enrich tumor initiating cells and represent a novel model for study of cancer stem cells. PLoS One.2011; 6: e23383.

Tang DG. Understanding cancer stem cell heterogeneity and plasticity. Cell Res.2012; 22: 457-72.

Tang DG, Patrawala, L, Calhoun, T, Bhatia, B, Choy, G, Schneider-Broussard, R & Jeter, C. Prostate cancer stem/progenitor cells: identification, characterization, and implications. Mol Carcinog.2007; 46: 1-14.

Taylor RA, Toivanen, R, Frydenberg, M, Pedersen, J, Harewood, L, Australian Prostate Cancer, B, Collins, AT, Maitland, NJ & Risbridger, GP. Human epithelial basal cells are cells of origin of prostate cancer, independent of CD133 status. Stem Cells.2012; 30: 1087-96.

Till JE & Mcculloch, EA. A direct measurement of the radiation sensitivity of normal mouse bone marrow cells. Radiat Res.1961; 14: 213-22.

Timms BG & Hofkamp, LE. Prostate development and growth in benign prostatic hyperplasia. Differentiation.2011; 82: 173-83.

Trosko JE. From adult stem cells to cancer stem cells: Oct-4 Gene, cell-cell communication, and hormones during tumor promotion. Ann N Y Acad Sci.2006; 1089: 36-58.

Tsujimura A, Koikawa, Y, Salm, S, Takao, T, Coetzee, S, Moscatelli, D, Shapiro, E, Lepor, H, Sun, T-T & Wilson, EL. Proximal location of

mouse prostate epithelial stem cells a model of prostatic homeostasis. J Cell Biol.2002; 157: 1257-65.

Tudor D, Chaudry, F, Harper, L & Mackenzie, IC. The in vitro behaviour and patterns of colony formation of murine epithelial stem cells. Cell Prolif.2007; 40: 706-20.

Tudor D, Locke, M, Owen-Jones, E & Mackenzie, IC. Intrinsic patterns of behavior of epithelial stem cells. J Investig Dermatol Symp Proc.2004; 9: 208-14.

Ueberberg S & Schneider, S. Phage library-screening: a powerful approach for generation of targeting-agents specific for normal pancreatic islet-cells and islet-cell carcinoma in vivo. Regul Pept.2010; 160: 1-8.

Ulrich H, Trujillo, CA, Nery, AA, Alves, JM, Majumder, P, Resende, RR & Martins, AH. DNA and RNA aptamers: from tools for basic research towards therapeutic applications. Comb Chem High Throughput Screen.2006; 9: 619-32.

Visvader JE & Lindeman, GJ. Cancer stem cells in solid tumours: accumulating evidence and unresolved questions. Nat Rev Cancer.2008; 8: 755-68.

Vodnik M, Zager, U, Strukelj, B & Lunder, M. Phage display: selecting straws instead of a needle from a haystack. Molecules.2011; 16: 790-817.

Von Hoff DD, Clark, GM, Stogdill, BJ, Sarosdy, MF, O'brien, MT, Casper, JT, Mattox, DE, Page, CP, Cruz, AB & Sandbach, JF. Prospective clinical trial of a human tumor cloning system. Cancer research.1983; 43: 1926-31.

Wang G, Wang, Z, Sarkar, FH & Wei, W. Targeting prostate cancer stem cells for cancer therapy. Discov Med.2012; 13: 135-42.

Wang H, Rana, S, Giese, N, Buchler, MW & Zoller, M. Tspan8, CD44v6 and alpha6beta4 are biomarkers of migrating pancreatic cancer initiating cells. International journal of cancer. Journal international du cancer.2013.

Wang JCY & Dick, JE. Cancer stem cells: lessons from leukemia. Trends Cell Biol.2005; 15: 494-501.

Wang Y, Hayward, S, Cao, M, Thayer, K & Cunha, G. Cell differentiation lineage in the prostate. Differentiation.2001; 68: 270-9.

Waseem A, Dogan, B, Tidman, N, Alam, Y, Purkis, P, Jackson, S, Lalli, A, Machesney, M & Leigh, IM. Keratin 15 expression in stratified epithelia: downregulation in activated keratinocytes. The Journal of investigative dermatology.1999; 112: 362-9.

Weber K, Thomaschewski, M, Benten, D & Fehse, B. RGB marking with lentiviral vectors for multicolor clonal cell tracking. Nat Protoc.2012; 7: 839-49.

Wei C, Guomin, W, Yujun, L & Ruizhe, Q. Cancer stem-like cells in human prostate carcinoma cells DU145: the seeds of the cell line? Cancer Biol Ther.2007; 6: 763-8.

Wilson JD & Roehrborn, C. Long-term consequences of castration in men: lessons from the Skoptzy and the eunuchs of the Chinese and Ottoman courts. J Clin Endocrinol Metab.1999; 84: 4324-31.

Wilt TJ, Brawer, MK, Jones, KM, Barry, MJ, Aronson, WJ, Fox, S, Gingrich, JR, Wei, JT, Gilhooly, P, Grob, BM, Nsouli, I, Iyer, P, Cartagena, R, Snider, G, Roehrborn, C, Sharifi, R, Blank, W, Pandya, P, Andriole, GL, Culkin, D & Wheeler, T. Radical prostatectomy versus observation for localized prostate cancer. N Engl J Med.2012; 367: 203-13.

Wolff JM & Mason, M. Drivers for change in the management of prostate cancer - guidelines and new treatment techniques. BJU Int.2012; 109 Suppl 6: 33-41.

Work LM, Nicklin, SA, Brain, NJ, Dishart, KL, Von Seggern, DJ, Hallek, M, Buning, H & Baker, AH. Development of efficient viral vectors selective for vascular smooth muscle cells. Mol Ther.2004; 9: 198-208.

Writer MJ, Marshall, B, Pilkington-Miksa, MA, Barker, SE, Jacobsen, M, Kritz, A, Bell, PC, Lester, DH, Tabor, AB, Hailes, HC, Klein, N & Hart, SL. Targeted gene delivery to human airway epithelial cells with synthetic vectors incorporating novel targeting peptides selected by phage display. J Drug Target.2004; 12: 185-93.

Wu Y, Cain-Hom, C, Choy, L, Hagenbeek, TJ, De Leon, GP, Chen, Y, Finkle, D, Venook, R, Wu, X, Ridgway, J, Schahin-Reed, D, Dow, GJ, Shelton, A, Stawicki, S, Watts, RJ, Zhang, J, Choy, R, Howard, P, Kadyk, L, Yan, M, Zha, J, Callahan, CA, Hymowitz, SG & Siebel, CW. Therapeutic antibody targeting of individual Notch receptors. Nature.2010; 464: 1052-7.

Xiao Y & Isaacs, SN. Enzyme-linked immunosorbent assay (ELISA) and blocking with bovine serum albumin (BSA)-not all BSAs are alike. J Immunol Methods.2012.

Yamamoto H, Masters, JR, Dasgupta, P, Chandra, A, Popert, R, Freeman, A & Ahmed, A. CD49f is an efficient marker of monolayer- and spheroid colony-forming cells of the benign and malignant human prostate. PLoS One.2012; 7: e46979.

Yang XD, Jia, XC, Corvalan, JR, Wang, P & Davis, CG. Development of ABX-EGF, a fully human anti-EGF receptor monoclonal antibody, for cancer therapy. Crit Rev Oncol Hematol.2001; 38: 17-23.

Yauch RL, Dijkgraaf, GJ, Alicke, B, Januario, T, Ahn, CP, Holcomb, T, Pujara, K, Stinson, J, Callahan, CA, Tang, T, Bazan, JF, Kan, Z, Seshagiri, S, Hann, CL, Gould, SE, Low, JA, Rudin, CM & De Sauvage, FJ. Smoothened mutation confers resistance to a Hedgehog pathway inhibitor in medulloblastoma. Science.2009; 326: 572-4.

Yayon A, Aviezer, D, Safran, M, Gross, JL, Heldman, Y, Cabilly, S, Givol, D & Katchalski-Katzir, E. Isolation of peptides that inhibit binding of basic fibroblast growth factor to its receptor from a random phage-epitope library. Proceedings of the National Academy of Sciences of the United States of America.1993; 90: 10643-7.

Yu HQ, Dong, XY & Sun, Y. An alternating elution strategy for screening high affinity peptides from a phage display peptide library. Biochem Eng J.2004; 18: 169-75.

Yu SC, Ping, YF, Yi, L, Zhou, ZH, Chen, JH, Yao, XH, Gao, L, Wang, JM & Bian, XW. Isolation and characterization of cancer stem cells from a human glioblastoma cell line U87. Cancer Lett.2008; 265: 124-34.

Yuan SH, Martin, J, Elia, J, Flippin, J, Paramban, RI, Hefferan, MP, Vidal, JG, Mu, Y, Killian, RL, Israel, MA, Emre, N, Marsala, S, Marsala, M, Gage, FH, Goldstein, LS & Carson, CT. Cell-surface marker signatures for the isolation of neural stem cells, glia and neurons derived from human pluripotent stem cells. PLoS One.2011; 6: e17540.

Zeilstra J, Joosten, SP, Van Andel, H, Tolg, C, Berns, A, Snoek, M, Van De Wetering, M, Spaargaren, M, Clevers, H & Pals, ST. Stem cell CD44v isoforms promote intestinal cancer formation in Apc(min) mice downstream of Wnt signaling. Oncogene.2013.

Zhang K & Waxman, DJ. PC3 prostate tumor-initiating cells with molecular profile FAM65Bhigh/MFI2low/LEF1low increase tumor angiogenesis. Mol Cancer.2010; 9: 319.

Zhang Y, Chen, J, Hu, Z, Hu, D, Pan, Y, Ou, S, Liu, G, Yin, X, Zhao, J, Ren, L & Wang, J. Panning and identification of a colon tumor binding peptide from a phage display peptide library. J Biomol Screen.2007; 12: 429-35.